



HAL
open science

Synthesis, characterization, ring-opening metathesis polymerization of cyclobutenyl macromonomers obtained by "click" chemistry and RAFT polymerization

Dao Le

► **To cite this version:**

Dao Le. Synthesis, characterization, ring-opening metathesis polymerization of cyclobutenyl macromonomers obtained by "click" chemistry and RAFT polymerization. Other. Le Mans Université, 2012. English. NNT : 2012LEMA1010 . tel-00743217

HAL Id: tel-00743217

<https://theses.hal.science/tel-00743217>

Submitted on 18 Oct 2012

HAL is a multi-disciplinary open access archive for the deposit and dissemination of scientific research documents, whether they are published or not. The documents may come from teaching and research institutions in France or abroad, or from public or private research centers.

L'archive ouverte pluridisciplinaire **HAL**, est destinée au dépôt et à la diffusion de documents scientifiques de niveau recherche, publiés ou non, émanant des établissements d'enseignement et de recherche français ou étrangers, des laboratoires publics ou privés.

THESE

Présentée en vue de l'obtention du grade de

DOCTEUR

Spécialité : Chimie et Physicochimie des polymères

Par

Dao LE

Synthèse, caractérisation et polymérisation par ouverture de cycle
par métathèse de macromonomères cyclobuténiques obtenus par
chimie « click » et polymérisation RAFT

Soutenue le 20 septembre 2012, devant le jury composé de :

M. Jean-François LUTZ	Directeur de Recherche CNRS, Institut Charles Sadron, Strasbourg	Rapporteur
M. Jean-Luc SIX	Professeur, Université de Lorraine	Rapporteur
Mme Sophie M. GUILLAUME	Directeur de Recherche CNRS, Université de Rennes 1	Examinatrice
Mme Valérie HEROGUEZ	Directeur de Recherche CNRS, Université Bordeaux 1	Examinatrice
M. Laurent FONTAINE	Professeur, Université du Maine	Directeur de thèse
Mme Véronique MONTEBAULT	Maître de Conférences-HDR, Université du Maine	Co-directeur de thèse
Mme Sagrario PASCUAL	Maître de Conférences-HDR, Université du Maine	Co-encadrante

Luận văn này được gửi tới....

Cha mẹ...

Anh chị...

Vi...

Bạn bè và những người tôi yêu quý.

Ce travaux de thèse ont été réalisés dans l'Institut des Molécules et Matériaux du Mans (IMMM-UMR CNRS 6283) de l'Université du Maine grâce au soutien financement de l'Agence Nationale de la Recherche, France.

Je tiens à remercier en premier lieu le Pr. Laurent FONTAINE pour m'avoir accueilli au Département Méthodologie et Synthèse lors de mon stage de master II et aussi dans le cadre de ce travail de thèse. Je le remercie pour la confiance qu'il m'a accordée ainsi que pour les discussions scientifiques qui m'ont permis de découvrir le monde de la recherche.

Je voudrais remercier ma co-directrice de thèse, le Dr. Véronique MONTEBAULT, pour les connaissances qu'elle m'a transmises concernant tous les travaux de ma thèse. Je la remercie pour sa patience, sa disponibilité, sa gentillesse et son grand travail de correction de mon manuscrit de thèse ainsi que pour les conseils dans des journées difficiles.

Je souhaite associer à ces remerciements ma co-encadrante, le Dr. Sagrario PASCUAL, pour sa disponibilité, sa gentillesse, pour m'avoir fait bénéficier de ses connaissances sur la polymérisation RAFT et pour ses conseils précieux à mes travaux de thèse.

Merci au Dr. Jean-Claude SOUTIF pour les nombreux spectres MALDI-TOF qu'il a réalisé et pour nos discussions scientifiques..

Je remercie également le Dr. Valérie HEROGUEZ, tout d'abord de m'avoir reçu dans son laboratoire, le LCPO, lors de deux stages de un mois, qui m'ont permis de me former à la ROMP en milieu aqueux dispersé, ainsi que pour avoir accepté d'être membre de mon jury de thèse. Merci également à ses étudiants, le Dr. Floraine COLLETTE et le Dr. Minh Ngoc NGUYEN pour leur aide au LCPO.

Je tiens ensuite à remercier le Dr. Stéphanie LEGOUPY pour les connaissances qu'elle m'a transmises sur le cyclobutène.

Merci au Pr. Christophe CHASSENIEUX et au Dr. Martin E. LEVERE pour les caractérisations physico-chimiques dans le cadre de ce projet ANR. Merci à Dr. Erwan NICOL pour son aide aux mesures de spectroscopie de fluorescence.

Je remercie également le Dr. Sophie M. GUILLAUME, les professeurs Jean-François LUTZ et Jean-Luc SIX pour avoir accepté d'être

membres de mon jury de thèse ainsi que pour leurs judicieuses remarques.

J'adresse ensuite mes remerciements au Dr. Sandie PIOGE pour sa disponibilité et son aide précieuse à ma présentation de soutenance.

Merci à Anita LOISEAU pour sa disponibilité et son aide au quotidien au laboratoire.

Je remercie également l'ensemble du personnel du laboratoire, chercheurs, thésards, stagiaires, post-docs, permanentes pour leur disponibilité, leur sympathie. Merci à mes collègues au laboratoire : Hien, Thuy, Marie, Romain, Flavien, Pierre-Yves, Hoa, Charles, Anuwat, Faten, Nhung, Ekkazit, Nitinart, Wannapa, Wannarat, Khrisna pour l'ambiance amicale au laboratoire.

Un grand merci à ma famille qui m'a toujours soutenue. Et Vi, merci d'avoir été à mes côtés et de partager les bons moments ou les moments difficiles.

LIST OF ABBREVIATIONS

ADMET	Acyclic Diene Metathesis Polymerization
ACPA	4,4'-azobis(4-cyanopentanoyl acid)
AcOEt	Ethyl acetate
AE	Acrylate d'éthyle
AFM	Atomic Force Microscopy
AIBN	2,2'-Azobis(isobutyronitrile)
ATRP	Atom Transfer Radical Polymerization
Bu	Butadiene
BSA	Bovine Serum Albumin
CMC	Critical Micellar Concentration
ϵ -CL	ϵ -Caprolactone
CT	Camptothecin
COD	Cyclooctadiene
CTA	Chain Transfer Agent
CuAAC	Copper Catalyzed Azide-Alkyne Cycloadditions
DCC	<i>N,N'</i> -dicyclohexylcarbodiimide
DCM	Dichloromethane
DCTB	2-[(2 <i>E</i>)-3-(4- <i>tert</i> -butylphenyl)-2-methylprop-2-enylidene]malononitrile
D_h	Number-average hydrodynamic diameter
DLS	Dynamic Light Scattering
DMAEMA	2-(<i>N,N</i> -dimethylamino)ethyl methacrylate
DMAP	4-(<i>N,N</i> -dimethylamino)pyridine
DMF	Dimethylformamide
DNA	Deoxyribonucleic acid
DOX	Doxorubicin
\overline{DP}_n	Number-average degree of polymerization
\overline{DP}_w	Weight-average degree of polymerization
DSC	Differential Scanning Calorimetry
EA	Ethyl acrylate
EO	Ethylene Oxide

FTIR	Fourier Transformed InfraRed spectroscopy
HRMS	High Resolution Mass Spectroscopy
LA	L-lactide
MA	Methyl Acrylate
Macro-CTA	Macromolecular Chain Transfer Agent
MALDI-TOF	Matrix Assisted Laser Desorption/Ionization-Time Of Flight
MMA	Methyl Methacrylate
\overline{M}_n	Number-average molecular weight
\overline{M}_n SEC	\overline{M}_n measured by SEC, refractive index detector
\overline{M}_n SEC, PEO	\overline{M}_n measured by SEC, refractive index detector, poly(ethylene oxide) calibration
\overline{M}_n SEC, PS	\overline{M}_n measured by SEC, refractive index detector, polystyrene calibration
\overline{M}_n LLS	\overline{M}_n measured by SEC, laser light scattering detector
\overline{M}_n MALDI	\overline{M}_n measured by Matrix Assisted Laser Desorption/Ionization-Time Of Flight
\overline{M}_n NMR	\overline{M}_n measured by proton Nuclear Magnetic Resonance spectroscopy
M_p	Molecular weight at the maximum of the SEC peak
\overline{M}_w	Weight-average molecular weight
<i>n</i> BA	<i>n</i> -Butyl Acrylate
NaI	Sodium Iodide
NaTFA	Sodium Trifluoroacetate
NB	Norbornene
NMR	Nuclear Magnetic Resonance spectroscopy
PAA	Poly(acrylic acid)
PBu	Polybutadiene
PCL	Poly(ϵ -caprolactone)
PDI	Polydispersity index
PDMAEMA	Poly(2-(<i>N,N</i> -dimethylamino)ethyl methacrylate)
PEO	Poly(ethylene oxide)

PLA	Poly lactide
PMDETA	<i>N,N,N',N',N''</i> -pentamethyldiethylenetriamine
PMMA	Poly(methyl methacrylate)
PNB	Polynorbornene
PNIPAM	Poly(<i>N</i> -isopropylacrylamide)
PEO	Poly(oxyde d'éthylène)
PS	Polystyrene
<i>Pt</i> BA	Poly(<i>tert</i> -Butyl Acrylate)
RAFT	Reversible Addition–Fragmentation chain Transfer
RDRP	Reversible-Deactivation Radical Polymerization
RI	Refractive Index
ROMP	Ring-Opening Metathesis Polymerization
ROP	Ring-Opening Polymerization
rt	Room temperature
SANS	Small Angle Neutron Scattering
SAXS	Small Angle X-ray Scattering
SDS	Sodium dodecyl sulfate
SEC	Size Exclusion Chromatography
SLS	Static Light Scattering
Sn(Otc) ₂	Stannous octanoate
Sty	Styrene
<i>t</i> BA	<i>tert</i> -Butyl Acrylate
TD-SEC	Three Detection-Size Exclusion Chromatography
TEM	Transition Electron Microscopy
TGA	Thermo Gravimetric Analysis
THF	Tetrahydrofuran
TMSI	Trimethylsilyl iodide
UV-Vis	Ultraviolet-Visible spectrophotometry
XPS	X-ray Photoelectron Spectroscopy

Table of contains

Glossary

Introduction générale..... 1

Chapter I: Bibliography study of macromonomers synthesis and their ROMP in solution

Introduction	4
I- Synthesis by living anionic/cationic polymerization	5
<i>I-1. Synthesis by living anionic polymerization</i> 5	
<i>I-2. Synthesis from commercial PEO synthesized by anionic polymerization</i>	20
<i>I-3. Synthesis by living cationic polymerization</i>	30
II- Synthesis by ring-opening (metathesis) polymerization	31
<i>II-1. Synthesis by ring-opening polymerization of biodegradable macromonomers</i>	31
<i>II-2. Synthesis by ring-opening metathesis polymerization</i>	38
III- Synthesis by reversible-deactivation radical polymerization	41
<i>III-1. Synthesis by ATRP</i>	42
<i>III-2. Synthesis by RAFT polymerization</i>	47
Conclusion	55
References	56

Chapter II: Synthesis of PEO macromonomers by “click” reaction

Introduction	60
I- Synthesis of ω-oxanorbornenyl PEO macromonomers	61
<i>I-1. Alkyne-functionalized oxanorbornene precursor synthesis</i>	61
<i>I-2. ω-Oxanorbornenyl PEO macromonomers synthesis</i>	62
<i>I-3. Thermal stability of the macromonomers</i>	67
II- Synthesis of ω-cyclobutenyl PEO macromonomers	68
II-1. PEO macromonomers synthesis from succinimide-based cyclobutene	68
<i>II-1.1. Anhydride cyclobutene synthesis</i>	69
<i>II-1.2. Alkyne-functionalized cyclobutene precursor synthesis</i>	69
<i>II-1.3. Macromonomer synthesis by “click” reaction</i>	72
II-2. PEO macromonomers synthesis from bis(hydroxymethyl)cyclobutene	74
<i>II-2.1. Bis(hydroxymethyl)cyclobutene synthesis</i>	74
<i>II-2.2. PEO macromonomer synthesis from azido-functionalized cyclobutene precursor</i>	74
II-2.2.a. Synthesis of bis(azidomethyl)cyclobutene precursor	75
II-2.2.b. BisPEO macromonomer synthesis by “click” reaction	76
<i>II-2.3. PEO macromonomers synthesis from alkyne-functionalized cyclobutene precursors</i>	78
II-2.3.a. Synthesis of alkyne-functionalized cyclobutene precursors	78
II-2.3.b. Two PEO chains macromonomer synthesis by “click” reaction	82
II-2.3.c. One PEO chain macromonomers synthesis by “click” reaction	83
Conclusion	88
References	90

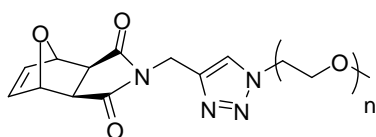
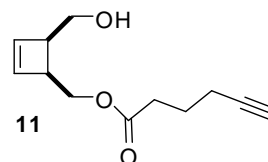
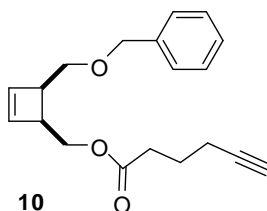
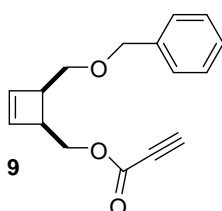
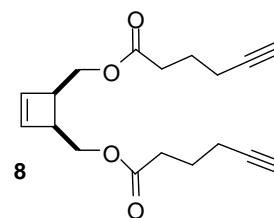
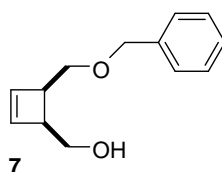
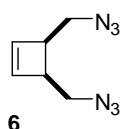
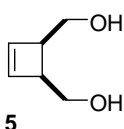
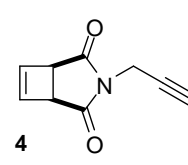
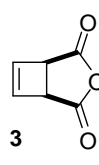
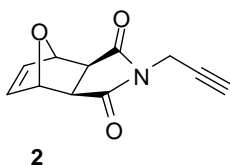
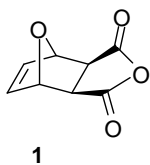
Chapter III: Synthesis of α -cyclobutenyl macromonomers by RAFT polymerization

Introduction	93
I- Synthesis of cyclobutene-based chain transfer agent synthesis	94
II- RAFT polymerization using cyclobutene-based chain transfer agent	96
<i>II-1. RAFT polymerization of ethyl acrylate</i>	96
<i>II-2. RAFT polymerization of N-isopropyl acrylamide</i>	102
III- Synthesis of cyclobutene-based block copolymers by RAFT polymerization	107
<i>III-1. Synthesis of cyclobutene-based PEO macromolecular chain transfer agent</i>	108
III-1.1. Synthesis of a dual cyclobutenyl-functionalized “click”-RAFT agent	108
III-1.2. Synthesis of a macromolecular chain transfer agent by “click” reaction....	109
<i>III-2. RAFT polymerization of N-isopropyl acrylamide using cyclobutene-based PEO macromolecular chain transfer agent</i>	111
Conclusion	114
References	115

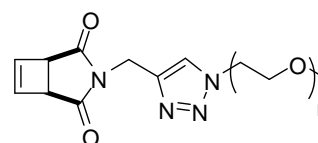
Chapter IV: Ring-Opening Metathesis Polymerization of oxanorbornenyl- and cyclobutenyl-functionalized macromonomers

Introduction	117
I- ROMP in solution	119
I-1. ROMP of oxanorbornenyl-functionalized macromonomers	119
<i>I-2. ROMP of cyclobutenyl-functionalized macromonomers</i>	124
<i>I-2.1. ROMP of succinimide-based cyclobutenyl PEO macromonomers</i>	125
<i>I-2.2. ROMP of unsymmetrical PEO macromonomers</i>	128
<i>I-2.3. ROMP of RAFT-derived macromonomers</i>	133
II- ROMP in dispersed media	135
<i>II-1. CMC determination of macromonomers</i>	135
<i>II-1.1. SLS measurements</i>	135
<i>II-1.2. Fluorescence spectroscopy</i>	136
<i>II-2. ROMP in dispersed media of oxanorbornenyl- and cyclobutenyl-functionalized macromonomers</i>	138
<i>II-2.1. ROMP in dispersed aqueous media of oxanorbornenyl macromonomer</i>	138
<i>II-2.2. ROMP in mini-emulsion of cyclobutenyl macromonomer</i>	141
Conclusion	144
References	145
Conclusion générale	152
Experimental section	153

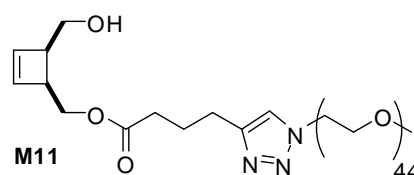
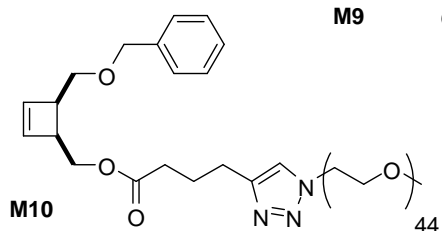
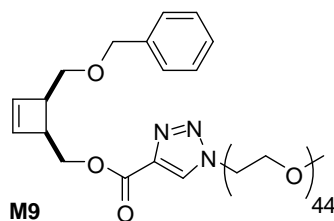
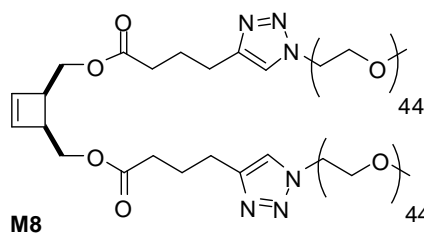
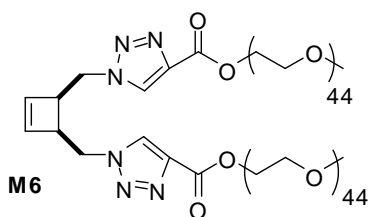
Structures of oxanorbornene, cyclobutene precursors and ω -oxanorbornenyl, ω -cyclobutenyl PEO macromonomers



M2-500, $n = 11$
M2-2000, $n = 44$
M2-5000, $n = 105$



M4-2000, $n = 44$
M4-5000, $n = 105$



Introduction générale

Les copolymères greffés constituent une classe de matériaux polymères particulièrement intéressants car leurs propriétés peuvent être modulées en fonction de la nature du squelette, de la composition, de la nature et de la densité des greffons.¹ Ils peuvent présenter des applications variées en tant que tensioactifs, vecteurs de principes actifs, compatibilisants, nanomatériaux.²

Les propriétés des copolymères greffés et la possibilité de moduler celles-ci *via* leur structure nous ont amenés à nous intéresser à cette classe particulière de polymères. Plus précisément, notre travail s'inscrit dans le cadre de la synthèse de copolymères greffés à squelette 1,4-polybutadiène et polyoxanorbornène possédant une haute densité de greffons de nature diverse, éventuellement amphiphiles.

La polymérisation par ouverture de cycle par métathèse (ROMP) a été choisie pour la synthèse du tronc, car celle-ci, grâce au développement de nouveaux amorceurs bien définis à base de ruthénium,³ est réalisable dans des conditions contrôlées. Elle présente d'autre part l'avantage de conduire, dans le cas des monomères dérivés du cyclobutène, à un polybutadiène strictement -1,4 qui n'est pas aisément accessible par d'autres techniques de polymérisation. L'approche « *grafting through* », aussi dénommée « technique macromonomère », a été choisie car elle permet de synthétiser des copolymères possédant une densité de greffons importante puisque chaque unité constitutive porte deux chaînes polymères.

Contrairement aux dérivés du norbornène pour lesquels un nombre relativement important de travaux ont été rapportés dans la littérature, les dérivés du cyclobutène n'ont été que peu étudiés en raison principalement de la difficulté de synthèse des monomères correspondants. La mise au point au sein du laboratoire d'une méthode efficace et sûre de préparation de l'anhydride cyclobutéinique par l'équipe de F. Huet⁴ a permis la préparation de nouveaux dérivés utilisables en tant que monomères pour la ROMP.⁵ Les précédents travaux conduits au laboratoire ont montré que des macromonomères cyclobutéiniques peuvent être préparés par polymérisation radicalaire

¹ Hadjichristidis, N.; Pispas, S.; Pitsikalis, M.; Iatrou, H.; Lohse, D. J. *Graft copolymers, Encyclopedia of Polymer Science and Technology*, 3rd Ed., John Wiley & Sons, Inc., Hoboken, New-York, **2004**.

² (a) Sakuma, S.; Hayashi, M.; Akashi, M. *Adv. Drug. Deliv. Rev.* **2001**, *47*, 21-37. (b) Xu, P.; Tang, H.; Li, S.; Rew, J.; Van Kirtle, E.; Murdoch, W. J.; Radosj, M.; Shen, Y. *Biomacromolecules* **2004**, *5*, 1736-1744.

³ Grubbs R. H. (Ed.), *Handbook of Metathesis*, vol. 3, Wiley-VHC, Weinheim, **2003**.

⁴ Gauvry, N.; Comoy, C.; Lescop, C.; Huet, F. *Synthesis* **1999**, 574-576.

⁵ Lapinte, V.; de Frémont, P.; Montembault, V.; Fontaine, L. *Macromol. Chem. Phys.* **2004**, *205*, 1238-1245.

contrôlée par transfert d'atome (ATRP) – tout en préservant la double liaison du cyclobutène – en utilisant des amorceurs cyclobuténiques renfermant un ou deux groupements bromoisobutyryle amorceurs d'ATRP. Leur polymérisation par ROMP a conduit à des troncs de type 1,4-polybutadiène greffés par divers homo- ou copolymères.⁶ Cette méthode souffre toutefois des limites inhérentes à la fois à la technique macromonomère et à l'ATRP. En effet, la polymérisation de macromonomères ne permet pas d'accéder à des masses molaires élevées⁷ et l'ATRP n'est utilisable qu'avec un nombre relativement limité de monomères.

Le premier objectif de ce travail a été de diversifier la nature des greffons en utilisant soit la polymérisation RAFT (*Reversible Addition-Fragmentation chain Transfer*), soit la chimie « click ». Deux stratégies de synthèse de macromonomères amphiphiles ont donc été considérées au cours de ce travail (Figure 1) :

- La première consiste en la synthèse de macromonomères de poly(oxyde d'éthylène) (POE) à extrémité oxanorbornène ou cyclobutène à partir de POE commerciaux par réaction de chimie « click » qui est susceptible de conduire à des conversions quantitatives.⁸
- La deuxième repose sur la polymérisation RAFT à l'aide de dérivés du cyclobutène renfermant un groupement apte à jouer le rôle d'agent de transfert de chaîne. Cette stratégie permet de synthétiser des macromonomères à partir d'une large gamme de monomères en raison de la tolérance de la technique RAFT vis-à-vis de nombreux groupements fonctionnels.⁹

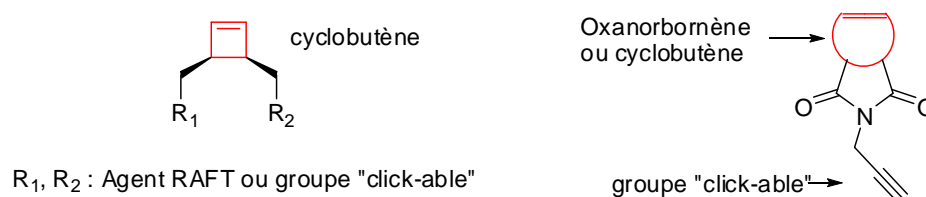


Figure 1. Structure des précurseurs de macromonomères polymérisables en ROMP.

⁶ Morandi, G.; Montebault, V.; Pascual, S.; Legoupy, S.; Fontaine, L. *Macromolecules* **2006**, *39*, 2732.

⁷ (a) Hadjichristidis, N.; Iatrou, H.; Pitsikalis, M.; Mays, J. *Progr. Polym. Sci.* **2006**, *31*, 1068. (b)

Hadjichristidis, N.; Pitsikalis, M.; Iatrou, H.; Pispas, S. *Macromol. Rapid. Commun.* **2003**, *24*, 979.

⁸ (a) Kolb, H.; Finn, M. G.; Sharpless, K. B. *Angew. Chem. Int. Ed.* **2001**, *40*, 2004. (b) Binder, W. H.; Sachsenhofer R. *Macromol. Rapid Commun.* **2007**, *28*, 15. (c) Fournier, D.; Hoogenboom, R. Schubert U. S. *Chem. Soc. Rev.* **2007**, *107*, 3654. (d) Lutz, J.F. *Angew. Chem. Int. Ed.* **2007**, *46*, 1018.

⁹ Chiefari, J.; Chong, Y. K.; Ercole, F.; Krstina, J.; Jeffery, J.; Le, T. P. T.; Mayadunne, R. T. A.; Meijs, G. F.; Moad, C.L.; Moad, G.; Rizzardo, E.; Thang, S. H. *Macromolecules* **1998**, *31*, 5559.

Le second objectif de ce travail a consisté à rechercher les moyens d'améliorer la polymérisation des macromonomères en solution par l'utilisation de systèmes amorceurs de Grubbs de dernière génération et en abordant la ROMP en milieu aqueux dispersé de macromonomères amphiphiles.

Le premier chapitre de ce mémoire est consacré à une étude bibliographique portant sur les voies d'accès aux macromonomères et leur polymérisation par ROMP pour accéder à des copolymères greffés.

La synthèse des macromonomères dérivés du cyclobutène et de l'oxanorbornène par chimie « click » fait l'objet d'un deuxième chapitre. Nous avons détaillé la synthèse des précurseurs cyclobutène et oxanorbornène qui contiennent un ou deux groupements « click-ables » et leur réaction en chimie « click » avec un poly(oxyde d'éthylène) (POE) fonctionnalisé afin d'accéder aux macromonomères correspondants.

Le chapitre trois porte sur la synthèse des macromonomères α -cyclobutényle par la polymérisation RAFT ainsi que la combinaison « click » et RAFT pour accéder à des macromonomères poly(oxyde d'éthylène)-*b*-poly(-*N*-isopropyl acrylamide) POE-*b*-PNIPAM.

Enfin, le quatrième chapitre présente la synthèse des copolymères greffés à squelette 1,4-polybutadiène et polyoxanorbornène par la ROMP en solution à partir des macromonomères. L'étude du comportement des macromonomères en solution aqueuse et des essais préliminaires ROMP en milieu aqueux dispersé sont également présentés.

Chapter I

Bibliography study of macromonomers synthesis and their ROMP in solution

Introduction

The development of well-defined based-molybdenum and based-ruthenium catalysts has allowed to use ring-opening metathesis polymerization (ROMP) as a living polymerization method to synthesize regular graft copolymers with controlled molecular and structural parameters. These graft copolymers can be synthesized according to three general strategies: the “grafting onto” method, in which side chains are preformed and then attached to the main chain polymer backbone; the “grafting from” method, in which the side chains are formed from active sites on the main chain backbone, these sites are able to initiate the polymerization leading to the synthesis of graft copolymer; the “grafting through” method or macromonomer method, in which the macromonomers, oligomeric or polymeric chains bearing a polymerizable end-group, are polymerized to give the graft copolymer.¹

The most commonly used method is the “grafting through” or macromonomer method which allows the control of grafts, backbone length, and grafting density. In such method, the polymerization of macromonomers affords brush polymers with an extremely high density of branching, since each monomeric unit bears a polymeric chain as a side group. Depending on the graft length and the degree of polymerization, the graft copolymer may adopt several conformations in solution, such as bottlebrush, comb-like, star-like or flower-like. The “grafting through” method requires the previous synthesis of macromonomers, which are polymer chains containing a polymerizable end-group. Nowadays, the synthesis of macromonomers can be accomplished by almost all the available polymerization techniques. Among them, controlled/living polymerization processes allow the synthesis of complex and well-defined polymer architectures.²

ROMP is a versatile and an efficient synthetic strategy for the polymerization of unsaturated constrained rings such as norbornene, oxanorbornene, cyclobutene or cyclooctene by using metal alkylidene initiator³. The absence of chain transfer and termination reactions in such polymerization systems allows synthesis of homopolymers, block copolymers or graft copolymers with narrow molecular weight distributions, and precise control of the functionality in both the initiation and the

termination sites.^{3,4} Moreover, the large number of catalyst systems based on transition metals available can tolerate a wide range of functionalities and the polymerization may be operated under mild conditions, such as room temperature and short time.

In this chapter, we thus introduce almost all examples for precise synthesis of graft copolymers by combination of living ROMP and controlled/living polymerization techniques such as anionic polymerization, ring-opening polymerization (ROP) and reversible-deactivation radical polymerization (RDRP) according to the “grafting through” method, both in solution and in dispersed media.*

Combination of ROMP and controlled/living polymerization methods has allowed to synthesize graft copolymers, which offer unique control over the molecular weight, the molecular weight distribution, and chain-end functionalization.

I- Synthesis by living anionic/cationic polymerization

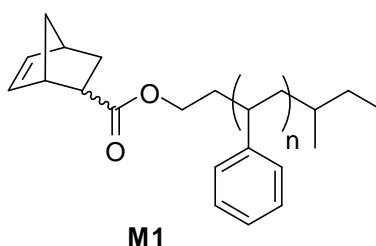
Among the living polymerization methods, anionic polymerization is the first technique which has been combined with ROMP to synthesized graft copolymers.

I-1. Synthesis by living anionic polymerization

In 1989, Norton *et al.* presented the first synthesis of polynorbornene-*g*-polystyrene by the copolymerization of ω -norbornenyl polystyrene (PS) macromonomers **M1** (Scheme I-1) and norbornene (NB).⁵ The macromonomers **M1** were prepared according to a two-step procedure. Hydroxyl-functionalized PS have been synthesized by anionic

* In this chapter, the synthesis of dendritic macromonomers was not considered. For more information, see references: (a) Percec, V.; Schlueter, D. *Macromolecules* **1997**, *30*, 5783-5790. (b) Percec, V.; Holerca, M. N. *Biomacromolecules* **2000**, *1*, 6-16. (c) Rajaram, S.; Choi, T.-L.; Rolandi, M.; Fréchet, J. M. J. *J. Am. Chem. Soc.* **2007**, *129*, 129, 9619-9621. (d) Nyström, A.; Malkoch, M.; Furó, I.; Nyström, D.; Unal, K.; Antoni, P.; Vamvounis, G.; Hawker, C.; Wooley, K.; Malmström, E.; Hult, A. *Macromolecules*, **2006**, *39*, 7241-7249.

polymerization of styrene (Sty) from *sec*-butyllithium as the initiator. The hydroxy functionality has then been used to react with 5-norbornene-2-carbonyl chloride to form ω -norbornenyl-PS macromonomer. A series of macromonomers were obtained with number-average molecular weight, measured by size exclusion chromatography with PS calibration ($\overline{M}_{n,SEC,PS}$), between 610 and 10 000 g/mol and low polydispersity index (PDI) in the range of 1.07-1.13.



Scheme I-1. ω -norbornenyl PS macromonomers^{†††} synthesized by Norton and coworkers.⁵

The graft copolymers were synthesized by copolymerization of macromonomer **M1** and NB at 80 °C using $WCl_6/Sn(CH_3)_4$ as the catalyst in chlorobenzene and a norbornene/macromonomer ratio range between 30/1 and 500/1. The crude products clearly contained a small amount of unreacted macromonomer and they were purified by precipitation in a methanol/acetone mixture. The $\overline{M}_{n,SEC,PS}$ of graft copolymers ranged between 15 000 and 105 000 g/mol but the PDIs were broad from 1.1 to 6.1.

The Sty/NB molar ratios and the percentage of grafts of the purified graft copolymers were determined by proton nuclear magnetic resonance spectroscopy (¹H NMR). Their values indicated that the graft copolymer composition was well controlled by adjusting the monomer/macromonomer feed ratio, the maximum percentage of grafts per

^{†††} ~~~~~: In this report, this symbol on “ROMP-able” macromonomers has been used to represent a mixture of *endo/exo* diastereoisomers.

↘: This symbol on “ROMP-able” macromonomers has been used to represent pure *exo* diastereoisomers.

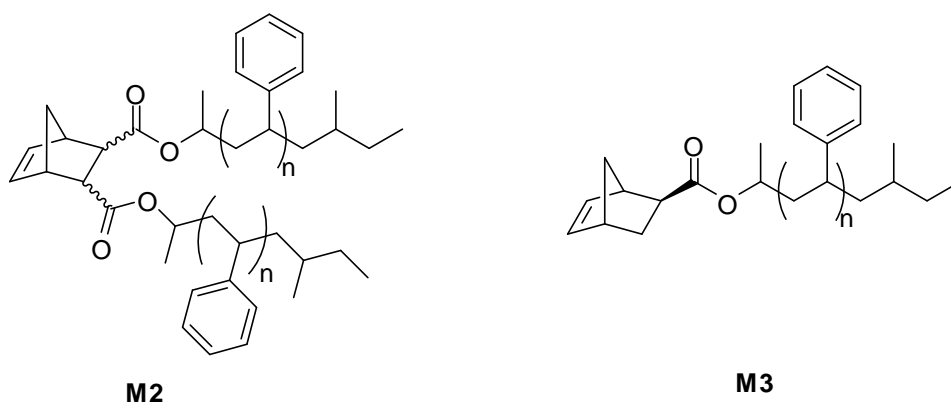
.....: This symbol has been used to represent pure *endo* diastereoisomers

↘: This symbol on “ROMP-able” macromonomers has been used when no information about the stereochemistry has been given.

↘: This symbol on cyclobutenyl “ROMP-able” macromonomers has been used to represent a *cis* stereochemistry.

main-chain of copolymer obtained was only 3%. The resulting films cast from solution were clear and transparent, indicating that phase separation occurs in domains smaller than the wavelength of visible light.

Feast *et al.* reported the first homopolymerization by ROMP of ω -norbornenyl PS macromonomers **M2** and **M3** (Scheme I-2). The macromonomers were synthesized by anionic polymerization of Sty, from *sec*-butyllithium as the initiator, which was then reacted with NB-dicarbonyl chloride to give **M2** or with NB-carbonyl chloride to give **M3**.⁶⁻⁸



Scheme I-2. ω -norbornenyl-PS macromonomers synthesized by Feast and coworkers.⁶⁻⁸

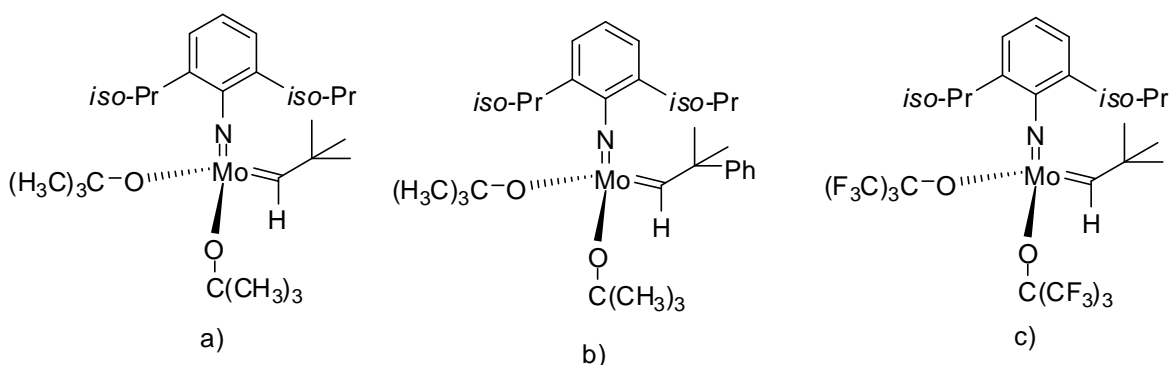
The homopolymerizations were first realized from macromonomer **M2** using the Schrock I and II catalysts (Scheme I-3) in benzene- d_6 . The macromonomer **M2**, with number-average degree of polymerization (\overline{DP}_n) of 4, 7 and 9 of Sty for each side chain, was successfully polymerized with narrow PDI (< 1.16) for a macromonomer/initiator ratio ≤ 27 . However, when attempts were made with macromonomers of \overline{DP}_n s 14, 24 and 46, in the same way, the size exclusion chromatography (SEC) traces showed two peaks. The lower molecular weight peaks all had the same retention time as the macromonomers and were accompanied by a higher molecular weight peak due to the graft copolymer. It appears that, as the length of the PS block in the macromonomer is increased, the metathesis reaction becomes sterically inhibited and eventually stops.⁶

A relationship between length of PS in macromonomer and length of polynorbornene (PNB) backbone of graft copolymer was established. ROMP of the macromonomer **M2**,

with \overline{DP}_n of 6 for Sty, was performed with a complete macromonomer conversion for a macromonomer/initiator ratio of 30.

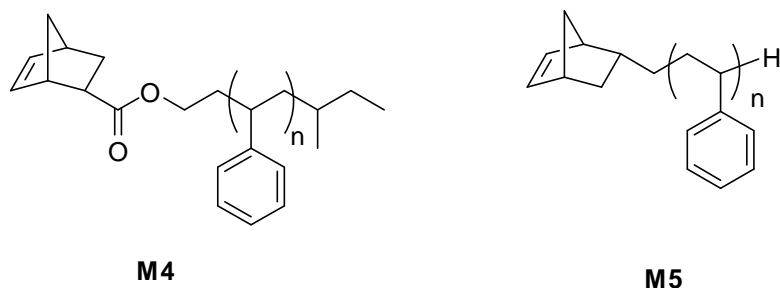
For the ROMP of macromonomer with \overline{DP}_n of 25 for Sty and macromonomer/initiator ratios of 5 and 11, the limit on the length of PNB backbone chain turns out to be less than 5 macromonomer repeating units. It was found that, as the length of PS in the macromonomer was increased, the length of the PNB backbone chain in the graft copolymer was decreased, an observation ascribed to steric hindrance.⁷

On the other hand, with only one graft per NB repeat unit (**M3**, $\overline{DP}_n = 13$), the ROMP was achieved with a complete conversion with a macromonomer/initiator ratio up to 200. The results clearly suggest that, with one PS graft on the NB unit (**M3**), in contrast to two PS grafts on the same NB unit (**M2**), graft copolymers with relatively long backbone and side chains can be prepared, probably as a consequence of lowered steric hindrance.⁸



Scheme I-3. Mo-based metathesis catalysts a) Schrock I, b) Schrock II and c) Schrock III.

Héroguez *et al.* have also reported the synthesis of ω -norbornenyl-PS macromonomer **M4** and α -norbornenyl-PS macromonomer **M5** (Scheme I-4), by the anionic polymerization of Sty.^{9,10} The ω -norbornenyl-PS macromonomer **M4** was obtained through deactivation of living PS anions by a norbornene-based deactivator, whereas the α -norbornenyl-PS macromonomer **M5** was derived from a norbornene-containing carbanionic initiator. Both macromonomers were obtained with $\overline{M}_{n,SEC,PS}$ ranging from 1 900 and 12 500 g/mol and low PDIs (1.02-1.05).



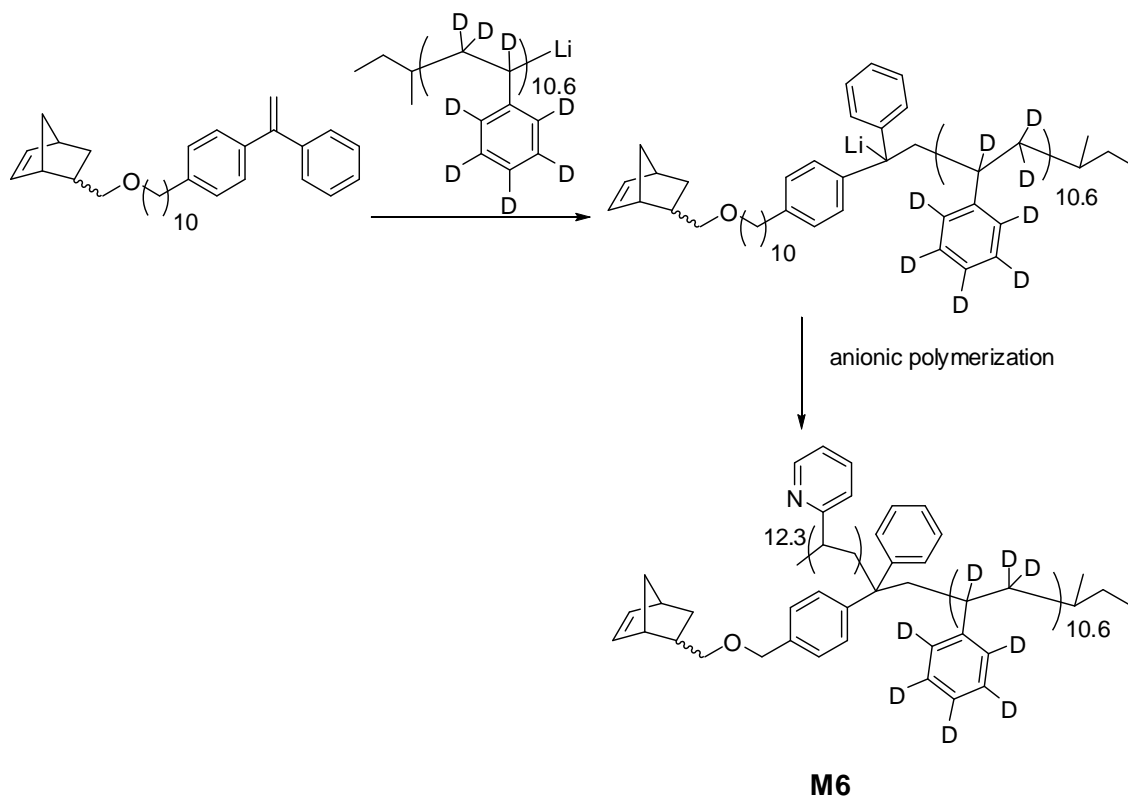
Scheme I-4. ω - and α -norbornenyl-PS macromonomers synthesized by Héroguez and coworkers.^{9,10}

The ROMP of **M4** ($\overline{M}_{n,SEC,PS} = 2\,700$ g/mol) in the presence of Schrock III catalyst in toluene at room temperature (rt) allowed a complete conversion for macromonomer/initiator ratios between 10 and 100. In the case of macromonomers exhibiting higher $\overline{M}_{n,SEC,PS}$ (4 800 and 11 000 g/mol), conversions ranging from 95 to 98 % were obtained. The graft copolymers were obtained with low PDIs (1.2-1.5) and the number-average molecular weights, measured by size exclusion chromatography with laser light scattering detector ($\overline{M}_{n,LLS}$), ranged between 4.1×10^4 and 4.9×10^5 g/mol. This was the first work on the homopolymerization of macromonomers that afforded access to samples of desired compacity without any fractionation or purification depending on two factors: the size of the macromonomer and the \overline{DP}_n 's of polymacromonomer.⁹

One family of macromonomers **M5** ($\overline{M}_{n,SEC,PS} = 2\,600$ g/mol) has also been subjected to ROMP, with macromonomer/initiator ratios of 10-100 and Schrock III catalyst as the initiator in toluene at rt. The polymerizations were completed after 30 min. The graft copolymers were obtained with low PDIs (1.2-1.5) and $\overline{M}_{n,LLS}$ between 3.7×10^4 and 3.0×10^5 g/mol.¹⁰

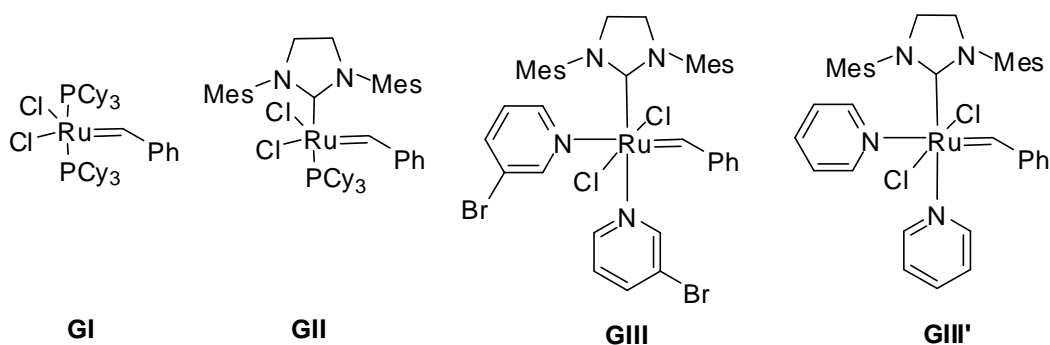
Cheng *et al.* reported a living linking method for the preparation of the polystyrene-*b*-poly(2-vinylpyridine) macromonomer **M6** (Scheme I-5) and its transformation into “double-brush” graft copolymers.¹¹ The macromonomer synthetic method is based on the terminal functionalization reaction of a living polymer with a norbornenyl-

functionalized living linking agent, followed by the polymerization of a second monomer, 2-vinylpyridine, initiated by the resulting macroinitiator.



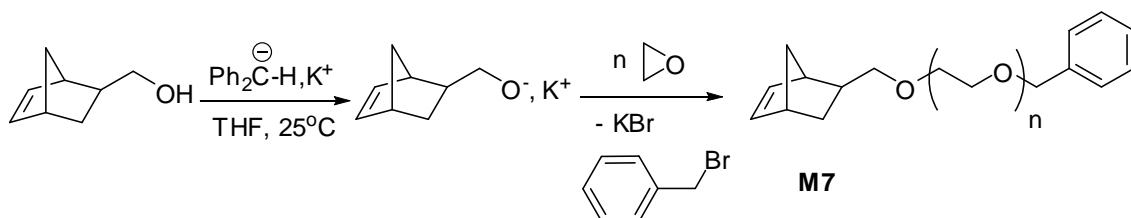
Scheme I-5. Norbornenyl-PS-*b*-poly(2-vinylpyridine) macromonomers synthesized by Cheng and coworkers.¹¹

ROMP of macromonomer **M6** with Grubbs I catalyst (Scheme I-6) in CDCl_3 at rt gave brush copolymers having unique double-brush architecture with each main-chain repeat unit carrying a diblock graft at block junction. After 4-6 h of polymerization, high macromonomer conversion (74-94%) was observed with macromonomer/initiator ratios between 10 and 25. The PDI values of copolymers were low (1.13-1.19), however, the apparent $\overline{M}_{n,SEC,PS}$ values of polymer were only 31-42% of the calculated number-average molecular weight (\overline{M}_n) values, in agreement with the unusual compactness of densely grafted structure of copolymer relative to linear structure of polystyrene standards.



Scheme I-6. Ru-based metathesis catalysts: (GI) Grubbs I, (GII) Grubbs II, (GIII) Grubbs III and (GIII') Grubbs III'.

The synthesis of macromonomers by anionic polymerization has also been extended to others monomers. Héroguez's group was the first to report the preparation of α -norbornenyl poly(ethylene oxide) (PEO) macromonomers **M7** (Scheme I-7) by anionic polymerization.¹² The α -norbornenyl-PEO macromonomers were prepared from hydroxymethylnorbornene and ethylene oxide (EO) with number-average molecular weight, measured by size exclusion chromatography with PEO calibration ($\overline{M}_{n,SEC,PEO}$), ranging from 1 500 to 4 700 g/mol and low PDIs (1.05-1.07).

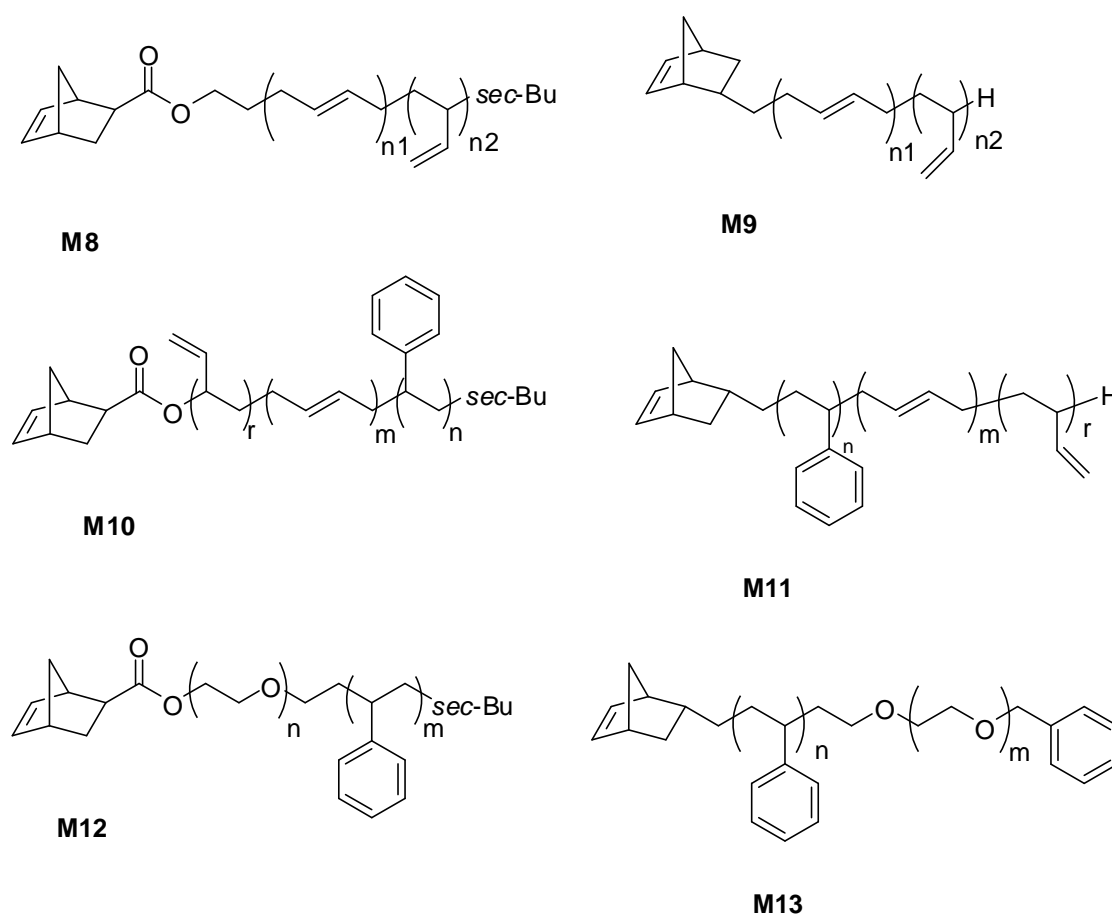


Scheme I-7. α -norbornenyl-PEO macromonomer synthesized by Héroguez and coworkers.¹²

ROMP of macromonomers ($\overline{M}_{n,SEC,PEO} = 1\ 500$ and $2\ 800$ g/mol) using Schrock III catalyst (Scheme I-3) as the initiator and toluene as the solvent at rt allows to achieve a complete conversion with $\overline{DP}_n = 5-25$ and relative low PDIs (< 1.3). In the case of macromonomers of higher \overline{M}_n (4 700 g/mol), the polymerization yield always reached a plateau value of 30%. Use of 1,2-diethoxyethane as the solvent makes an increase of the polymerization yield to 90%. This solvent, which is a stronger base than the repeating units of PEOs, helps to prevent the coordination of the metal vacant sites of the initiator by the oxygen atoms of PEO and allows the polymerization to proceed

almost to completion. With macromonomers of higher \overline{M}_n (11 000 g/mol), no polymerization occurred at all. In all cases, $\overline{M}_{n,LLS}$ of graft copolymers were much higher than the targeted values because the oxygen atoms of the PEO macromonomer were prone to interact with the metal carbene, and the proportion of initiator available for coordination with the olefinic unsaturation of the macromonomer obviously decreased.

Héroguez's group synthesized then a series of norbornenyl macromonomers including PS, PEO, polybutadiene (PBu) (**M8-M13**) (Scheme I-8) by anionic (co)polymerization.¹³⁻¹⁷



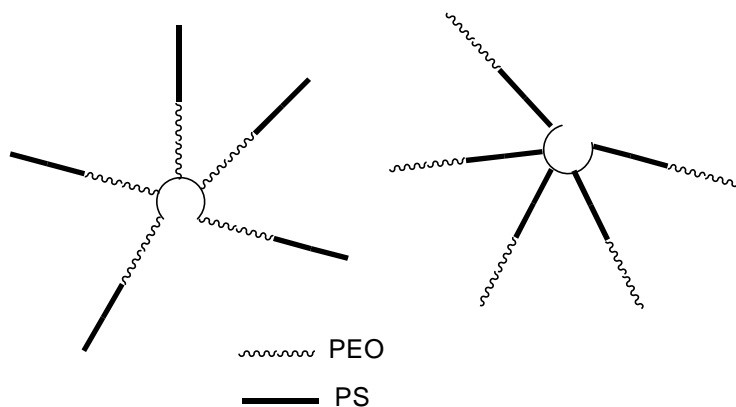
Scheme I-8. Norbornenyl-PS, -PBu and -PEO macromonomers synthesized by Héroguez and coworkers.¹³⁻¹⁷

The ω -norbornenyl-PBu macromonomer **M8** was obtained through deactivation of living polybutadienyl anions by a norbornene-based deactivator, whereas the α -

norbornenyl-PBu macromonomer **M9** was derived from a norbornene-containing carbanionic initiator (Scheme I-8).¹³ Both macromonomers were obtained with low PDIs (< 1.06) and $\overline{M}_{n,SEC,PS}$ ranging from 1.6×10^3 to 1.8×10^4 g/mol and contain *cis*-1,4-PBu units, *trans*-1,4-PBu units and 1,2-PBu units. It is well established that hydrocarbon solvents and lithium as counterion were required to obtain PBu with high 1,4-PBu units. The polymerization being carried out in toluene, the PBu samples obtained did not exhibit more than 14% of 1,2-PBu units. The ROMP was successfully realized in the presence of Schrock I catalyst in toluene which shows no interaction with the double bonds of PBu. The polymers were obtained with low PDIs (< 1.29) and $\overline{M}_{n,LLS}$ between 2.7×10^4 and 1.6×10^5 g/mol. Others catalysts (Schrock IV catalyst, $(\text{RuCl}_2\text{PPh}_3)_2(=\text{CH}-\text{CH}=\text{C}(\text{Ph})_2)$) showed a lower efficiency of polymerization.

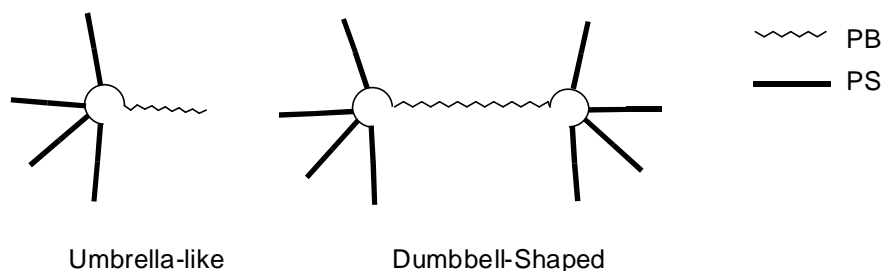
The α - and ω -norbornenyl PS-*b*-PBu macromonomers **M10** and **M11** (Scheme I-8) were prepared by sequential anionic polymerization of Sty and butadiene (Bu) following two pathways. The first route was based on the deactivation of growing PBu anions by norbornene-based deactivation (**M10**). The second route was the polymerization of Sty and Bu using norbornene-based anionic initiator (**M11**).^{14,15} Because of the higher reactivity of Bu, Sty was polymerized first in the two synthetic routes. The macromonomers **M10** and **M11** were homopolymerized with Schrock II catalyst in toluene at rt. The polymers were obtained with $\overline{M}_{n,LLS}$ between 4.1×10^4 and 1.8×10^5 g/mol and PDIs of 1.24-1.40.

The α and ω -norbornenyl PS-*b*-PEO macromonomers **M12** and **M13** (Scheme I-8) were prepared by the same methods than **M10** and **M11**.¹⁶ The homopolymerizations of PEO-*b*-PS macromonomer **M12** or PS-*b*-PEO macromonomer **M13** were realized with Schrock III catalyst in toluene to form star-shaped block copolymers (Scheme I-9). Macromonomer/initiator ratios of 10 and 20 were used for ROMP of macromonomers **M12** and **M13**, respectively. Amphiphilic spheres with hydrophilic or hydrophobic outer layers (Scheme I-9) were obtained with complete conversions of macromonomers, with PDIs of 1.10-1.40 and with $\overline{M}_{n,LLS}$ of 4.0×10^4 - 1.36×10^5 g/mol.^{16,17}



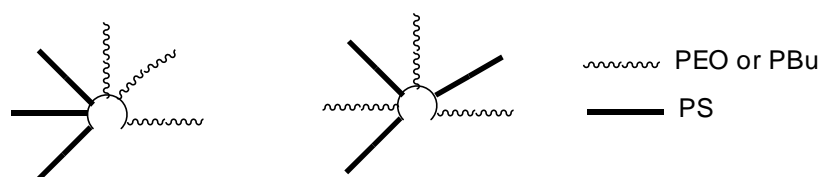
Scheme I-9. Amphiphilic spheres of PS/PEO synthesized by a combination of ROMP and anionic polymerization.^{16,17}

The copolymerization between different (macro)monomers has allowed the synthesis of various topologies. Umbrella-like, dumbbell-shaped (Scheme I-10) copolymers were prepared by sequential copolymerization of **M4** ($\overline{M}_{n,SEC,PS} = 2\,700$ g/mol) (Scheme I-4) and cyclooctadiene (COD) with Schrock II catalyst as the initiator, in toluene at rt.¹⁴ With the umbrella-like copolymers synthesis, the complete conversion of first step (polymerization of **M4**) was confirmed by SEC characterization. In a second step, COD was introduced in a single portion to the reaction mixture, but the distribution of $\overline{M}_{n,SEC,PS}$ of these final umbrella-like copolymers was large (1.9), reflecting the slow initiation rate of cycloolefin by the living alkylidene species carried by PS macromonomers. However, the PDI of umbrella-like copolymers could be narrowed down to 1.3 through the dropwise addition of COD in the second step with $\overline{M}_{n,LLS}$ of copolymers ranging from 3.5×10^4 to 1×10^5 g/mol. The dumbbell-shaped copolymers were obtained by sequential ROMP of **M5** (Scheme I-4), COD and again **M5**. The SEC results of PS polymacromonomer, umbrella-like copolymer and dumbbell-shaped one indicated that initiation of each of these sequential polymerizations occurred quantitatively. Because of the heterogeneity of composition, the authors chose to rely on NMR to evaluate the \overline{M}_n of the copolymers which ranged from 1×10^5 to 3.1×10^5 g/mol.



Scheme I-10. Umbrella-like and dumbbell-shaped copolymers of PS/PBu.¹⁴

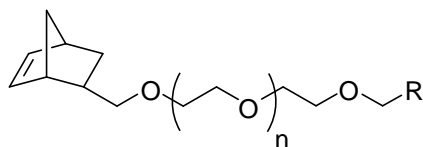
The sequential and statistical polymerizations of two different incompatible norbornene-terminated macromonomers **M4** ($\overline{M}_n = 2\,700$ g/mol) (Scheme I-4) and **M7** ($\overline{M}_n = 2\,800$ g/mol) (Scheme I-7) or **M4** ($\overline{M}_n = 1\,600$ g/mol) and **M8** ($\overline{M}_n = 2\,200$ g/mol) (Scheme I-8) were shown to give rise to Janus-type and miktoarm architectures (Scheme I-11). The conversion of the polymerization was complete with macromonomers/initiator ratios of 20-50, and the copolymers were obtained with $\overline{M}_{n,LLS}$ between 3.3×10^4 and 9.6×10^4 g/mol and relative low PDIs (< 1.45).



Scheme I-11. Janus-type and miktoarm architectures of PS/PEO or PBu.¹⁷

By the ROMP of PEO/PS/PBu macromonomers, the authors designed various architectures with unprecedented and peculiar topologies: Janus-type structures, heteroarmed spheres, amphiphilic architectures that had compact polymeric architectures that behave like unimicella systems with chemically different inner part and outer layer. It can be anticipated that some of these copolymers might find a specific application in the future.

Recently, Héroguez *et al.* investigated the synthesis of α -norbornenyl ω -functionalized PEO macromonomers **M14** and **M15** (Scheme I-12).¹⁸



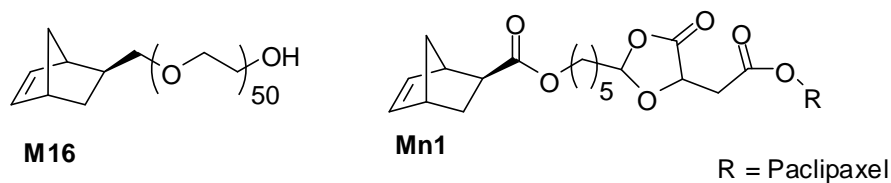
M14: R = COOH

M15: R = Gentamicin sulfate

Scheme I-12. α -norbornenyl ω -functionalized PEO macromonomers synthesized by Héroguez and coworkers.¹⁸

α -Norbornenyl PEO macromonomer was first synthesized according to the same method as already used for the synthesis of **M7** with a $\overline{M}_{n,SEC}$ of 3 640 g/mol and a low PDI (1.09). α -Norbornenyl- ω -carboxylic acid PEO macromonomer **M14** and α -norbornenyl- ω -gentamicin sulfate PEO macromonomer **M15** were then obtained by nucleophilic substitution from the hydroxyl end-group functionality of the α -norbornenyl PEO macromonomer. Carboxylic acid group was chosen because it could permit the anchoring on biomaterial surface and the local delivery of the drug on the site of infection. The triamino-functionalized gentamicin sulfate, a wide-spectrum antibiotic usually used to prevent infections in orthopedic surgery, was chosen as it could easily linked on ω -modified macromonomers through a pH-sensitive imine bond. High functionalization yields of 75 and 99% were obtained with both macromonomers **M14** and **M15**, respectively. Statistical copolymerization of **M14**, **M15** and NB was conducted in the presence of Grubbs I catalyst with a **M14/M15/NB/initiator** ratio of 4/4/160/1. The use of a dichloromethane (DCM)/ethanol mixture (35/65 v/v) for ROMP allowed to obtain high monomer and macromonomer conversions ($\geq 92\%$). The polynorbornene, insoluble in the medium, precipitates to form nanoparticles with hydrophobic core and hydrophilic PEO shell. Because of its hydrophilic properties, gentamicin sulfate is essentially located on the particle shells. Nanoparticles had z-average diameters of about 350 nm in DCM/ethanol mixture with a narrow distribution (~ 0.3). Gentamicin sulfate-functionalized nanoparticule system has proven its ability to be used as a pH-controlled drug delivery system.

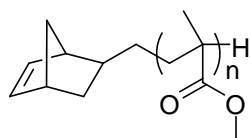
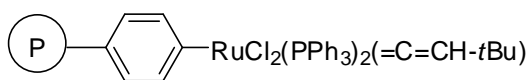
Cheng *et al.* presented the synthesis of α -*exo*-norbornenyl PEO macromonomer **M16**¹⁹ (Scheme I-13) by the same anionic polymerization method as reported by Héroguez *et al.*¹²



Scheme I-13. α -norbornenyl PEO macromonomer and monomer synthesized by Cheng and coworkers.¹⁹

Herein, the *exo*-oxanorbornene diastereoisomer was chosen as “ROMP-able” group due to its high polymerization reactivity. **M16** was obtained with a number-average molecular weight measured by proton nuclear magnetic resonance spectrometry ($\overline{M}_{n,NMR}$) of 2 400 g/mol and a PDI of 1.1. Monomer **Mn1** containing paclitaxel, a potential anti-cancer agent, was synthesized through a multi-step synthesis. The statistical copolymerizations of **M16** and **Mn1** were realized using both Grubbs I and III catalysts in DCM at rt with **M16**/initiator ratios of 25 and 100. Equimolar amounts of **M16** and **Mn1** were used to maintain significant grafting density and drug loading. When short backbones were targeted (**M16**/initiator ratio of 25), both Grubbs III and I catalysts were efficient initiators for ROMP and gave graft copolymers with low PDIs (1.04-1.11) within 15 min and 3 h, respectively. However, when high **M16**/initiator ratio of 100 was targeted, the ROMP initiated by Grubbs I catalyst became sluggish and yielded graft copolymer with a relative high PDI of 1.34 within 19 h. In contrast, ROMP initiated by Grubbs III catalyst was completed within 1.5 h and produced a graft copolymer with a low PDI of 1.09. Each graft copolymer contains high amount of paclitaxel, up to 24 wt%, as attested by ¹H NMR analysis. Under neutral conditions, *i.e.* pH = 7.0, the release of paclitaxel on graft copolymer was relatively slow but was much enhanced at pH of 5.5 as over 90% of the paclitaxel moieties were released within 6 h due to highly efficient cleavage of the acid-sensitive cycloacetal linkages.

Li *et al.* prepared an α -norbornenyl-poly(methyl methacrylate) (PMMA) macromonomer **M17** (Scheme I-14) by anionic polymerization of methyl methacrylate (MMA) using NB-CH₂Li as the initiator. Two norbornenyl-PMMA macromonomers were obtained with $\overline{M}_{n,SEC,PS}$ of 1 400 and 1 900 g/mol and PDI of 1.27.²⁰ A polymer-supported ruthenium carbene complex, generated *in situ*, for the ROMP of macromonomers was used in order to overcome the disadvantage of Grubbs catalysts of being highly moisture and oxygen sensitive as suggested by the authors.

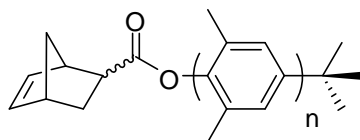
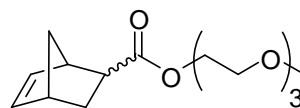
**M17**

polymer-supported ruthenium carbene complex

Scheme I-14. α -norbornenyl-PMMA macromonomer and polymer-supported ruthenium carbene complex synthesized by Li and coworkers.²⁰

ROMP of macromonomers was carried out using either $\text{RuCl}_2(\text{PPh}_3)_2(=\text{C}=\text{CH}t\text{Bu})$ and its polystyrene-supported counterpart generated *in situ* as an initiator in DCM at 25 °C. Yield of the ROMP catalyzed by the polymer supported ruthenium carbene complex (99%) was higher than that obtained by the homogeneous ruthenium carbene complex (75%) and PDIs of graft copolymers were roughly the same (2.5-2.6). One possible explanation of such high PDI of graft copolymer is the weak Π -coordination binding between the benzene ring on polystyrene chains and ruthenium atom in the ruthenium-carbene complex, which reduced the possibility of the highly labile metallocarbene species bimolecular disproportionation termination which is unnegligible without support.²¹⁻²²

In 1994, Grutke *et al.* presented the synthesis of norbornenyl poly(phenylene oxide) macromonomers **M18** (Scheme I-15) by a two-step procedure: Cu(II)-catalyzed polymerization from 4-*tert*-butyl-2,6-dimethylphenol with 4-bromo-2,6-dimethylphenol as the monomer, and esterification of the hydroxyl end-group of polymer with 5-norbornene-2-carboxylic acid chloride.²³

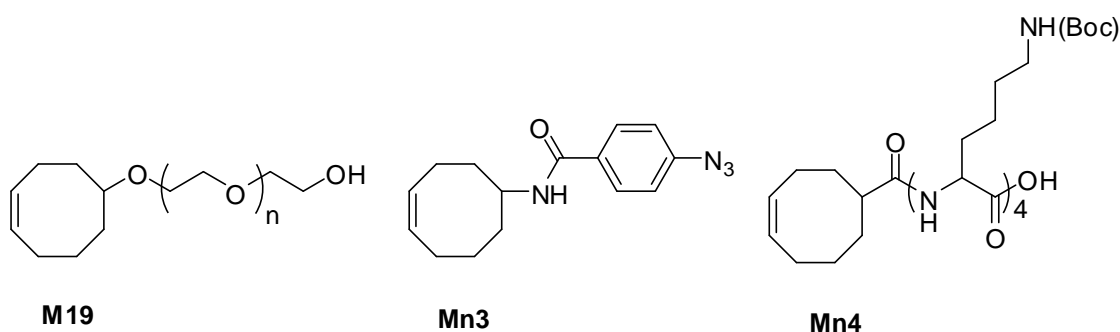
**M18****Mn2**

Scheme I-15. (Macro)monomers and monomer synthesized by Grutke and coworkers.²³

Five poly(phenylene oxide) macromonomers were obtained with $\overline{M}_{n, SEC, PS}$ in the range of 3 000 to 13 000 g/mol and PDI of 1.63-1.73. ROMP copolymerization of macromonomer **M18** and monomer **Mn2** (Scheme I-15) was realized in toluene with

RuCl₃ (hydrate) for 48 h at 110 °C with a macromonomer/initiator molar ratio of 60/1 and **M18/Mn2** molar ratios of 1/6-1/20. Graft copolymers were obtained with yields of 20-45% and $\overline{M}_{n,SEC,PS}$ of copolymers ranged between 1.3×10^5 and 2.5×10^5 g/mol. The copolymers were composed of both soft and hard segments, and these materials may find potential uses as thermoplastic elastomers or rubber-toughened plastics.

Emrick *et al.* have reported the only one example of synthesis and ROMP of a PEO macromonomer obtained by anionic polymerization with a “ROMP-able” entity different from norbornene. Two α -cyclooctenyl-PEO macromonomers **M19** (Scheme I-16) were obtained with PDI of 1.1 and $\overline{M}_{n,SEC,PS}$ s of 1 200 and 2 300 g/mol.²⁴ Amphiphilic graft copolymers were prepared by copolymerization of different ratios of cyclooctene/**M19** (91/9-80/20) with a 250/1 (macro)monomers/initiator ratio using Grubbs II catalyst and 1-hexene as the chain transfer agent in DCM at rt. The $\overline{M}_{n,SEC,PS}$ ranged from 1.5×10^4 to 4.2×10^4 g/mol and PDIs of 1.9-2.1 were obtained. The copolymers showed comonomer incorporation into the graft copolymer in agreement with the feed ratios. The macromonomer **M19** (weight-average molecular weight (\overline{M}_w) = 4 400 g/mol) was also copolymerized with cyclooctene and monomer **Mn3** (Scheme I-16) for membrane coating applications. The graft copolymer was prepared using Grubbs III catalyst from a **Mn3/M19/cyclooctene/GIII** ratio of 40/40/110/1 and had a $\overline{M}_{n,SEC,PS}$ of 3.5×10^4 g/mol and PDI of 1.7. The phenylazide-functionalized graft copolymers have been applied as an antifouling coating for poly(vinylidene fluoride) ultrafiltration membranes.



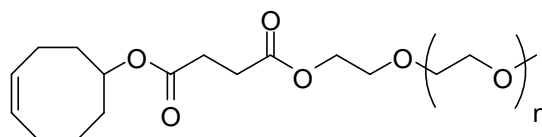
Scheme I-16. α -cyclooctenyl-PEO macromonomer and monomers synthesized by Emrick and coworkers.^{24,25}

The ROMP copolymerization of 50/50 **Mn4/M19** ($\overline{M_{n,SEC,PS}} = 1\ 200$ g/mol) molar mixture was performed, using Grubbs III catalyst in a **M19**/initiator molar ratio of 50 in 50/50 DCM/methanol (MeOH) at rt. The Boc-protected pentalysine/PEO graft copolymer was characterized by SEC in tetrahydrofuran (THF) to give $\overline{M_{n,SEC,PEO}}$ of 36 000 g/mol and PDI of 1.7. The combination of light scattering in solution at both high and low ionic strengths and SEC results showed that the copolymer chains likely formed aggregated structures composed of an average of three chains in water. The copolymers were used for deoxyribonucleic acid (DNA) complexation and delivery vectors.²⁵

I-2. Synthesis from commercial PEO synthesized by anionic polymerization

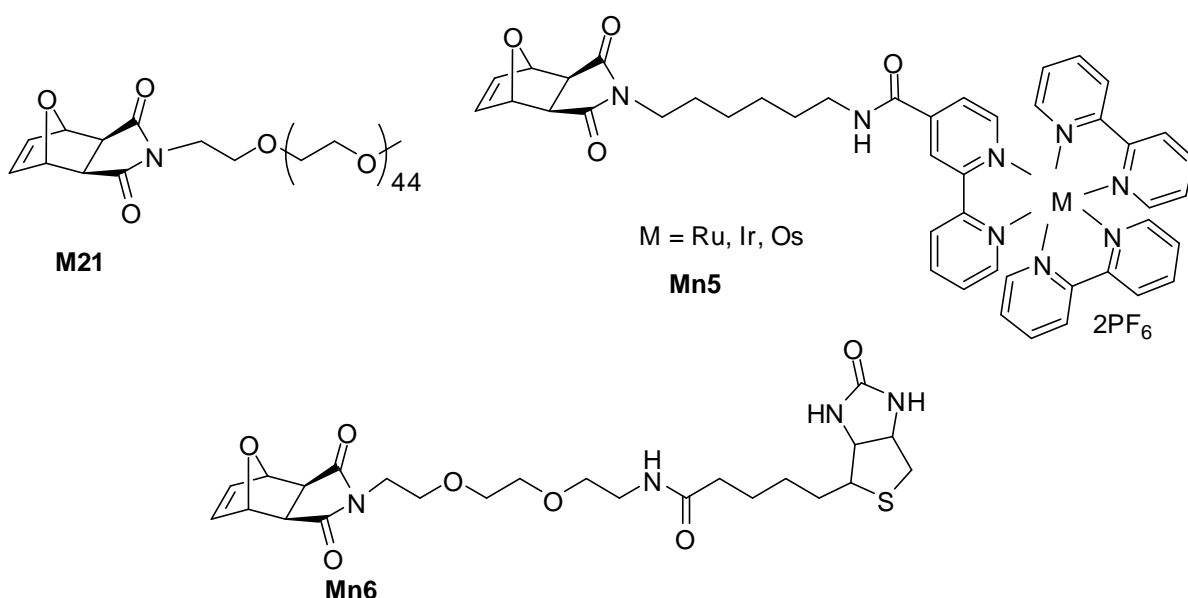
Numerous works of synthesis of graft copolymers by ROMP of macromonomers obtained from commercial PEO monomethyl ether synthesized by anionic polymerization have been reported.

Emrick's group presented the ω -cyclooctenyl macromonomer **M20** synthesis by esterification between an end-functionalized carboxylic acid cyclooct-5-enyl ester and two commercial PEO monomethyl ether of molecular weight of 750 and 1 000 g/mol (Scheme I-17).²⁶ Macromonomers were then copolymerized with cyclooctene in the presence of Grubbs I and II catalysts in DCM at rt and a (macro)monomers/initiator molar ratio ranging from 100 to 500. Initial molar ratios of macromonomer to cyclooctene range between 1/1 and 1/9.5. By using Grubbs I catalyst, the conversion is higher than 75%, and nearly complete with Grubbs II catalyst. The graft copolymers were obtained with $\overline{M_{n,SEC,PS}}$ between 1.4×10^5 and 5.4×10^5 g/mol and with PDIs of 1.21-2.20. These copolymers were expected to present possibilities for the synthesis of biofunctional macromolecules based on polyolefins, with potential applications in implant and biomedical coating.

**M20**

Scheme I-17. ω -cyclooctenyl-PEO macromonomer synthesized by Emrick and coworkers.²⁶

Sankaran *et al.* were interested in the synthesis by chemical modification of three classes of ROMP (macro)monomers: luminescent and electrochemiluminescent transition-metal-containing monomer (**Mn5**), biologically compatible macromonomer (**M21**) and bioconjugable monomer (**Mn6**) for drug delivery and tissue engineering applications (Scheme I-18).²⁷

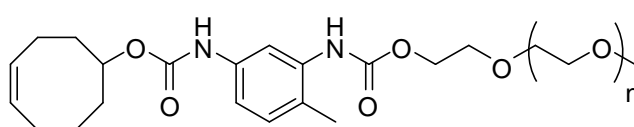


Scheme I-18. ω -oxanorbornenyl-PEO macromonomer and monomers synthesized by Sankaran and coworkers.²⁷

Macromonomer **M21** was synthesized by Mitsunobu coupling of *exo*-7-oxabicyclo[2.2.1]-hept-5-ene-2,3-dicarboximide and PEO monomethyl ether ($\overline{DP}_n = 44$). The ROMP was used to efficiently combine the macromonomer **M21** and two monomers into amphiphilic di- and triblock copolymers. The sequential copolymerization of **Mn5**, **M21** and **Mn6** was realized with Grubbs III catalyst as the initiator and **Mn5**/**M21**/**Mn6**/initiator ratios between 10/2/0/1 and 20/5/3/1 in DCM at rt. Most copolymerizations were complete in less than 20 min. Metal-containing

polymers could only be characterized by spectroscopic methods because of their interaction with the SEC stationary phase. The ^1H NMR analysis shows a quantitative incorporation of (macro)monomers into these graft copolymers. Finally, the self-assembly of copolymers in aqueous media formed star micelles with diameters between 4.2 and 43 nm and multiple luminescent metal units in their interior, biocompatible units to protect this core, and bioconjugable or bioconjugation units in their corona. These micellar aggregates were stable in the buffer aqueous conditions required for biological detection.

Shi *et al.* also presented the macromonomer synthesis from PEO monomethyl ether 1 000 g/mol and isocyanate-functionalized cyclooctene.²⁸ The infrared (FTIR) spectrum showed that the isocyanate group has completely reacted. The number-average molecular weight measured by matrix assisted laser desorption/ionization-time of flight (MALDI-TOF) mass spectrometry $\overline{M}_{n,MALDI}$ and PDI of macromonomer **M22** (Scheme I-19) are 1 085 g/mol and 1.02, respectively. The copolymerizations of PEO macromonomer **M22** and cyclooctene were performed in the presence of Grubbs II catalyst in DCM at rt with (macro)monomers/initiator molar ratio of 250 and macromonomer percentage from 5 to 20%. Four copolymers were obtained with $\overline{M}_{n,SEC,PS}$ from 1.15×10^5 to 2.69×10^5 g/mol and with PDIs of 1.64-2.54.

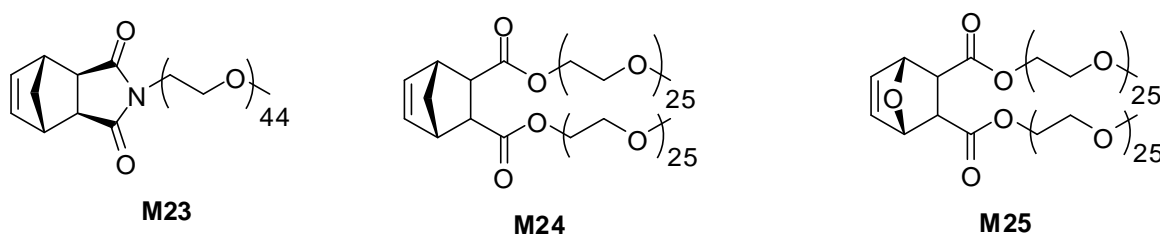


M22

Scheme I-19. ω -cyclooctenyl-PEO macromonomer synthesized by Shi and coworkers.²⁸

The surface properties of polycyclooctene-*g*-PEO films were evaluated through water contact angle and X-ray photoelectron spectroscopy (XPS). Water contact angle decreased from 87.7° to 65.8° along with increasing the content of PEO. Protein adsorption results showed that polycyclooctene-*g*-PEO copolymers had significant effect on preventing bovine serum albumin (BSA) from absorbing onto the polymer surface.

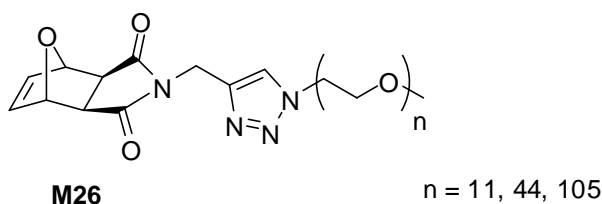
Alfred *et al.* have described the synthesis of (oxa)norbornene-functionalized PEO macromonomers (Scheme I-20) by esterification reaction of commercial PEO monomethyl ether 1 100 and 2 000 g/mol with (oxa)norbornene derivatives.²⁹ The authors presented the first homopolymerization by ROMP of PEO macromonomers. Norbornenyl-PEO macromonomers **M23** and **M24** with respectively one and two chains of PEO were obtained from PEO monomethyl ether. One oxanorbornenyl PEO macromonomer **M25** was also synthesized and contains two PEO chains of $\overline{M}_n = 1\ 100$ g/mol.



Scheme I-20. ω -norbornenyl-PEO and ω -oxanorbornenyl-PEO macromonomers synthesized by Alfred and coworkers.²⁹

The SEC and NMR characterizations of macromonomers **M24** and **M25** showed a few percent residual PEO which was only removed after polymerization of macromonomers by precipitation from diethyl ether. The authors first investigated the polymerization of macromonomer **M23** with Grubbs III catalyst in THF at rt, and were able to polymerize this macromonomer to $\overline{M}_{n,SEC,PS}$ of 1.5×10^4 g/mol with a macromonomer/initiator ratio of 18. However, the PDI obtained was broad (1.6) and the molecular distribution was multimodal. The ROMP of macromonomers **M24** and **M25** in the same conditions as previously described with macromonomer/initiator ratio of 27 and 8 for **M24** and **M25**, respectively, gave a quantitative conversion after 20 min. The PDIs were low (1.04-1.17). The facile ability of **M24** and **M25** to polymerize with PDIs below 1.17 suggests that the imide in **M23** plays a central role in its inability to yield polymers with narrow PDI, the difficulties seem to be caused by the combination of PEO with the imide functionality. The characterization of graft copolymer from **M25** by static light scattering (SLS) shows that it was aggregated in water, with a \overline{M}_w found by SLS larger by a factor of three than the value obtained by SEC in THF.

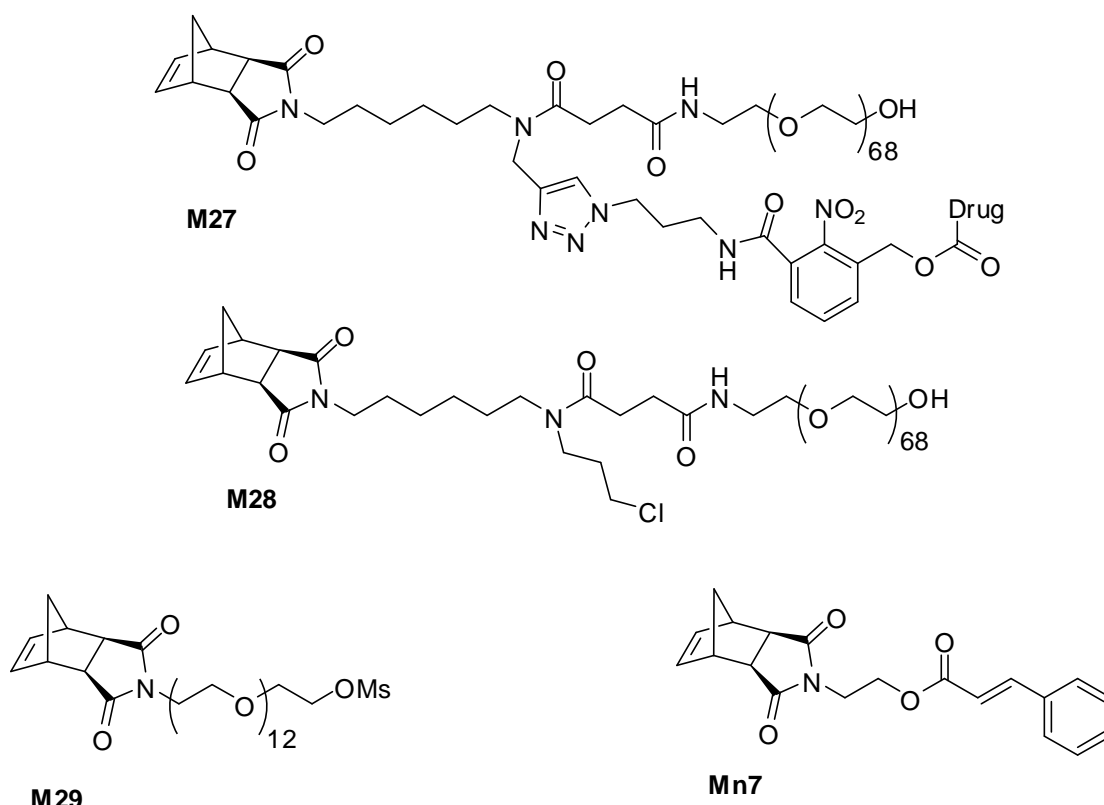
Le *et al.* presented the synthesis of PEO macromonomer **M26** by “click” reaction.³⁰ Three macromonomers (Scheme I-21) were prepared quantitatively from azide-functionalized PEO monomethyl ether of \overline{M}_n 500, 2 000 and 5 000 g/mol and alkyne-functionalized oxanorbornene by copper catalyzed azide-alkyne cycloadditions (CuAAC) “click” reaction. Pure *exo*-oxanorbornene diastereoisomers were chosen as “ROMP-able” group because of their higher reactivity in ROMP than their *endo*-counterparts.



Scheme I-21. ω -oxanorbornenyl-PEO macromonomers synthesized by Le and coworkers.³⁰

The Grubbs III catalyst was used for the ROMP of the macromonomers. The macromonomer of \overline{M}_n 500 g/mol ($n = 11$) was easily polymerized to near quantitative yield in DCM at rt in 1-4 h up to a macromonomer/initiator molar ratio of 100. The copolymers were obtained with $\overline{M}_{n,SEC,PS}$ ranging between 9 900 and 29 300 g/mol and with PDIs of 1.06-1.17. However, macromonomers of \overline{M}_n 2 000 and 5 000 g/mol were only able to form copolymers with relatively short backbone length with a macromonomer/initiator ratio of 10/1. ROMP with higher macromonomer/initiator ratios (50-100) was also realized but the conversion did not overcome 60%.

Grubbs *et al.* reported the macromonomer synthesis from PEO monomethyl ether and norbornene derivatives.³¹⁻³³ Macromonomer **M27** (Scheme I-22) was prepared from an azide-functionalized compound containing a drug and an alkyne-functionalized norbornene with quantitative conversions. Various series of macromonomers were synthesized, which contain hydrophilic chains, hydrophobic chains or doxorubicin (DOX) or camptothecin (CT) drugs.³¹⁻³²



Scheme I-22. ω -norbornenyl-PEO macromonomers synthesized by Grubbs's group.³¹⁻³³

M27 allowed to synthesize bivalent-brush polymers containing anticancer drugs with $\overline{M}_{n,LLS}$ from 3.3×10^4 to 4.99×10^5 g/mol and PDI of 1.04-1.38 by ROMP in the presence of Grubbs III' catalyst (Scheme I-6) in DCM at rt. The "grafting through" approach ensured that the weight percentage of drug loaded onto the brush copolymers was the same as the weight percentage of drug on the macromonomer and is independent of \overline{DP}_n and conversion. Thus, copolymers carry 8.5% CT and 12.6% DOX, respectively. These values could be increased by shortening the length of the PEO or designing a macromonomer linked to more than one drug molecule.³¹

For the macromonomer **M28** (Scheme I-22), the authors pursued a two-stage process to rapidly generate a series of azide-functional brush copolymers with variable \overline{DP}_n and hydrodynamic radii. Graft copolymers were prepared by ROMP of **M28** with Grubbs III' catalyst in DCM at rt, quenching of the polymerization by addition of ethyl vinyl ether, solvent exchange, and finally treatment with sodium azide for further attachment of a drug-alkyne derivative. The polymer characterization data demonstrated that ROMP of **M28** was well-controlled up to the highest \overline{DP}_n tested (400) with $\overline{M}_{n,LLS}$ up

to 1.96×10^6 g/mol and low PDIs (1.04-1.27). Chloride-azide exchange reaction occurred with equal efficiency for each \overline{DP}_n value. All polymers were highly soluble (>100 mg/mL) in water. Aqueous dynamic light scattering (DLS) measurements confirm that their nanoscopic dimensions increased with \overline{DP}_n and were tunable over a broad range (radii from 3 to 25 nm) of relevant sizes for drug delivery applications. Then, the drug (DOX) was attached to the polymers *via* CuAAC reaction and very high (>97%) conversions were reached. The authors are currently exploring applications for these materials in drug delivery.³¹

The macromonomer **M29** (Scheme I-22) was synthesized from aminohydroxyl PEO and *exo*-norbornene anhydride. PEO 600 g/mol was found to provide the desired solubility while retaining high reactivity during ROMP. Mesylate leaving groups were added to the end of the PEO chain for later displacement by radioactive fluoride. The sequential copolymerization of (macro)monomers **M29** and **Mn7** was carried out using Grubbs III' catalyst with **M29**/initiator ratios in the range 150-1200 and a **M29**/**Mn7** ratio of 3/1. All copolymerizations were complete in 30 min and the block graft copolymers were obtained with low PDI (1.01-1.78) and $\overline{M}_{n,LLS}$ up to 1.22×10^6 g/mol. Block graft copolymers were then dispersed in water to form micelles. The cross-linking reaction of cinnamoyl groups was accomplished by irradiation of the micelles with UV light in degassed water at rt. The conversion of the reaction was kept between 15 and 25% to remain the solubility of nanoparticles. Fluoride-18 was transported in nanoparticles hydrated and the fluoride-18-functionalized nanoparticles were used as an *in vivo* molecular imaging agent.³³

Miller *et al.* studied the organization of amphiphilic graft copolymers PNB-*g*-PEO at the air-water interface.³⁴ The copolymer was synthesized by anionic polymerization according to a literature procedure¹² and consists in a PNB backbone with a \overline{DP}_n of 50, and each repeating unit has a grafted PEO side chain with a \overline{DP}_n of 20. Graft copolymer has been spread at the air-water interface to form stable thin films. Neutron reflectometry has been used to determine the layer organization and the distribution of water in the near surface region occupied by the spread film. An examination of the reflectivity due to the PEO layers suggests that it is composed of two layers, one of

which has an uniform density of PEO segments with the second having a parabolic decay of segments. The exponent for the dependence of the PEO total layer thickness on the density of grafting of the water surface was 0.66, *i.e.*, stronger than predicted by theory for a brush-like layer. The near surface water layer self-partial structure factor could not be fitted with the often used uniform layer model. Attempts to model this parameter using multiple uniform layer models or a parabolic increase in water number density could not reproduce the features observed experimentally, suggesting that the near surface water layer is organized in a more complex manner than hitherto suspected when in the presence of PEO.

Cheng *et al.* studied the conformation of PNB-*g*-PEO in solvents with different polarity by small angle neutron scattering (SANS).³⁵ The copolymer was synthesized by ROMP of norbornenyl-PEO macromonomer and was composed of a PNB backbone with a \overline{DP}_n of 50, and each repeat unit has a grafted PEO side chain with a \overline{DP}_n of 6.6. The results demonstrated that the conformation of studied PNB-*g*-PEO polymer is controlled by interactions between the backbone, side chains and the solvent molecules. In deuterated toluene, the global conformation of the PNB backbone is not perturbed significantly by the presence of short PEO side chains and is described by the form factor of random-coil on length scales longer than 40 Å in 0.5 wt.% solution. In water, the chains are partially contracted already at 25 °C and the global conformation at this temperature is closed to cylindrical. At 74 °C, most of the polymers precipitate and the remaining few percent of the individual polymers in the solution collapse to form compact ellipsoids.

All macromonomers synthesized by anionic polymerization and their homopolymerization were summarized in the Table I-1. The living anionic polymerization has emerged as an important method for the synthesis of a variety of complex architectures of macromonomers with controlled molecular characteristics. The macromonomers were synthesized by two methods: functionalization of polymer chain, obtained by anionic polymerization (self-made or commercial), by a “ROMP-able” group such as NB, oxanorbornene or cyclooctene, or anionic polymerization from a “ROMP-able” group-containing carbanionic initiator. Most of the works are

concentrated on the “ROMP-able” NB group based on its high reactivity in ROMP. Oxanorbornene entity was also noticed as “ROMP-able” group because of its probability of biocompatibility of the resulting graft copolymers (Entries 14 & 15, Table I-1). A series of macromonomers were obtained with different polymer chains such as PS, PEO, PBu, PMMA or poly(phenylene oxide). The synthesized macromonomers present a \overline{M}_n range from 500 to 18 000 g/mol and have relative low PDIs (≤ 1.84) (Table I-1), containing one or two polymer chains, which is a homopolymer or a diblock polymer. ROMP technique has been performed for the synthesis of graft copolymers using essentially Schrock and Grubbs catalysts. The graft copolymers were obtained with relative low PDIs (1.04-2.50) and a wide range of \overline{M}_n ($\overline{M}_{n,LLS}$: 1.17×10^4 - 1.96×10^6 g/mol, $\overline{M}_{n,SEC,PS}$: 9.9×10^3 - 2.7×10^5 g/mol). It has been noted that the degree of polymerization of macromonomers is highly dependent on the chain length of macromonomers. It was shown that the macromonomer ceases to propagate as a consequence of steric hindrance induced by the size of the macromonomer. By using NB and Grubbs III' catalyst as high reactive “ROMP-able” group and initiator, the ROMP of macromonomers was well-controlled up to very high \overline{DP}_n tested (400), with $\overline{M}_{n,LLS}$ up to 1.96×10^6 g/mol and low PDI (1.27) (Entry 13, Table I-1). The sequential and statistical polymerization of macromonomers with (macro)monomers gave various topologies of graft copolymer such as umbrella-like, dumbbell-shaped, Janus-type or miktoarm (Entries 6-10, Table I-1) .

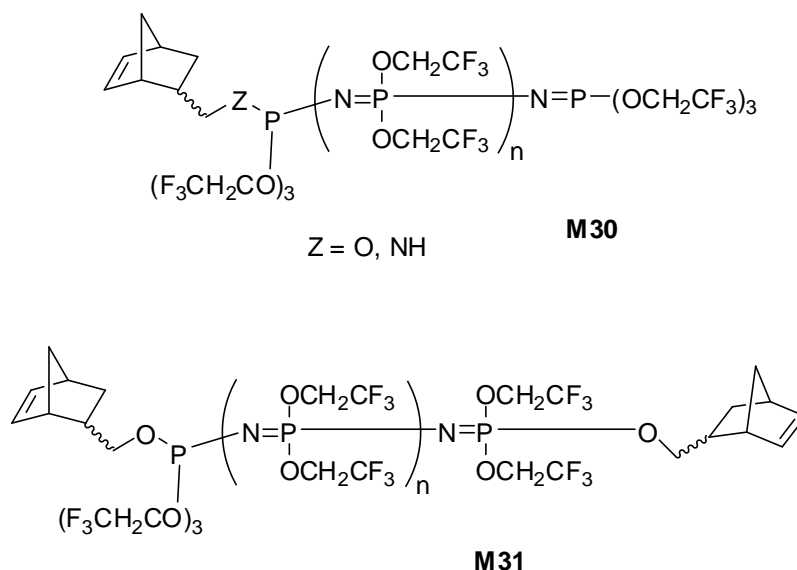
Table I-1. Macromonomers synthesized by anionic polymerization and their homopolymerization by ROMP

Entry	Macromonomer				Graft copolymer					Reference
	ROMP functionality	Nature of chain	$\overline{M}_{n,SEC} \times 10^{-3}$ (g/mol)	PDI	Initiator	[monomer] _o / [initiator] _o	$\overline{M}_{n,SEC} \times 10^{-4}$ (g/mol)	PDI	Macromonomer conversion (%)	
1	NB	bisPS	1.2 -2.1	1.06-1.12	Schrock I , II	5-30	n.d	1.07-1.16	n.d ^c	6-8
2	NB	PS	1.45-13.2	1.03-1.12		5-200	1.3-27 ^a	1.07-2.01	n.d ^c	
3	NB	PS	1.9-12.5	1.02-1.05	Schrock III	10-100	3.7-30 ^b	1.20-1.50	95-100	9-10
4	NB	PS	2.9	1.08	Grubbs I	10-25	1.17-4.06 ^b	1.13-1.19	74-94	11
5	NB	PEO	1.5-11	1.05-1.07	Schrock III	5-25	4.65-32.6 ^b	1.05-1.7	30-100	12
6	NB	PBu	1.6-18	<1.06	Schrock I	10-50	2.7-16 ^b	<1.29	~100	13
7	NB	PEO- <i>b</i> -PS	5.53-7.70	1.02-1.03	Schrock III	10-20	4.0-13.6 ^b	1.10-1.40	100	16, 17
8	NB	PS- <i>b</i> -PEO								
9	NB	PS- <i>b</i> -PBu	3.4-5.8	1.03-1.84	Schrock I	10-50	4.1-18 ^b	1.24-1.40	86-97	14, 15
10	NB	PBu- <i>b</i> -PS								
11	NB	PMMA	1.4-1.9	1.27	Supported Grubbs I	50	10.1 ^a	2.50	99	20
12	NB	monoPEO, bisPEO	2.2	~1.05	Grubbs III	10-27	1.5- 5.0 ^a	1.04-1.60	n.d ^c	29
13	NB	PEO	3.5	~1.04	Grubbs III'	15-400	3.3-196 ^b	1.04-1.38	~100	31, 32
14	Oxa-NB	bisPEO	2.2	~1.05	Grubbs III	8	1.2 ^a	1.17	~100	29
15	Oxa-NB	PEO	0.5-5.0	~1.10	Grubbs III	10-100	0.99-5.8 ^a	1.06-1.17	60-100	30

^a $\overline{M}_{n,SEC}$ determined by RI detector, PS standards, ^b $\overline{M}_{n,SEC}$ determined by multi-angle laser light scattering detector, ^cn.d: not determined.

I-3. Synthesis by living cationic polymerization

To our best knowledge, only Allcock *et al.* were interested in the synthesis of macromonomers by living cationic polymerization. They have reported the synthesis of norbornenyl polyphosphazenes macromonomers **M30** and **M31** (Scheme I-23) and their ROMP to give hybrid graft copolymers of polyphosphazene.³⁶



Scheme I-23. ω -norbornenyl-polyphosphazenes macromonomers synthesized by Allcock and coworkers.³⁶

Mono- and ditelechelic linear polyphosphazenes functionalized with a norbornene end-group were synthesized through termination of living poly(dichlorophosphazene)s with norbornenyl phosphoramine. Replacement of the chlorine atoms in each repeating unit of polymer by trifluoroethoxy groups by action of sodium trifluoroethoxide resulted in the production of mono- or ditelechelic norbornenyl-polyphosphazenes macromonomers **M30** and **M31**. The macromonomers were obtained with relative low PDIs (<1.47) and with $\overline{M}_{n,SEC,PS}$ of polymers ranging from 12 500 to 26 600 g/mol and from 10 300 to 54 700 g/mol with monotelechelic and ditelechelic macromonomers, respectively. Homo- and co-ROMP of monotelechelic macromonomer **M30** and NB using Grubbs I catalyst were carried out in THF at rt with initial molar ratios of macromonomer to norbornene between 100/0 and 1/99 and (macro)monomers/initiator ratio of 200/1. Confirmation that the ROMP reactions went to completion came from the examination of the reaction mixtures which showed no traces of the starting NBor

phosphazene macromonomer by ^1H and ^{31}P NMR spectroscopies. Graft copolymers were obtained with $\overline{M}_{n,SEC,PS}$ between 9.5×10^3 and 1.03×10^6 g/mol and PDIs from 1.29 to 2.07. The ditelechelic macromonomers **M31** were also homopolymerized by ROMP with Grubbs I catalyst, and the products were highly cross-linked, as evidenced by insolubility in organic solvents and could not be characterized.

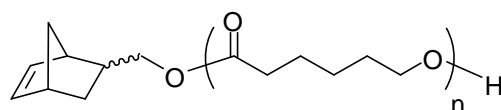
II- Synthesis by ring-opening (metathesis) polymerization

In recent years, a range of new catalytic processes have been developed that allowed the production of controlled architectures by a combination of ROMP and ROP or by ROMP exclusively.

II-1. Synthesis by ring-opening polymerization of biodegradable macromonomers

There is an increasing interest in methods that allow the preparation of polymers which degrade in a controlled fashion. In this respect, the preparation of macromolecular architectures remains an important challenge in biodegradable materials. Combination of ROMP and ROP allows to synthesize graft copolymers based on polyesters with a broad range of properties.

Mecerreyes *et al.* published the first synthesis of α -norbornenyl poly(ϵ -caprolactone) (PCL) macromonomers **M32** (Scheme I-24) by ROP of ϵ -caprolactone (CL) from 2-diethylaluminumoxymethyl-5-norbornene used as the initiator.³⁷

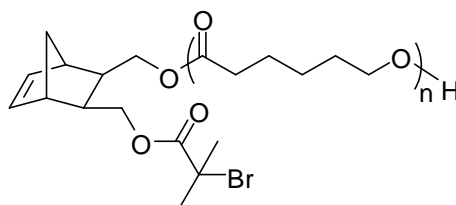


M32

Scheme I-24. α -norbornenyl-PCL macromonomer synthesized by Mecerreyes and coworkers.³⁷

The PDIs of macromonomers were low (< 1.20) for CL/NB ratio up to 90, but became broader (2.2) when the time required for the complete monomer conversion is exceeded 24h. $\overline{M}_{n,SEC,PS}$ of the macromonomers ranged from 2 100 to 9 600 g/mol. The macromonomers were then copolymerized by ROMP with NB in the presence of Grubbs II catalyst as the initiator in chlorobenzene at rt and a NB/initiator ratio of 57/1. CL molar fraction in the comonomer feed ranges from 0.3 to 0.6. The copolymerization of macromonomer and NB gave graft copolymers with high yields (60-90%), $\overline{M}_{n,SEC,PS}$ between 8.7×10^4 and 2.27×10^5 g/mol and PDIs of 1.25-2.00. The graft copolymers composition was controlled by the monomer/macromonomer feed molar ratio as evidenced by ^1H NMR by comparing relative intensities of NB backbone and of CL grafts signals. The homopolymerization of **M32** was also realized with **M32**/initiator ratios of 3-12. The graft copolymers were obtained with $\overline{M}_{n,SEC,PS}$ between 2.4×10^4 and 8.8×10^4 g/mol and low PDIs (1.10-1.15). Thermogravimetric analysis (TGA) and differential scanning calorimetry (DSC) analyses indicated that phase separation in the graft copolymers leads to microdomains which were smaller than in the corresponding homopolymer blends.

Xie *et al.* reported the synthesis of α -norbornenyl-PCL macromonomers **M33** (Scheme I-25) from a heterotrifunctional inimer and their ROMP/atom transfer radical polymerization (ATRP) for the preparation of brush copolymer containing a PNB backbone together with one hydrophobic PCL graft and one hydrophilic poly(2-(*N,N*-dimethylamino)ethyl methacrylate) (PDMAEMA) graft.³⁸



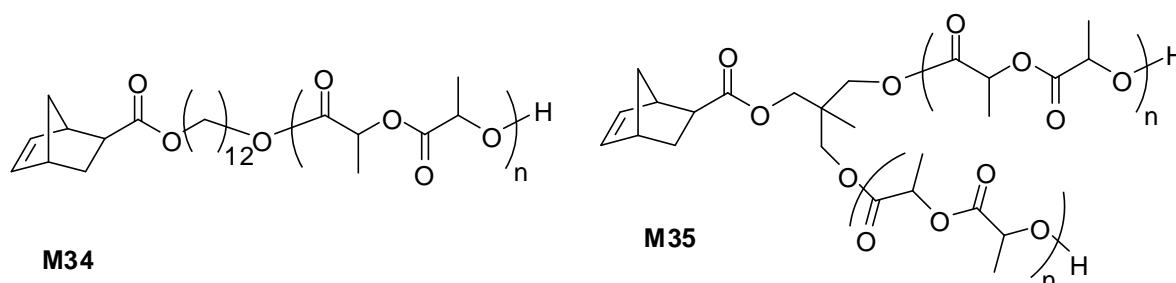
M33

Scheme I-25. α -norbornenyl-PCL macromonomer synthesized by Xie and coworkers.³⁸

Macromonomers **M33** were prepared via ROP of CL from hydroxyl-functionalized norbornene as initiator with the feed ratio of CL/inimer of 10/1 and 25/1, and stannous octanoate ($\text{Sn}(\text{Oct})_2$) as the catalyst. Two macromonomers were obtained with low PDI (1.1) with $\overline{M}_{n,SEC,PS}$ of 940 and 4 300 g/mol. Both macromonomers were contaminated

by unreacted CL and it was impossible to remove unreacted CL from the small macromonomer ($\overline{M}_{n,SEC} = 940$ g/mol). ROMP of the macromonomer ($\overline{M}_{n,SEC} = 4\ 300$ g/mol) was realized with Grubbs II catalyst in toluene at 60 °C and macromonomer/initiator ratios of 5, 20 and 50. A copolymer of $\overline{M}_{n,SEC,PS} = 2.4 \times 10^4$ g/mol and low PDI of 1.2 was obtained after 4 h with a macromonomer/initiator ratio of 5. The monomodal SEC profile attested a complete conversion. For a higher macromonomer/initiator ratio, a trimodal SEC profile was obtained resulting from unreacted macromonomer and the copolymer with a bimodal distribution. The small copolymer was then employed as macroinitiator for the ATRP of 2-(*N,N*-dimethylamino)ethyl methacrylate (DMAEMA) to achieve a brush copolymer containing one hydrophobic PCL graft and one hydrophilic PDMAEMA graft. The ^1H NMR analyses indicated that the initiation of ATRP did not occur quantitatively. PDIs of brush copolymers were relative broad (1.6-1.8).

Jha *et al.* presented the synthesis by ROP of macromonomers of polylactide (PLA) **M34** and **M35** (Scheme I-26) and their ROMP to prepare bottlebrush polymers.³⁹

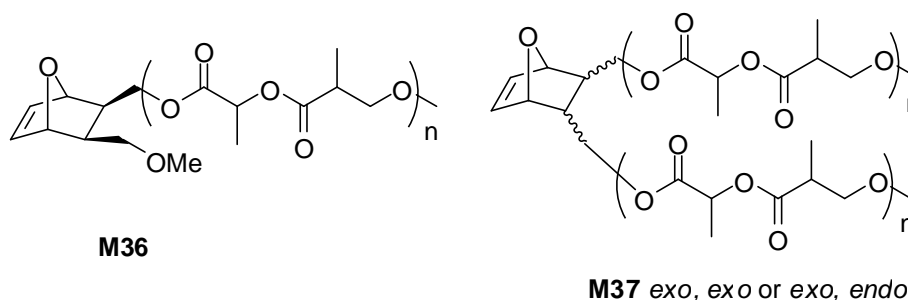


Scheme I-26. α -norbornenyl-PLA macromonomers synthesized by Jha and coworkers.³⁹

NBs with one or two alcohols were used as initiator for the ROP of L-lactide with $\text{Sn}(\text{Oct})_2$ as the catalyst. The macromonomers were obtained with low PDIs (1.06 – 1.19) and $\overline{M}_{n,SEC}$ (polylactide standards) between 4 300 and 52 000 g/mol. The polymerization of macromonomers was realized in the presence of Grubbs I and II catalysts in a macromonomer-to-initiator ratio of 51/1-1160/1 in DCM. With **M34**, Grubbs I catalyst gave a slow polymerization rate but high conversion and controlled molecular weights with $\overline{M}_{n,LLS}$ between 4.3×10^5 and 5.2×10^6 g/mol and low PDIs (<

1.19). After 23 h, a 95% conversion was obtained with macromonomer/initiator ratio up to 1160/1. By using the Grubbs II catalyst, the polymerization resulted in macromonomer conversions higher than 95% after 1.8 h of reaction, but also in higher PDI (1.30) and the $\overline{M}_{n,LLS}$ (1.3×10^7 g/mol) was significantly higher than the predicted one (5.0×10^6 g/mol). This result was consistent with the high rate of propagation relative to the rate of initiation for Grubbs' second generation catalyst. On the contrary, the ROMP of **M35** in presence of Grubbs II catalyst gave a high rate of polymerization, high conversion and the molecular weights distribution were well-controlled. The bottlebrush polymers were obtained with low PDIs (1.03-1.39) and very high molecular weights $\overline{M}_{n,LLS}$ (up to 1.2×10^7 g/mol). These results were in accordance with the hypothesis that steric crowding may influence the reactivity of the catalyst but did not prove it. More experiments are needed to determine the reasons behind the success of these macromonomers with Grubbs II catalyst.

Czelusniak *et al.* synthesized oxanorbornene-based macromonomers with either one or two PLA chains **M36** and **M37** (Scheme I-27).⁴⁰

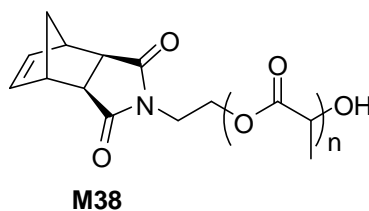


Scheme I-27. α -oxanorbornenyl-PLA macromonomers synthesized by Czelusniak and coworkers.⁴⁰

A series of macromonomers with different PLA chain lengths were prepared by ROP of DL-lactide (LA) in the presence of mono- or dihydroxyl derivatives of oxanorbornene as initiator and $\text{Sn}(\text{Oct})_2$ as the catalyst with $\overline{M}_{n,SEC,PS}$ from 1 400 to 8 300 g/mol and PDI of 1.20-1.90. All the α -oxanorbornenyl macromonomers (**M36**, **M37**) were contaminated with about 20 % PLA homopolymer which was polymerized from H_2O or 2-ethylhexanoic acid present as impurities in commercial $\text{Sn}(\text{Oct})_2$ acting as co-

initiators. Graft copolymers with PLA side chains and oxanorbornene backbones were synthesized from three PLA macromonomers, terminated with an oxanorbornene group, by ROMP in the presence of Grubbs I, II and III catalysts with macromonomer/initiator ratios of 1/5-1/50 in DCM or THF. The Grubbs III catalyst, in contrast to Grubbs I and II catalysts, presented the best results in ROMP including higher conversion. In THF, all ROMPs of one chain PLA macromonomers using **M36**/initiator ratios of 10 and 25 went to completion in 2 days. For (*endo*, *exo*)-PLA chains macromonomer **M37**, only one macromonomer with 5 LA units in each chain has been polymerized to completion with macromonomer/initiator ratio of 10. Polymerization of the (*exo*, *exo*)-PLA chains macromonomer **M37**, with 25 LA units in each chain, using macromonomer/initiator ratio of 10 and 25 went to completion in 24 and 48h, respectively. All the graft copolymers produced were contaminated with PLA homopolymer. The PDIs for the column-purified graft copolymers were in the range 1.05-1.14, indicating a well-behaved polymerization reaction. The degradation studies of graft copolymers with the same oxanorbornenyl backbone length and different lengths of PLA grafts indicated that the degradation rate increased with increasing length of PLA grafts. The degradation behavior of these materials depends also on configuration of PLA side chains on polyoxanorbornene backbone chain. The fastest degradation was observed in the case of graft copolymers with one *exo*-PLA side chain, in contrast with graft copolymers with two PLA side chains. The degradation test on the materials based on pure PLA and graft copolymer demonstrates that the rate of degradation of PLA is greatly reduced by attaching it to PNB backbone chain.

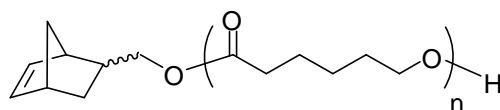
It is to be noted that Grubbs's group has synthesized the α -norbornenyl polylactide macromonomers **M38** (Scheme I-28) from ROP of LA using norbornene succinimide alcohol as the initiator and Sn(Oct)₂ as the catalyst.⁴¹



Scheme I-28. α -norbornenyl-PLA macromonomer synthesized by Grubbs's group.⁴¹

The macromonomers were obtained with $\overline{M}_{n,LLS}$ of 4 700-7 400 g/mol and PDIs of 1.06-1.12. The random and sequential copolymerization of **M38** with various macromonomers is described latter in this chapter.

Recently, Fu *et al.* have also reported the synthesis of α -norbornenyl PCL macromonomers **M39** (Scheme I-29) by ROP of CL from 5-norbornene-2-ol as the initiator and Sn(Oct)₂ as the catalyst.⁴²

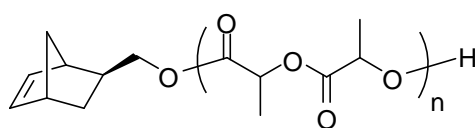


M39

Scheme I-29. α -norbornenyl-PCL macromonomer synthesized by Fu and coworkers.⁴²

Five macromonomers were obtained with relative low PDIs (1.15 – 1.24) and $\overline{M}_{n,LLS}$ between 2 000 and 9 500 g/mol. ROMP of these macromonomers were carried out using Grubbs III' catalyst in THF at rt and a macromonomer/initiator of 200 to form high molecular weight ($\overline{M}_{n,LLS} = 4.18 \times 10^5 - 2.99 \times 10^6$ g/mol) graft copolymers with low PDIs (1.24-1.34). The inclusion complexation of the prepared PNB-*g*-PCL bottlebrush copolymers and α -cyclodextrins afforded novel bottlebrush polypseudorotaxanes with a length of 350 ± 50 nm and a width of 50 ± 10 nm. The formation of bottlebrush polypseudorotaxanes was confirmed by NMR, X-ray diffractogram analysis and DLS measurements.

Wooley's group reported the synthesis of α -norbornenyl polylactide macromonomers **M40** (Scheme I-30) from ROP of D,L-lactide using norbornene-2-methanol as the initiator and 1,8-diazabicyclo[5.4.0]-undec-7-ene as the catalyst.⁴³

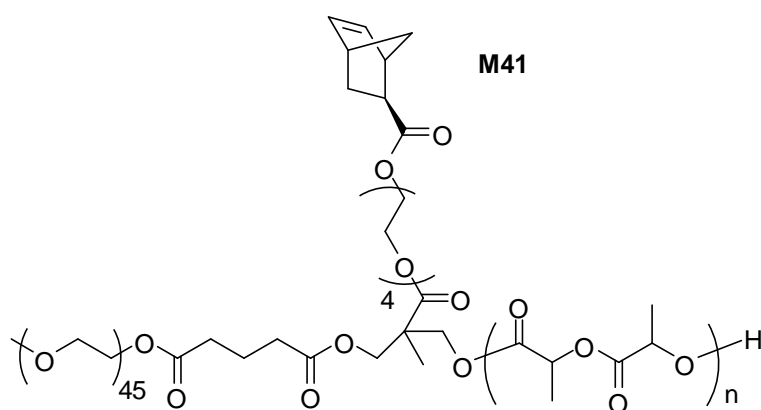


M40

Scheme I-30. α -norbornenyl-PLA macromonomer synthesized by Wooley's group.⁴³

Three α -norbornenyl-PLA macromonomers were synthesized with \overline{DP}_n of 15, 30, and 45 (**M40-15**, **M40-30** and **M40-45**) and low PDI of 1.20, 1.11, and 1.10, respectively. The authors attempted the synthesis of dumbbell-shaped triblock brush copolymer $P(\text{NB-}g\text{-PLA}_{45})_{30}\text{-}b\text{-}P(\text{NB-}g\text{-PLA}_{15})_{100}\text{-}b\text{-}P(\text{NB-PLA}_{45})_{30}$ with “balls” and “bar” composed of **M40-45** and **M40-15**, respectively, by sequential polymerization of **M40-45**, **M40-15** and then **M40-45** again, using Grubbs III’ catalyst as the initiator in toluene at rt. The triblock brush copolymer showed high macromonomers conversions (91%) and a low PDI of 1.14 with $\overline{M}_{n,SEC,PS}$ of 6.6×10^5 g/mol. Atomic force microscopy (AFM) revealed dumbbell-shaped macromolecular architectures with “balls” consisting of **M40-45** “bars” made of **M40-15** and the width and length of the middle block were measured to be 18 ± 3 nm and 55 ± 9 nm, respectively, which are close to the calculated values (0.62 and 0.45 nm per monomeric unit for PNB backbone and PLA side chain, respectively).

Recently, Cheng *et al.* presented the synthesis of amphiphilic PEO-*b*-PLA norbornenyl macromonomer **M41** by a combination of esterification and ROP (Scheme I-31).⁴⁴



Scheme I-31. ω -norbornenyl PEO-*b*-PLA macromonomer synthesized by Cheng and coworkers.⁴⁴

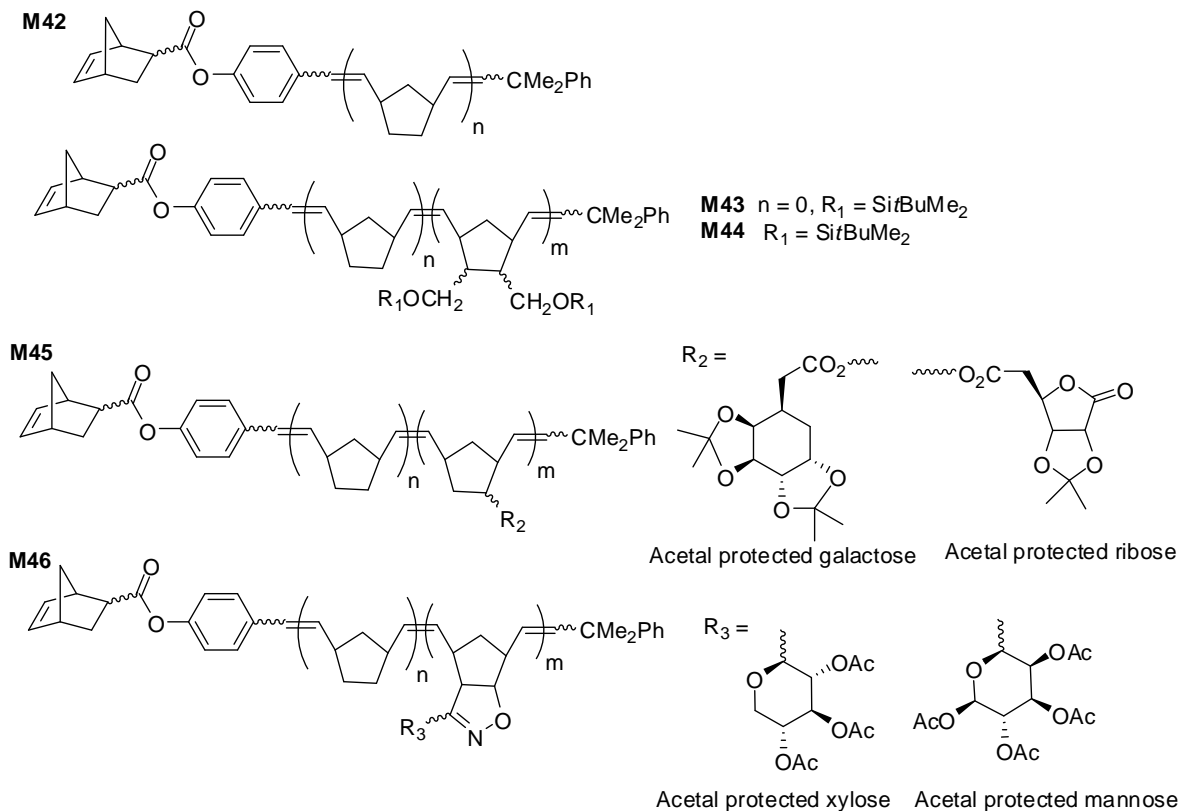
Esterification of ω -acid-functionalized PEO with an excess of *exo*-NB-based diol was first realized to form PEO-based NB-functionalized alcohol which was then used as initiator for the ROP of LA. ω -Norbornenyl PEO-*b*-PLA macromonomers **M41** were obtained with low PDIs (1.03-1.10) and $\overline{M}_{n,NMR}$ between 4 260 and 8 900 g/mol. The ROMP of macromonomers was then carried out using Grubbs III catalyst as the initiator

with macromonomer/initiator ratios ranging from 50 to 250. High conversions were obtained (49-100%). The graft copolymers obtained after passing polymerization solution through short columns of silica gel to trap unreacted macromonomers presented low PDIs (1.11-1.23) and $\overline{M}_{n,LLS}$ ranging from 3.43×10^5 to 1.09×10^6 g/mol.

II-2. Synthesis by ring-opening metathesis polymerization

Successive ROMP has also been studied in order to reach graft copolymers which could function as scaffold for the display of active ligands in orientations inaccessible with linear polymers.

Nomura *et al.* were the first to present the synthesis of polymacromonomers by successive ROMP. Different ω -norbornenyl macromonomers **M42**, **M43**, **M44**, **M45** and **M46** (Scheme I-32) were prepared by ROMP of norbornene and derivatives using Schrock I, II and III catalysts.⁴⁵⁻⁴⁸

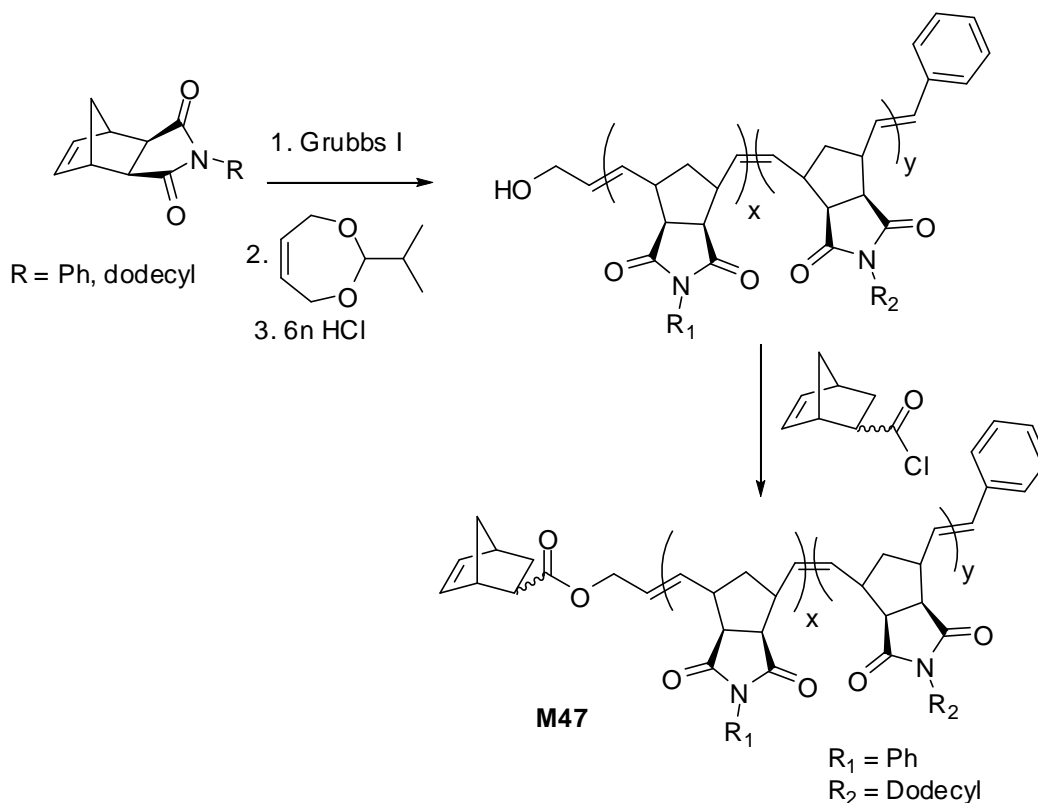


Scheme I-32. ω -norbornenyl-PNB macromonomers synthesized by Nomura and coworkers.⁴⁵⁻⁴⁸

Homopolymerization and copolymerization of **M42**, **M43** and **M44** were realized by using Schrock II and III catalysts with macromonomer/initiator ratios of 20-50 in toluene at 25 °C, to give various polymacromonomers with $\overline{M}_{n,SEC,PS}$ between 3.9×10^4 and 1.42×10^5 g/mol and low PDIs (< 1.40). Hydrolysis of polymacromonomers containing **M43** and **M44** gives access to amphiphilic copolymers ($\overline{M}_{n,MALDI} = 3.27 \times 10^4 - 1.15 \times 10^5$ g/mol).

PNB-g-PNB containing a variety of carbohydrate residues (galactose, ribose, xylose, mannose) were also prepared by ROMP of **M45** and **M46** then quenched with 4-Me₃SiO-C₆H₄CHO. The phenol-terminated PNB-g-PNB was obtained by removing *t*BuMe₂Si end-group under mildly acidic conditions. Amphiphilic (PNB-g-PNB)-*b*-PEO were synthesized by coupling reaction of phenol terminus PNB-g-PNB of **M45** and PEO-mesyate ($\overline{M}_n = 2\ 200$ and $4\ 600$ g/mol). The resulting (PNB-g-PNB)-*b*-PEO have been obtained with a 82-85% yield and an increase of the $\overline{M}_{n,SEC,PS}$ was observed from 5.85×10^4 to 6.11×10^4 and 6.4×10^4 g/mol with PEO 2 200 and 4 600 g/mol, respectively, and a resulting narrow polydispersity (PDI = 1.08-1.11).

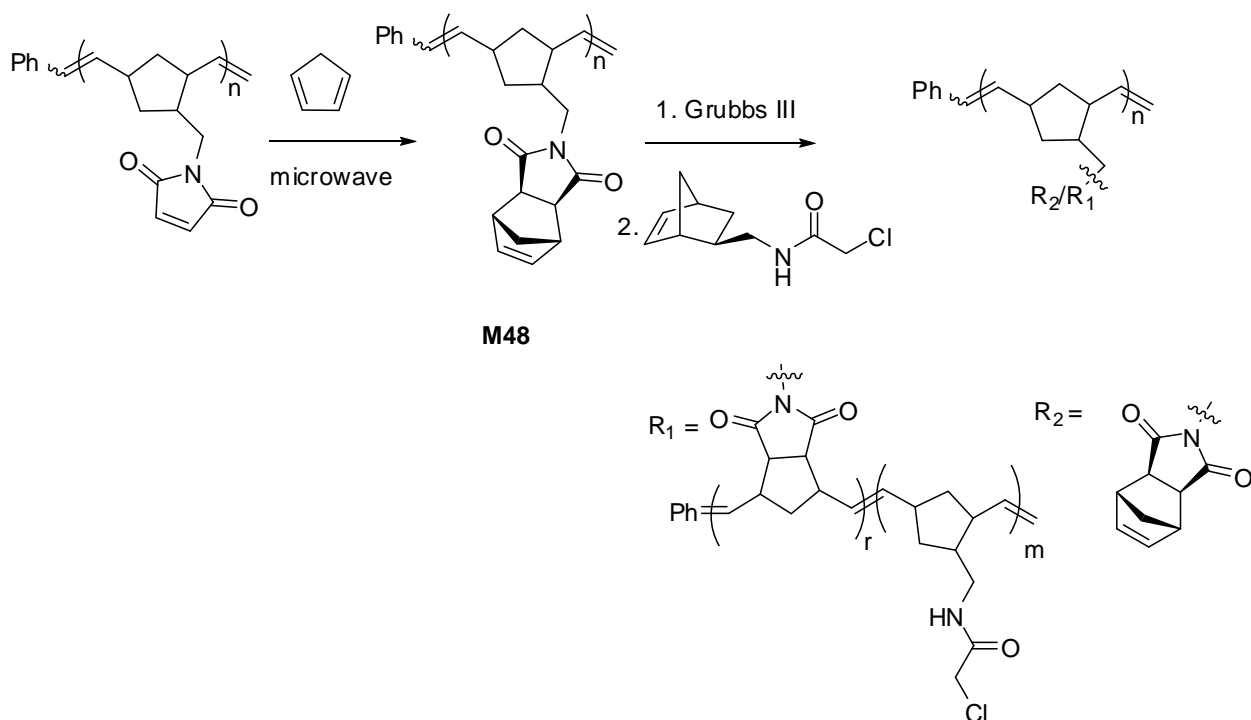
Hilf *et al.* used the same approach as Nomura to synthesize ω-norbornenyl macromonomers **M47** (Scheme I-33).⁴⁹ The authors prepared monohydroxy-terminated polymers *via* ROMP (co)polymerization of dodecylnorbornene dicarboximide and phenylnorbornene dicarboximide with Grubbs I catalyst employing 2-isopropyl dioxepine as the sacrificial monomer. Subsequent reaction with freshly prepared norbornene-5-carboxylic acid chloride gave macromonomers carrying norbornene end-groups *via* ester linkages.



Scheme I-33. ω -norbornenyl-PNB macromonomer synthesized by Hilf and coworkers.⁴⁹

PDIs ≤ 1.1 were obtained for all macromonomers, with $\overline{M}_{n,LLS}$ from 3.3×10^3 to 1.5×10^4 g/mol. All macromonomers were subsequently polymerized with the Grubbs I catalyst in DCM at rt. The \overline{DP}_n s of polymers, calculated according to the $(\overline{M}_{n,LLS}$ of copolymer)/ $(\overline{M}_{n,LLS}$ of macromonomer) ratio, varied between 3 and 8 with PDIs of 1.10-1.38 for most samples.

Allen *et al.* also used the ROMP of NB to synthesize ω -norbornenyl-PNB macromonomers **M48** (Scheme I-34).⁵⁰ A linear polymer was synthesized by ROMP with each side chain containing a maleimide group, which has been converted to norbornene moieties *via* a Diels-Alder reaction in a microwave. The $\overline{M}_{n,SEC,PS}$ of macromonomer **M48** ranged from 6 200 to 11 000 g/mol and PDIs from 1.50 to 3.43.



Scheme I-34. ω -norbornenyl-PNB macromonomer synthesized by Allen and coworkers.⁵⁰

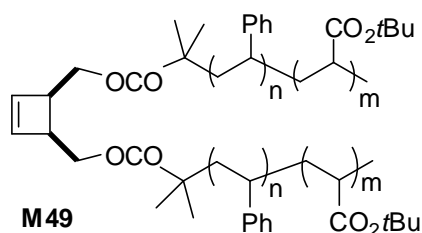
Graft copolymers were obtained by sequential copolymerization of **M48** and norbornene- α -chloroacetamide comonomer (Scheme I-34) using Grubbs III catalyst in DCM with 5-55 equivalents of initiator per 100 potentially reactive main-chain sites. The addition of initiator and comonomer in macromonomer solution was realized at -78 °C, and the mixture was stirred vigorously and then allowed to warm to rt. This comonomer was chosen because it contains an α -chloroacetamide group, which can be used to append biologically active ligands. The $\overline{M}_{n,SEC,PS}$ of graft copolymers ranged from 1.5×10^4 to 2.6×10^4 g/mol with PDIs of 1.89 - 3.18 and the graft density was between 8 and 26%.

III- Synthesis by reversible-deactivation radical polymerization

Reversible-deactivation radical polymerization process has allowed to give access to a wide range of new macromonomers from monomers such as Sty, MMA, *n*-butyl acrylate (*n*BA), *tert*-butyl acrylate (*t*BA) or methyl acrylate (MA).

III-1. Synthesis by ATRP

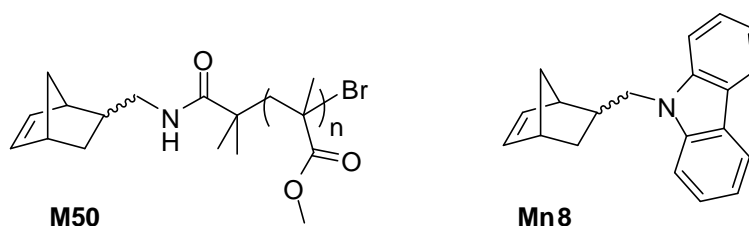
Morandi *et al.* presented the first synthesis of graft copolymers by combination of ATRP/ROMP according to the “grafting through” method.⁵¹ α -Cyclobutenyl macromonomer **M49** (Scheme I-35) was prepared by ATRP, then polymerized by ROMP to achieve graft copolymers. The difunctional ATRP initiator was synthesized by reaction of 2-bromoisobutyryl bromide with *cis*-3,4-bis(hydroxymethyl)cyclobutene. A series of macromonomers **M49** was prepared by sequential ATRP copolymerizations of Sty and *t*BA using Cu(I)Br/*N,N,N',N',N''*-pentamethyldiethylenetriamine (PMDETA) as the catalytic system, with $\overline{M}_{n,SEC,PS}$ in the range of 4 300 and 7 200 g/mol, low PDIs (1.15-1.20) and *t*BA molar ratios of 43-66%. α -Cyclobutenyl polystyrene-*b*-poly(acrylic acid) PS-*b*-PAA macromonomers were then prepared by acidolysis and were successfully employed as stabilizers in emulsion polymerization of styrene.⁵²



Scheme I-35. α -cyclobutenyl-PS-*b*-PtBA macromonomers synthesized by Morandi and coworkers.⁵¹⁻⁵²

The Grubbs I catalyst was used for ROMP of macromonomers in a macromonomer-to-initiator ratio of 10 in toluene at 50 °C but the reactivity is not enough to achieve a complete conversion. By using the Grubbs II catalyst, two graft copolymers PBu-*g*-(PS-*b*-PtBA) were obtained, with low PDIs (1.21-1.25) and $\overline{M}_{n,SEC,PS}$ of 8 200 and 10 400 g/mol, from macromonomers $\overline{M}_{n,SEC,PS}$ of 4 300 and 6 700 g/mol, respectively. The removal of *tert*-butyl groups led to amphiphilic PBu-*g*-(PS-*b*-PAA). This work constitutes the only example of synthesis of graft copolymers with a 1,4-PBu backbone according to the “grafting through” strategy.

Liaw *et al.* have synthesized the α -norbornenyl-PMMA macromonomer **M50** (Scheme I-36) by ATRP.⁵³

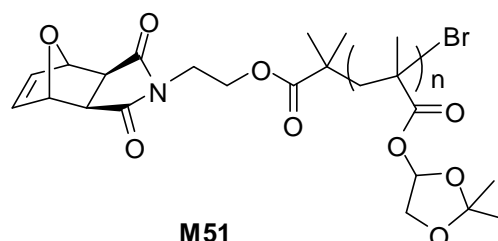


Scheme I-36. α -norbornenyl-PMMA macromonomers and monomer synthesized by Liaw and coworkers.⁵³

Four macromonomers were obtained with $\overline{M_{n,SEC,PS}}$ between 6.39×10^3 and 1.66×10^4 g/mol. The PDI values of these macromonomers were in the range between 1.3 and 1.5. The ROMP of macromonomer of $\overline{M_{n,SEC,PS}} = 6.39 \times 10^3$ g/mol was carried out with Grubbs I catalyst and a macromonomer/initiator ratio of 26 in DCM at 25 °C. The copolymer was obtained with $\overline{M_{n,SEC,PS}}$ of 6.4×10^4 g/mol and high PDI of 4.5 and was a kind of star-like high *cis* macromolecule (*cis/trans* = 72/28). The macromonomers with higher molecular weight than 6.39×10^3 g/mol could not be polymerized *via* ROMP by Grubbs I catalyst. The authors have studied the copolymerization of their macromonomers ($\overline{M_{n,SEC,PS}} > 1.0 \times 10^4$ g/mol) with carbazole-containing norbornene comonomer **Mn8** to synthesize branched copolymers. ROMP with **M50/Mn8**/initiator ratio of 350/6.7/1 gives access to a graft copolymer with $\overline{M_{n,SEC,PS}}$ of 4.76×10^4 g/mol and PDI of 1.78. Fluorescence spectrum of copolymer exhibited a strong carbazole fluorescence emission due carbazole moiety.

Morandi *et al.* presented the synthesis of α -oxanorbornenyl macromonomer **M51** (Scheme I-37) by ATRP⁵⁴ of (2,2-dimethyl-1,3-dioxolan-4-yl)methyl methacrylate using α -oxanorbornenyl initiator and using CuBr/iminopyridine as the catalyst. Well-defined macromonomers were obtained with $\overline{M_{n,SEC,PS}}$ ranging from 3 500 to 8 500 g/mol and PDI of 1.22 to 1.26. The Grubbs I catalyst was first used for the ROMP of macromonomer 6 000 g/mol in toluene at 50 °C, but the results show a bimodal distribution of the SEC trace. The Grubbs II catalyst has allowed to polymerize macromonomers of $\overline{M_{n,SEC,PS}}$ of 3 500 g/mol and 6 000 g/mol in toluene, at 60°C

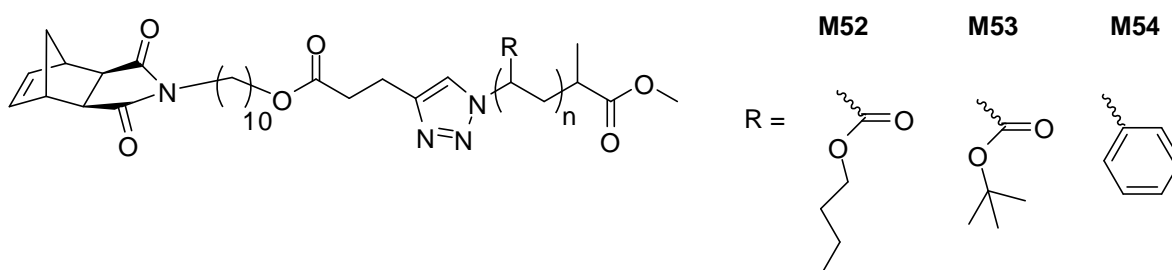
with a macromonomer/initiator ratio of 20. After 6h, complete conversions were obtained with low PDIs (1.25 and 1.56, respectively). Graft polymers were then deprotected of the ketal functionality to give polyoxanorbornene-*g*-poly(glycerol methacrylate), a class of polymers employed for the preparation of biocompatible materials.



Scheme I-37. α -oxanorbornenyl macromonomer synthesized by Morandi and coworkers.⁵⁴

Another route was also developed to synthesize ω -ROMP-functional macromonomers from ATRP by two-stage process: ATRP of monomer and then reaction with “ROMP-able” group to give macromonomer carrying “ROMP-able” end-group.

Grubbs’s group combined ATRP and CuAAC “click” reaction to synthesize ω -norbornenyl macromonomer **M52**, **M53** and **M54** (Scheme I-38).^{41,55}



Scheme I-38. ω -norbornenyl-*Pn*BA, -*Pt*BA, -PS macromonomers synthesized by Grubbs’s group.^{41,55}

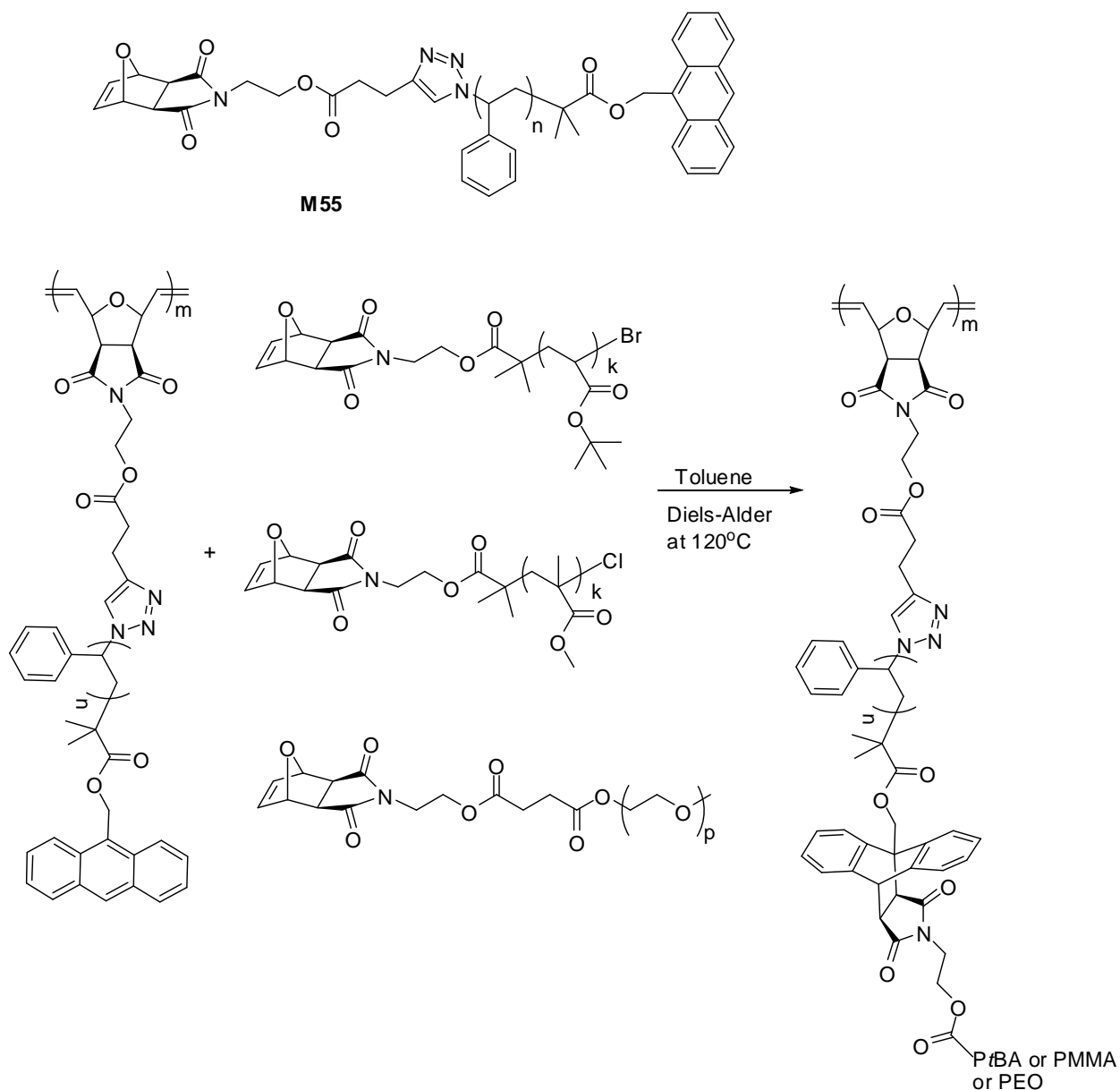
ATRPs of *n*BA, *t*BA and Sty were conducted using a CuBr/PMDETA catalytic system to produce a variety of side chain polymers with different \overline{M}_w and functionalities. Their bromide end-groups were quantitatively transformed to azides through nucleophilic substitution reaction. Next, the azido-terminated polymers were coupled in a stoichiometric amount of alkyne end-functionalized norbornene monomer to give

macromonomers with $\overline{M}_{n,LLS}$ between 2 200 and 6 600 g/mol and a PDI of 1.02. The homopolymerization of **M52**, **M53** and **M54** with Grubbs III' catalyst (Scheme I-6) in THF at rt with macromonomer-to-initiator ratios of 50-400 achieved graft copolymers of high $\overline{M}_{n,LLS}$ from 2.67×10^5 to 2.62×10^6 g/mol and low PDI ~1.03.

The sequential and random copolymerizations of macromonomers **M38** (Scheme I-28) and **M52** (Scheme I-38) gave asymmetric brush block copolymers with $\overline{M}_{n,LLS}$ between 4.5×10^5 and 1.88×10^6 and low PDIs. In general, the polymerization rates of PLA and polyacrylate macromonomers was higher than that of PS macromonomers, as measured from kinetic plots. Such as behaviour is related to the local steric congestion around the propagating metallocycle or different solvent quality for various polymers, as suggested by the authors. The brush block copolymer (macromonomers/initiator ratio = 200) with the same number of PLA and PnBA side chains self-assembled in the melt state into highly ordered, large lamellar domains over 100 nm as revealed by small angle X-ray scattering (SAXS). The domain size was dictated by the backbone length. Asymmetric brush copolymers containing different numbers of two types of side chains did not form well-ordered morphologies. This may be attributed to the reduced backbone flexibility of brush polymers and their increased difficulty to adopt coiled conformations.⁴¹

Tunca and coworkers used the same combination of “click” CuAAC reaction and ATRP for the macromonomer **M55** synthesis.⁵⁶ The azide-functionalized PS was first synthesized by ATRP polymerization from an anthracene derivative used as initiator and subsequent nucleophilic substitution of bromide end-group. The macromonomer **M55** was prepared by CuAAC “click” reaction with alkyne-functionalized oxanorbornene (Scheme I-39). One polymer was synthesized by ROMP in presence of Grubbs I catalyst at room temperature for 24h with macromonomer/initiator ratio of 10 in DCM. SEC analysis of the graft copolymer shows a $\overline{M}_{n,LLS}$ of 3.45×10^4 g/mol which is close to the theoretical one ($\overline{M}_n = 3.69 \times 10^4$ g/mol) and a low PDI (1.17). The copolymer contains anthracene groups as end-groups of the PS side chains which allows the preparation of graft block copolymers of polyoxanorbornene-*g*-(PS-*b*-PEO) or

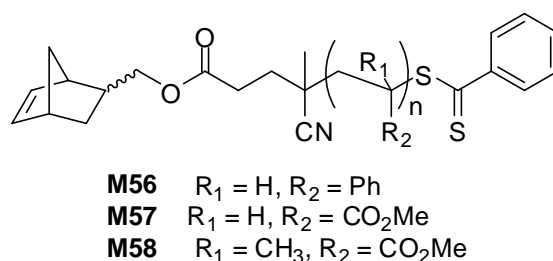
polyoxanorbornene-*g*-(PS-*b*-PMMA) or polyoxanorbornene-*g*-(PS-*b*-PtBA) by Diels-Alder “click” reaction through “grafting onto” method. Monitoring of the Diels-Alder reaction using ultraviolet-visible spectrophotometry (UV-Vis) revealed high reaction efficiencies (90-95%). The graft block copolymers were obtained with $\overline{M}_{n,LLS}$ range between 4.22×10^4 and 6.34×10^4 g/mol and PDIs of 1.10-1.3.



Scheme I-39. ω -norbornenyl-PS macromonomer, its ROMP and subsequent Diels-Alder reaction of graft copolymer synthesized by Tunca and coworkers.⁵⁶

III-2. Synthesis by RAFT polymerization

In 2006, Patton *et al.* were the first to use reversible addition-fragmentation chain transfer (RAFT) polymerization for norbornenyl macromonomer synthesis.⁵⁷ A chain transfer agent (CTA) containing norbornene (NB-CTA) was designed by coupling the 4-cyano-4-((thiobenzoyl)sulfanyl)pentanoic acid with a 5-norbornene-2-methanol. The homopolymerization of Sty, MMA and MA was carried out in the presence of 2,2'-azobis(isobutyronitrile) (AIBN) used as a radical initiator and the CTA containing NB under typical homogeneous RAFT conditions to achieve macromonomers **M56**, **M57** and **M58** (Scheme I-40).

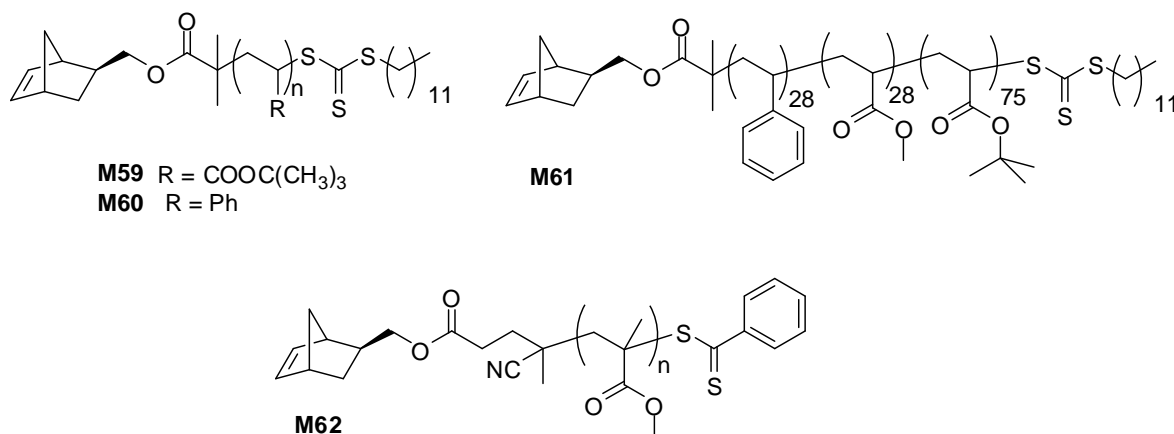


Scheme I-40. α -norbornenyl-PS, PMA, PMMA macromonomers synthesized by Patton and coworkers.⁵⁷

An initially high monomer-to-CTA ratio ($[M]_0/[CTA]_0$, 600/1 for Sty and MMA and 500/1 for MA) was used to minimize the potential polymerization of norbornenyl group. The PDIs of NB-PS, NB-PMMA and NB-PMA macromonomers were ≤ 1.2 at 27.7%, 41.5% and 21.9% monomer conversion of RAFT polymerization, respectively. An excellent agreement between the $\overline{M}_{n,SEC}$ (PS and PMMA as standards) and the theoretical \overline{M}_n in all cases was observed, indicating the norbornenyl group on CTA remained essentially intact over the course of the reaction. A PNB-*g*-PMMA copolymer was prepared from the norbornene-functionalized PMMA macromonomer ($\overline{M}_{n,SEC} = 6715$ g/mol, PDI = 1.18) with Grubbs I catalyst using standard ROMP conditions.⁵⁸ A low number-average degree of polymerization ($\overline{DP}_n = 8$) was targeted to avoid steric hindrance effects. Under these conditions, near-quantitative conversion was obtained, and a good agreement between the target \overline{M}_n (5.3×10^4 g/mol) and the experimental one

($\overline{M}_{n,SEC} = 4.8 \times 10^4$ g/mol, PMMA as standards), and a low PDI (1.15) was observed, indicating a well-controlled polymerization.

Wooley's group also presented the combination of RAFT polymerization and ROMP to synthesize a series of graft copolymers.⁵⁹⁻⁶² Norbornenyl-functionalized RAFT initiator was designed by combining an *exo*-norbornenyl functionality and a S-1-dodecyl-S'-(α, α' -dimethyl- α' -acetic acid)trithiocarbonate or a 4-cyano-4-(phenylcarbonothioylthio)-pentanoic acid. CTA containing NB was then used in the polymerization of *t*BA, Sty, MA and MMA to afford the NB-*Pt*BA, NB-PS, NB-PS-*b*-PMA-*b*-*Pt*BA and NB-PMMA macromonomers **M59**, **M60**, **M61** and **M62** (Scheme I-41).



Scheme I-41. α -norbornenyl-PMA, -PS, -*Pt*BA and -PMMA macromonomers synthesized by Wooley's group.⁵⁹⁻⁶²

To suppress the potential norbornenyl group radical polymerization, a series of experiments was conducted to optimize the polymerization conditions. Ultimately, the polymerization was performed in butan-2-ol at 51 °C in a monomer/CTA/AIBN ratio of 310/1/0.1 and quenched at 40% conversion. By this method, the RAFT polymerization was controlled, as indicated by retention of both the norbornenyl terminus and the trithiocarbonate terminus in the resulting macromonomer. Two macromonomers **M59** were obtained with $\overline{M}_{n,SEC,PS}$ of 4.67×10^3 g/mol⁵⁹ and 1.6×10^4 g/mol⁶⁰ and PDI < 1.16. One macromonomer **M60** was obtained with $\overline{M}_{n,SEC,PS}$ of 4.56×10^3 g/mol and PDI < 1.12.⁶⁰

The brush copolymer synthesis was achieved by ROMP of the terminal norbornenyl group of the NB-*Pt*BA macromonomer **M59** ($\overline{M}_{n,SEC,PS} = 1.6 \times 10^4$ g/mol), using the Grubbs III catalyst in DCM at rt with macromonomer/initiator ratio of 320/1. As observed by SEC, the *Pt*BA molecular brushes had a $\overline{M}_{n,SEC,PS}$ value of about 1×10^6 g/mol and an uniform size distribution, with a PDI, similar to that of the macromonomer, of 1.20 and about 93% of the macromonomer had been incorporated into the final brush structure. The *t*-butyl groups were cleaved by reaction with trimethylsilyl iodide (TMSI) and subsequent hydrolysis to afford water-soluble PAA brushes which could be used for further chemical modification, in addition to their observed pH-responsive transformations.⁵⁹

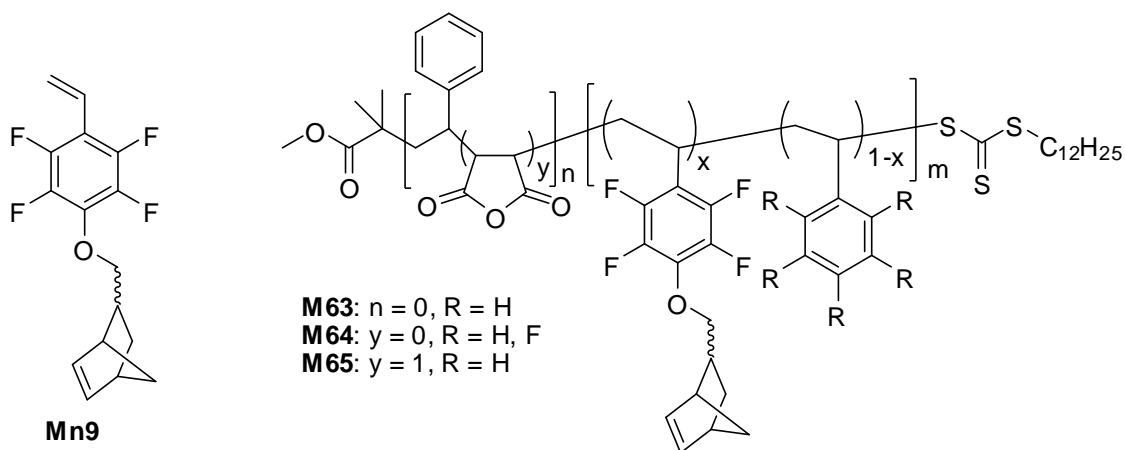
The sequential ROMP of **M59** ($\overline{M}_{n,SEC,PS} = 4.67 \times 10^3$ g/mol) and **M60** was also realized in the presence of Grubbs III catalyst with a **M59/M60**/initiator ratio of 50/50/1. The well-defined structure of P(NB-*g-Pt*BA)-*b*-P(NB-*g-PS*) was supported by SEC, with low PDIs (< 1.20) and a $\overline{M}_{n,SEC,PS}$ of 1.97×10^5 g/mol. The amphiphilic diblock graft copolymer P(NB-*g-PAA*)-*b*-P(NB-*g-PS*) was obtained after deprotection of P(NB-*g-Pt*BA)-*b*-P(NB-*g-PS*) with TMSI and hydrolysis of the intermediate trimethylsilyl esters. The final amphiphilic diblock graft copolymer was investigated as nanoscopic building blocks for the assembly of supramolecular nanostructures in aqueous medium. Both AFM and transmission electron microscopy (TEM) results showed that the copolymer had a broad size distribution. The capacity of hierarchical supramolecular assembly into complex, functional nano- and microscopic objects is currently studied.⁶⁰

The triblock macromonomer **M61** was synthesized from a NB-CTA by sequential RAFT polymerizations of St, MA and *t*BA.⁶¹ The RAFT processes were stopped at low monomer conversion ($\leq 35\%$) to prevent the participation of norbornenyl groups in the multiple radical polymerizations. The final macromonomer had a $\overline{M}_{n,SEC,PS}$ of 15 900 g/mol and a PDI of 1.20. ROMP of **M61** was carried out in the presence of Grubbs III' catalyst in DCM at rt with a **M61**/initiator ratio of 100/1. After 1 h, over 95% macromonomer conversion to graft copolymer was obtained. The resulting graft copolymer had a $\overline{M}_{n,SEC,PS}$ of $1.52 \cdot 10^6$ g/mol and a low PDI of 1.15. Finally, PNB-*g*-(PS-*b*-PMA-*b-Pt*BA) was converted to an amphiphilic block brush copolymer PNB-*g*-

(PS-*b*-PMA-*b*-PAA) by acidolysis of the *tert*-butyl groups. The amphiphilic block brush copolymer exhibited cylindrical morphologies with diameters of 18 ± 2 nm and lengths of 92 ± 21 nm as measured by TEM.

Most recently, Wooley's group investigated the synthesis of brush copolymers by a tandem RAFT polymerization and ROMP. First, an *exo*-NB-PMMA macromonomer **M62** (Scheme I-41) was synthesized by selective RAFT polymerization of MMA using NB-functionalized dithiobenzoate CTA.⁶² As analyzed by SEC, the macromonomer **M62** had a PDI of 1.12 and a $\overline{M}_{n,SEC,PS}$ of 4 600 g/mol. The compatibility of Grubbs III' catalyst with MMA monomer was checked by ROMP of **M62** in a mixed solvent of toluene/MMA (60/40 v/v). After 1h, SEC analysis showed a high macromonomer conversion (91%), which suggested a highly efficient transformation of the NB terminal group in ROMP by Grubbs III' catalyst in the presence of MMA monomer. Two brush copolymers were then synthesized by the sequential RAFT polymerization and ROMP in a one-pot process. The feed ratio of RAFT polymerization was used as optimized by the kinetics study ($[MMA]_0:[NB-CTA]_0:[AIBN]_0 = 200:1:0.1$, 50 vol % of toluene at 65 °C). The RAFT polymerizations were stopped after 3 and 5 h, to obtain **M62** with $\overline{M}_{n,SEC,PS}$ of 4 700 and 6 450 g/mol, respectively. In the next step, Grubbs III' (0.01 equiv) in stock solution was added to the crude macromonomer solutions to initiate the ROMP. The polymerizations were stopped after 1 h by adding several drops of ethyl vinyl ether. High macromonomer conversions (92-94%) were obtained in both ROMPs. AFM images of graft copolymers showed bottlebrush-like morphologies with average contour lengths of 66 ± 13 nm and 68 ± 12 nm, respectively.

Wooley's group has also reported the synthesis of multiple NB-functionalized macromonomers **M63**, **M64** and **M65** (Scheme I-42) by RAFT polymerization.⁶³ Multiple reactive NB functionalities have been incorporated onto the backbone of well-defined statistical and diblock copolymers previously synthesized by selective RAFT copolymerization.



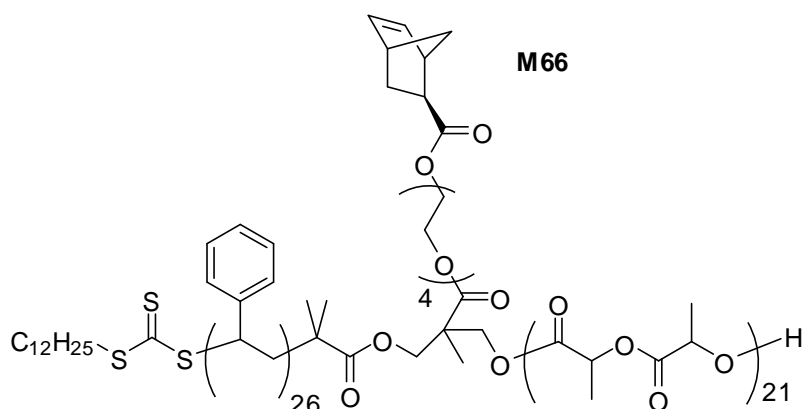
Scheme I-42. NB-functionalized macromonomers synthesized by Wooley's group.⁶³

RAFT copolymerization of **Mn9** and Sty was carried out using AIBN as the radical initiator, S-1-dodecyl-S'-(α, α' -dimethyl- α'' -acetic acid)trithiocarbonate as the RAFT agent with **Mn9**/Sty/CTA/AIBN = 41/59/1/0.1. The macromonomer **M63**, obtained at 78% conversion of **Mn9** and 58% conversion of Sty after 12h of copolymerization, had a $\overline{M}_{n,LLS}$ of 1.35×10^4 g/mol and a PDI of 1.23, which was in agreement with the theoretical value of 1.31×10^4 g/mol. The macromonomer characterization suggested that nearly all of the NB groups remained intact during the RAFT copolymerization process and the molar percentage of **Mn9** was about 53% in macromonomer, which also agreed with relative degrees of polymerization based on the monomer conversion. But it was considered that if the **M63** was used as a macroCTA for the synthesis of block copolymers, the relatively high local concentration of NB groups along the polymer backbone might induce side reactions during the chain extension by RAFT polymerization. So, the macromonomers **M64** and **M65** were synthesized by RAFT copolymerization of **Mn9** with comonomers using PS ($\overline{M}_{n,LLS} = 4.4 \times 10^3$ g/mol) or poly(styrene-*alt*-maleic anhydride) ($\overline{M}_{n,LLS} = 8.1 \times 10^3$ g/mol) as macroCTAs. The macromonomers **M64** and **M65** were obtained with low PDIs (1.09-1.22), and $\overline{M}_{n,LLS}$ of 1.1×10^4 and 1.27×10^4 g/mol, respectively. The incorporation of the NB side-chain groups was quite high, because of the high conversion of **Mn9**, about 50% in all cases.

The ROMP of NB-functionalized macromonomer **M64** was conducted using Grubbs I catalyst with macromonomer/initiator ratio of 50/1 in DCM at rt. As measured by ^1H

NMR spectroscopy and SEC analysis, the successful transformation of **M64** into a star block copolymer had occurred. By SEC, star polymer was found to have a $\overline{M}_{n,LLS}$ of 4.96×10^5 g/mol and a narrow molecular weight distribution (PDI = 1.23). The number-average hydrodynamic diameter ($D_{h,n}$) measured by DLS (from a THF solution of 2.5 mg/mL) was 8 ± 2 nm, suggesting that star polymer existed as nanoscale objects.

Recently, Cheng *et al.* have reported the first synthesis of macromonomers **M66** (Scheme I-43) by simultaneous RAFT polymerization and ROP.⁶⁴



Scheme I-43. α -norbornenyl-PS/PLA macromonomer synthesized by Cheng and coworkers.⁶⁴

The authors first synthesized a multifunctional agent containing a trithiocarbonate functionality for RAFT polymerization, a hydroxyl group as an initiator site for ROP and an *exo*-NB functionality as “ROMP-able” group. By selecting AIBN as the initiator for RAFT polymerization of Sty and 4-(*N,N*-dimethylamino)pyridine (DMAP) as the organocatalyst for ROP of LA, simultaneous polymerizations were conducted at 59 °C in the presence of the multifunctional agent with an agent/Sty/LA/AIBN/DMAP molar ratio of 1/70/35/0.1/4 and 30 wt % of 1,2-dichloroethane for the synthesis of macromonomer **M66**. The polymerization was stopped at 24 h with 34% conversion of Sty and 71% conversion of LA. MALDI-TOF mass spectrometry analysis of macromonomer showed a narrow, monomodal molecular weight distribution with the molecular weight of the highest peak of 6319.83 g/mol, which was close to the calculated value. ROMP of **M66** was realized with Grubbs III catalyst in DCM at rt for 1 h with different macromonomer/initiator ratios (59-176/1). High conversions of ROMP were determined by SEC analysis (86-95%). Pure PNB-*g*-PS/PLAs were obtained by passing the polymerization solutions through short columns of silica gel

with $\overline{M}_{n,LLS}$ ranging from 4.3×10^5 to 8.9×10^5 g/mol and low PDIs (1.15-1.28). The observation of “gradual Janus” and left-right Janus conformations of copolymers by TEM after annealing provided the direct experimental evidence to prove the PNB-g-PS/PLA copolymers as a type of Janus nanomaterial.

All macromonomers synthesized by reversible-deactivation radical polymerization and their ROMP were summarized in the Table I-2. The results demonstrated the compatibility of the ATRP and RAFT polymerization together with ROMP in the “grafting through” method. ATRP and RAFT polymerization are controlled radical polymerization techniques that allow for the preparation of well-defined polymers from vinylic monomers. In case of ATRP, the macromonomers were synthesized by two methods: ATRP from a NB, oxa-NB or cyclobutene “ROMP-able” group-containing ATRP initiator or functionalization of polymer chain obtained by ATRP, by a “ROMP-able” group such as NB or oxa-NB. In contrast, in case of RAFT polymerization, the authors used a dual-functional molecule that serves as a RAFT agent and carries the NB unit which allows to obtain the norbornenyl-functionalized macromonomers directly from RAFT polymerization. Initial high monomer to CTA ratios are used to suppress the potential NB group radical polymerization. Finally, the macromonomers were obtained with relative low PDIs (1.02-1.50), $\overline{M}_{n,SEC,PS}$ of 2 200-16 600 g/mol with different polymer chains, such as PS, PtBA, PnBA, PMMA, PMA, poly(glycerol-MMA). The ROMP of macromonomers was realized in presence of the Grubbs catalysts. Almost all graft copolymers were obtained with low PDIs (1.03-1.56) and in a wide range of $\overline{M}_{n,SEC}$ between 8.2×10^3 - 2.62×10^6 g/mol.

Table I-2. Macromonomers synthesized by ATRP, RAFT and their homopolymerization by ROMP

Entry	Macromonomer				Graft copolymer					Ref.
	ROMP functionality	Nature of chain	$\overline{M}_{n,SEC} \times 10^{-3}$ g/mol	PDI	Initiator	$\frac{[\text{monomer}]_0}{[\text{initiator}]_0}$	$\overline{M}_{n,SEC} \times 10^{-4}$ g/mol	PDI	Macromonomer conversion (%)	
ATRP										
1	Cyclobutene	PS- <i>b</i> -PrBA	4.3-7.2	1.16-1.20	Grubbs I and II	10	0.82-1.04 ^a	1.21-1.25	~100	52
2	NB	PMMA	6.39 -16.6	1.3-1.5	Grubbs I	26-400	4.76-6.4 ^a	1.78-4.5	n.d ^c	53
3	Oxa-NB	Poly(Glycerol-MMA)	3.5-8.5	1.22-1.26	Grubbs II	20	1.1-2.4 ^a	1.25-1.56	~100	54
4	NB	PMA, PrBA, PS	2.2- 6.6	1.02	Grubbs III'	50-400	26.7-262 ^b	1.03	~100	55
5	Oxa-NB	PS	4.1	1.12	Grubbs III	10	4.03 ^b	1.17	n.d	56
RAFT polymerization										
6	NB	PS, PMMA, PMA	0.69-24.7	1.07-1.34	Grubbs I	8 (only NB-PMMA)	4.8 ^a	1.15	~100	57
7	NB	PrBA, PS, PMMA, PMA	4.67 -16	<1.20	Grubbs III	26-400	19.7- 152 ^b	~1.2	93-100	58-62
8	NB	PS derivative, P(Sty- <i>alt</i> -maleic anhydride)	11-13.5	~1.23	Grubbs I	60	49.6 ^b	1.23	~100	63
9	NB	PS/PLA	8.6	1.14	Grubb III	59-95	43.5-89.2 ^b	1.1-1.28	86-95	64

^a $\overline{M}_{n,SEC}$ determined by RI detector, PS standards, ^b $\overline{M}_{n,SEC}$ determined by multi-angle laser light scattering detector, ^cn.d: not detected

Conclusion

Since 1989, about 50 articles reporting graft copolymer synthesis by ROMP according to the “grafting through” method have been published. The ROMP of (macro)monomers was realized by using metal alkylidene initiators such as Schrock catalysts and Grubbs catalysts and various topologies of well-defined graft copolymers were obtained: bottlebrush, comb-like, star-like or flower-like... The results indicate that the combination of ROMP with others techniques of polymerization is one of the most important strategies for the synthesis of graft copolymers according to the “grafting through” method.

In there, macromonomer synthesis was essentially realized by two routes: in the first route, α -“ROMP-able”-macromonomers were prepared from a “ROMP-able” entity containing an initiating group; in the second route, ω -“ROMP-able”-macromonomers were synthesized by post-modification, *i.e.*, polymerization of the monomer and subsequent functionalization of the macromolecular chain by a “ROMP-able” group. Norbornene is usually used as the “ROMP-able” group because of its high reactivity in ROMP, but other “ROMP-able” groups have also been reported such as oxanorbornene, cyclobutene and cyclooctene. Macromonomers have been synthesized in the literature by almost all the available polymerization techniques such as anionic polymerization, cationic polymerization, ROP, ROMP and RDRP, which are chosen according to the nature of the monomer to be polymerized. A wide range of monomers was successfully polymerized: Sty, EO, Bu, MMA, MA, *t*BA, *n*BA, LA, CL or NB. There is no universal technique for polymerization of all monomers. Nevertheless, among the available techniques, the RDRP is one of the most efficient and versatile methods thanks to its high tolerance to a wide range of functionalities. Recently, the simultaneous combination of different polymerization techniques, such as RAFT and ROP, has been described for synthesizing complex non-symmetrical block macromonomers.

In this work, we investigated the preparation of macromonomers using the “click” copper-catalyzed azide-alkyne cycloaddition methodology and RAFT polymerization such techniques can be applied to a wide range of polymers.

References

1. Hadjichristidis, N.; Pitsikalis, M.; Iatrou H. *Adv. Polym. Sci* **2005**, *189*, 1-124.
2. Hadjichristidis, N.; Iatrou, H.; Pitsicalis, M.; Mays J. *Prog. Polym. Sci.* **2006**, *31*, 1068-1132.
3. Grubbs R. H. (Ed.), *Handbook of Metathesis*, vol. 1&3, Wiley-VHC, Weinheim, 2003.
4. Schrock, R. R.; Hoveyda. A. H. *Angew. Chem. Int. Ed* **2003**, *42*, 4592-4633.
5. Norton, R. L.; McCarthay T. J. *Macromolecules* **1989**, *22*, 1022-1025.
6. Feast, W. J.; Gibson, V. C.; Johnson, A. F.; Khosravi, E.; Mohsin M. A. *Polymer*, **1994**, *35*, 3542-3548.
7. Feast, W. J.; Gibson, V. C.; Johnson, A. F.; Khosravi, E.; Mohsin M. A. *J. Mol. Catal. A: Chem.* **1997**, *115*, 37-42.
8. Rizmi, A. C. M.; Khosravi, E.; Feast, W. J.; Mohsin, M. A.; Johnson A. F. *Polymer*, **1998**, *39*, 6605-6610.
9. Breunig, S.; Héroguez, V.; Gnanou, Y.; Fontanille, M. *Macromol. Symp.* **1995**, *95*, 151-166.
10. Héroguez, V.; Gnanou, Y.; Fontanille, M. *Macromol. Rapid Commun.* **1996**, *17*, 137-142.
11. Cheng, C.; Yang, N.-L *Macromolecules* **2010**, *43*, 3153-3155.
12. Héroguez, V.; Breunig, S.; Gnanou, Y.; Fontanille, M. *Macromolecules* **1996**, *29*, 4459-4464.
13. Héroguez, V.; Six, J. L.; Gnanou, Y.; Fontanille, M. *Macromol. Chem. Phys.* **1998**, *199*, 1405-1412.
14. Héroguez, V.; Amédéo, E.; Grande, D.; Fontanille, M.; Gnanou, Y. *Macromolecules* **2000**, *33*, 7241-7248.
15. Grande, D.; Six, J. L.; Héroguez, V.; Gnanou, Y.; Fontanille, M. *Macromol. Symp.* **1998**, *128*, 21-37.
16. Héroguez, V.; Gnanou, Y.; Fontanille, M. *Macromolecules* **1997**, *30*, 4791-4798.
17. Grande, D.; Six, J. L.; Breunig, S.; Héroguez, V.; Fontanille, M.; Gnanou, Y. *Polym. Adv. Technol.* **1998**, *9*, 601-612.
18. Pichavant, L.; Bourget, C.; Durrieu, M.-C. ; Héroguez, V. *Macromolecules* **2011**, *44*, 7879-7887.

19. Zou, J.; Jafr, G.; Themistou, E.; Yap, Y.; Wintrob, Z. A. P.; Alexandridis, P.; Ceacareanu, A. C.; Cheng, C. *Chem. Commun.* **2011**, *47*, 4493-4495.
20. Li, H.; Zhang, W.; Wang, Y.; He, B. *Polym. Adv. Technol.* **2003**, *14*, 226-229.
21. Li, H.; Wang, Z.; He, B. *J. Mol. Catal. A: Chem.* **1999**, *147*, 83-88.
22. Li, H.; Wang, Z.; He, B. *J. Mol. Catal. A: Chem.* **2000**, *159*, 121-125.
23. Grutke, S.; Hurley, J. H.; Risse, W. *Macromol. Chem. Phys.* **1994**, *195*, 2875-2885.
24. Revanur, R.; McCloskey, B.; Breitenkamp, K.; Freeman, B. D.; Emrick, T. *Macromolecules* **2007**, *40*, 3624-3630.
25. Breitenkamp, R. B.; Ou, Z.; Breitenkamp, K.; Muthukumar, M.; Emrick, T. *Macromolecules* **2007**, *40*, 7617-7624.
26. Breitenkamp, R. B.; Simeone, J.; Jin, E.; Emrick, T. *Macromolecules* **2002**, *35*, 9249-9252.
27. Sankaran, N. B.; Rys, A. Z.; Nassif, R.; Nayak, M. K.; Metera, K.; Chen, B.; Bazzi, H. S.; Sleiman, H. F. *Macromolecules* **2010**, *43*, 5530-5537.
28. Shi, H.; Shi, D.; Yao, Z.; Luan, S.; Jin, J.; Zhao, J.; Yang, H.; Stagnaro, P.; Yin, J. *Polym. Chem.* **2011**, *2*, 679-684.
29. Alfred, S. T.; Al-badri, Z. M.; Madkour, A. E.; Lienkamp, K.; Tew, G. N. *J. Polym. Sci., Part A: Polym. Chem.* **2008**, *46*, 2640-2648.
30. Le, D.; Montembault, V.; Soutif, J.-C.; Rutnakornpituk, M.; Fontaine, L. *Macromolecules* **2010**, *43*, 5611-5617.
31. Johnson, J. A.; Lu, Y. Y.; Burts, A. O.; Xia, Y.; Durrell, A. C.; Tirrell, D. A.; Grubbs, R. H. *Macromolecules* **2010**, *43*, 10326-10335.
32. Johnson, J. A.; Lu, Y. Y.; Burts, A. O.; Lim, J.-H.; Finn, M. G.; Koberstein, J. T.; Turro, N. J.; Tirrell, D. A.; Grubbs, R. H. *J. Am. Chem. Soc.* **2011**, *133*, 559-566.
33. Matson, J. B.; Grubbs, G. H. *J. Am. Chem. Soc.* **2008**, *130*, 6731-6733.
34. Miller, A. F.; Richards, R. W. *Macromolecules* **2000**, *33*, 7618-7628.
35. Cheng, G.; Hua, F.; Melnichenko, Y. B.; Hong, K.; Mays, J. W.; Hammouda, B.; Wignall, G. D. *Eur. Polym. J.* **2008**, *44*, 2859-2864.
36. Allcock, H. R.; de Denus, C. R.; Prange, R.; Laredo, W. R. *Macromolecules* **2001**, *34*, 2757-2765.
37. Mecerreyes, D.; Dahan, D.; Lecomte, P.; Dubois, P.; Demonceau, A.; Noel, A. F.; Jérôme, R. *J. Polym. Sci., Part A: Polym. Chem.* **1999**, *37*, 2447-2455.
38. Xie, M.; Dang, L.; Han, H.; Wang, W.; Liu, J.; He, X.; Zhang, Y. *Macromolecules* **2008**, *41*, 9004-9010.

39. Jha, S.; Dutta, S.; Bowden, N. B. *Macromolecules* **2004**, *37*, 4365-4374.
40. Czelusniak, I.; Khosravi, K.; Kenwright, A. M.; Ansell, C. W. G. *Macromolecules* **2007**, *40*, 1444-1452.
41. Xia, Y.; Olsen, B. D.; Kornfield, J. A.; Grubbs, R. H. *J. Am. Chem. Soc.* **2009**, *131*, 18525-18532.
42. Fu, Q.; Ren, J. M.; Qiao, G. G. *Polym. Chem.* **2012**, *3*, 343-351.
43. Li, A.; Li, Z.; Zhang, S.; Sun, G.; Policarpio, D. M.; Wooley, K. L. *ACS Macro Lett.* **2012**, *1*, 241-245.
44. Li, Y.; Zou, J.; Das, B. P.; Tsianou, M.; Cheng, C. *Macromolecules*, **2012**, *45*, 4623-4629.
45. Nomura, K.; Takahashi, S.; Imanishi, Y. *Polymer* **2000**, *41*, 4345-4350.
46. Nomura, K.; Takahashi, S.; Imanishi, Y. *Macromolecules* **2001**, *34*, 4712-4723.
47. Murphy, J. J.; Nomura, K. *Chem. Commun.* **2005**, 4080-4082.
48. Murphy, J. J.; Furusho, H.; Paton, R. M.; Nomura, K. *Chem. Eur. J.* **2007**, *13*, 8985-8997.
49. Hilf, S.; Kilbinger, A. F. M. *Macromol. Rapid Commun.* **2007**, *28*, 1225-1230.
50. Allen, M. J.; Wangkanont, K.; Raines, R. T.; Kiessling, L. L. *Macromolecules* **2009**, *42*, 4023-4027.
51. Morandi, G.; Montembault, V.; Pascual, S.; Legoupy, S.; Fontaine, L. *Macromolecules* **2006**, *39*, 2732-2735.
52. Morandi, G.; Piogé, S.; Montembault, V.; Pascual, S.; Legoupy, S.; Fontaine, L. *Materials Science and Engineering C* **2009**, *29*, 367-371.
53. Liaw, D. J.; Huang, C. C.; Ju, J. Y. *J. Polym. Sci., Part A: Polym. Chem.* **2006**, *44*, 3382-3392.
54. Morandi, G.; Mantovani, G.; Montembault, V.; Haddleton, D. M.; Fontaine, L. *New J. Chem.* **2007**, *31*, 1826-1829.
55. Xia, Y.; Kornfield, J. A.; Grubbs, R. H. *Macromolecules* **2009**, *42*, 3761-3766.
56. Durmaz, H.; Dag, A.; Cerit, N.; Sirkecioglu, O.; Hizal, G.; Tunca, U. *J. Polym. Sci., Part A: Polym. Chem.* **2010**, *48*, 5982-5991.
57. Patton, D. L.; Advincula, R. C. *Macromolecules* **2006**, *39*, 8674-8683.
58. Bielawski, C. W.; Benitez, D.; Morita, T.; Grubbs, R. H. *Macromolecules* **2001**, *34*, 8610-8618.
59. Li, Z.; Zhang, K.; Ma, J.; Cheng, C.; Wooley, K. L. *J. Polym. Sci., Part A: Polym. Chem.* **2009**, *47*, 5557-5563.

60. Li, Z.; Ma, J.; Cheng, C.; Zhang, K.; Wooley, K. L. *Macromolecules* **2010**, *43*, 1182-1184.
61. Ma, J.; Lee, N. S.; Wooley, K. L. *J. Am. Chem. Soc.* **2011**, *133*, 1228-1231.
62. Li, A.; Ma, J.; Sun, G.; Li, Z.; Cho, S.; Clark, C.; Wooley, K. L. *J. Polym. Sci., Part A: Polym. Chem.* **2009**, *50*, 1681-1688.
63. Ma, J.; Cheng, C.; Wooley, K. L. *Aust. J. Chem.* **2009**, *62*, 1507-1519.
64. Li, Y.; Themistou, E.; Zou, J.; Das, B. P.; Tsianou, M.; Cheng, C. *ACS Macro Lett.* **2012**, *1*, 52-56.

Chapter II

Synthesis of PEO macromonomers by “click” reaction

Introduction*

Poly(ethylene oxide) (PEO) is a neutral, hydrophilic, highly mobile, synthetic polymer and non-toxic, which has found numerous applications in fields such as biomaterials and biotechnologies.¹ Because of the unique properties of PEO, a wide range of complex structures of graft copolymers with PEO side chains has been designed in various ways, and hydrophilic PEO segments are usually combined with any hydrophobic component forming amphiphilic graft copolymers.² We were interested in the synthesis of PEO graft copolymers by the “grafting through” approach. The “grafting through” method requires the synthesis of PEO macromonomers in which a polymerizable functional group is incorporated to the chain-end. The synthesis of macromonomers can be accomplished by two methods: the α -functional macromonomer synthesis, in which the polymerization is initiated by an initiator containing the polymerizable group; the ω -functional macromonomer synthesis, in which the polymer chains were functionalized with polymerizable groups after the synthesis of polymer chains.

In this chapter, we have chosen the ω -functional macromonomer strategy for the PEO macromonomers synthesis which allows using commercially available PEO with different molecular weights, having one or two –OH end-groups which can be used to easily functionalize with polymerizable groups. The “click” reaction was chosen for the functionalization of PEO for its high efficiency with a high tolerance towards functional groups and solvents.³ The ring-opening metathesis polymerization (ROMP) will be used to polymerize the PEO macromonomers as it is a versatile and an efficient synthetic strategy for the polymerization of unsaturated constrained rings such as norbornene, oxanorbornene, cyclobutene or cyclooctene by using metal alkylidene initiators.⁴

We present the synthesis of alkyne- or azido-functionalized oxanorbornene and cyclobutene precursors and the synthesis of various ω -cyclobutenyl PEO macromonomers and ω -oxanorbornenyl PEO macromonomers by “click” reaction.

* Part of this chapter was published in *Macromolecules* **2010**, *43*, 5611-5617.

The oxanorbornene-based group was chosen as the “ROMP-able” entity for two reasons. First, pure *exo*-oxanorbornene diastereoisomers are easily prepared starting from *exo*-7-oxabicyclo[2.2.1]hept-5-ene-2,3-dicarboxylic anhydride, available in high yield through Diels-Alder cycloaddition.⁵ Indeed, it is well known that *exo*-diastereoisomers are much more reactive in ROMP than their *endo*- counterparts.⁶⁻¹² Second, as pointed out by Czelusniak *et al.*,¹³ it is expected that the oxygen in the oxanorbornene group makes the backbone more hydrophilic¹⁴ and hence increases the probability of biocompatibility of the resulting graft copolymers.

The 3,4-disubstituted cyclobutene functionality was also selected as the “ROMP-able” entity of the macromonomers because the ROMP of cyclobutene affords an exclusively linear polybutadiene with a strictly 1,4-type microstructure. Because of their unique properties, PBu graft copolymers could be used for a variety of applications, such as nanomaterials, thermoplastic elastomers, impact-resistant plastics, compatibilizers, polymeric emulsifiers, and nanoparticles for drug delivery.¹⁵⁻¹⁷ In this case, the *cis* stereochemistry was preferred to the *trans* one as a previous study has highlighted the higher reactivity of *cis*-3,4-disubstituted cyclobutenes compared to their *trans* analogues in ROMP.¹⁸

I- Synthesis of ω -oxanorbornenyl PEO macromonomers

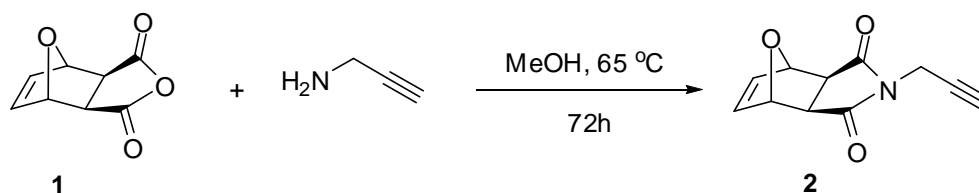
ω -Oxanorbornenyl PEO macromonomers have been synthesized by “click” reaction between azido-terminated PEO of different molecular weights and alkyne-functionalized oxanorbornene. This precursor is easily obtained in a pure *exo* stereochemistry by Diels-Alder cycloaddition from furan and maleic anhydride.⁵

I-1. Alkyne-functionalized oxanorbornene precursor synthesis

The oxanorbornene-based monomer with an alkyne functionality was designed and prepared from *exo*-7-oxabicyclo[2.2.1]hept-5-ene-2,3-dicarboxylic anhydride (**1**)[#] and

[#] A glossary containing chemical structures of all compounds (**1** - **11** and **M2** – **M11**) is attached to this chapter.

N-propargylamine, and the synthetic route is illustrated in Scheme II-1. An excess of *N*-propargylamine is necessary to increase the yield, and the suitable ratio of *N*-propargylamine to **1** was 1.5:1. Under these conditions, *exo-N*-prop-2-ynyl-7-oxabicyclo[2.2.1]hept-5-ene-2,3-dicarboximide (**2**) was obtained with 81 % yield. The proton nuclear magnetic resonance spectroscopy (^1H NMR) spectrum (Figure II-1) shows the resonance signal of $\text{N-CH}_2\text{-C}\equiv\text{CH}$ at 4.24 ppm, while the signal of $\text{CH}=\text{CH}$ protons at 6.54 ppm are still observed, and importantly the integration area ratio of the characteristic resonances of 2:2 is in agreement with the ratio of corresponding protons, which demonstrates that full condensation occurred. Furthermore, the molecular weight ($M + \text{H}^+ = 204.0661$) of **2** from high resolution mass spectroscopy (HRMS) analysis was in good accordance with the calculated value ($M + \text{H}^+ = 204.2060$).



Scheme II-1. Synthesis of oxanorbornene precursor **2**.

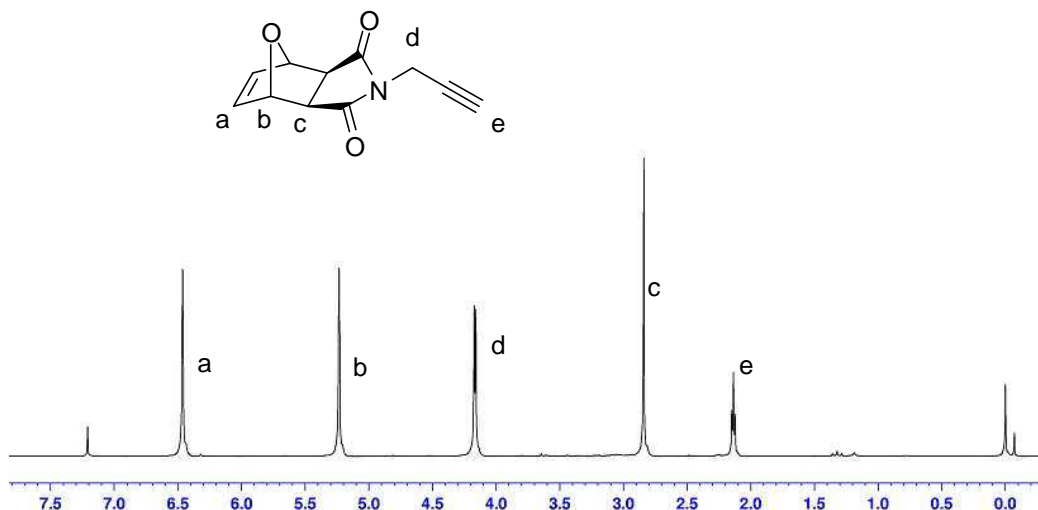


Figure II-1. ^1H NMR spectrum of **2**; solvent: CDCl_3 .

I-2. ω -Oxanorbornenyl PEO macromonomers synthesis

First, azido-terminated linear PEO monomethyl ether chains (PEO-N_3 ; $M_{n,NMR} = 554$, 2010 and 4590 g/mol, Table II-1) have been synthesized from hydroxyl-terminated PEO

monomethyl ether chains (PEO-OH) with different molecular weights.

PEO-OH were first converted to mesylate-terminated PEO monomethyl ether chains (PEO-OSO₂CH₃) by reaction with methanesulfonyl chloride, followed by transformation of mesylate chain-end groups into azido groups *via* reaction with sodium azide (NaN₃) in dichloromethane (DCM) for PEO-N₃ 500¹⁹ or in tetrahydrofuran (THF) for PEO-N₃ 2 000 and PEO-N₃ 5 000²⁰. The presence of an azido group at the chain-end was checked by ¹³C NMR spectroscopy as shown in Figure II-2 for PEO-N₃ 500. The carbon bearing the azido group appears at 50.7 ppm, whereas the one carrying the terminal hydroxyl is located at 61.7 ppm. Moreover, the chain-end functionality was proved to be quantitative, as evidenced by the disappearance of the CH₂OH peak (5, Figure II-2, A) of PEO-OH spectrum and the disappearance of the -O-SO₂CH₃ peak (6', Figure II-2, B) of the PEO-O-SO₂CH₃ spectrum in the final ¹H NMR spectrum of PEO-N₃ (Figure II-C).

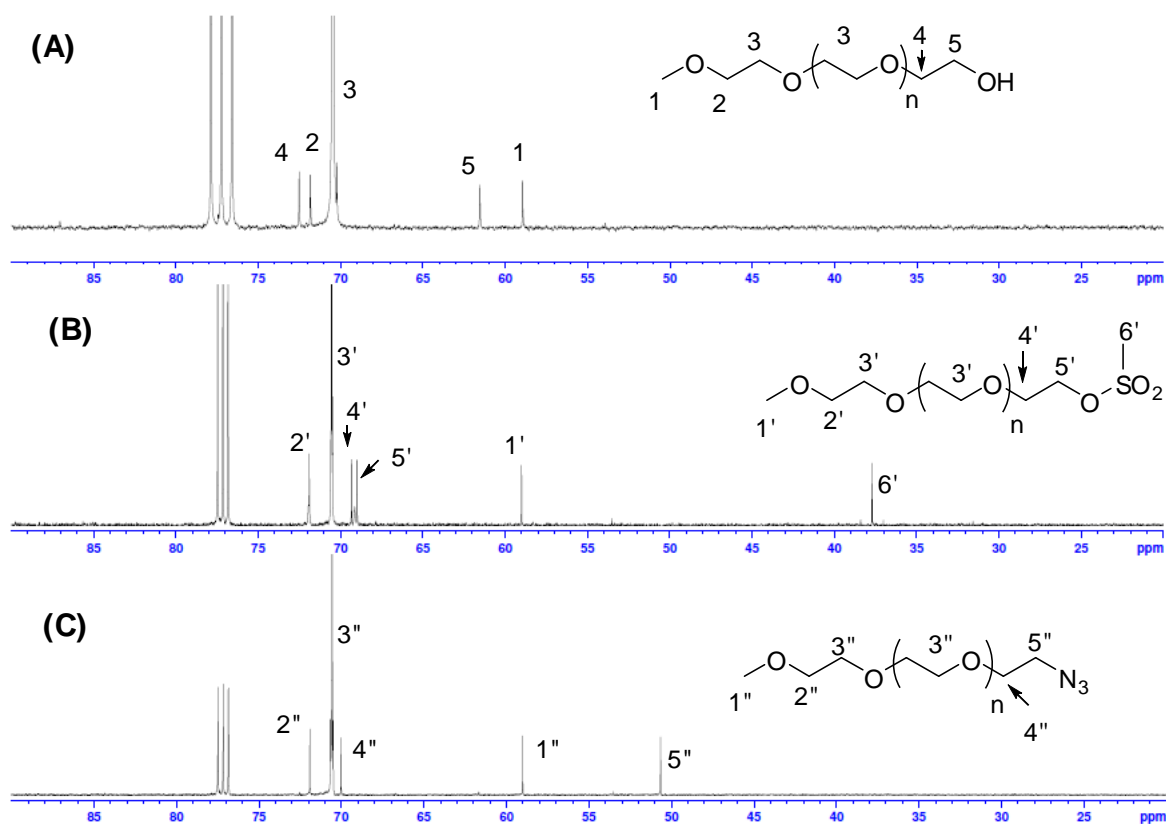


Figure II-2. ¹³C NMR spectra of (A) PEO-OH, (B) PEO-OSO₂CH₃, and (C) PEO-N₃

500 ($M_{n,NMR} = 554$ g/mol); solvent: CDCl₃.

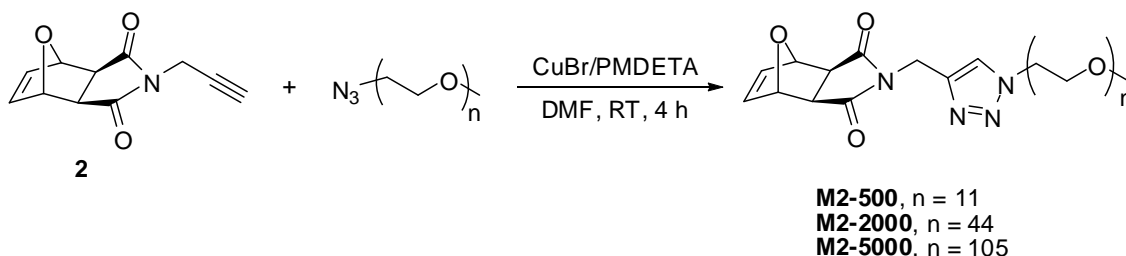
The characteristic of POE-N₃ are reported in Table II-1.

Table II-1. Characteristics of the azido-terminated linear PEO monomethyl ethers 500, 2 000 and 5 000.

Sample name	$\overline{M}_{n,theor}^a$ (g/mol)	$\overline{M}_{n,NMR}^b$ (g/mol)	$\overline{M}_{n,SEC}^c$ (g/mol)	$M_{p,SEC}^d$ (g/mol)	PDI ^c
PEO-N ₃ 500	500	554	- ^e	720	- ^e
PEO-N ₃ 2 000	2 000	2 037	3 200	3 200	1.05
PEO-N ₃ 5 000	5 000	4 614	7 600	8 100	1.06

^a Supplier data. ^b Number-average molecular weight determined by ¹H NMR by comparing integration area ratio of the CH₃- peak and of the -CH₂-O- peak, CDCl₃ as the solvent. ^c Number-average molecular weight and polydispersity measured by SEC in THF with RI detector, calibration with linear polystyrene standards. ^d $M_{p,SEC}$: Molecular weight at the peak maximum of the SEC trace. ^e Part of the peak was outside the calibration window.

Macromonomers were then synthesized by coupling azido-terminated PEO-N₃ and alkyne-functionalized oxanorbornene precursor **2** (Scheme II-2). The “click” reactions were carried out in *N,N*-dimethylformamide (DMF) at room temperature using a stoichiometric molar ratio between PEO-N₃ and alkynyl groups in the presence of a catalytic amount of Cu(I)Br with *N,N,N',N',N''*-pentamethyldiethylenetriamine (PMDETA) as the ligand (Scheme II-2). After 4 h of reaction, “click” chemistry afforded the targeted ω -*exo*-oxanorbornenyl PEO monomethyl ether macromonomers with different molecular weights **M2-500***, **M2-2000** and **M2-5000**, obtained from PEO-N₃ 500, 2 000 and 5 000, respectively.



Scheme II-2. Synthesis of ω -oxanorbornenyl PEO macromonomers **M2-500**, **M2-2000** and **M2-5000**.

* Name of macromonomers: As an example, **M2-500** corresponds the macromonomer (**M**) obtained from the oxanorbornene compound (**2**) and with a PEO-(**500**).

The ^1H NMR spectrum of **M2-500** (Figure II-3) clearly indicates the shift of the alkyne proton from 2.20 ppm (e, Figure II-3) to 7.68 ppm (e', Figure II-3) as well as the shift of the methylene group next to the alkyne group from 4.24 ppm (d, Figure II-1) to 4.78 ppm (d', Figure II-3), which corresponds to the proton linked to the triazole ring. The “click” reaction occurred in a quantitative way since integrations of norbornenyl olefin peak (a' at 6.50 ppm, Figure II-3) and the proton on the triazole ring (e' at 7.68 ppm, Figure II-3) gave a 2:1 ratio. The same conclusions could be drawn from the reactions between **2** and PEO- N_3 2 000 or 5 000. The results of the coupling reactions are reported in Table II-2.

The SEC analysis shows that the coupling product **M2-500** has a slightly higher molecular weight than the PEO- N_3 500 precursor, determined by SEC in THF with linear PS standards (Table II-2).

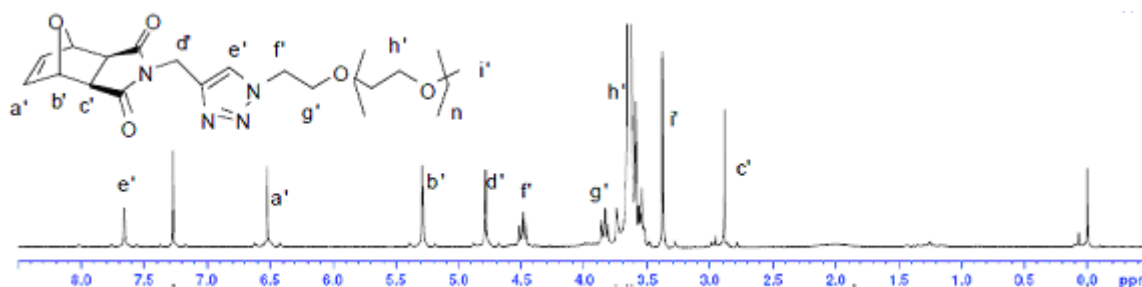


Figure II-3. ^1H NMR spectrum of ω -*exo*-oxanorbornenyl PEO monomethyl ether **M2-500**; solvent: CDCl_3 .

Table II-2. Characteristics of ω -*exo*-oxanorbornenyl PEO macromonomers **M2-500**, **M2-2000** and **M2-5000**.

Sample name	Conv. ^a (%)	Yield ^b (%)	$M_{n,NMR}$ ^c (g/mol)	$M_{n,SEC}$ ^d (g/mol)	PDI ^d
M2-500	> 95	80	757	890	1.05
M2- 2000	> 95	85	2 240	3 400	1.06
M2-5000	> 95	78	4 817	7 800	1.05

^a Determined by ^1H NMR from the reaction mixture, CDCl_3 as the solvent. ^b After purification. ^c Number-average molecular weight determined by ^1H NMR, CDCl_3 as the solvent. ^d Number-average molecular weight and polydispersity measured by SEC in THF with RI detector, calibration with linear polystyrene standards.

The MALDI-TOF mass spectrum of **M2-2000** is shown in Figure II-4. It is interesting to note that besides the expected product, *i.e.*, the macromonomer plus one sodium ion, an additional series was observed which differs by 68 mass units from the main series. The difference in mass of each signal of both series was roughly estimated as 44, indicating the signals were assignable to PEO homologues. This second series has also been detected on MALDI-TOF mass spectrum of **M2-500**. For **M2-5000**, this second series is the only one detected. Since no side reactions were detectable by ^1H NMR spectrum of **M2-2000**, the fragment signals can be ascribed to the retro-Diels-Alder reaction (Scheme II-3) caused by ionization.²¹

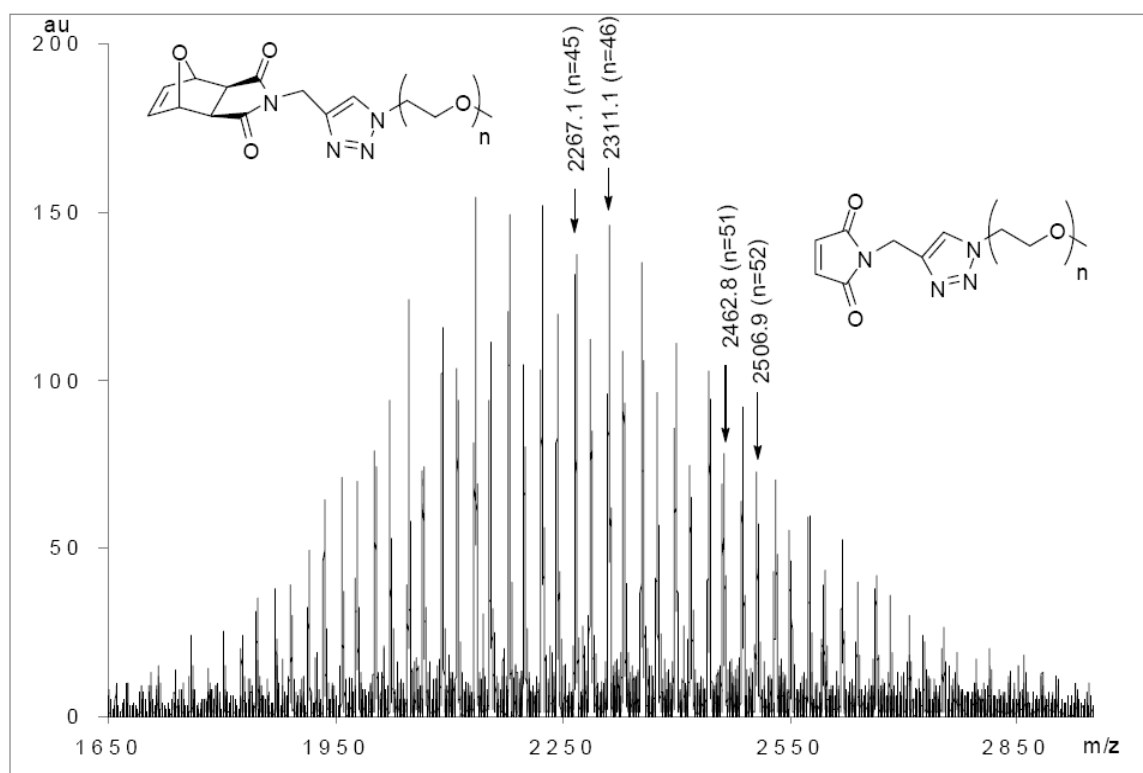
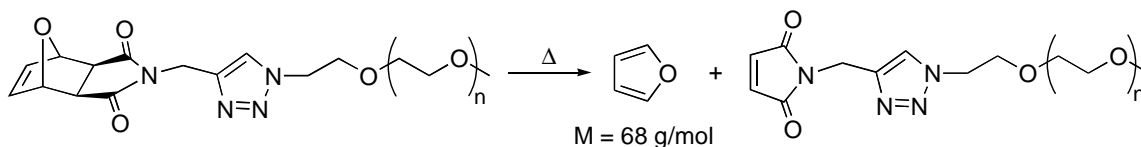


Figure II-4. MALDI-TOF mass spectrum of ω -*exo*-oxanorborenyl PEO monomethyl ether macromonomer **M2-2000** (matrix: 2-[(2*E*)-3-(4-*tert*-butylphenyl)-2-methylprop-2-enylidene]malononitrile (DCTB) + sodium trifluoroacetate (NaTFA)).

The thermal stability of these macromonomers has been studied in order to check the facile conversion of the oxanorborenyl moieties by retro-Diels-Alder reaction.



Scheme II-3. Retro-Diels-Alder reaction of macromonomers.

I-3. Thermal stability of the macromonomers

The conversion of the ω -*exo*-norbornenyl end-group of the macromonomer to a maleimide group could also be monitored by thermo gravimetric analysis (TGA) (Figure II-5). **M2-2000** TGA thermogram clearly exhibits a first loss of 3.07 weight % between 134 and 150 °C, which is attributed to the release of furan²² (calculated % weight loss = 3.04 for **M2-2000**, $\overline{M}_{n,NMR} = 2\,240 \text{ g/mol}$). Additionally, the macromonomers exhibited a major thermal degradation at 405 °C (50% weight loss). The presence of the maleimide functionality was checked after a thermal treatment of **M2-2000** at 250 °C. The resulting ¹H NMR spectrum (Figure II-6) clearly shows the disappearance of the oxatricyclo vinyl signals (*CH=CH* and *CH-O* protons at 6.50 and 5.29 ppm, respectively) and the appearance of the maleimide peak at 6.74 ppm. It should be noted that such maleimide end-functionalized PEO can undergo further Diels-Alder cycloaddition or thiol-ene reaction, giving access to modular block copolymers, stars, bioconjugates, and other functional telechelics.²³

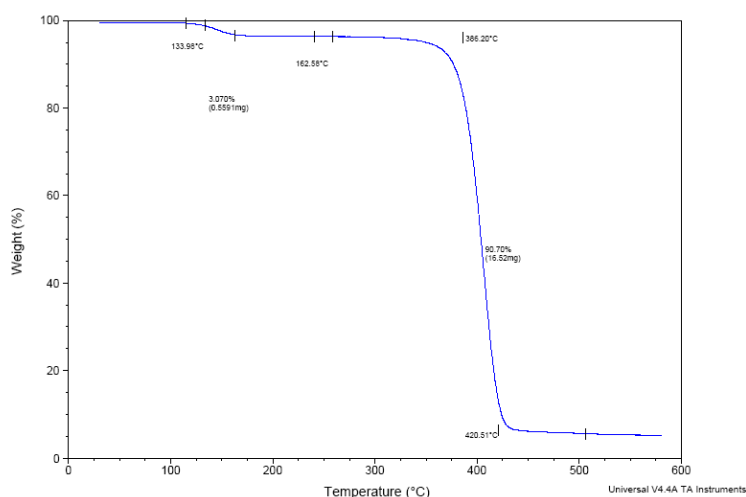


Figure II-5. TGA thermogram of ω -*exo*-oxanorbornenyl PEO monomethyl ether macromonomer **M2-2000** ($\overline{M}_{n,NMR} = 2\,240 \text{ g/mol}$; 3.04 wt % oxanorbornenyl functionality).

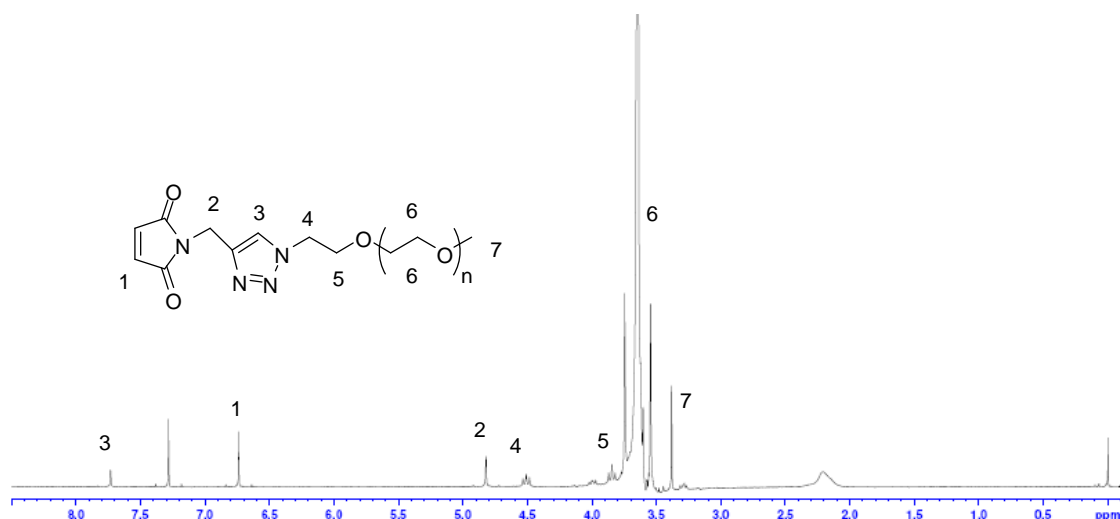


Figure II-6. ^1H NMR spectrum of ω -maleimide PEO monomethyl ether 2 000 obtained after heating **M2-2000** at 250 °C; solvent: CDCl_3 .

This synthetic strategy has then been applied for the synthesis of PEO macromonomers end-functionalized by a cyclobutenyl “ROMP-able” group.

II- Synthesis of ω -cyclobutenyl PEO macromonomers

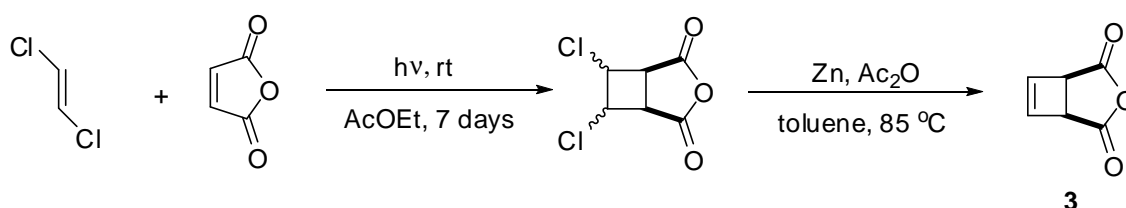
Various PEO macromonomers with a cyclobutene end-group have been targeted from succinimide-based cyclobutene and *cis*-3,4-difunctionalized cyclobutene. The *cis* stereochemistry was preferred to the *trans* one as previous studies have highlighted the higher reactivity of *cis*-3,4-disubstituted cyclobutenes compared to their *trans* analogues in ROMP.¹⁸ In this work, all cyclobutene precursors were synthesized from *cis*-cyclobut-3-ene-1,2-dicarboxylic anhydride.

II-1. PEO macromonomers synthesis from succinimide-based cyclobutene

ω -Cyclobutenyl PEO macromonomers have been first synthesized according to the same procedure as used for the synthesis of ω -oxanorbornenyl PEO macromonomers. This procedure needs the previous synthesis of the succinimide-based cyclobutene from cyclobutene dicarboxylic anhydride and *N*-propargylamine.

II-1.1. Anhydride cyclobutene synthesis

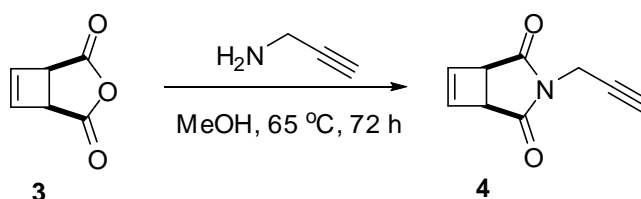
The *cis*-cyclobut-3-ene-1,2-dicarboxylic anhydride precursor **3** (Scheme II-4) is available by photochemical [2 + 2] cycloaddition between maleic anhydride and acetylene. Although this reaction involves inexpensive reagents, it is cumbersome and not totally safe. This hazardous character of the monomers synthesis may explain the limited number of studies dedicated so far to the ROMP of cyclobutene derivatives compared to their norbornene counterpart.^{4,24-32} In our laboratory, a new safe and original synthetic route was developed using (*Z* + *E*)- or (*E*)-dichloroethene as acetylene equivalents (Scheme II-4).³³ The photochemical step at room temperature is safer and less cumbersome. The subsequent step consists in the reductive chlorine elimination in the presence of activated zinc. The best results were obtained in the presence of 12 equivalents of acetic anhydride and 25 equivalents of activated zinc in toluene at 85 °C and the conversion was complete within 3 days, as indicated by ¹H NMR. **3** was isolated in 60% yield after purification by distillation (bp_{0.3 mbar} = 80-120 °C).



Scheme II-4. Synthesis of *cis*-cyclobut-3-ene-1,2-dicarboxylic anhydride **3**.

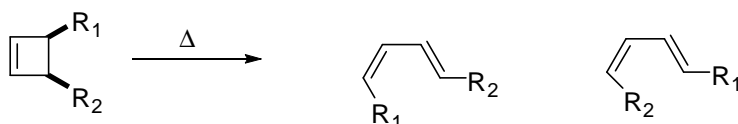
II-1.2. Alkyne-functionalized cyclobutene precursor synthesis

The cyclobutene-based monomer **4** (Scheme II-5) with an alkyne functionality was first prepared in a one step process from *cis*-cyclobut-3-ene-1,2-dicarboxylic anhydride **3** and *N*-propargylamine in the same conditions as used for the oxanorbornene precursor **2**, *i.e.* in MeOH at 65 °C for 72 h (Scheme II-1).



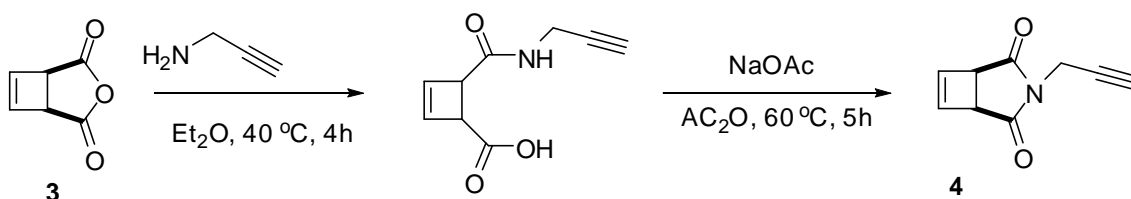
Scheme II-5. Synthesis of alkyne-functionalized cyclobutene precursor **4** by a one step process.

However, under these conditions, the formation of dienes by ring-opening of cyclobutene was observed, as evidenced by the appearance of the double bond resonances on the ^1H NMR spectrum (Figure II-7, A) of the two isomeric (*Z*, *E*)-dienes (Scheme II-6) at 4.00-4.20 and 5.90-6.75 ppm, respectively. This result is in accordance with the previous studies on the thermal ring-opening of cyclobutene derivatives.³⁴⁻³⁸



Scheme II-6. Thermal ring-opening of cyclobutene derivatives.

Therefore, a two-steps process was then used with a shorter reaction time and a lower temperature (Scheme II-7) in diethyl ether according to a literature procedure.³⁹



Scheme II-7. Synthesis of alkyne-functionalized cyclobutene precursor **4**.

An intermediate amido acid was isolated and used without further purification for the second step. The ^1H NMR spectrum (Figure II-7, B) shows the double peak of $\text{CH}=\text{CH}$ protons at 6.35 and 6.47 ppm indicating an unsymmetrical structure while the carboxylic peak was still observed at 8.90 ppm. The methylene group of *N*-propargylamine totally shifted from 3.45 ppm to 4.00 ppm (5, Figure II-7, B) and the integrations of one cyclobutene olefin peak (1, Figure II-7, B) and the $\text{C}\equiv\text{CH}$ proton peak (6, Figure II-7, B) gave a 1:1 ratio indicating the formation of amido acid.

Under mild conditions, *i.e.* 60 °C for 5 h, *N*-prop-2-ynyl-*cis*-cyclobut-3-ene-1,2-dicarboximide **4** was obtained in a 70 % yield. The ^1H NMR spectrum (Figure II-7, C) shows the signal of $\text{CH}=\text{CH}$ protons at 6.47 ppm, and the presence of a doublet peak at 4.24 ppm attributed to the $\text{N}-\text{CH}_2-\text{C}\equiv\text{CH}$. The integration area ratio of the characteristic resonances is in good agreement with the ratio of corresponding protons (Figure II-7, C, 2:2) which demonstrates that full condensation occurred. In this case, the thermal ring-

opening of cyclobutene derivative was not observed anymore. Furthermore, the molecular weight ($M + H^+ = 162.0555$) of **4** from HRMS analysis was in good agreement with the calculated value ($M + H^+ = 162.0500$).

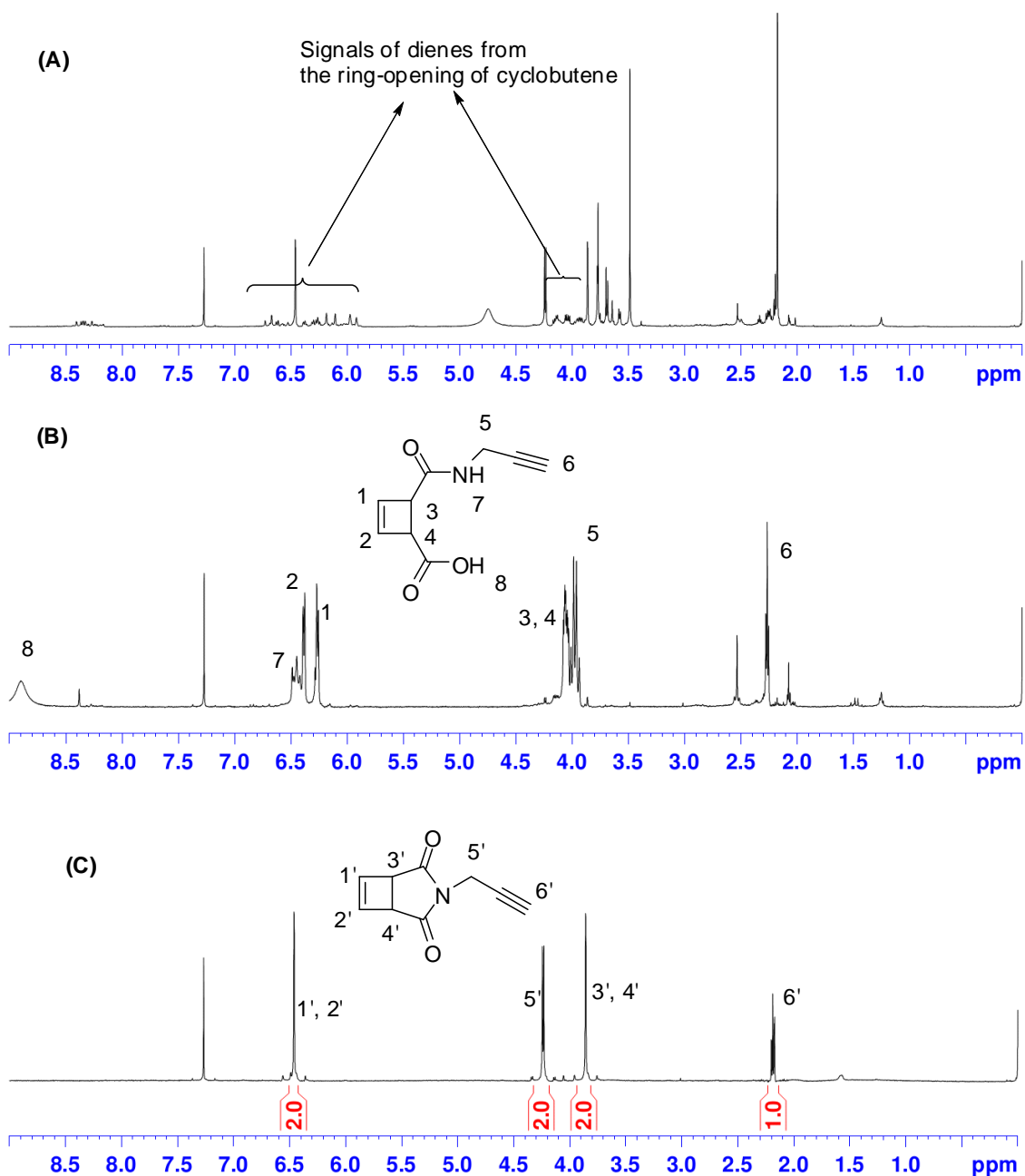
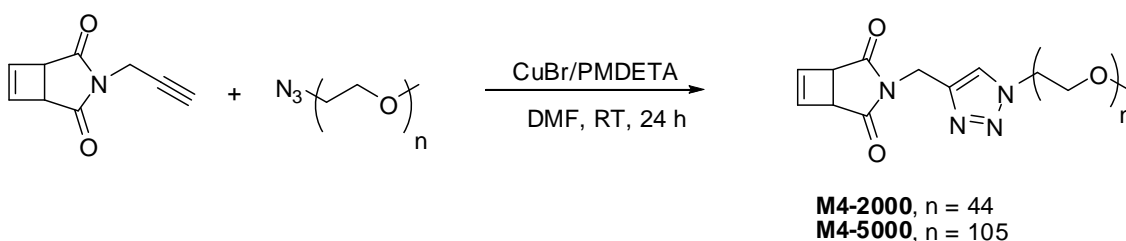


Figure II-7. ^1H NMR spectra of (A) ring-opening of *cis*-cyclobut-3-ene-1,2-dicarboxylic anhydride **3**, (B) amido acid and (C) *N*-prop-2-ynyl-*cis*-cyclobut-3-ene-1,2-dicarboximide **4**; solvent: CDCl_3 .

II-1.3. Macromonomer synthesis by “click” reaction

Macromonomers were then synthesized by “click” reaction between POE-N₃ 2 000 and 5 000 and a stoichiometric amount of alkyne-containing cyclobutene **4** in DMF at room temperature in the presence of a catalytic amount of CuBr with PMDETA as the ligand (Scheme II-8). ¹H NMR spectrum of **M4-2000** (Figure II-8) obtained from POE-N₃ 2 000 clearly showed the end-group transformation. When the terminal azido group was transformed to a triazole ring, the methylene group next to the azido group resonance of the PEO-N₃ disappears at 3.60 ppm and a new methylene group next to the triazole group appears at 4.50 ppm (5, Figure II-8). Moreover, the methylene group of **4** next to the alkyne group disappears at 4.24 ppm and a new methylene group next to the triazole group appears at 4.78 ppm (3, Figure II-8). The newly formed triazole proton (4, Figure II-8) was also observed at 7.70 ppm. Integrations of cyclobutene olefin peak (1, Figure II-8), the signal of the proton on the triazole ring (4, Figure II-8) and the methoxy end-group (8, Figure II-8) peak gave 2:1 and 2:3 ratios, respectively, indicating complete “click” coupling. The same conclusions could be drawn from the reactions between **4** and PEO-N₃ 5 000.



Scheme II-8. Synthesis of ω -cyclobutenyl PEO macromonomers **M4-2000** and **M4-5000**.

Furthermore, the structure of macromonomers **M4-2000** and **M4-5000** was confirmed by MALDI-TOF analysis. For example, the MALDI-TOF mass spectrum of **M4-5000** (Figure II-9) showed a constant value between peaks of $m/z = 44.03$, corresponding to one ethylene oxide unit. The peaks at $m/z = 4863.70$ (calculated value = 4864.15) and at $m/z = 4907.64$ (calculated value = 4908.18) are attributed to sodium-ionized **M4-5000**, where number of ethylene oxide (EO) units are 105 and 106, respectively.

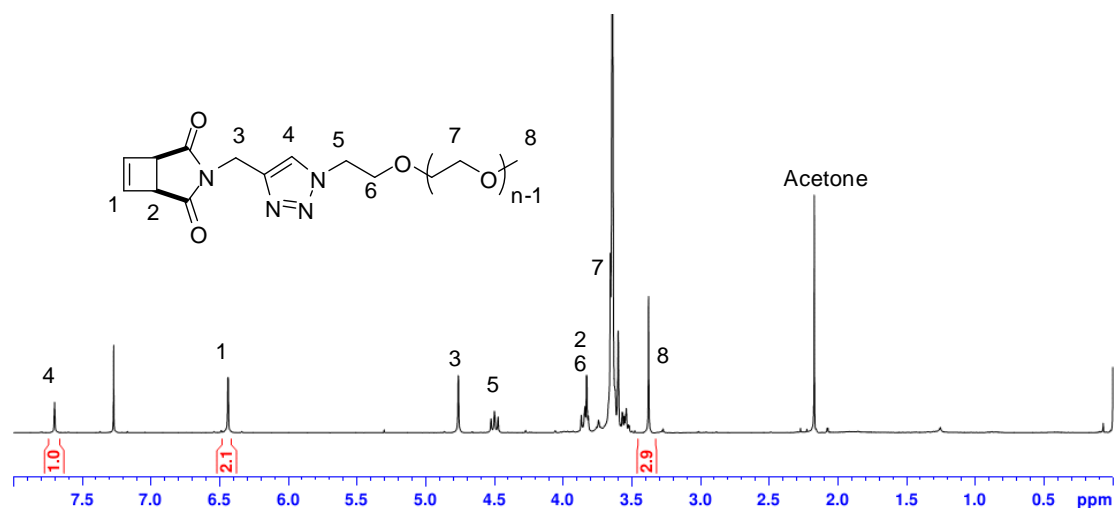


Figure II-8. ^1H NMR spectrum of ω -cyclobutenyl PEO monomethyl ether **M4-2000**; solvent: CDCl_3 .

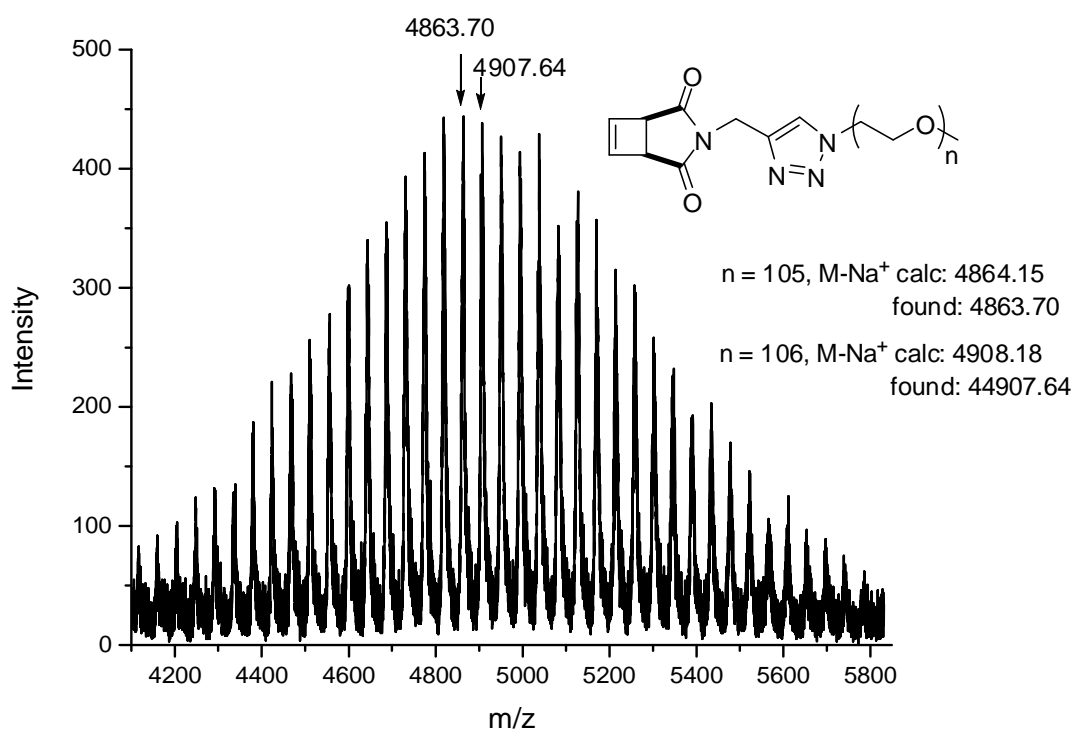


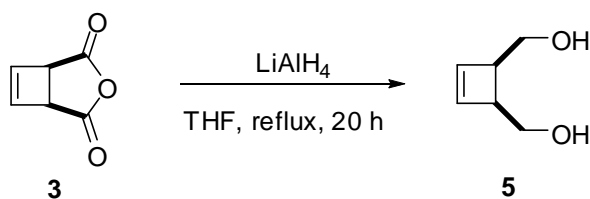
Figure II-9. MALDI-TOF mass spectrum of ω -cyclobutenyl PEO monomethyl ether macromonomer **M4-5000** (matrix: DCTB + NaTFA).

II-2. PEO macromonomers synthesis from bis(hydroxymethyl)cyclobutene

A series of original cyclobutenyl- azido- and alkyne-functionalized precursors was synthesized from the bis(hydroxymethyl)cyclobutene **5** (Scheme II-9) that contains a “ROMP-able” cyclobutene moiety and two hydroxymethyl groups that allowed 2-fold and unsymmetrical functionalization.

II-2.1. Bis(hydroxymethyl)cyclobutene synthesis

Bis(hydroxymethyl)cyclobutene **5** has been synthesized by reduction of **3** (Scheme II-9) using an excess of LiAlH_4 as the reducing agent in THF in 92% yield after purification by extraction with DCM and diethyl ether. The formation of bis(hydroxymethyl)cyclobutene was confirmed by ^1H NMR spectroscopy and the molecular weight ($M + \text{H}^+ = 115.0768$) of **5** from HRMS analysis was in good agreement with the calculated value ($M + \text{H}^+ = 115.0766$).



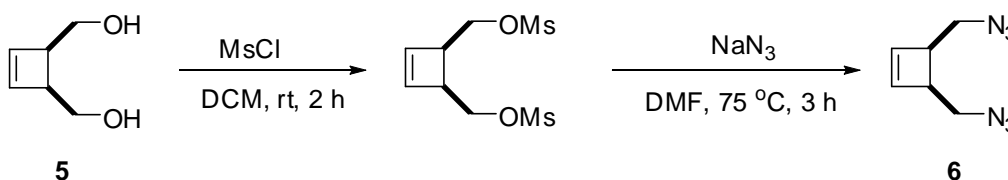
Scheme II-9. Synthesis of bis(hydroxymethyl)cyclobutene **5**.

II-2.2. PEO macromonomer synthesis from azido-functionalized cyclobutene precursor

The hydroxyl groups of **5** can be converted to azido or alkyne groups through activation and subsequent nucleophilic substitution. The azido-functionalized and alkyne-functionalized cyclobutene precursors will be reacted with alkyne-terminated or azido-terminated PEO, respectively, by “click” coupling to form PEO macromonomers.

II-2.2.a. Synthesis of bis(azidomethyl)cyclobutene precursor

Compound **5** has been transformed to bis(azido)cyclobutene **6** by a two-step procedure (Scheme II-10). **5** was first converted to mesylate-functionalized cyclobutene by reaction with methanesulfonyl chloride in 74% yield. Mesylate groups were then transformed into azido groups *via* reaction with NaN_3 in DMF in 66% yield. The structure of bis(azido)cyclobutene was confirmed by ^1H NMR (Figure II-10), with the shift of the peak of the methylene group of **6** from 3.6-3.8 ppm next to 3.4-3.5 ppm (5 & 6, Figure II-10) and the disappearance of the peak of hydroxyl groups at 4.25 ppm.



Scheme II-10. Synthesis of bis(azidomethyl)cyclobutene precursor **6**.

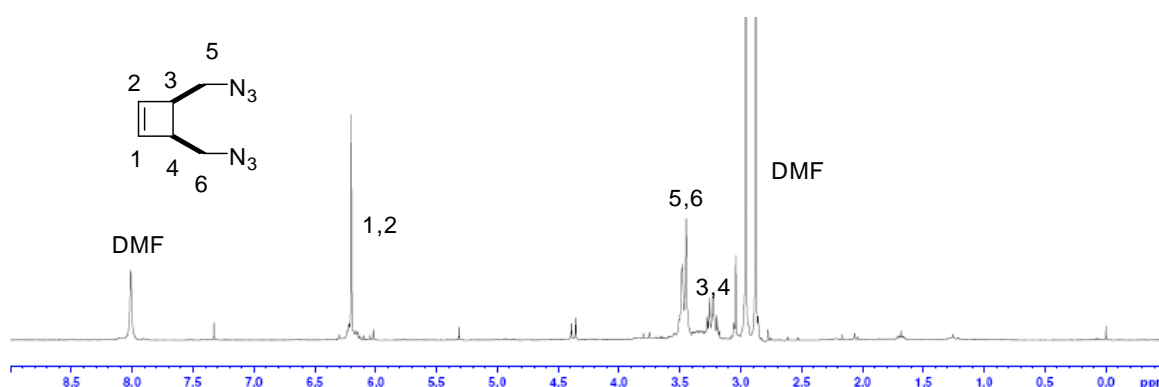
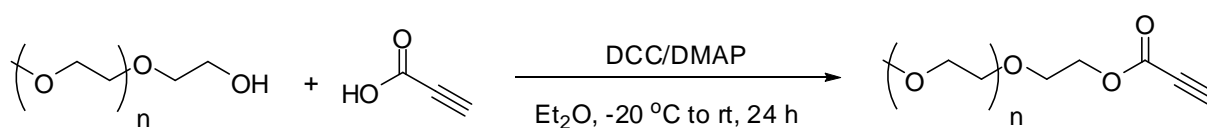


Figure II-10. ^1H NMR spectrum of bis(azido)cyclobutene **6**; solvent: CDCl_3 .

Organic azides are potentially-explosive substances and small molecules containing the azido functionality tend to decompose violently which may result in injury if proper safety precautions are not used. The organic azides with number of carbon/number of nitrogen ratio smaller than 3 should be stored as solutions below room temperature and less than 5 grams of material.^{3a} Compound **6** having $\text{N}_\text{C}/\text{N}_\text{N} = 1$ was thus purified using column chromatography and should be handled with care.

II-2.2.b. BisPEO macromonomer synthesis by “click” reaction

Alkyne-terminated end-chain PEO 2 000 was prepared by esterification of hydroxyl-terminated PEO monomethyl ether and propynoic acid according to a literature procedure (Scheme II-11).³⁹ In order to get good yields, 4-(*N,N*-dimethylamino)pyridine (DMAP) and *N,N'*-dicyclohexylcarbodiimide (DCC) had to be added to the mixture because some polymerization occurred when the acid and DMAP were directly mixed together. Moreover, low addition temperature (-20 °C to rt) had to be used to minimize polymerization risks of the unstable anhydride intermediate.⁴⁰



Scheme II-11. Synthesis of alkyne-terminated PEO 2 000.

The MALDI-TOF mass spectrum (Figure II-11) showed only one series of the expected alkyne-terminated PEO. The difference in mass of each signal of the series was roughly estimated as 44, indicating the signals were assignable to the PEO homologues. The peak at $m/z = 1912.36$ was assigned to a PEO consisting of 41 EO units ionized by a sodium ion and featuring a methyl group at one chain-end and a propynoate group at the other chain-end (calculated value $m/z = 1912.25$). Moreover, the SEC trace of alkyne-terminated PEO also showed a monomodal molecular distribution with low PDI (1.06) (Figure II-12, A).

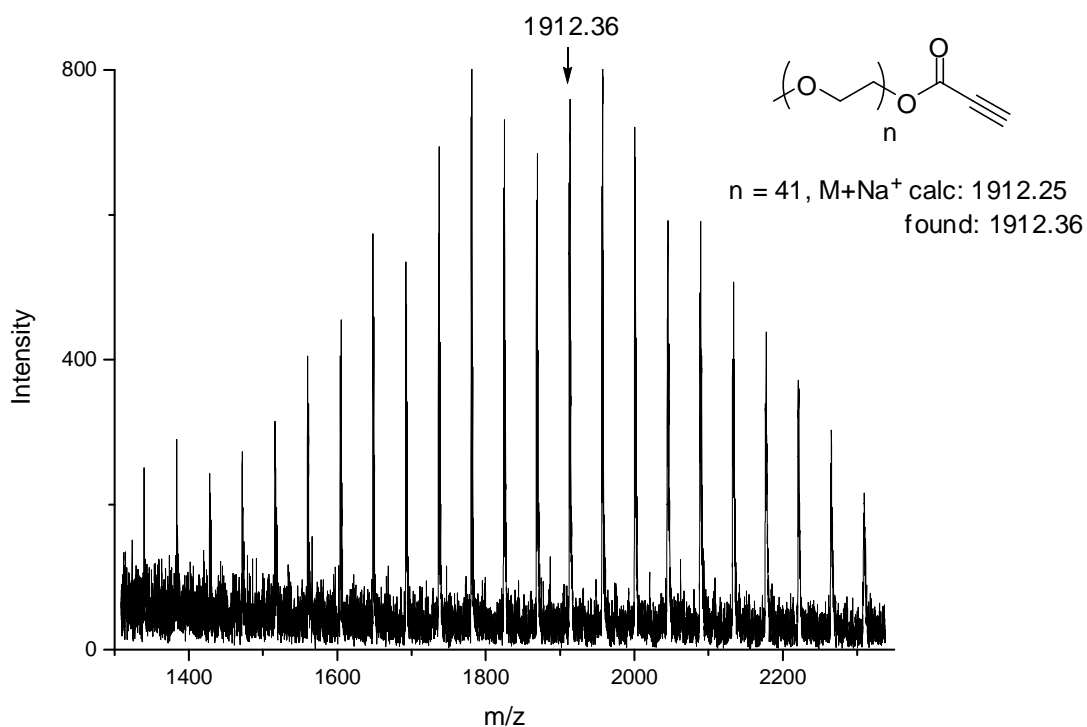
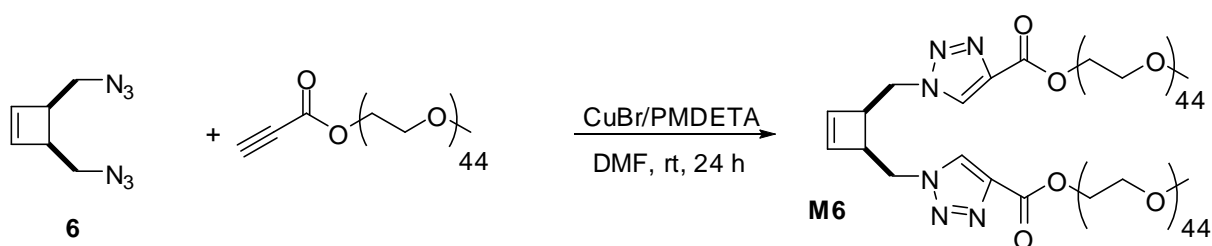


Figure II-11. MALDI-TOF mass spectrum of alkyne-terminated PEO 2 000 (matrix: DCTB + NaTFA).

The two PEO chains macromonomer **M6** (Scheme II-12) was then synthesized by “click” reaction between **6** and 2 equivalents of alkyne-terminated PEO, in the same conditions as already used for the synthesis of the former macromonomers **M2** and **M4**.



Scheme II-12. Synthesis of two chains PEO macromonomer **M6**.

The ^1H NMR showed the characteristic resonance signal of proton on the triazole ring at 8.3 ppm, indicating the “click” coupling has occurred. The integration ratio for protons of cyclobutene olefin and of triazole ring is approximately 2:2 indicating the percentage of reacted **6** was nearly quantitative. However, the SEC chromatogram (Figure II-12, B) of the macromonomer showed two populations. The high molecular weight peak is the

two PEO chains macromonomer, and the low molecular weight peak is correlative either to alkyne-terminated PEO or to one PEO chain macromonomer. The macromonomer could not be purified by precipitation or dialysis.

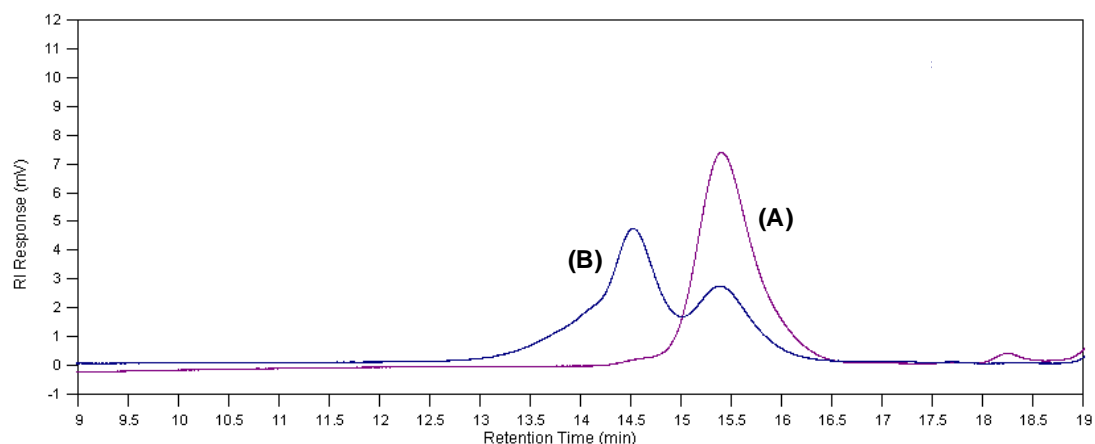


Figure II-12. SEC traces of (A) alkyne-terminated PEO 2 000 and (B) two chains PEO macromonomer **M6**.

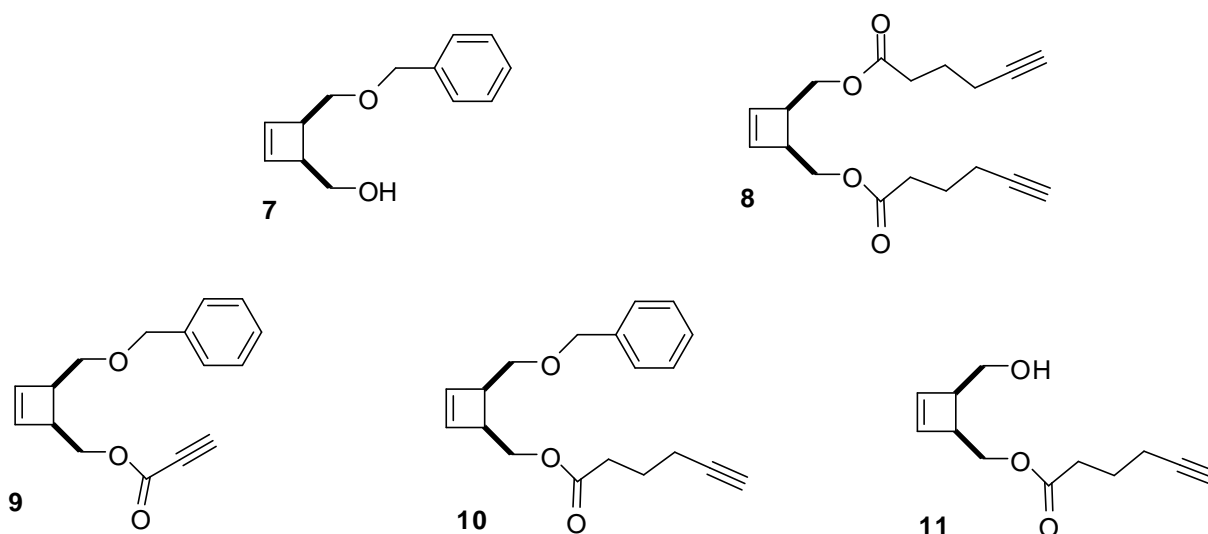
This result is possibly due to the fact that the determination of the exact stoichiometry between alkyne and azido groups becomes difficult when the mass fraction of alkyne chain-end group on the PEO chain is low.⁴¹⁻⁴⁴ In this case, it is not possible to use an excess amount of **6** because that is favorable to form one chain PEO macromonomers.

The second strategy consisting in “click” reaction between the POE-N₃ and symmetrical and unsymmetrical alkyne-functionalized cyclobutenes has then been studied as a more safety procedure. Furthermore, the unsymmetrical functionalization of cyclobutene derivatives is supposed to be easier.³⁵

II-2.3. PEO macromonomers synthesis from alkyne-functionalized cyclobutene precursors

II-2.3.a. Synthesis of alkyne-functionalized cyclobutene precursors

A series of original alkyne-functionalized cyclobutene precursors **8**, **9**, **10** and **11** (Scheme II-13) were synthesized from **5** which contains two hydroxymethyl groups that allowed symmetrical and unsymmetrical functionalization.



Scheme II-13. Protected cyclobutene **7** and alkyne-functionalized cyclobutene precursors **8**, **9**, **10** and **11**.

In order to synthesize a two PEO chains macromonomers by a safe and one step “click” reaction, **8** containing two alkyne groups was synthesized from **5**.

Precursors **9** and **10** were prepared from **5** by a two-steps procedure. First, one hydroxyl group was protected benzyl ether group by using benzyl bromide in DMF. 1.1 equivalent of benzyl bromide was used to ensure protection of only one hydroxyl group. The benzylation was terminated after 4 h and pure product 4-benzyloxymethyl-3-hydroxymethyl cyclobutene **7** was obtained in 51 % yield after purification by silica gel column chromatography using cyclohexane/ethyl acetate (AcOEt) (v/v 5/1) as the eluent. The benzyl group has been chosen as the protecting group because of its high hydrophobicity. Furthermore, it can easily be deprotected by various reagents.^{45,46} The protected cyclobutene **7** was then reacted with propynoic acid using DCC/DMAP as the catalyst. The reaction was realized at low temperature (-20 °C to rt) to minimize polymerization risks of the unstable anhydride intermediate.⁴⁰ The precursor **9** was obtained in 45 % yield after silica gel column chromatography purification using DCM as the eluent. Precursor **10** was also prepared by esterification of **7** and 5-hexynoic acid according to the same procedure and was obtained in 60% yield. **10** presents an additional hydrophobic (-CH₂-)₃ chain according to **9**, which is expected to increase the hydrophobicity of the resulting macromonomers in order to use them in ROMP in aqueous dispersed media.

11 containing two functional orthogonal groups, alkyne and hydroxyl, is supposed to allow the synthesis of macromonomers with two different chains. The alkyne group will be used to introduce a PEO chain by “click” reaction. The hydroxyl group could be used directly as initiator for ring-opening polymerization (ROP) or could be modified in atom transfer radical polymerization (ATRP) initiator⁴¹ or reversible addition-fragmentation chain transfer agent (RAFT) polymerization to introduce a new polymer chain such as polystyrene, poly(*N*-isopropyl acrylamide) (PNIPAM), polymethacrylates. **8** and **11** were simultaneously prepared from **5** and 5-hexynoic acid by esterification in the same conditions as already reported for **9** and **10**. In this reaction, the amount of 5-hexynoic acid influences the percentage of **8** and **11** obtained as reported in Table II-3. Conversions were calculated from ¹H NMR spectrum of the reaction mixture and were based on (**8** or **11**)/**5** ratio. Conversions were about 30% for both **8** and **11** by using 1.0 equivalent of acid. Higher conversions were obtained by increasing the amount of acid (Run 2, Table II-3). If the amount of acid is equal to 2.0 equivalents, only **8** is obtained as the final product.

Table II-3. Synthesis of alkyne-functionalized cyclobutene **8** and **11**.

Run	Equivalent of 5-hexynoic acid	Equivalent of 5	11		8	
			Conversion (%)	Yield (%)	Conversion (%)	Yield (%)
1	1.0	1.0	34	30	33	30
2	1.5	1.0	50	35	50	40
3	2	1.0	0	-	100	75

The ¹H NMR spectra (Figure II-13) of the resulting cyclobutene precursors showed the signal of *CH=CH* protons of cyclobutene at 6.0-6.1 ppm, and the presence of a peak at 2.9 ppm (**7**, Figure II-13, A) or 2.0 ppm (**10**, Figure II-13, B; **8**, Figure II-13, C and **7**, Figure II-13, D) attributed to the *-C≡CH*. The integration area ratios of the characteristic signals are in agreement with the ratios of corresponding protons (Figure II-13, 2:2 for **8**, and 2:1 for **9**, **10**, **11**) which demonstrates that full condensation occurred. Moreover, the molecular weights of **9**, **10** and **11** from HRMS analysis ($M^+ = 256.1117$, 298.1583 and 208.1019 , respectively) were in good agreement with the calculated values ($M^+ = 256.110$, 298.1569 and 208.1099 , respectively).

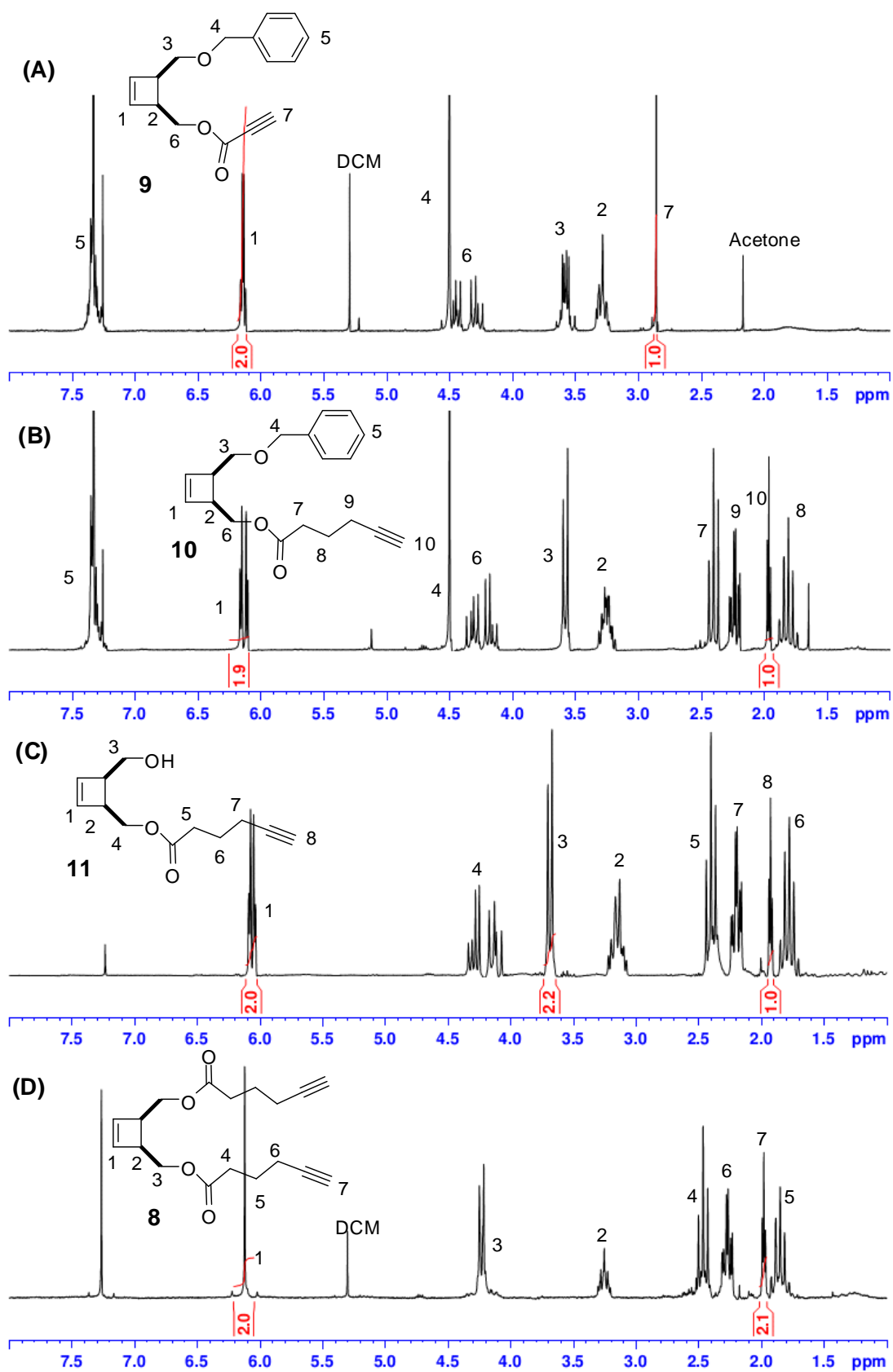


Figure II-13. ^1H NMR spectra of (A) **9**, (B) **10**, (C) **11** and (D) **8**; solvent: CDCl_3 .

II-2.3.b. Two PEO chains macromonomer synthesis by “click” reaction

Two PEO chain macromonomer **M8** (Figure II-14) was prepared from **8** and PEO-N₃ 2 000 by “click” reaction in the conditions reported for **M6**. Two equivalents of azido-terminated PEO were used for the reaction. ¹H NMR spectroscopy clearly showed the end-group transformation. The newly formed triazole proton was observed at 7.50 ppm (7, Figure II-14). When the terminal azido group was transformed to a triazole ring, a new methylene group next to the triazole group appears at 4.50 ppm (8, Figure II-14). The integration ratio for protons of cyclobutene olefin and of triazole ring is approximately 2:2 indicating the percentage of reacted **8** was nearly quantitative. However, the SEC trace and MALDI-TOF spectrum of the isolated product showed a bimodal distribution corresponding to two PEO chains macromonomer **M8** and either to one PEO chain macromonomer or to PEO-N₃ in excess, as already observed for **M6**.

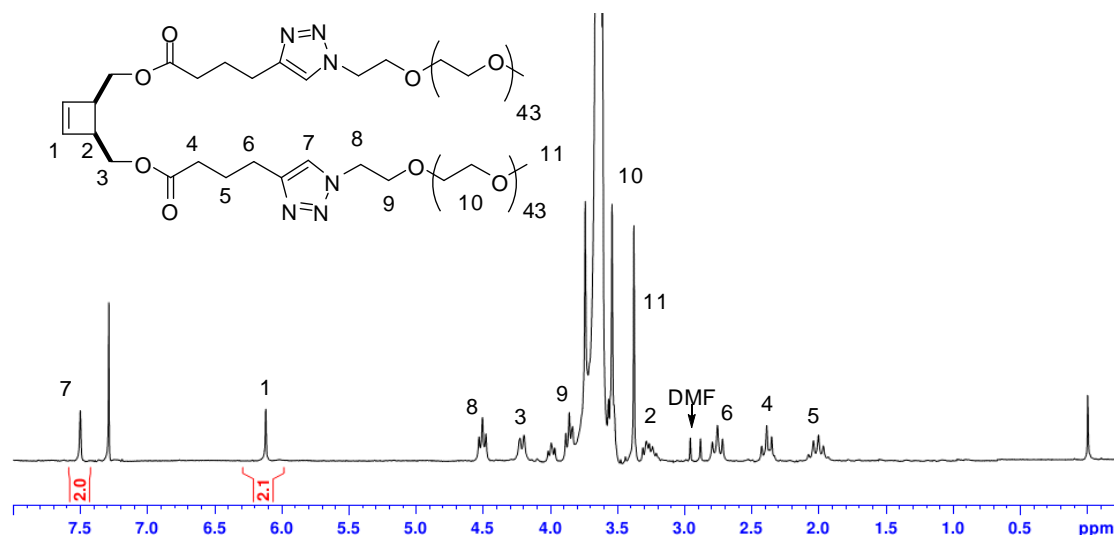
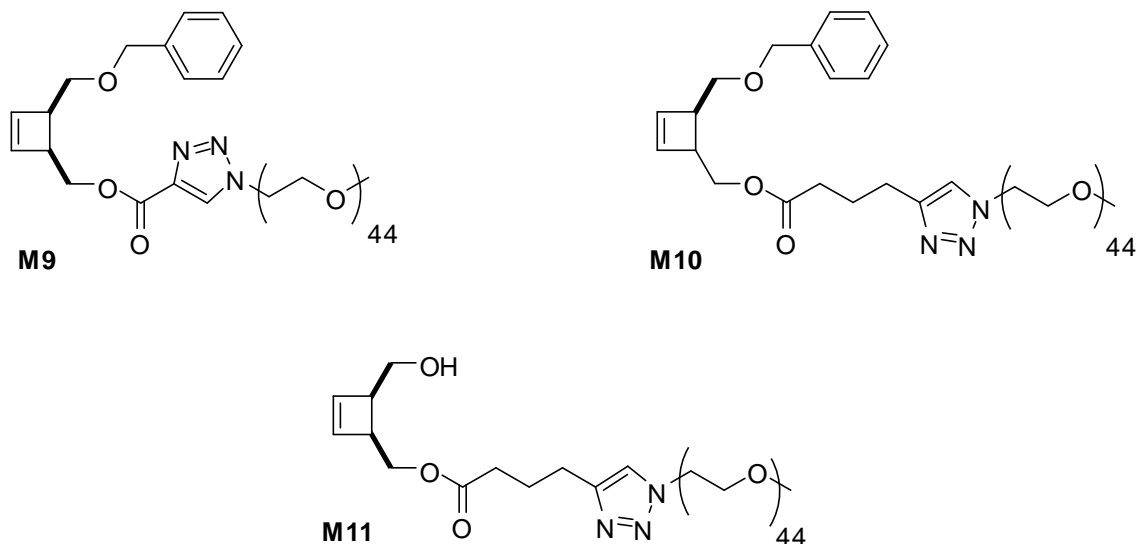


Figure II-14. ¹H NMR spectrum of two PEO chains macromonomer **M8**; solvent: CDCl₃.

Results obtained for the synthesis of two PEO chains macromonomers **M6** and **M8** indicated the difficulty of a quantitative coupling using “click” reaction between polymers and alkyne/azido-containing multifunctional compounds because of the less precisely balanced stoichiometry between azido and alkyne groups.³⁸ Therefore, the synthesis of one PEO chain macromonomers was then developed from unsymmetrical mono-alkyne cyclobutene, based on the success of the synthesis of macromonomers **M2** and **M4**.

II-2.3.c. One PEO chain macromonomers synthesis by “click” reaction

One PEO chain macromonomers **M9**, **M10**, **M11** (Scheme II-14) were then prepared in turn from PEO-N₃ 2 000 and an equivalent of **9**, **10** and **11**, respectively, by “click” reaction in the presence of CuBr/PMDTA as the catalyst in DMF at room temperature.



Scheme II-14. One PEO chain macromonomers **M9**, **M10** and **M11**.

The ¹H NMR spectra (Figure II-15) of macromonomers showed the appearance of the proton on the triazole ring for **M10** and **M11** at 7.5 ppm (10, Figure II-15, B; 8, Figure II-15, C) and next to 8.2 ppm for **M9** (7, Figure II-15, A) because of the electroattractive carbonyl group in β position. The methylene group next to the triazole ring (8, Figure II-15, A; 11, Figure II-15, B and 9, Figure II-15, C) appears at 4.5 ppm. In all cases, integrations of cyclobutene olefin peak, of the triazole ring signal and of the methoxy end-group peak gave 2:1 and 2:3 ratios, respectively, indicating complete “click” coupling. The results of the coupling reactions were reported in Table II-4. The SEC results show that the coupling products have slightly higher molecular weights than the PEO-N₃ 2 000 precursor: such results are consistent with the formation of the macromonomers. Moreover, all macromonomers have low PDIs (< 1.07).

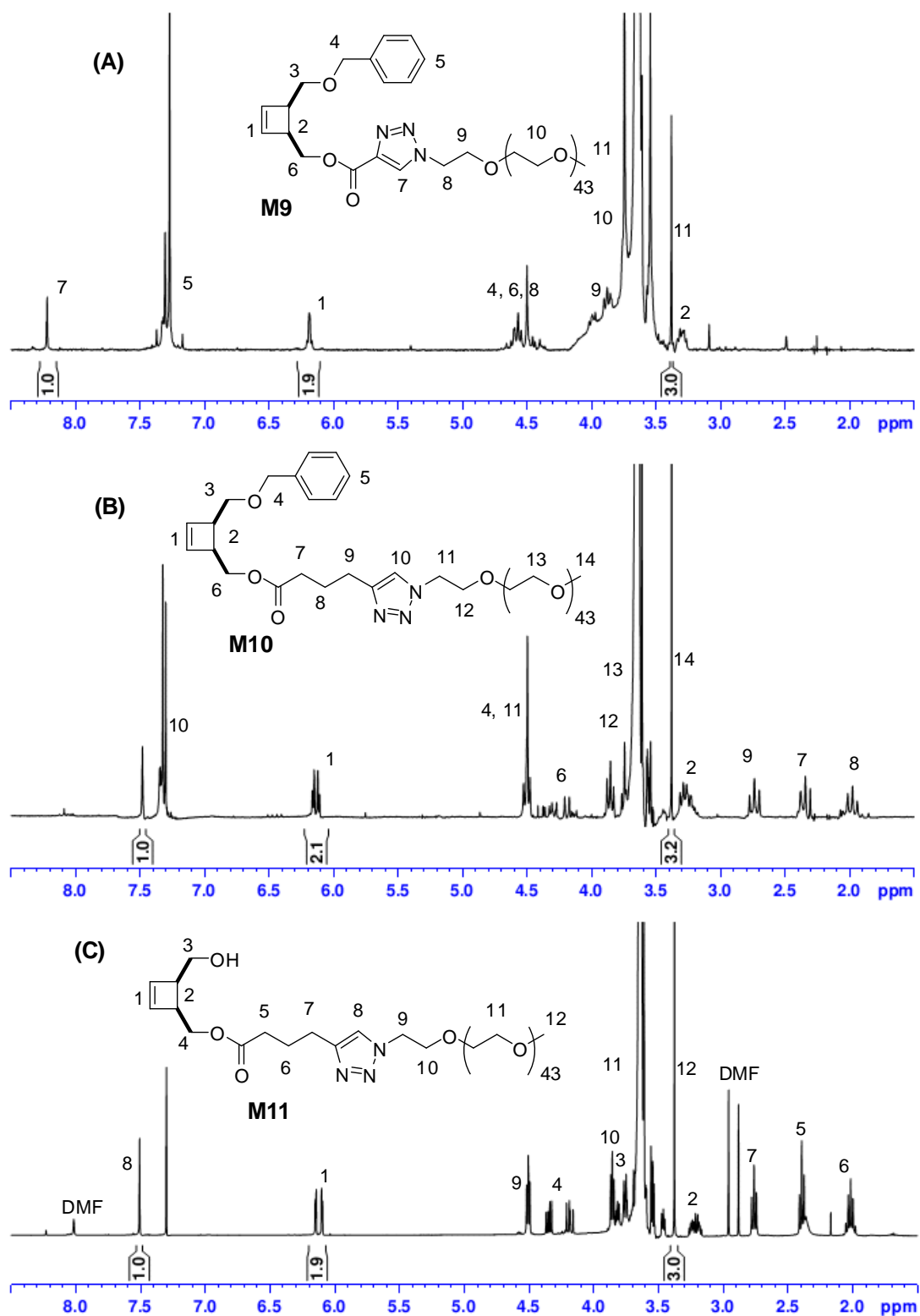


Figure II-15. ^1H NMR spectra of (A) **M9**, (B) **M10** and (C) **M11**; solvent: CDCl_3 .

Table II-4. Characteristics of ω -cycobutenyl PEO monomethyl ether macromonomers **M9**, **M10** and **M11**.

Sample name	Conv. ^a (%)	Yield ^b (%)	$\overline{M}_{n,NMR}$ ^c (g/mol)	$\overline{M}_{n,SEC}$ ^d (g/mol)	PDI ^d
POE-N ₃ 2 000	-	-	2037	3200	1.05
M9	> 95	70	2 293	3 400	1.05
M10	> 95	75	2 335	3 450	1.07
M11	> 95	73	2 245	3 400	1.05

^a Determined by ¹H NMR from the reaction mixture, CDCl₃ as the solvent. ^b After purification. ^c Number-average molecular weight determined by ¹H NMR, CDCl₃ as the solvent. ^d Number-average molecular weight and polydispersity measured by THF SEC with RI detector, calibration with linear polystyrene standards.

Structure of macromonomers was also confirmed by MALDI-TOF analysis. MALDI-TOF mass spectra showed only one series of peaks for each macromonomer (Figure II-16). The difference in mass between each peak in all spectra is estimated as 44, which indicates that the signals are assignable to the PEO homologues. The major peaks labeled 2097.82 (Figure II-16, A), 2140.31 (Figure II-16, B) and 2049.25 (Figure II-16, C) are made up of sodium-ionized macromonomers **M9**, **M10**, **M11**, respectively, with 40 ethylene oxide units (calculated values = 2097.31, 2139.58 and 2049.20, respectively).

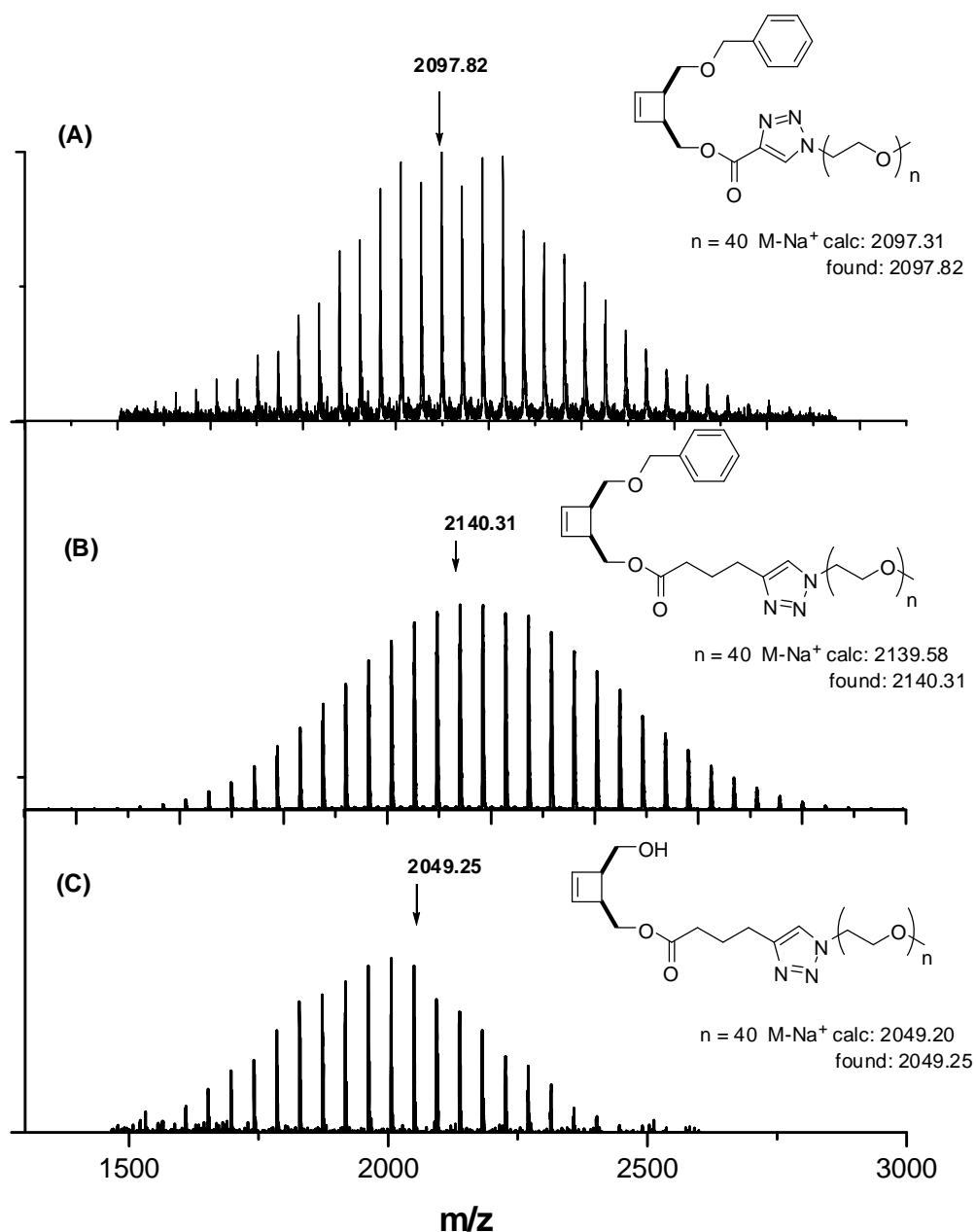


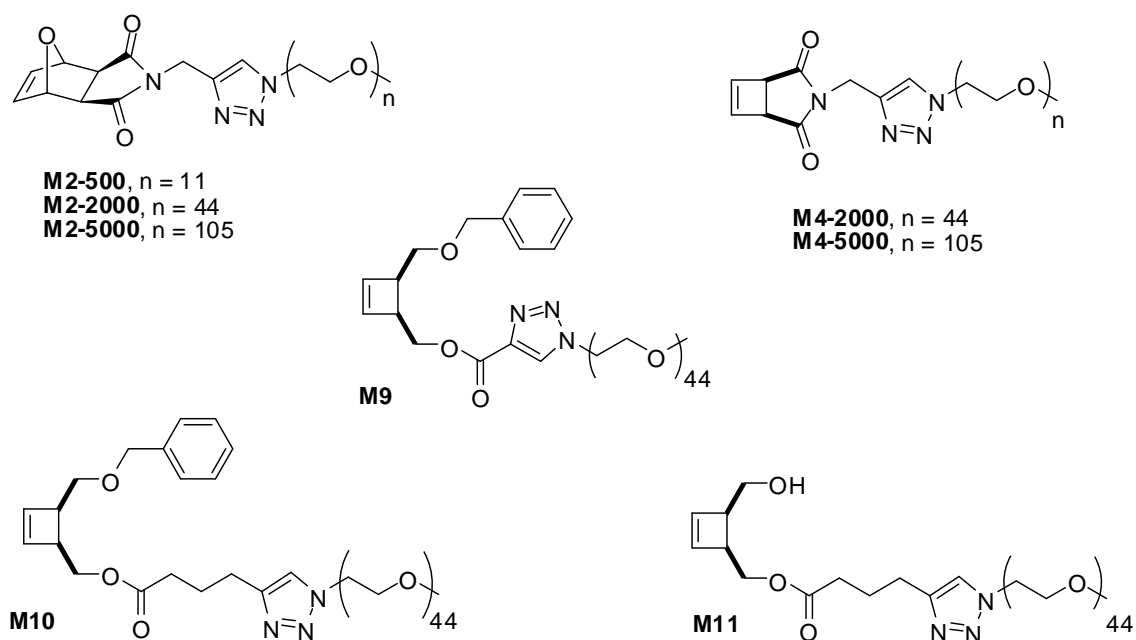
Figure II-16. MALDI-TOF mass spectra of ω -cyclobutenyl PEO monomethyl ether macromonomers (A) **M9**, (B) **M10** and (C) **M11** (matrix: DCTB + NaTFA).

Previous studies indicated that symmetric or unsymmetric cyclobutene precursors were stable up to 100 °C for a duration of 2h,³⁵ which allows to realize the ROMP in a wide range of temperatures. Accordingly, thermal stability of macromonomers was studied. The thermal behavior of one PEO chain macromonomer **M10** was evaluated by TGA under N₂ conditions in order to determine the degradation temperature. The macromonomer showed no change of weight at 200 °C exhibiting only one-step

Conclusion

A series of original PEO macromonomers with a “ROMP-able” group has been synthesized according to a “click” reaction strategy from commercially available PEO.

Three ω -oxanorbornenyl PEO macromonomers were synthesized by “click” reaction between PEO- N_3 of different molecular weights and a succinimide-based oxanorbornene precursor (Scheme II-15). The 1H NMR, MALDI-TOF and SEC results of the resulting macromonomers indicated that the “click” coupling of PEO and oxanorbornene precursors occurred in a quantitative way.



Scheme II-15. PEO macromonomers with a “ROMP-able” group synthesized in this work by “click” reaction.

This strategy has also been applied with the cyclobutene as “ROMP-able” entity. Succinimide-based cyclobutene precursor was synthesized from cyclobutene dicarboxylic anhydride in high yield and engaged in a “click” reaction with PEO- N_3 2 000 and 5 000 to form two ω -cyclobutenyl PEO macromonomers 2 000 and 5 000 (Scheme II-15).

A series of cyclobutene precursors was then synthesized from 3,4-bis(hydroxymethyl) cyclobutene (prepared from cyclobutene dicarboxylic anhydride) that contained one or two alkyne or azido groups. First, symmetric bis(alkyne) and bis(azido)-functionalized cyclobutene precursors were synthesized. The further “click” reaction didn’t allow to obtain a quantitative functionalization of PEO. For this reason, unsymmetric cyclobutene precursors were developed from *cis*-3,4-bis(hydroxymethyl)cyclobut-1-ene with one alkyne group and an orthogonal protecting or non protecting group and different hydrophobic chains. They contain:

- An orthogonal protecting group and one alkyne group, introduced from propynoic acid and 5-hexynoic acid, this latter allowing to move away the “ROMP-able” group and being expected to increase the hydrophobicity of the resulting macromonomer.
- One alkyne group and a hydroxyl functionality which could be used directly as initiator for ROP or could be modified in ATRP initiator³⁸ or RAFT agent to introduce a new polymer chain, as studied in the next chapter of this work.

The “click” reaction was realized between PEO-N₃ 2 000 and the unsymmetric precursors. The near quantitative functionalization of PEO 2 000 with “ROMP-able” cyclobutene precursors (Scheme II-15) has been confirmed by ¹H NMR, MALDI-TOF mass and SEC analysis.

References

1. Harris, J. M. *Poly(Ethylene Glycol) Chemistry: Biotechnical and Biomedical Applications*, Plenum Press, New York, 1992.
2. Neugebauer, D. *Polym. Int.* **2007**, *56*, 1469-1498.
3. (a) Kolb, H.C.; Finn, M.G.; Sharpless, K.B. *Angew. Chem., Int. Ed.* **2001**, *40*, 2004.
(b) Kolb, H. C.; Sharpless, K. B. *Drug Discovery Today* **2003**, *8*, 1128-1137.
4. Grubbs, R. H. (Ed.), *Handbook of Metathesis*, vol. 1&3, Wiley-VHC, Weinheim, 2003.
5. Woodward, R. B.; Baer, H. *J. Am. Chem. Soc.* **1948**, *70*, 1161-1166.
6. Castner, K. F.; Calderon, N. *J. Mol. Catal.* **1982**, *15*, 47-59.
7. Seehof, N.; Grutke, S.; Risse, W. *Macromolecules* **1993**, *26*, 695-700.
8. Wolfe, P. S.; Wagener, K. B. *Macromolecules* **1999**, *32*, 7961-7967.
9. Rule, J. D.; Moore, J. S. *Macromolecules* **2002**, *35*, 7878-7882.
10. Lapinte, V.; Fontaine, L.; Montembault, V.; Campistron, I.; Reyx, D. *J. Mol. Catal. A: Chem.* **2002**, *190*, 117-129.
11. Lapinte, V.; Brosse, J. C.; Fontaine, L. *Macromol. Chem. Phys.* **2004**, *205*, 824-833.
12. Nishihara, Y.; Inoue, Y.; Nakayama, Y.; Shiono, T.; Takagi, K. *Macromolecules* **2006**, *39*, 7458-7460.
13. Czelusniak, I.; Khosravi, E.; Kenwright, A. M.; Ansell, C. W. G. *Macromolecules* **2007**, *40*, 1444-1452.
14. Hamilton, J. G.; Kay, J.; Rooney, J. J. *J. Mol. Catal. A: Chem.* **1998**, *133*, 83-91.
15. Pakula, T.; Zhang, Y.; Matyjaszewski, K.; Lee, H.; Boerner, H.; Qin, S.; Berry, G. C. *Polymer* **2006**, *47*, 7198-7206.
16. Braun, D.; Fischer, M.; Kozera, A. *Eur. Polym. J.* **1996**, *32*, 791-800.
17. Keskkula, H.; Paul, D. R.; McCreedy, K. M.; Henton, D. E. *Polymer* **1987**, *28*, 2063-2069.
18. Lapinte, V.; de Frémont, P.; Montembault, V.; Fontaine, L. *Macromol. Chem. Phys.* **2004**, *205*, 1238-1245.
19. Gao, H.; Matyjaszewski, K. *J. Am. Chem. Soc.* **2007**, *129*, 6633-6639.

20. Samanta, D.; Kratz, K.; Zhang, X.; Emrick, T. *Macromolecules* **2008**, *41*, 530-532.
21. Mantovani, G.; Lecolley, F.; Tao, L.; Haddleton, D. M.; Clerx, J.; Cornelissen, J. J. L. M.; Velonia, K. *J. Am. Chem. Soc.* **2005**, *127*, 2966-2973.
22. Blicke, F. F.; Godt, H. C. Jr. *J. Am. Chem. Soc.* **1954**, *76*, 2835-2836.
23. Sumerlin, B. S.; Vogt, A. P. *Macromolecules* **2010**, *43*, 1-13.
24. Perrot, M. G.; Novak, B. M. *Macromolecules* **1996**, *29*, 1817-1823.
25. Perrot, M. G.; Novak, B. M. *Macromolecules* **1995**, *28*, 3492-3494.
26. Charvet, R.; Novak, B. M. *Macromolecules* **2001**, *34*, 7680-7685.
27. Wu, Z.; Wheeler, D. R.; Grubbs, R. H. *J. Am. Chem. Soc.* **1992**, *114*, 146-151.
28. Wu, Z.; Grubbs, R. H. *Macromolecules* **1995**, *28*, 3502-3508.
29. Maughon, B. R.; Weck, M.; Mohr, B.; Grubbs, R. H. *Macromolecules* **1997**, *30*, 257-265.
30. Maughon, B. R.; Grubbs, R. H. *Macromolecules* **1997**, *30*, 3459-3469.
31. Weck, M.; Mohr, B.; Maughon, B. R.; Grubbs, R. H. *Macromolecules* **1997**, *30*, 6430-6437.
32. Lee, J. C.; Parker, K. A.; Sampson, N. S. *J. Am. Chem. Soc.* **2006**, *128*, 4578-4579.
33. Gauvry, N.; Comoy, C.; Lescop, C.; Huet, F. *Synthesis* **1999**, 574-576.
34. Niwayama, S.; Houk, K. N. *Tetrahedron Lett.* **1993**, *34*, 1251-1258.
35. Pioge, S.; Morandi, G.; Legoupy, S.; Montembault, V.; Pascual, S.; Fontaine, L. *Macromolecules* **2008**, *41*, 9595-9601.
36. Gauvry, N.; Lescop, C.; Huet, F. *Eur. J. Org. Chem.* **2006**, 5207-5218.
37. Boucheron, C.; Guillarme, S.; Legoupy, S.; Dubreuil, D.; Huet, F. *Synthesis* **2006**, *4*, 633-636.
38. Gourdel-Martin, M. E.; Huet, F. *Tetrahedron Lett.* **1996**, *37*, 7745-7748.
39. Cava, M. P.; Deana, A. A.; Muth, K.; Mitchell, M. J. *Organic Synthesis, Coll.* **1973**, *5*, 944.
40. Balas, L.; Jousseume, B.; Langwost, B. *Tetrahedron* **1989**, *30*, 4525-4527.
41. Gao, H.; Matyjaszewski, K. *Macromolecules* **2006**, *39*, 4960-4965.
42. Riva, R.; Schmeits, S.; Jérôme, C.; Jérôme, R.; Lecomte, P. *Macromolecules* **2007**, *40*, 796-803.
43. Opsteen, J. A.; van Hest, J. C. M. *Chem. Commun.* **2005**, 57-59.

44. Engler, A. C.; Lee, H.; Hammon, P. T. *Angew. Chem. Int. Ed.* **2009**, *48*, 9334-9338.
45. Green, T. W.; Wuts, P. G. M. *Protective Groups in Organic Synthesis*, Wiley-Interscience, New York, **1999**, 76-86 & 708-711.
46. Congreve, M. S.; Davison, E. C.; Fuhry, M. A. M.; Holmes, A. B.; Payne, A. N.; Robinson, R. A.; Ward, S. E. *Synlett.* **1993**, 663-664.

Chapter III

Synthesis of α -cyclobutenyl macromonomers by RAFT polymerization

Introduction

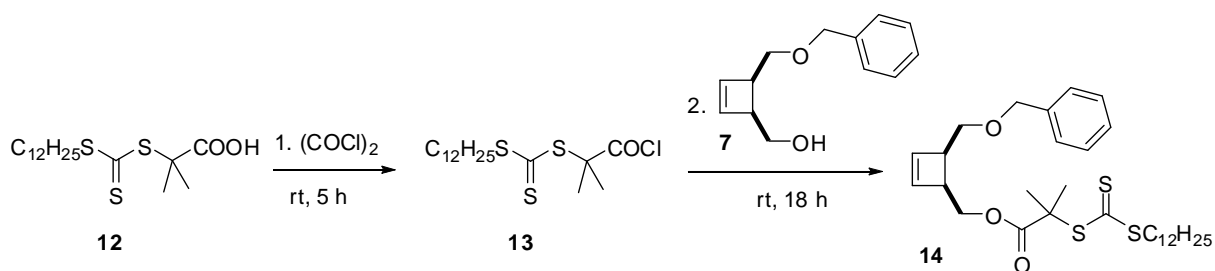
Reversible addition-fragmentation chain transfer (RAFT) process is one of the most versatile controlled/living free radical methods to prepare complex macromolecular structures. It can be used with a wide range of monomers such as (meth)acrylates, styrene, (meth)acrylamides and is tolerant towards a variety of functional groups such as hydroxyl, acid, and amide.¹⁻³ Recently, a number of studies have demonstrated the compatibility of RAFT polymerization together with ring-opening metathesis polymerization (ROMP) in the “grafting through” approach.⁴⁻¹⁰ This strategy has given access to a series of polynorbornene backbone-based brush copolymers with a variety of morphologies by using styrene (Sty), *tert*-butyl acrylate (*t*BA), methyl acrylate (MA) and methyl methacrylate (MMA). Herein, we are interested in this “grafting through” strategy to synthesize polybutadiene graft copolymers from macromonomers with self-assembling properties allowing the polymerization in dispersed media. Furthermore, RAFT polymerization gives access to macromonomers with water-soluble and thermo-sensitive properties. The latter could be used for the preparation of responsive water-soluble molecular brushes¹¹ in solution or in dispersed media from polyacrylamide macromonomers¹² or double-hydrophilic macromonomers.¹³

In this chapter, we present the synthesis of a new cyclobutene-based chain transfer agent from a trithiocarbonate chain transfer agent and its efficiency in RAFT polymerization of acrylate and acrylamide monomers to form α -cyclobutenyl macromonomers. The combination of “click” and RAFT polymerization was also used to prepare cyclobutene-based block copolymers from cyclobutene-based chain transfer agent, poly(ethylene oxide) (PEO) and acrylic monomers. Firstly, a PEO-based RAFT agent was synthesized from a dual-functionalized “click”-RAFT agent cyclobutene by “click” reaction. It was then used as a macromolecular chain transfer agent (macro-CTA) for the RAFT polymerization of *N*-isopropyl acrylamide (NIPAM) affording cyclobutene-based poly(ethylene oxide)-*b*-poly(*N*-isopropylamide) (PEO-*b*-PNIPAM) copolymers.

I- Synthesis of cyclobutene-based chain transfer agent synthesis

S-1-dodecyl-S'-(α , α' -dimethyl- α'' -acetic acid) trithiocarbonate **12** (Scheme III-1) was chosen as the RAFT agent because of its high chain-transfer efficiency and control over radical polymerization.¹⁴ Moreover, it was proven to be compatible with the “ROMP-able” norbornenyl functionality as α -norbornenyl macromonomers have been successfully synthesized by RAFT polymerization.⁵⁻¹⁰ Furthermore, its carboxylic functionality allows for the facile introduction of different functional groups such as butene-1,4-diol¹⁵, alkyne group¹⁶ or a polymeric chain¹⁷ into the RAFT agent structure by esterification.

The chain transfer agent (CTA) containing a cyclobutene group **14** (Scheme III-1) was synthesized by esterification between acyl chloride **13** and alcohol **7**.¹⁵ Compound **7** has been chosen as cyclobutene-containing reagent because it has two functional orthogonal groups, benzyl and hydroxyl, which are supposed to allow the synthesis of macromonomers with two different chains. The hydroxyl group will be used to introduce a CTA; the benzyl group can easily be deprotected by various reagents¹⁸ and the resulting hydroxyl functionality could be further modified in an initiating group, a CTA or a “clickable” moiety.



Scheme III-1. Synthesis of cyclobutene-functionalized CTA **14**.

Acyl chloride **13** was prepared *in situ* from the commercially available CTA **12** and an excess of oxalyl chloride. After removal of the chlorinating agent in vacuo, **13** was immediately reacted with a stoichiometric amount of **7** resulting in an evolution of HCl gas. Purification of the reaction mixture by silica gel column chromatography eluted with dichloromethane (DCM) provides **14** in high yield (80%) as a yellow oil. ¹H NMR and HRMS analyses confirmed the structure and the purity of **14**. ¹H NMR spectrum

(Figure III-1) shows a shift of the methylene group next to the hydroxyl group (10, Figure III-1, A) from around 3.65 ppm to 4.25 ppm (10', Figure III-1, B) corresponding to the protons linked to the acetyl group. The vinyl protons of cyclobutene also shifted from 5.95-6.05 ppm (1 & 2, Figure III-1, A) to 6.08-6.18 ppm (1' & 2', Figure III-1, B) indicating the modification of the OH functionality. Integration area ratios of the cyclobutene olefin peaks (1' & 2', Figure III-1, B) and the methyl peak of the CTA (14', Figure III-1, B) gave a 2:3 ratio which demonstrated a quantitative coupling. Moreover, high resolution mass spectrometry (HRMS) analysis revealed a molecular weight for **14** ($M + H^+ = 551.2687$) in exact agreement with the calculated value ($M + H^+ = 551.2687$).

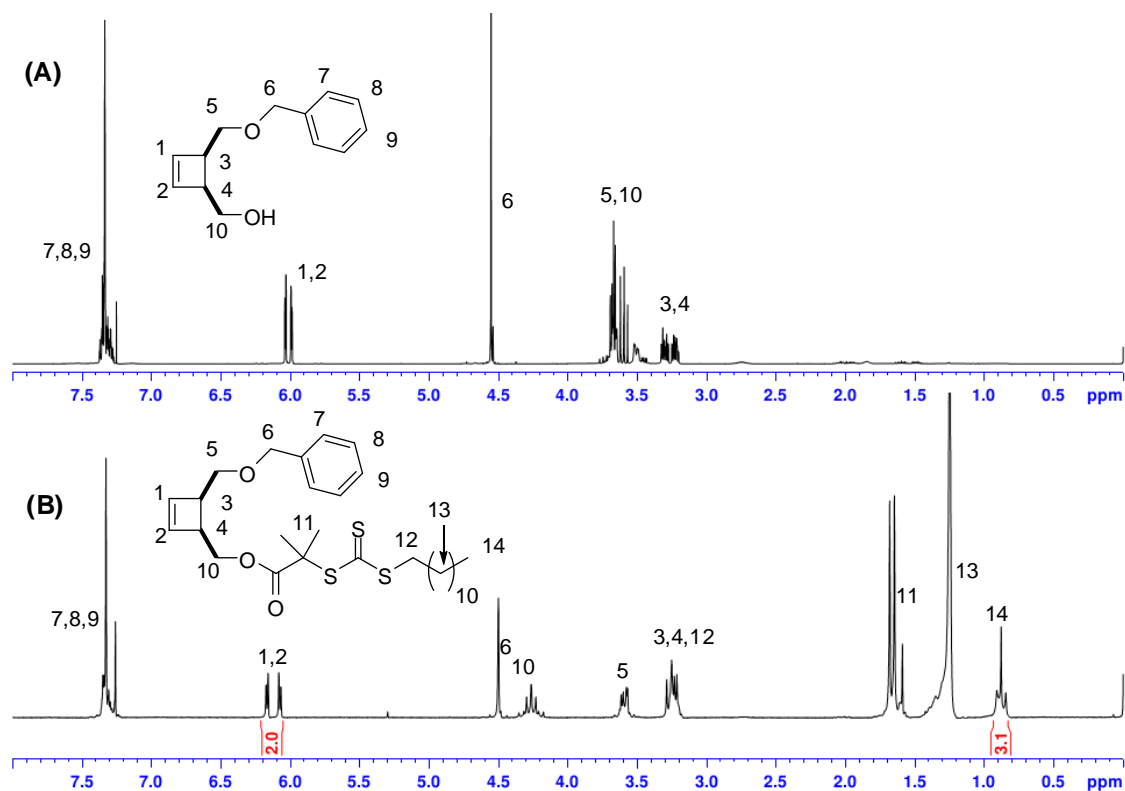


Figure III-1. ^1H NMR spectra of (A) *cis*-4-benzyloxymethyl-3-hydroxymethylcyclobut-1-ene **7** and (B) cyclobutene-based CTA **14**; solvent: CDCl_3 .

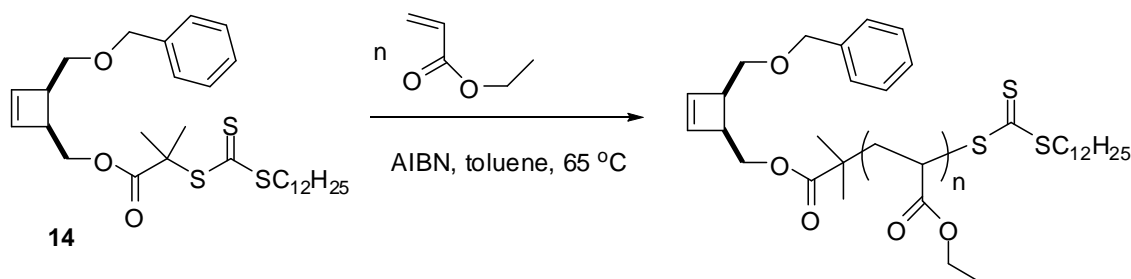
This new CTA has then been tested to prove its efficiency to promote RAFT polymerization of acrylate and acrylamide monomers.

II- RAFT polymerization using cyclobutene-based chain transfer agent

The ability of **14** to mediate RAFT polymerization has been studied using ethyl acrylate (EA) and *N*-isopropyl acrylamide (NIPAM) as monomers.

II-1. RAFT polymerization of ethyl acrylate

CTA **14** was first engaged in RAFT polymerization of EA with 2,2'-azobis(isobutyronitrile) (AIBN) as the radical initiator in toluene at 65 °C¹⁴ (Scheme III-2).



Scheme III-2. RAFT polymerization of EA using cyclobutene-functionalized CTA **14**.

The kinetics of RAFT polymerization of EA using CTA **14** has been performed using the following conditions: $[EA]_0/[14]_0/[AIBN]_0/[DMF]_0 = 100/1/0.1/30$ in toluene (1/1 v/v) at 65 °C. *N,N*-dimethylformamide (DMF) was used as the internal standard in order to determine the monomer conversion, calculated from ¹H NMR analysis, using equation 1:

$$\text{Conversion} = \left(1 - \frac{I_H^t / I_{DMF}^t}{I_H^o / I_{DMF}^o} \right) \times 100 \quad (1)$$

where, I_H^o and I_H^t are the integrations for the vinyl protons of EA at 5.70-5.80 ppm at initial moment and over time of polymerization, respectively, while I_{DMF}^o and I_{DMF}^t are the integrations for the formamide proton of DMF at 8.02 ppm at initial moment and

over time of polymerization, respectively (Figure III-2). Details of the kinetic investigations are listed in Table III-1.

Table III-1. RAFT polymerization of EA using **14** as the CTA and AIBN as the initiator in toluene at 65 °C.

Run	Time (min)	Conversion ^a (%)	$\overline{M}_{n,calc.}^b$ (g/mol)	$\overline{M}_{n,SEC}^c$ (g/mol)	PDI ^c
1	30	23	2 850	3 700	1.11
2	60	48	5 350	5 770	1.08
3	90	64	6 950	7 800	1.06
4	120	72	7 550	8 600	1.08
5	150	75	8 050	8 670	1.08

^a Monomer conversions were determined using ¹H NMR spectroscopy by comparing the integrations of the vinyl resonances (at 5.70 - 5.80 ppm) and the formamide proton resonance of DMF (at 8.02 ppm). ^b

$\overline{M}_{n,calc.} = ([EA]_0/[14]_0) * (\text{molar mass of EA}) * (\text{EA conversion}) + \text{molar mass of the chain-ends.}^c$
Number-average molecular weight and polydispersity index measured by steric exclusion chromatography (SEC) in tetrahydrofuran (THF) with refractive index (RI) detector, calibration with linear polystyrene standards.

75% conversion of EA (Entry 5, Table 1) has been reached after 150 min, which is in good agreement with the efficiency of trithiocarbonate **12** in the RAFT polymerization of EA.¹⁴

During the RAFT process, the ln([M]₀/[M]) versus time plot (Figure III-3, B) clearly showed linearity up to 72 % of monomer conversion which is compatible with a constant concentration of propagating species. The deviation from linearity can be attributed to biradical coupling reactions.

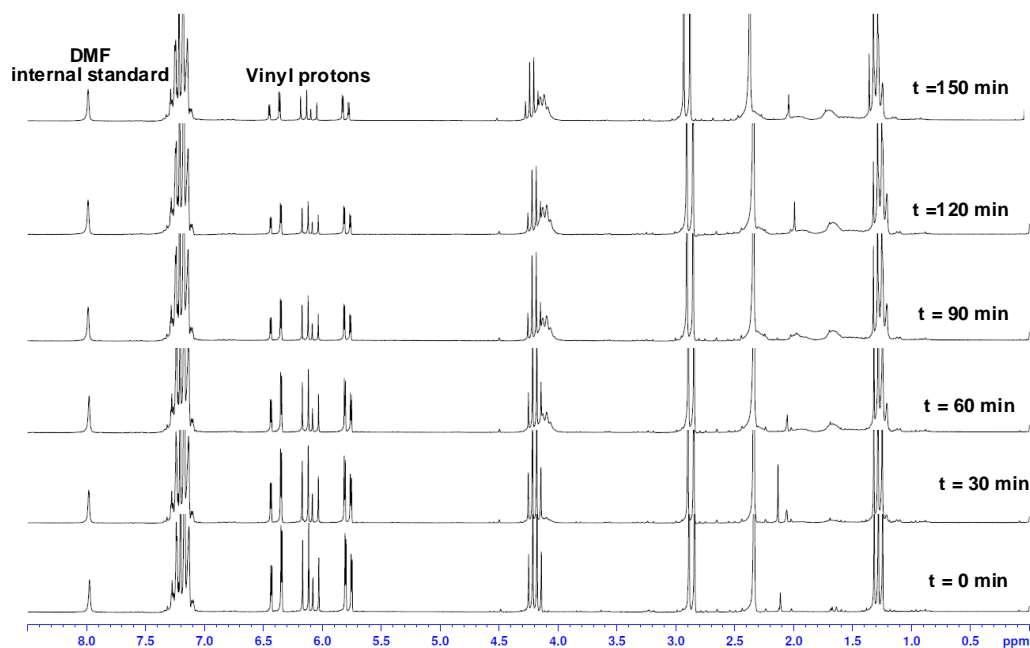


Figure III-2. ^1H NMR spectra of the raw polymerization with time for the RAFT polymerization of EA using **14** as the CTA; solvent: CDCl_3 .

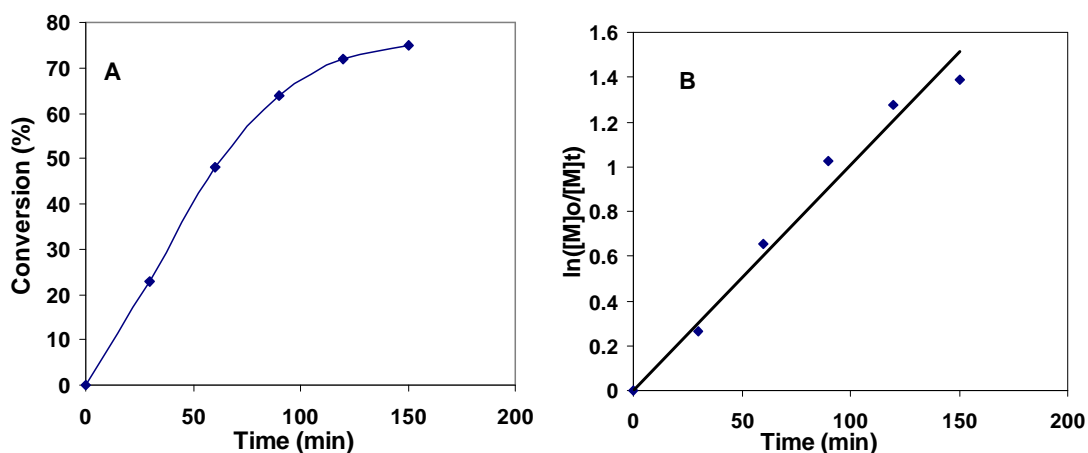


Figure III-3. (A) Evolution of monomer conversion with time and (B) first-order kinetic plot for the RAFT polymerization of EA using CTA **14**.

As shown in Figure III-4, the number-average molecular weight measured by SEC with RI detector ($\overline{M}_{n,SEC}$) values are close to the calculated ones. The $\overline{M}_{n,SEC}$ increased linearly with conversion. The polydispersity index (PDI) first decreases with conversion to reach low values (1.06 at 64% conversion). Then, above 72% conversion, PDI begins to increase, since the probability of termination reactions increases when the monomer concentration decreases.¹⁹⁻²¹

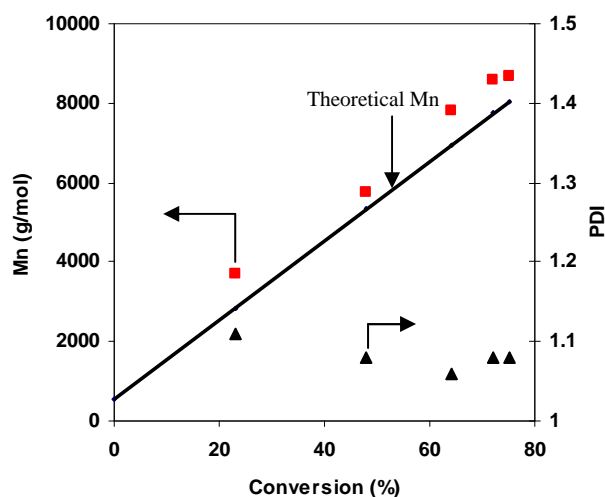


Figure III-4. Evolution of $M_{n,SEC}$ and PDI with conversion for the RAFT polymerization of EA using CTA 14.

The SEC chromatograms (Figure III-5) show a shift towards higher molecular weights as the polymerization time increases. Symmetrical chromatograms are also observed throughout the polymerization up to 48% of monomer conversion.

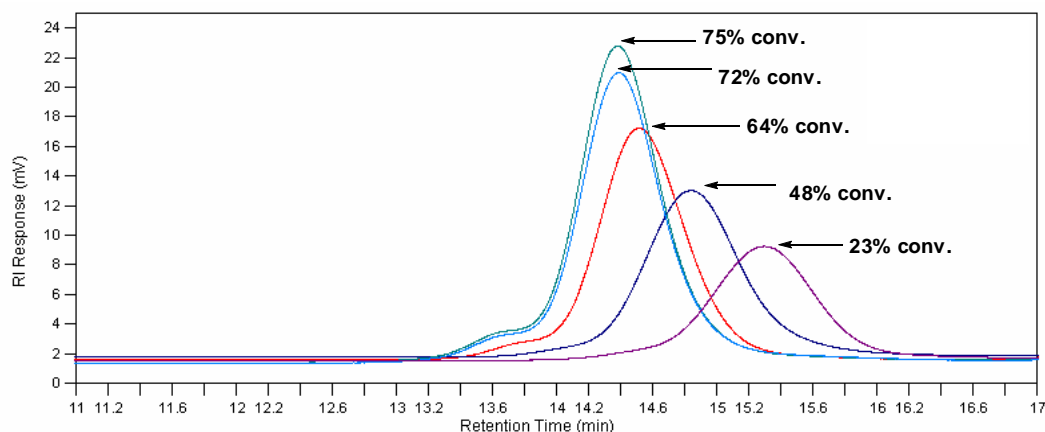


Figure III-5. Evolution of SEC traces (using RI detection) with time for the RAFT polymerization of EA using CTA 14.

The high molecular weight shoulder observed in the SEC trace at high conversion (> 64%) is consistent with radical coupling reactions. This hypothesis is in accordance with previous studies on the polymerization of EA using CTA 12¹⁴, as it was demonstrated a loss of molecular weight control and a resulting PDI of 1.43 when a

high molecular weight EA homopolymer ($\overline{M}_{n,SEC} = 6800$ g/mol) was targeted. To check the occurrence of cyclobutenyl copolymerization, a RAFT polymerization was realized with an initially low monomer to CTA ratio (40/1). The RAFT polymerization was allowed to reach a high monomer conversion to create the conditions of the eventual polymerization of cyclobutene. Monomer conversion was determined from ^1H NMR spectroscopy by following the disappearance of the vinyl peaks of EA at 5.80 ppm, using the methylene peak at 4.50 ppm (6, Figure III-6) of CTA **14** as an internal standard.

After 24h of polymerization, the EA monomer conversion reached 90%. The ^1H NMR spectrum of the resulting polymer after purification by precipitation in water (Figure III-6) showed the presence of the double bond of cyclobutene at 6.1-6.2 ppm (1 & 2, Figure III-6), and the ratio of vinyl peak integration of cyclobutene and the methyl peak integration of CTA at 0.9 ppm (18, Figure III-6) is approximately 2/3, indicating that the cyclobutenyl group of **14** remains intact during the polymerization.

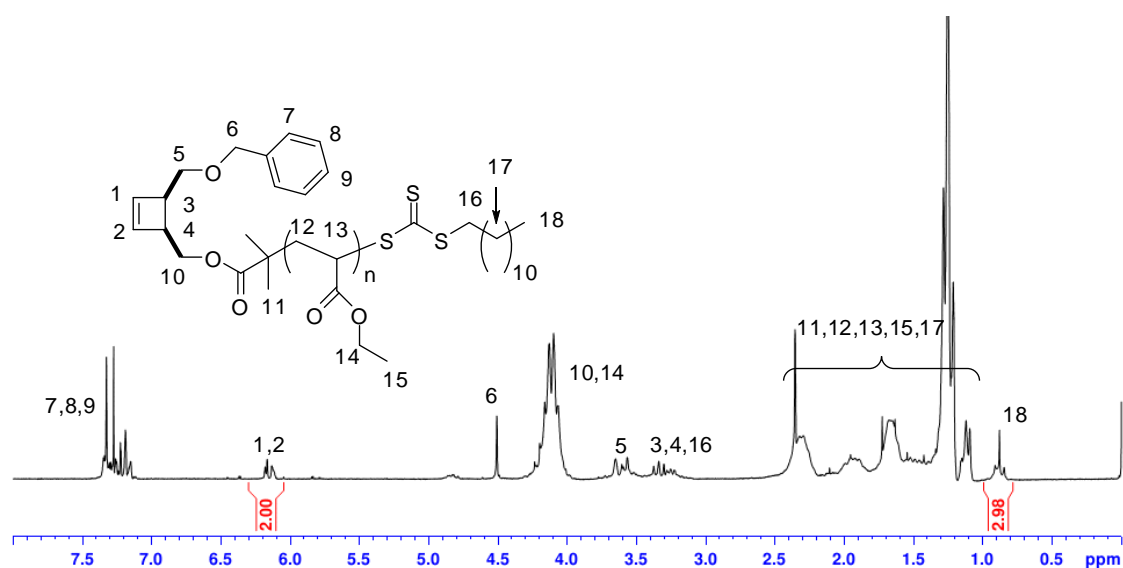


Figure III-6. ^1H NMR spectrum of α -cyclobutenyl poly(ethyl acrylate) macromonomer; solvent: CDCl_3 .

SEC chromatogram with RI detector (Figure III-7, A) showed an unimodal molecular distribution with PDI of 1.06 also confirming the well-controlled polymerization. The retention of the trithio-moiety terminus in the resulting polymer was confirmed by the presence of a peak on the SEC chromatogram with ultraviolet-visible (UV-Vis) detector

at 309 nm (Figure III-7, B), corresponding to the absorption of the chromophoric C=S bond of the RAFT agent.

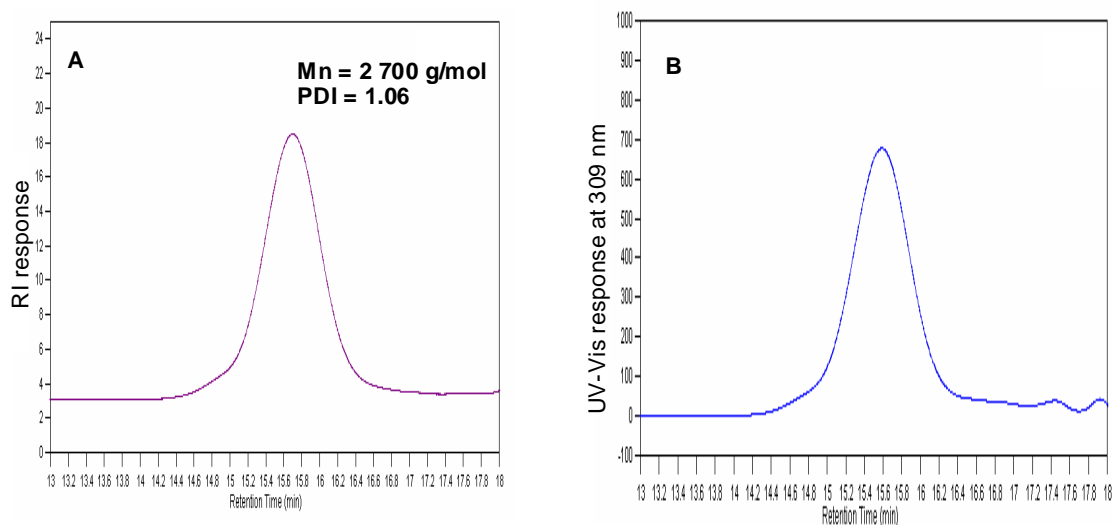


Figure III-7. SEC traces of α -cyclobutenyl poly(ethyl acrylate) with (A) RI detector and (B) UV-Vis detector at 309 nm.

Furthermore, the exact structure of the polymer was confirmed by matrix assisted laser desorption/ionization-time of flight (MALDI-TOF) mass spectrometry analysis. The MALDI-TOF mass spectrum showed only one series of peaks which has a constant value between peaks of $m/z = 100.05$ (Figure III-8), corresponding to one EA unit (calculated value = $100.05 \text{ g}\cdot\text{mol}^{-1}$). The peaks at $m/z = 1874.00$ (calculated value = 1873.91) and at $m/z = 1973.98$ (calculated value = 1973.96) are attributed to sodium-ionized polymer with a 4-benzyloxymethyl-3-hydroxymethylcyclobut-1-ene group at one chain-end and a trithiocarbonate moiety with a dodecyl chain at the other chain-end, where number of EA units are 13 and 14, respectively.

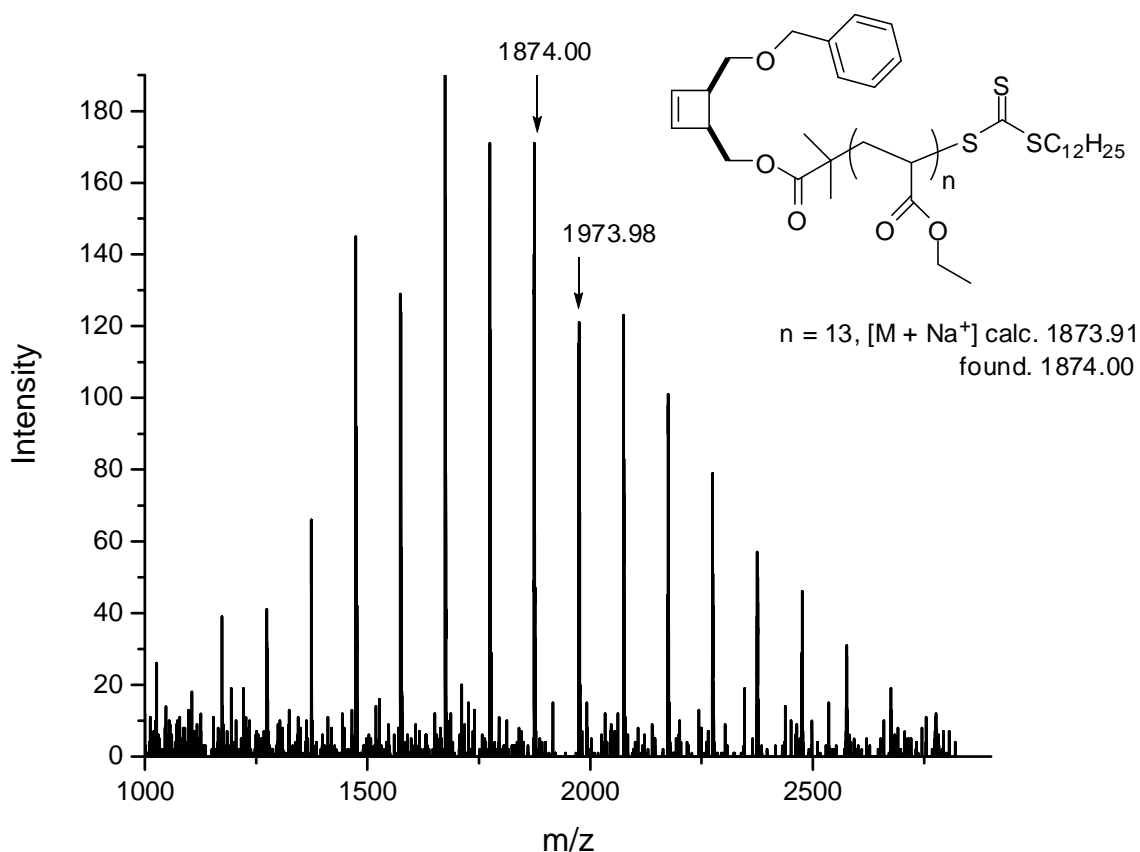
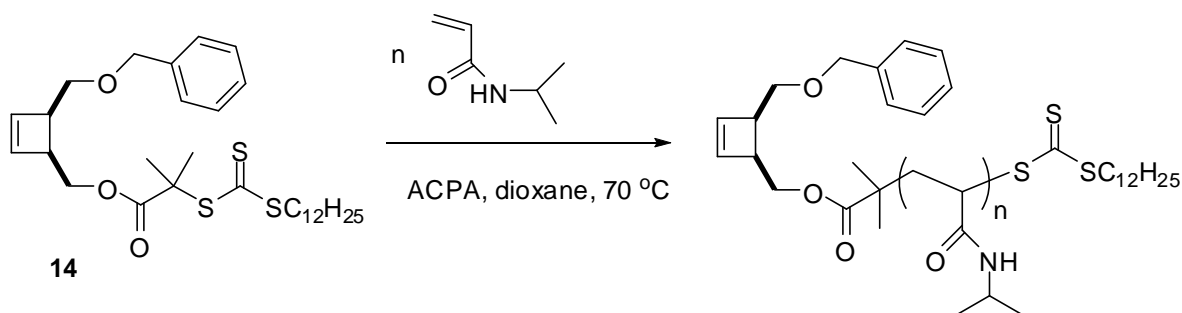


Figure III-8. MALDI-TOF mass spectrum of α -cyclobutenyl poly(ethyl acrylate); matrix: 2-[(2*E*)-3-(4-*tert*-butylphenyl)-2-methylprop-2-enylidene]malononitrile (DCTB) + sodium iodide (NaI).

All data presented demonstrated that the RAFT polymerization of EA mediated by CTA **14** is well-controlled and importantly the cyclobutene-moiety of CTA **14** is conserved under the RAFT polymerization conditions, allowing to synthesize macromonomers with α -terminated cyclobutenyl group quantitatively.

II-2. RAFT polymerization of *N*-isopropyl acrylamide

NIPAM was polymerized in dioxane at 70 °C over selected time intervals using **14** as the RAFT CTA and 4,4'-azobis(4-cyanopentanoyl acid) (ACPA) as the radical initiator²² (Scheme III-3).



Scheme III-3. RAFT polymerization of NIPAM using cyclobutene-functionalized CTA **14**.

The initial $[\text{NIPAM}]_0/[\mathbf{14}]_0/[\text{ACPA}]_0/[\text{DMF}]_0$ was maintained at 100/1/0.1/30. Monomer conversions were monitored as a function of time by comparison of the integration of the vinyl resonances (5.55-5.65 ppm) of NIPAM and the formamide proton resonance of DMF (8.02 ppm) and based on equation 1. Experimental data for the RAFT polymerization of NIPAM are summarized in Table III-2.

Table III-2. RAFT polymerization of NIPAM using **14** as the CTA and ACPA as the initiator in dioxane at 70 °C.

Run	Time (min)	Conversion ^a (%)	$\overline{M}_{n,calc.}^b$ (g/mol)	$\overline{M}_{n,SEC}^c$ (g/mol)	PDI ^c
1	30	34	4 390	4 700	1.14
2	75	72	8 680	10 000	1.08
3	120	86	10 260	10 900	1.11
4	150	93	11 050	11 500	1.11
5	180	94	11 170	10 560	1.14

^a Monomer conversions were determined using ¹H NMR spectroscopy by comparing the integration of the vinyl resonances (at 5.55-5.65 ppm) and the formamide proton resonance of DMF (at 8.02 ppm). ^b

$\overline{M}_{n,calc.} = ([\text{NIPAM}]_0/[\mathbf{14}]_0) \cdot (\text{molar mass of NIPAM}) \cdot (\text{NIPAM conversion}) + \text{molar mass of the chain-end}$. ^c Number-average molecular weight and polydispersity index measured by SEC in DMF with RI detector, calibration with linear polystyrene standards.

The ¹H NMR spectra (Figure III-9) showed a decrease of the vinyl peaks of the monomer at 5.50-6.30 ppm with time, and a nearly quantitative disappearance of the vinyl protons peaks was observed after 180 min of polymerization.

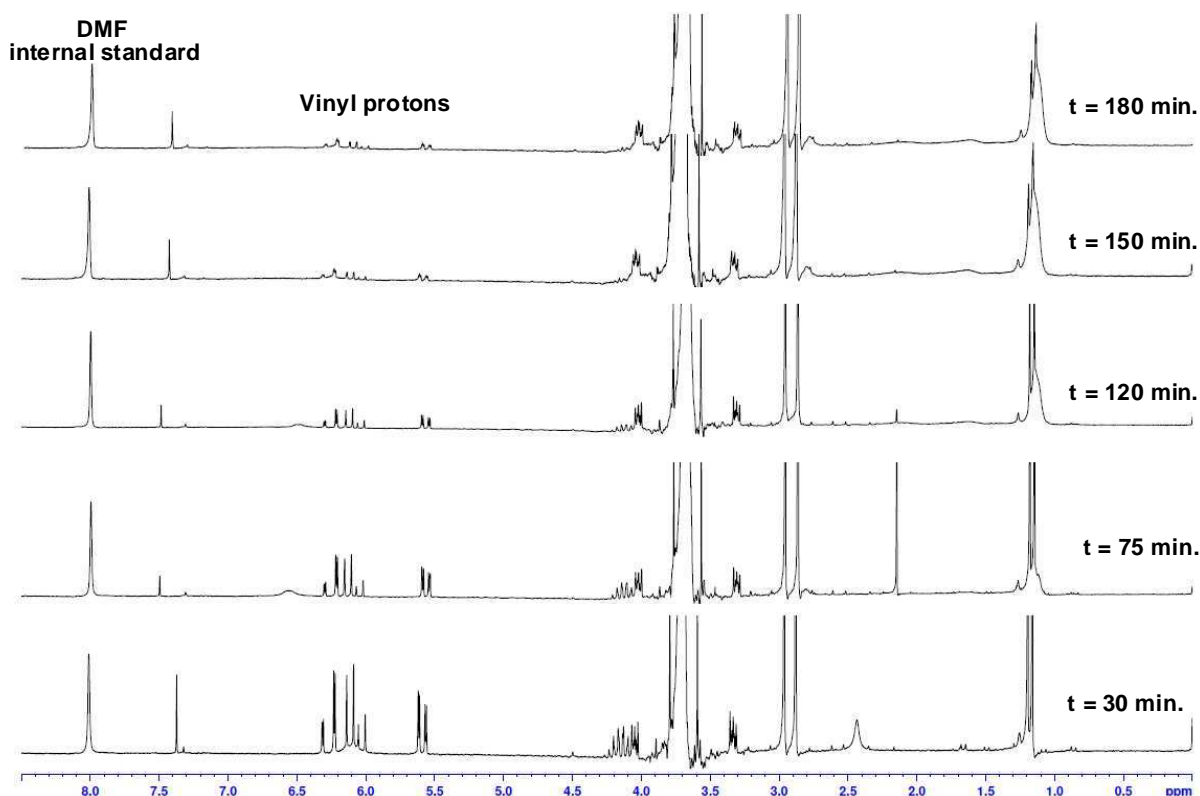


Figure III-9. ^1H NMR spectra of the raw polymerization with time for the RAFT polymerization of NIPAM mediated by CTA **14**; solvent: CDCl_3 .

The pseudo-first-order kinetic plot remains mostly linear at low-to-high conversion (93%) indicating a constant radical concentration over the polymerization of NIPAM mediated by CTA **14** (Figure III-10, A).

Figure III-10B shows the evolution of $\overline{M}_{n,SEC}$ and PDI during the RAFT polymerization of NIPAM. Molecular weight increased gradually with time up to 93%. From the inset, we can observe a linear increase of $\overline{M}_{n,SEC}$ with conversion (up to 93%). The $\overline{M}_{n,SEC}$, determined by SEC in DMF with RI detector, are somewhat higher than those predicted by theory. Similar molecular weight overshots have also been observed for the polymerization of other acrylamide monomers.²³ Low PDIs were also observed over the polymerization (≤ 1.14). Significantly, the SEC traces are unimodal and free from high molecular weight termination products (Figure III-11).

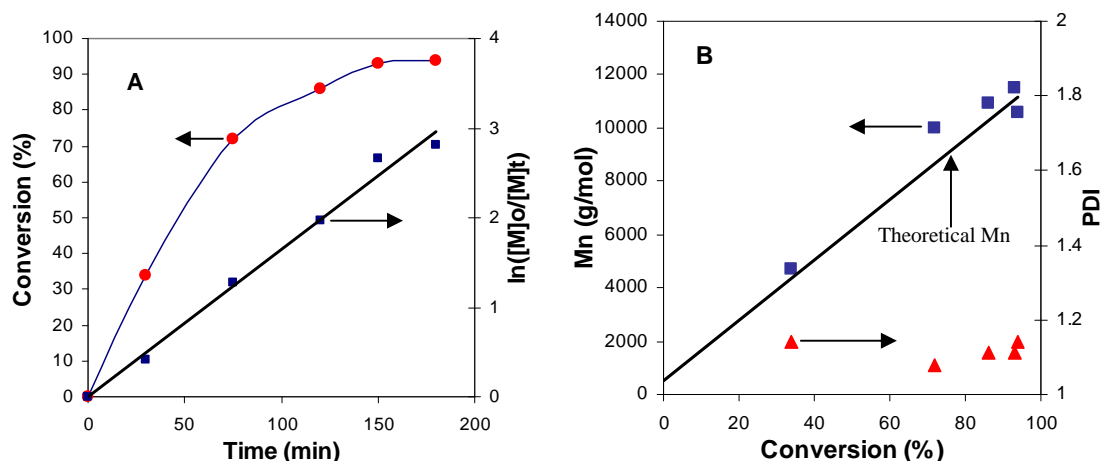


Figure III-10. (A) Evolution of monomer conversion with time and first-order kinetic plot and (B) evolution of molecular weight and PDI with conversion for the RAFT polymerization of NIPAM mediated by CTA **14**.

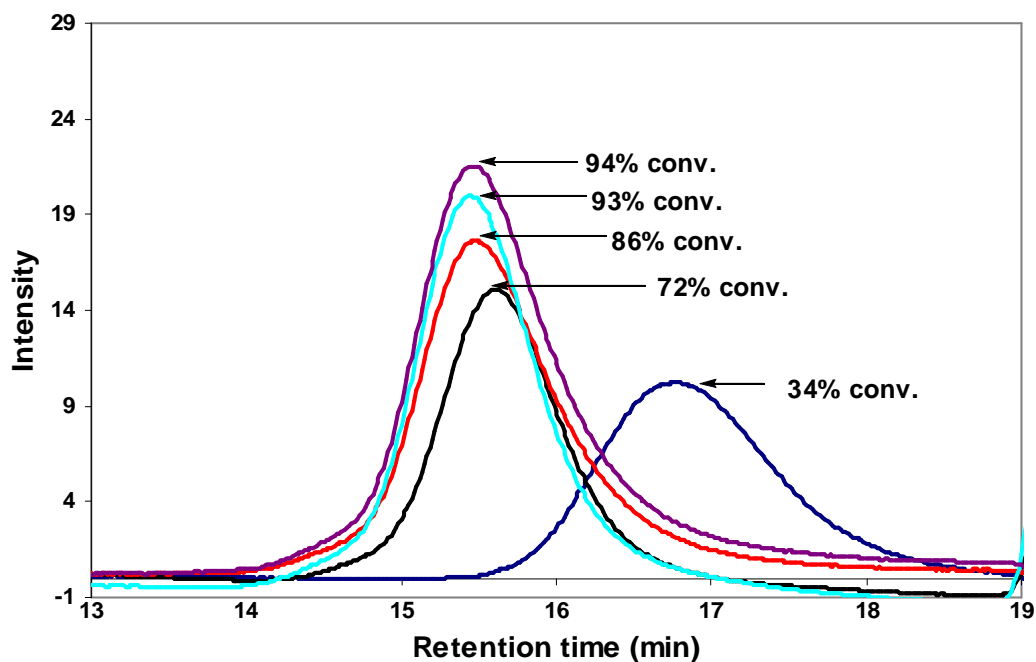


Figure III-11. Evolution of SEC traces (using RI detection) with time for the RAFT polymerization of NIPAM mediated by CTA **14**.

The ^1H NMR spectrum (Figure III-12) of the polymer issued from Run 1, Table III-2 after purification by precipitation from diethyl ether showed the double bond of cyclobutene at 6.1-6.2 ppm (1 & 2, Figure III-12), and the ratio of vinyl peak integration of cyclobutene at 6.10-6.17 ppm and the methylene peak integration (6, Figure III-12) at

4.50 ppm is approximately 2/2, indicating the cyclobutenyl group on **14** remains intact over the course of the polymerization.

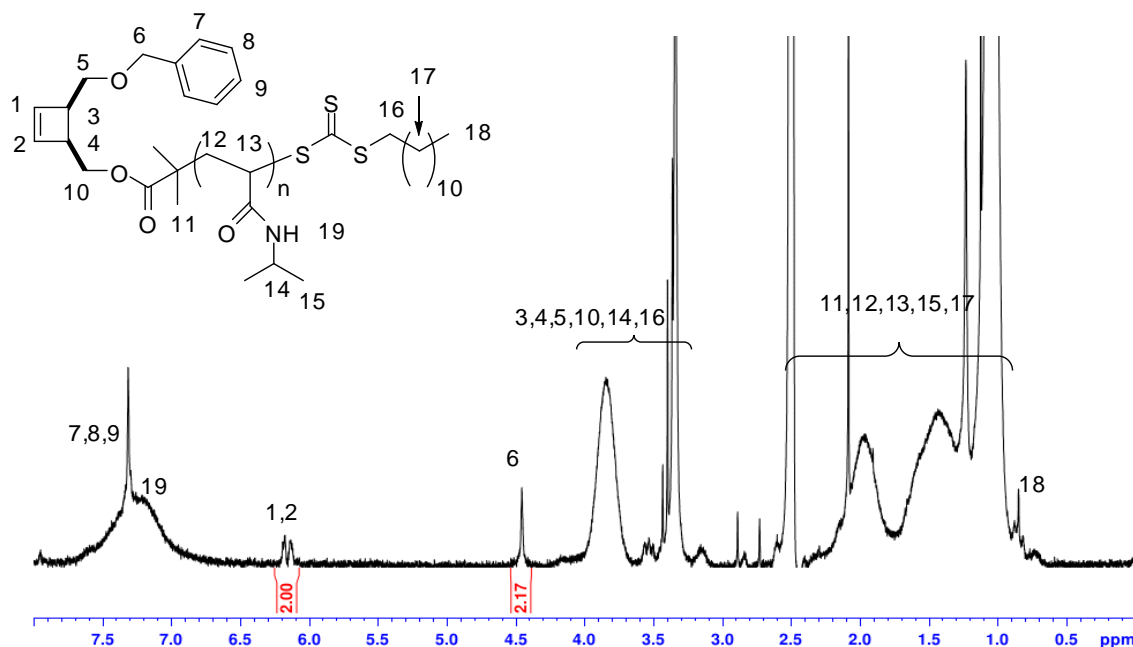


Figure III-12. ^1H NMR spectrum of α -cyclobutenyl poly(*N*-isopropyl acrylamide) (PNIPAM) macromonomer (Run 1, Table III-2); solvent: $\text{DMSO } d_6$.

Furthermore, the MALDI-TOF mass spectrum (Figure III-13) showed only one series of peaks of the expected α -cyclobutenyl PNIPAM. The difference in mass of each signal of the series was roughly estimated as 113.07 (calculated value = $113.16 \text{ g}\cdot\text{mol}^{-1}$), indicating the signals were assignable to the PNIPAM homologues. The peaks at $m/z = 3062.25$ and at 3175.51 were assigned to a PNIPAM consisting of 22 and 23 NIPAM units with a 4-benzyloxymethyl-3-hydroxymethylcyclobut-1-ene group at one chain-end and a trithiocarbonate moiety with a dodecyl chain at the other chain-end ionized by a sodium ion, respectively (calculated value $m/z = 3062.79$ and 3175.95).

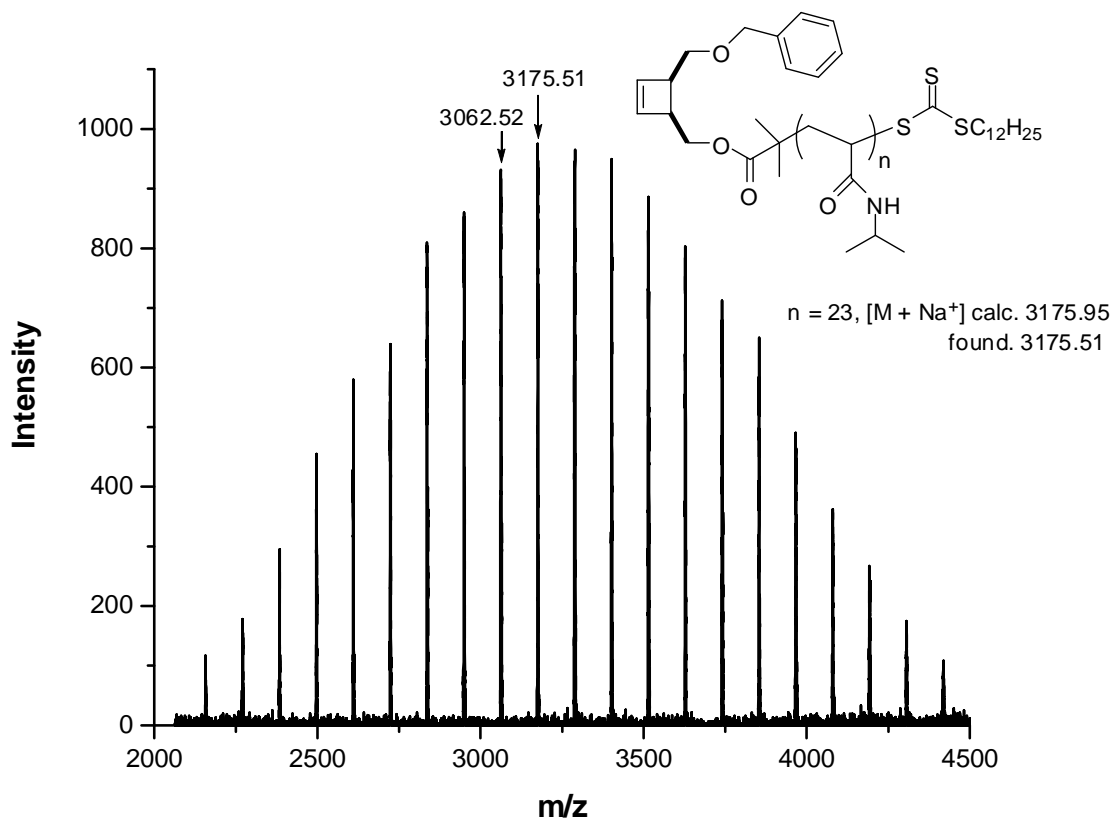


Figure III-13. MALDI-TOF mass spectrum of α -cyclobutenyl PNIPAM; matrix: DCTB + NaI.

All together, these data indicate that the RAFT polymerization of NIPAM mediated by CTA **14** is well-controlled and that the cyclobutene-moiety of CTA **14** was conserved during the polymerization.

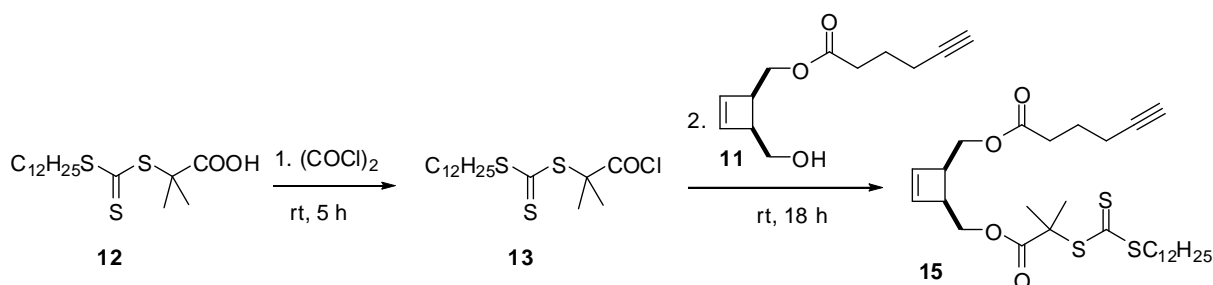
III- Synthesis of cyclobutene-based block copolymers by RAFT polymerization

The ability of the trithiocarbonate moiety to mediate RAFT polymerization was then used to synthesize unsymmetrical macromonomers with one polymer chain issued from RAFT polymerization, and one PEO chain obtained from “click” reaction. Such macromonomer is expected to show thermo-responsive properties that could be used for the polymerization in dispersed media.

III-1. Synthesis of cyclobutene-based PEO macromolecular chain transfer agent

III-1.1. Synthesis of a dual cyclobutenyl-functionalized “click”-RAFT agent

The cyclobutenyl-functionalized “click”-RAFT agent **15** was synthesized from precursor **11**. **15** comprises a trithiocarbonate chain transfer functionality for RAFT polymerization, an alkyne group for ‘click’ reaction, and a cyclobutene functionality as the “ROMP-able” group (Scheme III-4).



Scheme III-4. Synthesis of a dual cyclobutenyl-functionalized “click”-RAFT agent **15**.

The coupling reaction was realized under the same conditions as previously reported for CTA **14**. Purification of the reaction mixture by silica gel column chromatography eluted with DCM provides **15** in high yield (80%) as a yellow oil. ^1H NMR spectrum of the purified product shows a shift of the methylene peak next to the hydroxyl group of **11** from 3.70 ppm to 4.25 ppm (10, Figure III-14) indicating a linking with acetyl group. Integration area ratios of the cyclobutene olefin peaks (1 & 2, Figure III-14) and the methyl peak of the CTA moiety (14, Figure III-14) gave a 2:3 ratio, which demonstrated a quantitative coupling between **13** and **11**. Furthermore, the integrations of cyclobutene olefin peaks (1 & 2, Figure II-14) and the $\text{C}\equiv\text{CH}$ proton peak (9, Figure II-14) gave a 2:1 ratio, indicating that the alkyne group remained intact after introduction of the trithiocarbonate functionality.

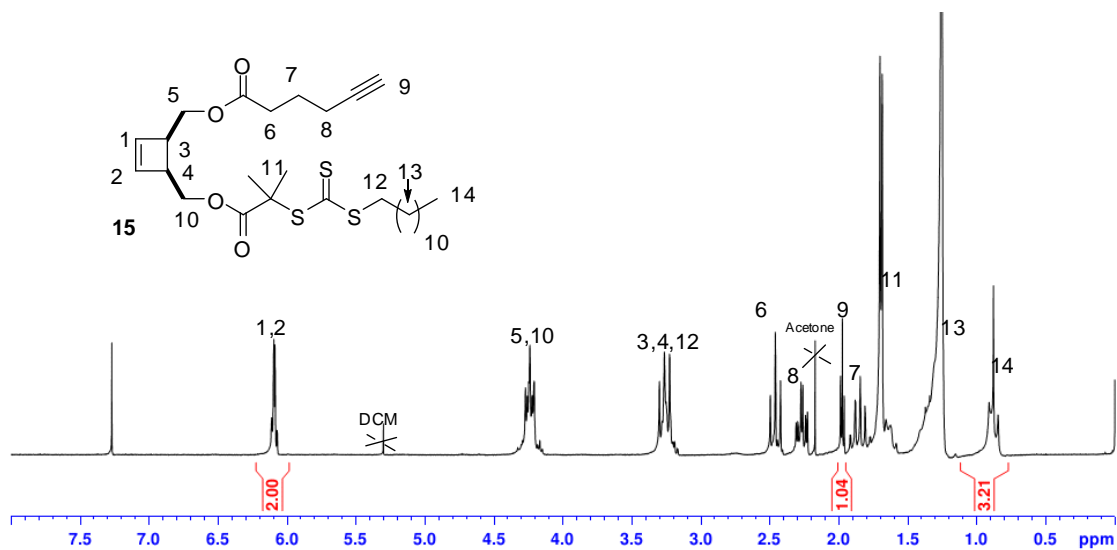
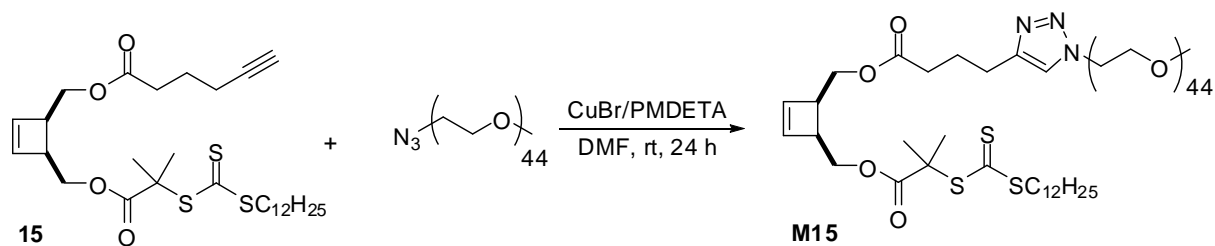


Figure III-14. ^1H NMR spectrum of the dual-functionalized “click”-RAFT agent cyclobutene **15**; solvent: CDCl_3 .

The synthesis of cyclobutene-based PEO-*b*-PNIPAM block copolymers can be done according to two pathways. The first one consists in the RAFT polymerization of NIPAM in the presence of **15** as the CTA followed by a “click” reaction with a PEO chain. Previous studies on the combination of RAFT polymerization and “click” reaction have shown the compatibility of those two reactions.^{16,24} However, the “click” reaction between two polymers has been already reported in the chapter II and has proven not to be quantitative. Consequently, the second strategy consisting in the synthesis of PEO-based RAFT agent from **15** and PEO- N_3 chain by “click” reaction, which will then be used as the macro-CTA for the RAFT polymerization has been chosen to achieve cyclobutene-based block copolymers.

III-1.2. Synthesis of a macromolecular chain transfer agent by “click” reaction

Cyclobutene-based PEO macro-CTA **M15** has been synthesized from CTA **15** and azide-terminated PEO 2 000 g/mol by “click” reaction under the same conditions as previously reported for PEO macromonomers in chapter II (Scheme III-5).



Scheme III-5. Synthesis of PEO-based RAFT agent **M15** by “click” reaction.

^1H NMR spectroscopy showed a nearly quantitative conversion from the alkyne group to triazole five-membered ring after 24h reaction time, as observed by loss of the acetylene proton signal at 1.97 ppm (9, Figure III-14) and appearance of the triazole proton resonating at 7.50 ppm (14, Figure III-15). Integrations of cyclobutene olefin peaks, the triazole ring signal and the methoxy end-group peak gave approximately a 2:1:3 ratio, indicating “click” coupling has occurred.

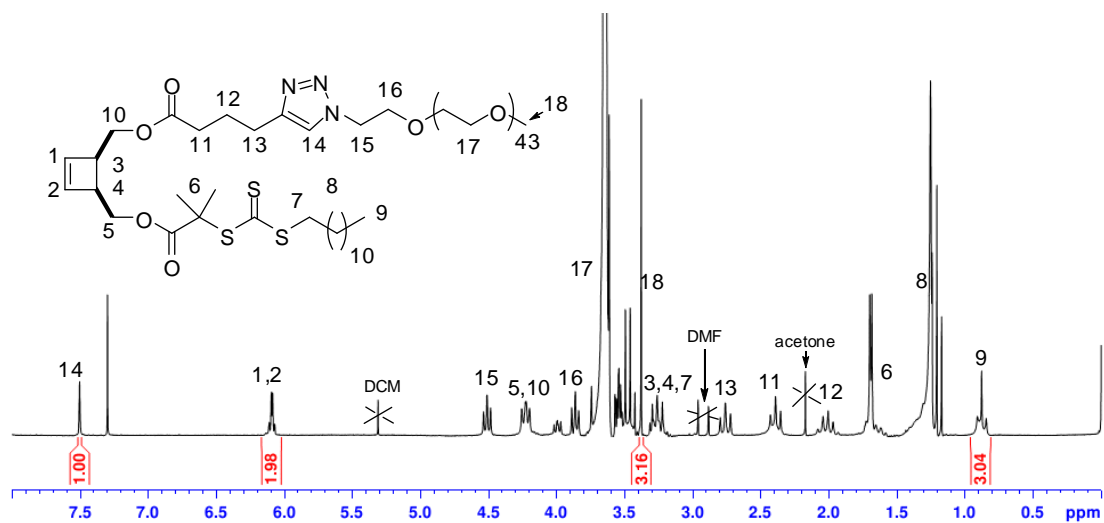


Figure III-15. ^1H NMR spectrum of the cyclobutene-based PEO macro-CTA **M15**; solvent: CDCl_3 .

The SEC trace using RI detector showed that the coupling product has a slightly higher molecular weight than the PEO- N_3 2 000. The SEC trace using UV-Vis detector (Figure III-16) also showed the absorption at 309 nm corresponding to the $\text{C}=\text{S}$ bond of trithiocarbonate-moiety, and confirming the trithiocarbonate functionalization of PEO.

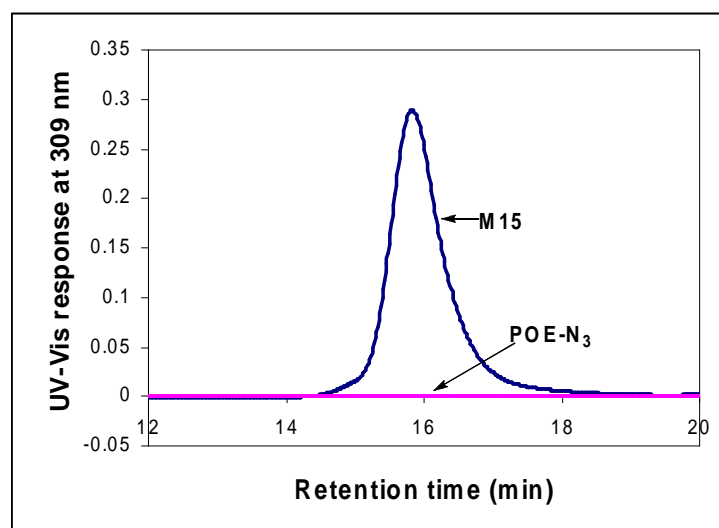
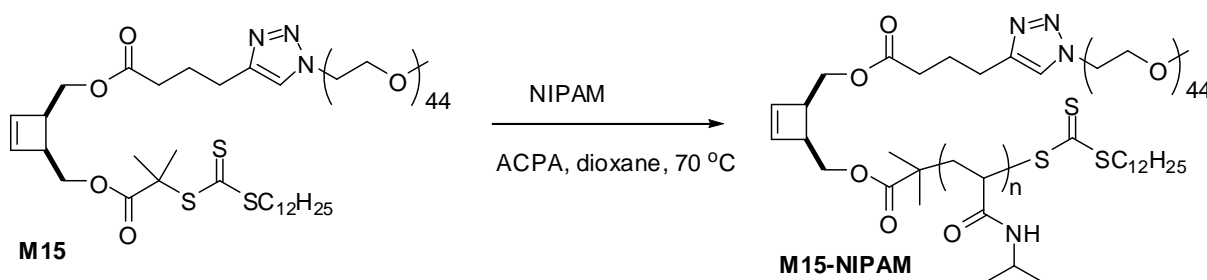


Figure III-16. SEC traces using UV-Vis detection at 309 nm for the PEO-N₃ and cyclobutene-based PEO macro-CTA **M15**.

This result confirms that the azide-alkyne copper-catalyzed cycloaddition is compatible with the trithiocarbonate functionality. This macro-CTA has then been engaged in RAFT polymerization of NIPAM in order to obtain a cyclobutene-based PEO-*b*-PNIPAM with water-soluble and thermo-sensitive properties.

III-2. RAFT polymerization of *N*-isopropyl acrylamide using cyclobutene-based PEO macromolecular chain transfer agent

The synthesis of a cyclobutene-based PEO-*b*-PNIPAM was performed according to the same conditions as already reported for the RAFT polymerization of NIPAM with **14** as the CTA (Scheme III-6).



Scheme III-6. RAFT polymerization of NIPAM mediated by the macro-CTA **M15**.

The reaction was monitored by ^1H NMR spectroscopy by following the decrease of the vinyl peaks of the monomer at 5.55-5.65 ppm comparing with the formamide proton peak of DMF at 8.02 ppm used as an internal reference with time. The results, reported in Table III-3, showed that the RAFT polymerization stopped at 34 % monomer conversion probably because of the contact with oxygen. Nevertheless, the SEC trace of the block copolymer is symmetric unimodal curve, shifted towards shorter elution time as compared with **M15** (Figure III-17). However, the molecular weights are always higher than those predicted by calculation because of the higher hydrodynamic volume of PEO as compared with polystyrene (PS) standards of SEC. Furthermore, the ^1H NMR spectrum of the block copolymer after precipitation in diethyl ether shows a signal with a chemical shift of 6.17 ppm, which corresponds to the vinyl protons of cyclobutene group. The ratio of vinyl peak integration of cyclobutene and the methyl peak integration of **M15** at 4.50 ppm (3, Figure III-18) is approximately 2:2, indicating that the cyclobutenyl group on **M15** remains intact during the polymerization.

Table III-3. RAFT polymerization of NIPAM using **M15** as the CTA and ACPA as the initiator in dioxane at 70 °C.

Run	Time (min)	Conversion ^a (%)	$\overline{M}_{n,calc}$ ^b (g/mol)	$\overline{M}_{n,SEC}$ ^c (g/mol)	PDI ^c
1	30	23	5 100	10 070	1.10
2	75	34	6 390	11 400	1.12
3	120	34	6 390	11 400	1.12

^a Monomer conversions were determined using ^1H NMR spectroscopy by comparing the integration of the vinyl resonances (at 5.55-5.65 ppm) and the formamide proton resonance of DMF (at 8.02 ppm). ^b

$$\overline{M}_{n,calc} = ([\text{NIPAM}]_0/[\text{M15}]_0) * (\text{molar mass of NIPAM}) * (\text{NIPAM conversion}) + \text{molar mass of M15}.^c$$

^c Number-average molecular weight and polydispersity index measured by SEC in DMF with RI detector, calibration with linear polystyrene standards.

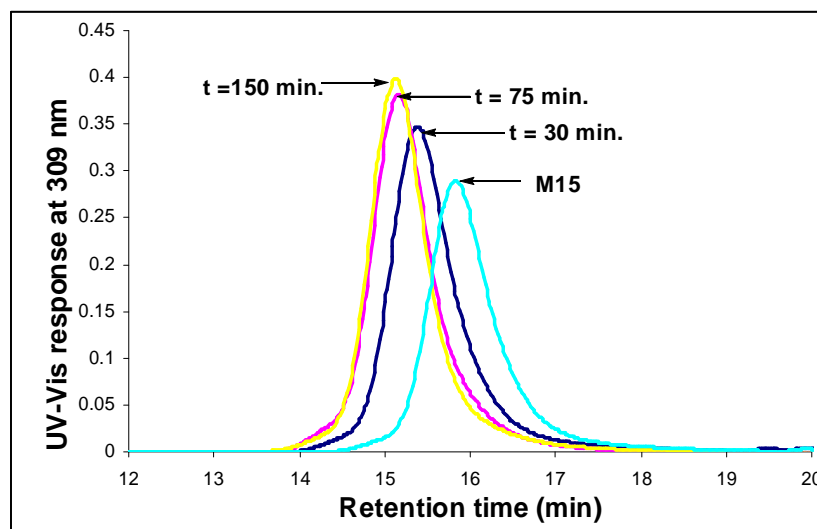


Figure III-17. SEC traces using UV-Vis detection at 309 nm for the cyclobutene-based PEO macro-CTA and cyclobutene-based PEO-*b*-PNIPAM block copolymers.

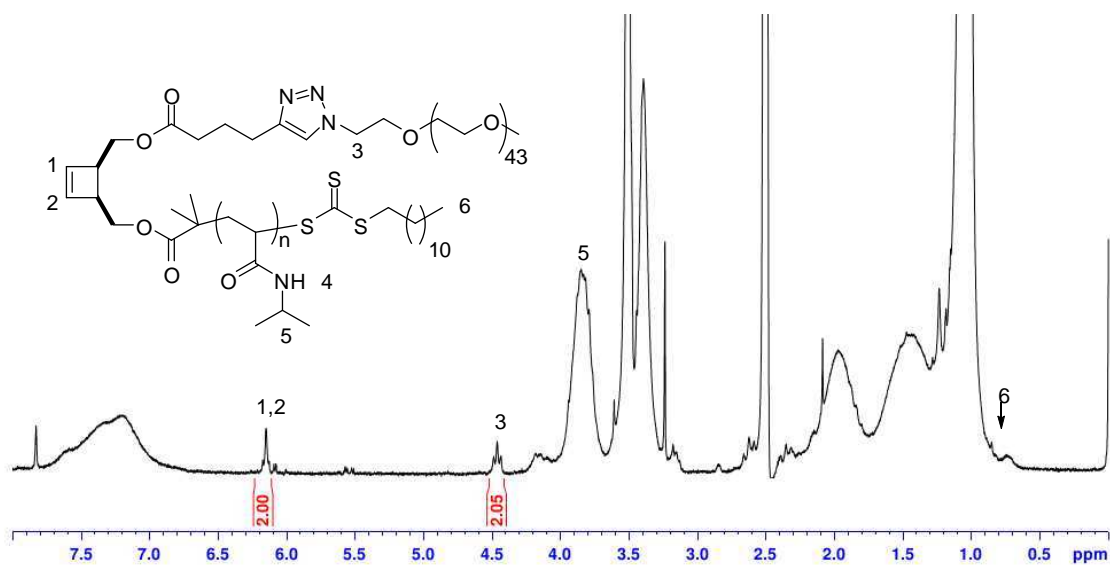
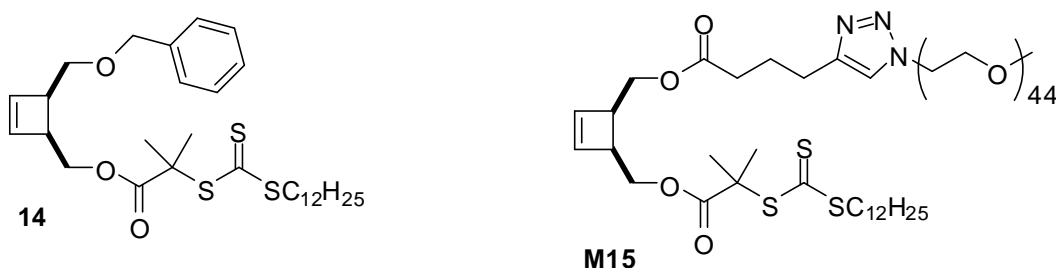


Figure III-18. ^1H NMR spectrum of cyclobutene-based PEO-*b*-PNIPAM block copolymer; solvent: $\text{DMSO-}d_6$.

Conclusion

The synthesis of α -cyclobutenyl macromonomers issued from RAFT polymerization has been studied in order to give access to new macromonomers with potential self-assembling properties. An original CTA agent **14** (Scheme III-7) has first been obtained from the cyclobutenyl precursor **7** and its ability to promote RAFT polymerization of EA and NIPAM has been demonstrated.



Scheme III-7. Cyclobutene-based (macro)chain transfer agents.

The RAFT polymerization studies of EA and NIPAM monomers show the high efficiency of CTA **14** with a well-controlled polymerization. The cyclobutene-moiety of CTA **14** remains intact in both RAFT polymerization conditions (of EA and NIPAM). This method enables the synthesis of well-defined α -cyclobutenyl-functionalized macromonomers with controlled molecular weight and composition as well as narrow molecular weight distribution (PDIs ≤ 1.14).

Cyclobutene-based PEO-*b*-PNIPAM block copolymers have then been prepared by combination of “click” reaction with PEO chain and RAFT polymerization of NIPAM mediated by **M15** (Scheme III-7). The copolymers show an unimodal and well narrow molecular weight distribution (PDIs ≤ 1.12) with $\overline{M}_{n,SEC}$ from 10 700 to 11 400 g/mol.

References

1. Chiefari, J.; Chong, Y. K. ; Ercole, F.; Krstina, J.; Jeffery, J.; Le, T. P. T.; Mayadunne, R. T. A; Meijs, G. F.; Moad, C. L.; Moad, G.; Rizzardo, E.; Thang, S. H. *Macromolecules* **1998**, *31*, 5559-5562.
2. Moad, G.; Rizzardo, E.; Thang, S. H. *Aust. J. Chem.* **2005**, *58*, 379-410.
3. Barner-Kowollik, K. (Ed), *Handbook of RAFT polymerization*, Wiley-VHC, Weinheim, **2008**.
4. Patton, D. L.; Advincula, R. C. *Macromolecules* **2006**, *39*, 8674-8683.
5. Li, Z.; Zhang, K.; Ma, J.; Cheng, C.; Wooley, K. L. *J. Polym. Sci., Part A: Polym. Chem.* **2009**, *47*, 5557-5563.
6. Ma, J.; Cheng, C. ; Wooley, K. L. *Aust. J. Chem.* **2009**, *62*, 1507-1519.
7. Li, Z.; Ma, J.; Cheng, C.; Zhang, K.; Wooley K. L. *Macromolecules* **2010**, *43*, 1182-1184.
8. Li, Z.; Ma, J.; Lee, N. S.; Wooley, K. L. *J. Am. Chem. Soc.* **2011**, *133*, 1228-1231.
9. Li, Y.; Themistou, E.; Zou, J.; Das, B. P.; Tsianou, M.; Cheng C. *ACS Macro Lett.* **2012**, *1*, 52-56.
10. Li, A.; Ma, J.; Sun, G.; Li, Z.; Cho, S. ; Clark, C.; Wooley, K. L. *J. Polym. Sci., Part A: Polym. Chem.* **2012**, *50*, 1681-1689.
11. Li, C.; Gunari, N.; Fischer, K.; Janshoff, A.; Schmidt, M. *Angew. Chem. Int. Ed.*, **2004**, *43*, 1101-1104.
12. Chen, M. Q.; Kishida, A.; Akashi, M. *J. Polym. Sci., Part A: Polym. Chem.* **1996**, *34*, 2213-2220.
13. Berlinova, I. V.; Iliev, P. V.; Vladimirov, N. G.; Novakov, C. P. *J. Polym. Sci., Part A: Polym. Chem.* **2007**, *45*, 4720-4732.
14. Lai, J. T.; Filla, D.; Shea, R. *Macromolecules* **2002**, *35*, 6754-6756.
15. Mahanthappa, M. K.; Bates, F. S.; Hillmyer, M. A. *Macromolecules* **2005**, *38*, 7890-7894.
16. Harvison, M. A.; Lowe, A. B. *Macromol. Rapid Commun.* **2011**, *32*, 779-800.
17. Rieger, J.; Stoffelbach, F.; Bui, C.; Alaimo, D.; Jerome, C.; Charleux, B. *Macromolecules* **2008**, *41*, 4065-4068.

18. (a) Green, T.W.; Wuts, P. G. M. *Protective Groups in Organic Synthesis*, Wiley-Interscience, New York, **1999**, 76-86 & 708-711.
(b) Congreve, M. S.; Davison, E. C.; Fuhry, M. A. M.; Holmes, A. B.; Payne, A. N.; Robinson, R. A.; Ward, S. E. *Synlett* **1993**, 663-664.
19. Goto, A.; Fukuda, T. *Prog. Polym. Sci.* **2004**, *29*, 329-385.
20. (a) Kwak, Y.; Goto, A.; Fukuda, T. *Macromolecules* **2004**, *37*, 1219-1225.
(b) Kwak, Y.; Goto, A.; Tsujii, Y.; Murata, Y.; Komatsu, K.; Fukuda, T. *Macromolecules* **2002**, *38*, 3026-3029.
(c) Kwak, Y.; Goto, A.; Komatsu, K.; Sugiura, Y.; Fukuda, T. *Macromolecules* **2004**, *37*, 4434-4440.
21. (a) Monteiro, M. J.; de Brouwer, H.; *Macromolecules* **2001**, *34*, 349-352.
(b) Monteiro, M. J. *J. Polym. Sci., Part A: Polym. Chem.* **2005**, *43*, 3189-3204.
22. Levere, M. E.; Ho, H. T.; Pascual, S.; Fontaine, L. *Polym. Chem.* **2011**, *2*, 2878-2887.
23. (a) Donovan, M. S.; Sumerlin, B. S.; Lowe, A. B.; McCormick, C. L. *Macromolecules* **2002**, *35*, 8663-8666.
(b) Donovan, M. S.; Sanford, T. A.; Lowe, A. B.; Sumerlin, B. S.; Mitsukami, Y.; McCormick, C. L. *Macromolecules* **2002**, *35*, 4570-4572.
(c) Vasilieva, Y. A.; Thomas, D. B.; Scales, C. W.; McCormick, C. L. *Macromolecules* **2004**, *37*, 2728-2737.
(d) Favier, A.; Charreyre, M.-T.; Chaumont, P.; Pichot, C. *Macromolecules* **2002**, *35*, 8271-8280.
(e) Convertine, A. J.; Lokitz, B. S.; Vasileva, Y.; Myrick, L. J.; Scales, C. W.; Lowe, A. B.; McCormick, C. L. *Macromolecules* **2006**, *39*, 1724-1730.
24. Gregory, A.; Stenzel, M. H. *Progr. Polym. Sci.* **2012**, *37*, 38-105.

Chapter IV

Ring-Opening Metathesis Polymerization of oxanorbornenyl- and cyclobutenyl- functionalized macromonomers

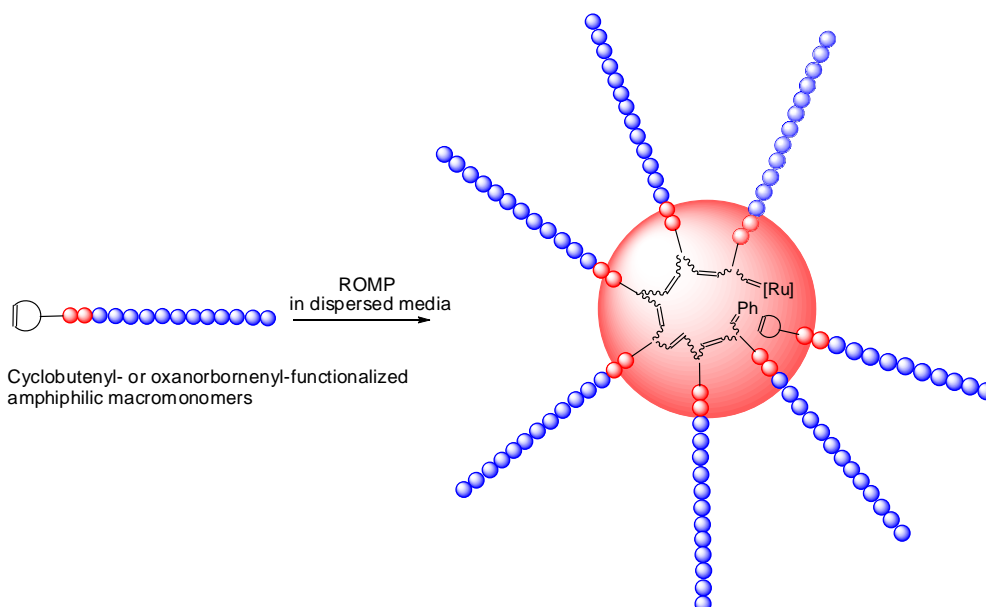
Introduction

The synthesis of graft copolymers has been widely studied since the development of living polymerization processes and allows to design well-defined structures. Amongst the main synthetic approaches that have been developed, the “grafting through” strategy, which relies on polymerization of appropriate macromonomers, has proven to be one of the most useful ways to get well-defined graft copolymers since it allows a good control on grafts, on backbone lengths, and on grafts density.

Although the “grafting through” approach offers versatility in the construction of complex macromolecular systems, it is likely to encounter steric hindrance during the polymerization of high molecular weight or sterically-bulky macromonomers. To overcome this issue, ring-opening metathesis polymerization (ROMP) has often been used, which is driven by the release of enthalpy from cyclic monomer structures and affords a polymer backbone with relatively loose grafting density^{1,2}. Furthermore, ROMP has proven to be orthogonal with reversible deactivation radical polymerizations (RDRP) and numerous works have reported the synthesis of graft copolymers from macromonomers obtained by RDRP with the “ROMP-able” (oxa)norbornenyl functionality.³⁻⁹

ROMP of macromonomers with the “ROMP-able” cyclobutenyl functionality was first reported by our group in 2006.¹⁰ This “ROMP-able” functionality has not been much exploited because of the hazardous character of such monomer synthesis.¹¹⁻¹³ The previous works reported about the ability of cyclobutenyl macromonomers to polymerize by ROMP have shown that the cyclobutenyl functionality is less reactive than the norbornenyl functionality despite its high ring strain of about 30 kcal/mol.^{10,14-17} Furthermore, polymerization of cyclobutenyl- or oxanorbornenyl-functionalized macromonomers is still deficient in preparing very high molecular weight copolymers. Use of ROMP in dispersed aqueous media such as mini-emulsion has to be considered as it has been previously shown that radical polymerization of amphiphilic macromonomers in selective solvents can lead to unusually rapid reactions and products having high molecular weights, because such macromonomers are organized into micelles with the hydrophobic polymerizable end-groups concentrated in the cores (Scheme IV-1).¹⁸⁻²⁰ Although ROMP^{21,22} and acyclic diene metathesis

ADMET polycondensation²³ in aqueous emulsion have been previously described in the literature, to our knowledge, no study has been reported up to now concerning the use of amphiphilic macromonomers for ROMP in mini-emulsion. Nevertheless, Héroguez *et al.* have recently reported the use of amphiphilic macroinitiators for ROMP in a mini-emulsion process.²⁴⁻²⁶



Scheme IV-1. Schematic representation of ROMP of cyclobutenyl- or oxanorbornenyl-functionalized macromonomers in dispersed media.

In this chapter, we first report the ROMP in solution of amphiphilic cyclobutenyl- and oxanorbornenyl-functionalized macromonomers previously synthesized in order to check the reactivity and the compatibility of poly(ethylene oxide) (PEO), of poly(meth)acrylate or of poly(meth)acrylamide macromonomers towards ROMP. Indeed, we have previously observed that cyclobutenyl-functionalized polystyrene macromonomers were much less reactive in ROMP than their poly(styrene-*b*-*tert*-butyl acrylate) homologues; such result shows the eventual influence of the structure of the macromonomer.¹¹

The surfactant properties of the macromonomers have then been studied using complementary techniques to assess critical micellar concentration (CMC) in order to establish their ability to stabilize an interface like common surfactants do. Such macromolecular structures can be used as stabilizers in (mini-)emulsion processes. The ability of the macromonomers having a CMC to be used as *surfmers* (*surfactant-monomer*) in ROMP in dispersed aqueous media has then been investigated.

I- ROMP in solution

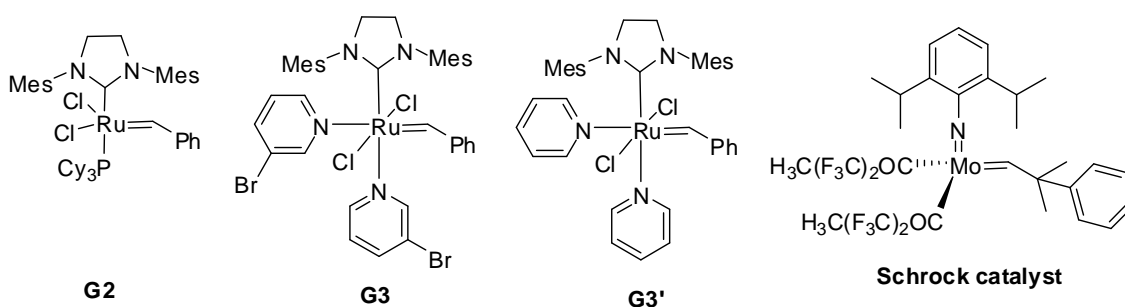
The reactivity in ROMP in solution of the oxanorbornenyl and cyclobutenyl macromonomers previously synthesized has been studied. Third generation Grubbs' catalyst (**G3**) with 3-bromopyridine ligand was used because it exhibits much higher values of k_i relative to k_p than the first and second generation Grubbs' catalysts (**G1** & **G2**) and hence yields polymers with narrow molecular weight distributions.²⁷⁻²⁹ **G3** has also proved to be efficient for the ROMP of (oxa)norbornene-terminated poly(ethylene oxide)³⁰, poly(meth)acrylate^{7,31-32}, polystyrene^{7,31-32}, poly(ϵ -caprolactone)³³ and polylactide³⁴⁻³⁶.

I-1. ROMP of oxanorbornenyl-functionalized macromonomers*

The oxanorbornenyl macromonomers **M2** with molecular weights ranging from 500 to 5000 g/mol were subjected to ROMP (Scheme IV-2), using **G3** (Scheme IV-3), and the living polymers were terminated using ethyl vinyl ether to give the final product.



Scheme IV-2. ROMP of oxanorbornenyl macromonomers **M2**.



Scheme IV-3. Structure of Grubbs and Schrock catalysts.

Reactions were carried out in dichloromethane (DCM) with various macromonomer-to-catalyst ratios ($[M]_0/[I]_0$) at room temperature with a macromonomer concentration of 0.05 M (Table IV-1). DCM was preferred to tetrahydrofuran (THF) since **M2-2000** and **M2-5000** show a poor solubility in THF at the concentrations used. **M2-500** was easily

* Part of this chapter was published in *Macromolecules* **2010**, *43*, 5611-5617.

polymerized to near quantitative yield in 1-4 h depending on the desired molecular weight (Table IV-1, runs 1-4).

^1H NMR spectroscopy indicated the disappearance of the vinyl proton signal at 6.50 ppm as shown in Figure IV-1 and the emergence of the *trans* and *cis* vinyl proton resonances at 6.05 and 5.75 ppm (1 *trans* & *cis*), respectively (Figure IV-1, Table IV-1, run 2). NMR spectroscopy also evidenced that the triazole moieties are preserved throughout the ROMP process (resonances in ^1H NMR at 7.72 ppm; 5). Size Exclusion Chromatography (SEC) traces of the polymers are shown in Figure IV-2. As can be seen (Figure IV-2, (B) & (C)), the line profile is perfectly symmetrical with no observable high or low molecular weight shoulders. All polymers issued from **M2-500** were obtained with low polydispersities (Table IV-1, runs 1, 2 & 4) ranging from 1.06 to 1.17. These results are in contrast to those already reported in literature³⁷⁻³⁹, where broad polydispersities were observed, typically around 1.6, when (co)polymerizing PEO functionalized imide monomer (however using other Ru-based catalysts), suggesting to be caused by the combination of PEO with the imide functionality³⁸. The number-average molecular weights (\overline{M}_n) obtained SEC in THF, calibrated with polystyrene, were as much lower than the targeted ones as the $[\text{M}]_0/[\text{I}]_0$ ratio is high (Table IV-1, runs 1-4). This disparity can be attributed to different hydrodynamic volumes of these polymers compared to linear polystyrene standards.⁴⁰ It is also well-known in the literature that the measured values for the molecular weights underestimate the true molecular weights of comb polymers by up to a factor of 10.⁴¹ Additionally, THF is a poor solvent for PEO in which the copolymer contracts substantially, leading to a dramatic decrease in hydrodynamic volume.⁴² However, the weight-average molecular weights (\overline{M}_w) determined by static light scattering[^] are in rather good agreement with the targeted values (Table IV-1, runs 2 & 4) indicating most catalyst initiated the ROMP process. These values, *i.e.* 40 650 and 61 050 g/mol, can be related to the weight-average degree of polymerizations (\overline{DP}_w) of 54 and 83, for $[\text{M}]_0/[\text{I}]_0$ ratios of 50 and 100, respectively which evidences the near quantitative conversion of the macromonomers.

[^] This work has been done by Dr. M. E. Levere with the framework of a 9 months post-doctoral position financed by the ANR under contract ANR_08_BLAN_0104 (“cycloROMP”)

Table IV-1. ROMP of oxanorbornenyl PEO macromonomers using **G3** catalyst ^a

Run	Macromonomer	[M] ₀ /[I] ₀ ^b	$\overline{M}_{n,theo}$ ^c (g/mol)	t (h)	Conv. ^d ¹ H NMR (%)	Conv. ^e SEC (%)	$\overline{M}_{n,SEC}$ ^f (g/mol)	\overline{M}_w ^g	PDI ^f	Trans /cis ^h
1	M2-500	10	7 661	1	100	99	9 900	-	1.06	50/50
2	M2-500	50	37 941	1	100	99	22 800	40 650	1.17	50/50
3	M2-500	100	75 791	1	90	90	20 000	-	1.09	50/50
4	M2-500	100	75 791	4	100	100	23 500	61 050	1.15	50/50
5	M2-2000	10	22 491	1	100	98	29 300	-	1.07	43/57
6	M2-2000	50	112 091	1	25	-	-	-	-	-
7	M2-2000	50	112 091	4	61	58	37 700	-	1.10	43/57
8	M2-2000	50	112 091	24	60	60	46 300	-	1.04	43/57
9	M2-2000	100	224 091	24	-	5	-	-	-	-
10	M2-5000	10	48 261	4	90	90	57 800	-	1.06	75/25
11	M2-5000	10	48 261	24	-	90	57 800	-	1.06	-
12	M2-5000	50	240 941	24	-	61	67 500	-	1.08	-
13	M2-5000	100	481 791	24	-	1	-	-	-	-

^a Results are representative of at least duplicated experiments. ^b Macromonomer to Grubbs' catalyst **G3** ratio. ^c $\overline{M}_{n,theo} = \overline{M}_n \text{ macromonomer} \times ([M]_0/[I]_0) \times \text{Conv. NMR} + M_{\text{ext.}}$. ^d Determined by comparing the peak areas of oxanorbornenyl ring of the grafted copolymer and residual macromonomer from ¹H NMR of the crude product. ^e Determined by comparing the peak areas of grafted copolymer and residual macromonomer from steric exclusion chromatography (SEC) measurement of the crude product. ^f Number-average molecular weight and polydispersity measured by SEC in THF with refractive index (RI) detector, calibration with linear polystyrene standards. ^g Determined by static light scattering. ^h Determined by comparing the peak areas of H_{cis} and H_{trans} of the CH= groups of the backbone from ¹H NMR of the grafted copolymer.

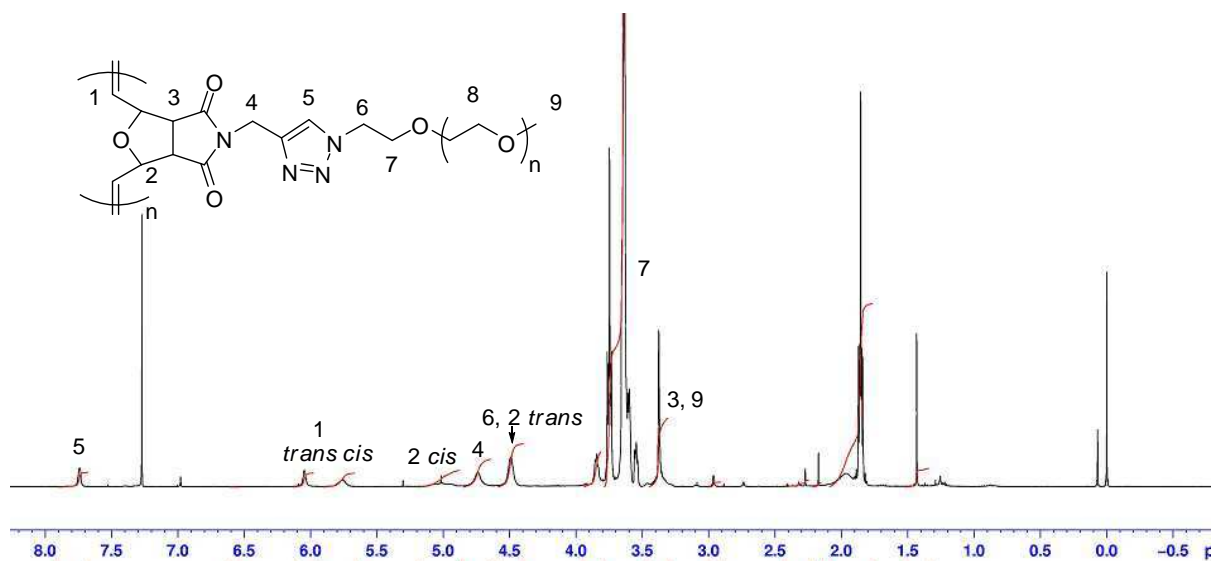


Figure IV-1. ^1H NMR spectrum of polyoxanorbornene-*g*-PEO 500 (Table IV-1, run 2);
solvent: CDCl_3 .

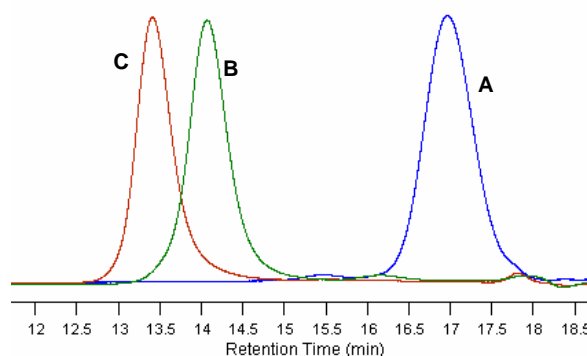


Figure IV-2. SEC traces of (A) ω -*exo*-oxanorbornenyl PEO monomethyl ether **M2-500**, (B) polyoxanorbornene-*g*-PEO 500 (Table IV-1, run 1) and (C) polyoxanorbornene-*g*-PEO 500 (Table IV-1, run 2).

However, **M2-2000** and **M2-5000** were only able to form polyoxanorbornene-*g*-PEO with relatively short backbone length (Table IV-1, runs 5 & 10). The resulting grafted copolymers have been characterized using both SEC and NMR techniques. The grafted copolymers had apparent molecular weights higher than the macromonomers precursors, and the molecular weight distribution of the grafted copolymers remained as narrow as $\text{PDI} = 1.06 - 1.07$ (Table IV-1, runs 5 & 10, Figures VI-3 & VI-4). The ^1H NMR results were similar to the one shown in Figure VI-1. Increase of the reaction time for macromonomer-to-catalyst ratios of 50 and 100 didn't allow a complete conversion

of the macromonomers (Table IV-1, runs 6-9 & 12). The macromonomer chain length seems to be a critical factor towards the conversion, probably due to the limiting effect of the macromonomer steric hindrance during the propagation step. Furthermore the rich-oxygen macromonomers could give competitive coordination with the ruthenium with the result of lowering the rate of polymerization. Indeed, such competitive coordination of catalyst has already been described for PEO macromonomers⁴³ or ether-containing monomers.⁴⁴

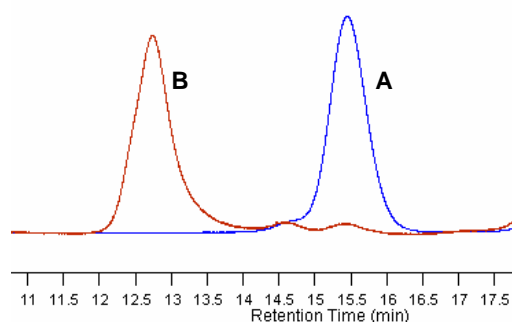


Figure IV-3. SEC traces of (A) ω -*exo*-oxanorbornenyl PEO monomethyl ether **M2-2000**, and (B) polyoxanorbornene-*g*-PEO 2000 (Table IV-1, run 5).

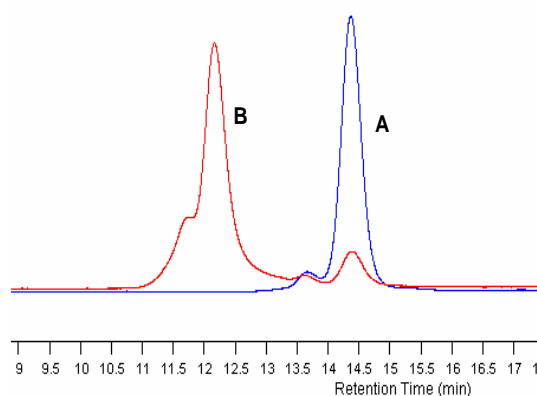


Figure IV-4. SEC traces of (A) ω -*exo*-oxanorbornenyl PEO monomethyl ether **M2-5000**, and (B) polyoxanorbornene *g*-PEO 5000 (Table IV-1, run 10).

Polyoxanorbornene-*g*-PEO 500 was shown by ¹H NMR to have a backbone tacticity that was equally *cis* and *trans* (Table IV-1, runs 1-4) whereas polyoxanorbornene-*g*-PEO 2000 and 5000 had tacticities that were 57% and 75% *trans*, respectively. Similar

results have already been mentioned in the literature for polynorbornene-*g*-PEO 700, 1200 and 2300.⁴⁵

The thermal behavior of polyoxanorbornene-*g*-PEO copolymers (Table IV-1, runs 1, 5 & 10) was evaluated by thermo gravimetric analysis (TGA) under N₂ conditions in order to determine the degradation temperature of each copolymer (Figure IV-5). The polyoxanorbornene-*g*-PEO copolymers exhibited a one-step degradation process, and the temperature range of the first 5 % weight loss decomposition was determined to lie between 372 and 386 °C, indicating no influence of the PEO length.

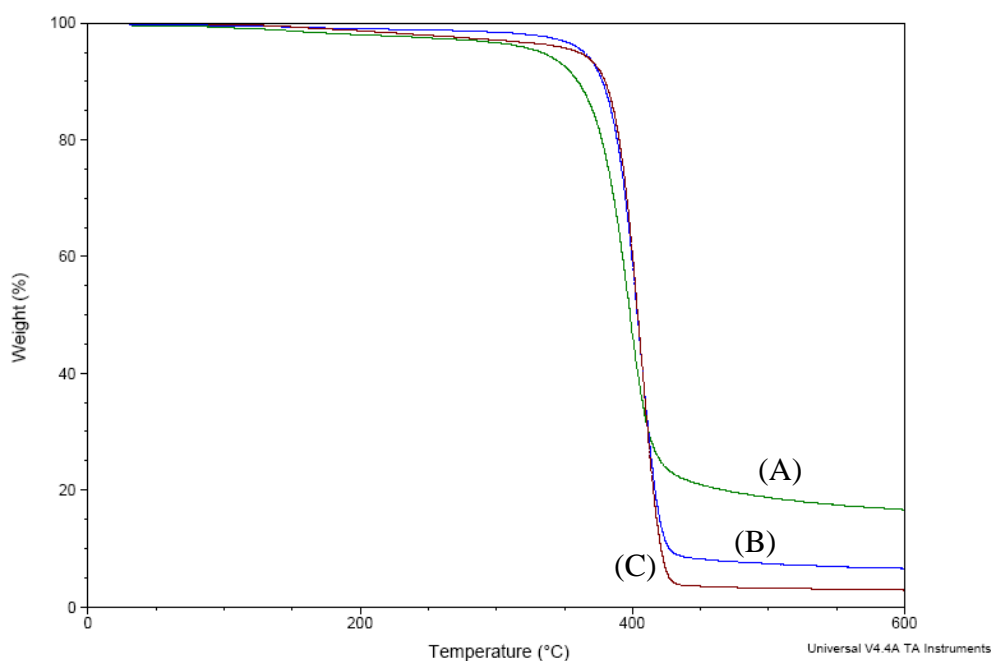


Figure IV-5. TGA thermograms of (A) polyoxanorbornene -*g*-PEO 500, (B) polyoxanorbornene *g*-PEO 2000 and (C) polyoxanorbornene *g*-PEO 5000 with a heating rate of 10 °C/min under nitrogen.

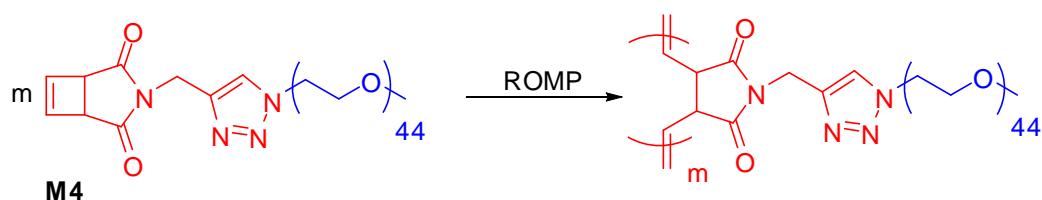
1-2. ROMP of cyclobutenyl-functionalized macromonomers

ROMP of cyclobutenyl PEO macromonomers is expected to afford graft copolymers with a strictly 1,4-polybutadiene backbone and an exact control over the placement of the PEO grafts resulting from a pure head-to-head arrangement.

I-2.1. ROMP of succinimide-based cyclobutenyl PEO macromonomers

Polymerization of the ω -cyclobutenyl PEO macromonomer **M4-2000**, which has a similar symmetrical structure as the ω -*exo*-oxanorbornenyl POE macromonomer **M2-2000** was first performed according to the conditions already reported (Scheme IV-4).

ROMP of ω -cyclobutenyl PEO macromonomers with **G3** as the initiator did not occur whatever the PEO length. Another third generation Grubbs' catalyst containing substitutionally labile pyridine and chloride ligands (**G3'**, Scheme IV-3) and exhibiting both fast initiation and high reactivity^{3,29,46,47} was tested for the polymerization, but all failed to produce polymer with no detectable yield. Such behaviour is related to the electronic effects of the allylic substituents obtained after initiation.⁴⁸⁻⁵⁰ The Π -acceptor carbonyl groups in 3 and 4 positions on the cyclobutene decrease activation barriers for the ring-opening.⁵¹⁻⁵³ Moreover, the coordination to the emerging ruthenium carbene metal center could result in a stable chelation through the 5-membered ring between metal center and oxygen after the initiation step that disfavors the propagation step.^{44,54-57}



Scheme IV-4. ROMP of ω -cyclobutenyl PEO macromonomer **M4-2000**.

The molybdenum Schrock initiator Mo-(NAr)(CHCMe₃)(OCMe(CF₃)₂)₂ was then used for the polymerization*. Its efficiency has been proven by successful polymerization of 3,4-disubstituted cyclobutenes with different functional groups such as ester and ether which do not polymerize with the first generation Grubbs' catalyst.^{12,13} However, this catalyst is limited by the high oxophilicity of the metal center, which renders them sensitive to oxygen and moisture, and the polymerization requires an inert atmosphere and rigorously purified, dried, and degassed solvents and reagents.⁵⁸

* This work has been done in the LCPO, Bordeaux University under the supervision of Dr. V. Héroguez.

Toluene was chosen as the solvent because it generally gives the most monodisperse polymer.^{12,13} Macromonomers were twice lyophilized to eliminate traces of water before polymerization. Reactions were carried out in dried and deoxygenated toluene and were terminated by adding benzaldehyde in excess with $[M]_0/[I]_0$ ratios of 6 and 10 at room temperature with a macromonomer concentration of 0.05 M. **M4-2000** was polymerized to quantitative yield in 16 and 24 h (Table VI-2).

Table IV-2. ROMP of cyclobutenyl PEO macromonomers **M4-2000** using Schrock catalyst.

Run	Macromonomer	$[M]_0/[I]_0^a$	$\overline{M}_{n,theo}^b$ (g/mol)	t (h)	Conv. ^c ¹ H NMR (%)	$\overline{M}_{n,SEC}^d$ (g/mol)	PDI ^d
1	M4-2000	6	13 200	16	~100	15 000	1.17
2	M4-2000	10	22 000	24	~100	22 000	1.10

^a Macromonomer to Schrock catalyst ratio. ^b $\overline{M}_{n,theo} = \overline{M}_n \text{ macromonomer} \times ([M]_0/[I]_0) \times \text{Conv. NMR} + M_{\text{extr.}}$. ^c Determined by comparing the peak areas of cyclobutenyl ring of the grafted copolymer and residual macromonomer from ¹H NMR of the crude product. ^d Number-average molecular weight and polydispersity measured by SEC in THF with RI detector, calibration with linear polystyrene standards.

¹H NMR spectroscopy indicated the disappearance of the vinyl proton signal of the macromonomer at 6.44 ppm and the appearance of the vinyl proton resonances of the backbone at 5.20-5.60 ppm. NMR spectroscopy also evidenced that the triazole moieties are preserved throughout the ROMP process (resonances in ¹H NMR at 7.72 ppm; triazole-H). However, SEC traces of the resulting copolymers showed the presence of a major high molecular weight peak and a minor low molecular weight peak (Figure IV-6, A and B). The low molecular weight peak had the same retention time as that of PEO-N₃ still present after “click” coupling as the stoichiometric alkyne-azide ratio is hard to reach with macromolecular structures. This hypothesis has been checked by the MALDI-TOF analysis of the **M4-2000** (Figure IV-7). The MALDI-TOF mass spectrum of **M4-2000** presents two populations, the major population corresponds to **M4-2000** ionized by Na⁺ (calculated value = 2134.29, experimental value = 2135.12 for n = 43), the minor one corresponds to PEO-N₃ ionized by Na⁺ (calculated value = 2061.35, experimental value = 2060.14 for n = 45).

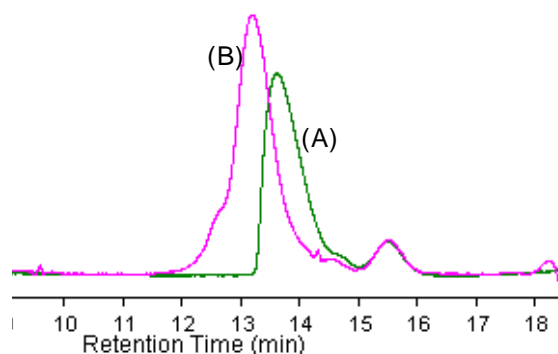


Figure IV-6. SEC traces of polybutadiene-*g*-PEO 2000 with (A) $[M]_0/[I]_0$ of 6 and (B) $[M]_0/[I]_0$ of 10 (Table IV-2, runs 1 & 2).

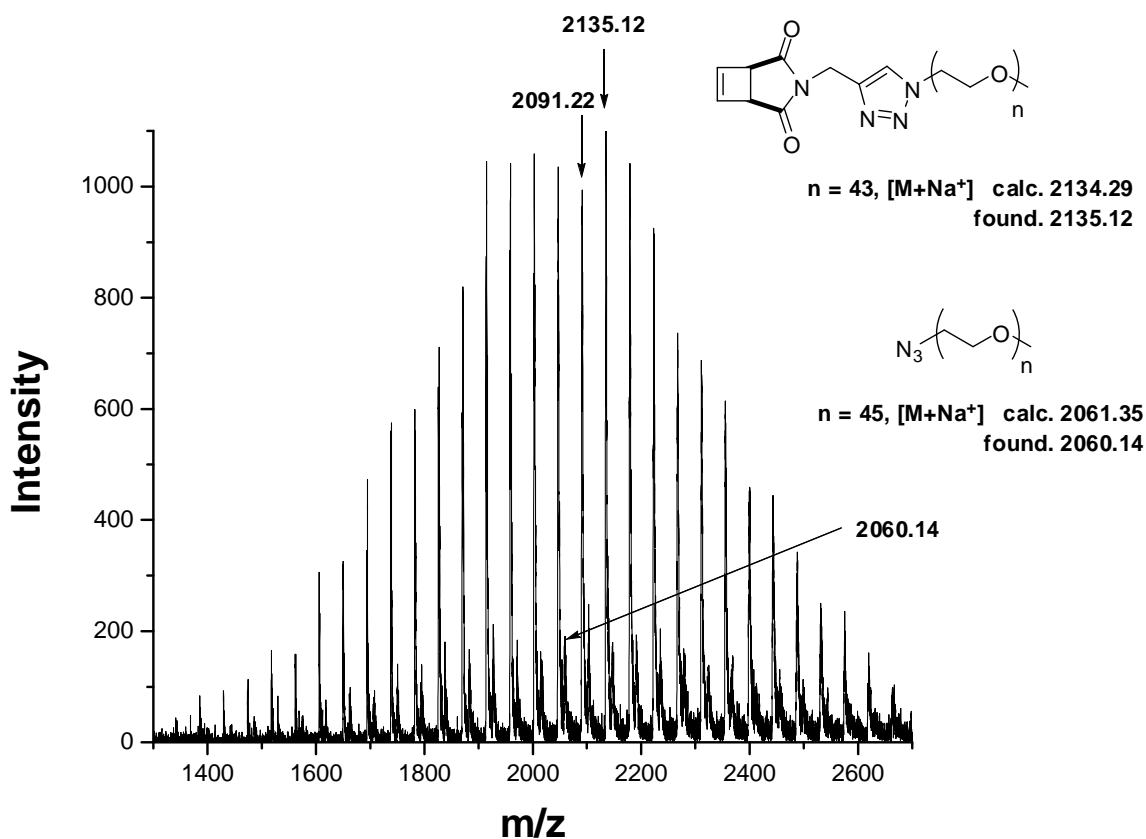


Figure IV-7. MALDI-TOF mass spectrum of **M4-2000** containing PEO- N_3 (matrix: 2-[(2*E*)-3-(4-*tert*-butylphenyl)-2-methylprop-2-enylidene]malononitrile (DCTB) + sodium trifluoroacetate (NaTFA)).

In the case of $[M]_0/[I]_0 = 6$ (Table IV-2, run 1), the high molecular weight peak shows a shoulder which has been attributed to double molecular weight PEO present in the

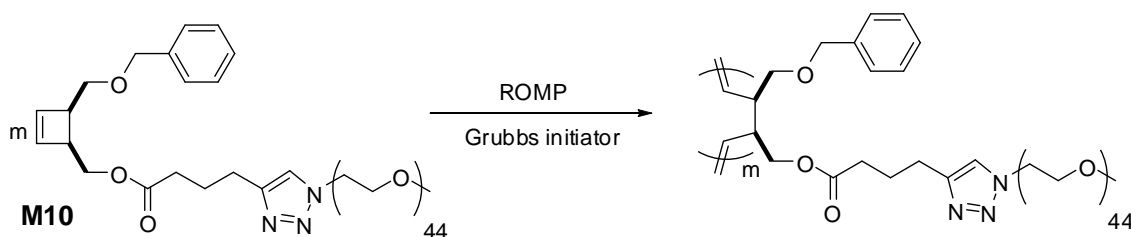
commercial product (Figure IV-6, A). In addition, the high molecular weight peak detected for the polymer issued from $[M]_0/[I]_0$ ratio of 10 (Table IV-2, run 2) presents a high molecular weight shoulder (Figure IV-6, B), which could be due to the back-biting between two polymeric chains.

The ability of unsymmetrical POE, poly(ethyl acrylate) and poly(*N*-isopropyl acrylamide) macromonomers to polymerize by ROMP has been studied.

I-2.2. ROMP of unsymmetrical PEO macromonomers

Macromonomer **M10** was chosen to study the reactivity of ω -cyclobutenyl PEO macromonomers towards ROMP in solution among all the synthesized macromonomers as it shows a critical micellar concentration (CMC) in water (reported latter in this chapter) that is expected to be powerful for the studies of ROMP in dispersed aqueous media.

The third generation Grubbs catalyst has first been chosen as its efficiency to initiate the polymerization of 1-substituted cyclobutenes bearing a large variety of side groups such as ether, ester and amine in solution has been proven.^{57,59-61} Reactions were carried out in DCM with a $[M]_0/[I]_0$ ratio of 10 at room temperature (Scheme IV-5) with a macromonomer concentration of 0.01 and 0.1 M (Table IV-3, runs 1-2).



Scheme IV-5. ROMP of ω -cyclobutenyl PEO macromonomer **M10**.

Table IV-3. ROMP of cyclobutenyl PEO macromonomer **M10** using **G2** and **G3** catalysts

Run	Catalyst	Solvent	$[M]_0/[I]_0^a$	$[M]_0^b$ (mol/L)	$\overline{M}_{n,theo}^c$ (g/mol)	t (h)	Temperature (°C)	Conv. ^d ¹ H NMR (%)	$\overline{M}_{n,SEC}^e$ (g/mol)	PDI ^e
1	G3	DCM	10	0.01	23 000	3	25	~75	bimodal	1.17
2	G3	DCM	10	0.1	23 000	3	25	~100	15 000	1.17
3	G2	Toluene	10	0.01	23 000	148	70	~100	19 800	1.07
4	G2	Toluene	20	0.01	46 000	48	70	~100	26 900	1.11
5	G2	Toluene	30	0.01	69 000	48	70	~100	38 000	1.10

^a Macromonomer to Grubbs' catalyst ratio. ^b initial concentration of macromonomer solution ^c $\overline{M}_{n,theo} = \overline{M}_{n,macromonomer} \times ([M]_0/[I]_0) \times \text{Conv. NMR} + M_{extr.}$ ^d Determined by comparing the peak areas of vinyl proton of the grafted copolymer and residual macromonomer from ¹H NMR of the crude product. ^e Number-average molecular weight and polydispersity measured by SEC in THF with RI detector, calibration with linear polystyrene standards.

When a green solution of **G3** was added to a colorless solution of monomer, the color immediately changed to yellow, which implies the immediate initiation of the polymerization. After 3h, at low macromonomer concentration, **M10** was polymerized to 75% conversion. By increasing the macromonomer concentration from 0.01 up to 0.1 mol/L, a quantitative polymerization was observed as shown by the disappearance of the vinyl proton signal of **M10** at 6.10 ppm and the appearance of the vinyl proton resonances of grafted copolymer at 5.10-5.50 as indicated in the ^1H NMR spectrum (Figure IV-8).

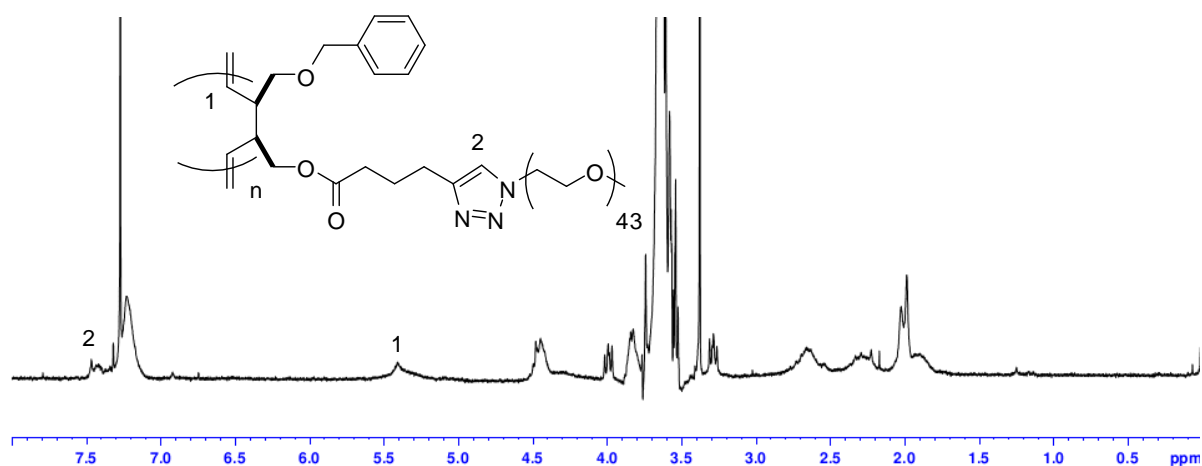


Figure IV-8. ^1H NMR spectrum of 1,4-polybutadiene-*g*-PEO 2000 from **M10** (Table IV-3, run 2); solvent: CDCl_3 .

However, the SEC trace showed the presence of a major high molecular weight peak and a minor low molecular weight peak (Figure IV-9, A). The low molecular weight peak had the same retention time that the PEO- N_3 or macromonomer **M10** and has been removed by reprecipitation of a solution of the crude copolymer in THF into diethyl ether. The filtrate was evaporated and the resulting residue has been analyzed by ^{13}C NMR spectroscopy. The ^{13}C NMR spectrum of the residue (B, Figure IV-10) showed the presence of PEO- N_3 and of 1,4-polybutadiene-*g*-PEO. Macromonomer **M10** was not observable in this residue. This result confirmed that the minor low molecular weight peak corresponds to PEO- N_3 in excess after the “click” coupling and that ROMP was quantitative. The SEC trace of purified polymer showed an asymmetric distribution (PDI = 1.14, Figure IV-9, B) with a small extension towards low molecular weight

which is caused by the back-biting of polybutadiene with Grubbs and Schrock type catalysts.⁶²⁻⁶⁴

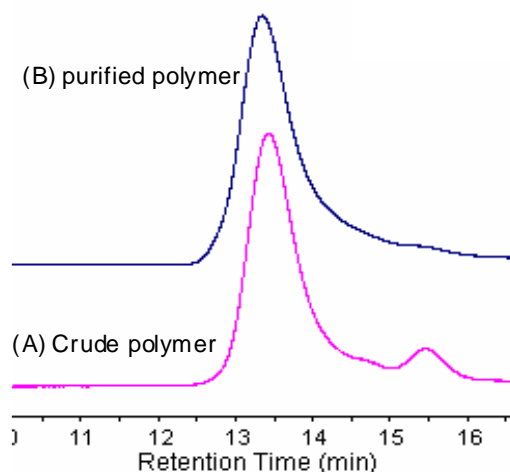


Figure IV-9. SEC traces of polybutadiene-g-PEO synthesized from ROMP of **M10** initiated by **G3** (A) before and (B) after purification.

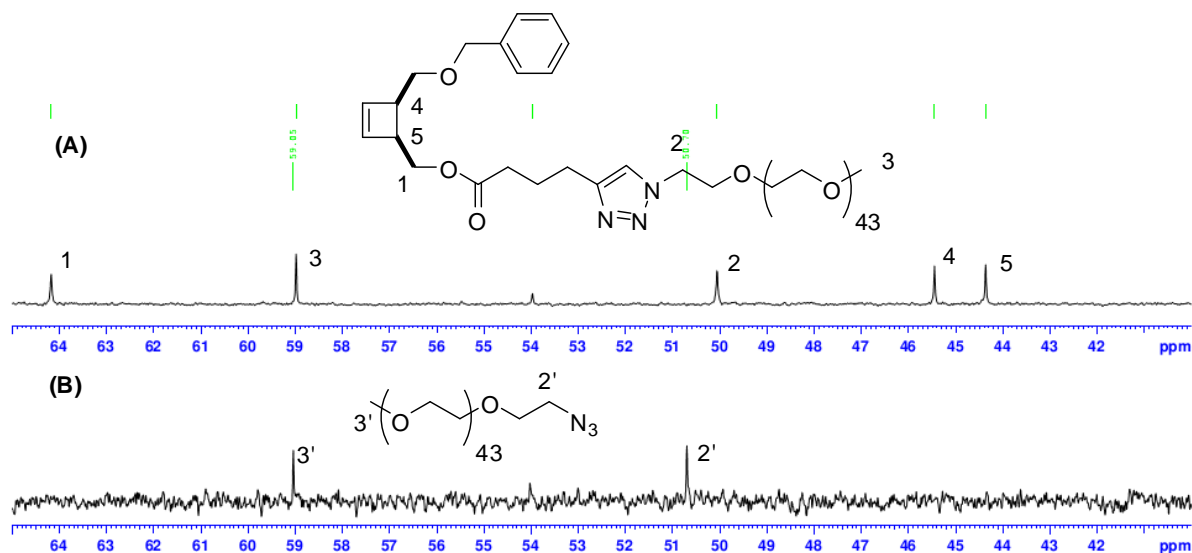


Figure IV-10. ¹³C NMR spectra of (A) cyclobutenyl PEO macromonomer **M10** and (B) residual PEO-N₃ separated from crude polymer; solvent: CDCl₃.

To minimize the chain transfer phenomenon, ROMP using first- or second-generation Grubbs catalyst (**G1** & **G2**) was realized.^{11,34} The reactivity of **G1** catalyst ((Cy₃P)₂RuCl₂(CHPh)) seems to be too low towards cyclobutenyl polystyrene-*b*-

poly(*tert*-butyl acrylate) macromonomers, probably as a consequence of the steric hindrance effect of the polymeric chain, as already observed with a cyclobutenyl and a norbornenyl macromonomer bearing two polymeric chains.^{11,34} The **G2** catalyst ((IMesH₂)-(Cy₃P)RuCl₂(CHPh)), one of the most active ROMP catalysts commercially available, is less used despite its higher activity, as the polymerizations are, in general, less controlled.⁶⁵ However, it has already been used for polymerization of hindered macromonomers such as cyclobutenyl and norbornenyl macromonomers, leading to well-defined graft copolymers with narrow polydispersity indices.^{11,34} In particular, previous studies in our laboratory have demonstrated the efficiency of initiator **G2** to polymerize α -cyclobutenyl polystyrene-*b*-poly(*tert*-butyl acrylate) macromonomers in toluene at 50-70 °C for 7 days.¹¹

The first attempt using **G2** and macromonomer **M10** was performed according to the conditions reported for α -cyclobutenyl polystyrene-*b*-poly(*tert*-butyl acrylate) macromonomers. The ROMP was carried out in toluene with a [M]₀/[I]₀ ratio of 10 at 70 °C with a macromonomer concentration of 0.01 M. After 7 days, the ¹H NMR spectroscopy indicated the disappearance of the vinyl proton signal of **M10** at 6.10 ppm. The SEC trace showed the presence of a major high molecular weight peak and a minor low molecular weight peak (Figure IV-11, A). The low molecular weight peak corresponds to unreacted PEO-N₃ as already shown. In contrast to the ROMP using **G3**, the high molecular weight peak was unimodal and symmetric indicating a well-defined 1,4-polybutadiene-*g*-PEO copolymer, with a low polydispersity index (PDI = 1.07, $\overline{M}_{n,SEC} = 19\,800$ g/mol) (Table IV-3, run 3) without any chain transfer phenomenon.

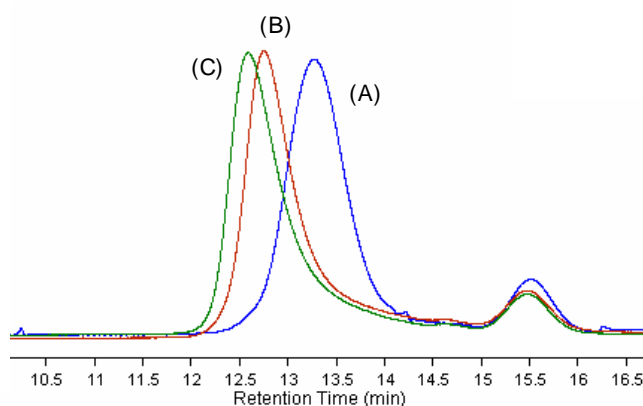


Figure IV-11. SEC traces of 1,4-polybutadiene-*g*-PEO from **M10** initiated by **G2** with [M]₀/[I]₀ of (A) 10, (B) 20 and (C) 30.

The same conditions were successfully applied to ROMP of **M10** with $[M]_0/[I]_0$ ratios of 20 and 30. ^1H NMR spectroscopy showed that a complete macromonomer conversion was obtained after 48 h, in all cases (Table IV-3, runs 4 & 5). Furthermore, the unimodal SEC traces (Figure IV-11, B & C) of the graft copolymers obtained showed a consistent shift towards high molecular weight with increasing the $[M]_0/[I]_0$ ratio, while the polydispersity indices remain low indicating that well-defined graft copolymers have been prepared. The small amount of residual PEO- N_3 can be simply removed through reprecipitation of a solution of the crude polymer in THF into diethyl ether thanks to the difference in solubility between PEO- N_3 and graft copolymers. The SEC trace of purified polymer showed only one peak of graft copolymer (Figure IV-12, B).

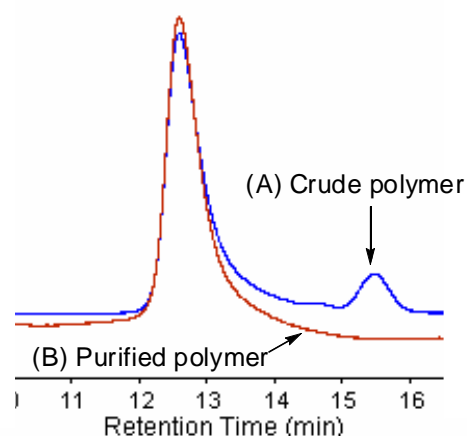


Figure IV-12. SEC traces of 1,4-polybutadiene-*g*-PEO from **M10** initiated by **G2** with $[M]_0/[I]_0$ of 30 (A) before and (B) after purification.

I-2.3. ROMP of RAFT-derived macromonomers

The reactivity and compatibility of α -cyclobutenyl poly(ethyl acrylate) and poly(*N*-isopropyl acrylamide) macromonomers **M14-EA** and **M14-NIPAM** towards ROMP have then been studied. **G3** was used as the initiator. α -Cyclobutenyl poly(ethyl acrylate) macromonomers with $\overline{M}_{n,SEC} = 5\,350$ g/mol (Table III-1, run 2) and α -cyclobutenyl poly(*N*-isopropyl acrylamide) macromonomer with $\overline{M}_{n,SEC} = 4\,700$

g/mol (Table III-2, run 1) were subjected to ROMP in DCM with a $[M]_0/[I]_0$ ratio of 10 at room temperature with a macromonomer concentration of 0.05 M (Table IV-4).

Table IV-4. ROMP of α -cyclobutenyl macromonomer **M14** using **G3** catalyst in DCM with $[M]_0/[I]_0$ of 10.

Run	Macromonomer	Time (h)	Conv. ^1H NMR ^a (%)	$\overline{M}_{n,theo}$ ^b (g/mol)	$\overline{M}_{n,SEC}$ ^c (g/mol)	PDI ^c
1	M14-EA	2	65	53 000	bimodal distribution	
2	M14-EA	24	70	53 000		
3	M14-NIPAM	24	0	47 000	-	-

^a Determined by comparing the peak areas of vinyl proton of the grafted copolymer and residual macromonomer from ^1H NMR of the crude product. ^b $\overline{M}_{n,theo} = \overline{M}_n \text{ macromonomer} \times ([M]_0/[I]_0) \times \text{Conv. NMR} + M_{\text{extr}}$. ^c Number-average molecular weight and polydispersity measured by SEC in THF with RI detector, calibration with linear polystyrene standards.

The ROMP of α -cyclobutenyl poly(*N*-isopropyl acrylamide) macromonomer did not occur at all (Table IV-4, run 3). This behaviour could be explained by the high concentration of acrylamide groups that can result in inhibition of the catalytic cycle in initiation step by competitive binding to the ruthenium metal center.^{66,67} *In situ* deactivation of the amine-containing group, *via* Bronsted⁶⁸⁻⁶⁹ or Lewis acid addition,⁷⁰ has been reported to affect metathesis reaction of amine-containing compounds.

In contrast, the ROMP of poly(ethyl acrylate) macromonomer was effective, leading to 1,4-polybutadiene-*g*-poly(ethyl acrylate) with 70% conversion after 24h of reaction (Table IV-4, runs 1 & 2). This relatively low yield of ROMP of high molecular weight macromonomer is believed to mirror the difficulty of the macromonomer double bonds to get coordinated to the vacant site of the transition metal.⁴³ These macromonomers showed a similar behaviour as macromonomer **M10**, and it is expected that the use of more favorable conditions, *i.e.* **G2** catalyst in toluene at 70 °C, could allow to reach a quantitative conversion.

II- ROMP in dispersed media

The previously synthesized macromonomers are composed of a poly(ethylene oxide) hydrophilic block and a hydrophobic sequence terminated with an unsaturation. It is expected that such structures could be used as *surfmers* in (mini-)emulsion ROMP. Such a strategy has the advantage to bring closer the polymerizable groups into the core. The surfactant properties of the ω -cyclobutenyl or ω -oxanorbornenyl PEO macromonomers have been studied by static light scattering (SLS) and by steady state fluorescence spectroscopy using pyrene as a probe to determinate the CMC.

II-1. CMC determination of macromonomers

II-1.1. SLS measurements

A range of PEO macromonomers have been analysed using SLS. A summary of the macromonomers properties is listed in Table IV-5.[#]

Table IV-5. Characterization of the PEO macromonomers in pure water by static light scattering.

Run	Sample	M_w^a (g/mol)	$M_{n,NMR}^b$ (g/mol)	$2A_2$ ($\times 10^{-6}$) ^c
1	M2-500	481	757	-55.4
2	M2-2000	2 381	2 240	9.31
3	M2-5000	5 250	4 817	6.75
4	M9	2 383	2 293	-0.0045
5	M10	2 029	2 235	-28.13

^a Determined by static light scattering. ^b $M_{n,NMR} = M_{n,PEO} + M_{extr}$ where $M_{n,PEO}$ is the number-average molecular weight of poly(ethylene oxide) determined by ¹H NMR spectroscopy and M_{extr} is the molar mass of the chain-end. ^c determined by Zimm plot.

In all cases, the weight-average molecular weights M_w of the macromonomers, calculated using the Zimm methodology, are in good agreement with the values

[#] This work has been done by M. E. Levere in collaboration with Pr. C. Chassenieux, within the framework of a 9 months post-doctoral position (January-September 2010) financed by the ANR under contract ANR_08_BLAN_0104 ("cycloROMP")

calculated by ^1H NMR spectroscopy. The second virial coefficient, A_2 , provides a measure of the aggregation behaviour of the macromonomers in solution, with a more positive value indicating increased solute-solvent interactions and a more negative value indicating increased solute-solute interactions (*i.e* more aggregation).

When a short PEO chain in macromonomer **M2-500** is used, the second virial coefficient determined by the gradient of the Zimm plot is negative, indicating that interactions between the chains are occurring. As the PEO chain increases in length, the second virial coefficient of the macromonomer becomes positive, suggesting that there is less aggregation between these macromonomers. This is because the ratio of the hydrophobic end-groups with respect to the water soluble PEO chain decreases and so, the hydrophobic chain-end is less able to exert an influence over the behaviour of the macromonomer in aqueous solution. As such, **M2-2000** and **M2-5000** did not aggregate in solution.

Similar result has been obtained with cyclobutene-based macromonomer **M9**, which do not aggregate in water. Changing the structure of the macromonomer by inserting a hydrophobic chain $(-\text{CH}_2)_3$ exerts a strong influence over the behaviour of the macromonomer in aqueous solution. The cyclobutene-based macromonomer **M10** shows a negative second virial coefficient, indicating attractive forces between the polymer chains. It is predicted from these results that raising the concentration sufficiently may eventually cause the macromonomer **M10** to aggregate in solution.

II-1.2. Fluorescence spectroscopy

The CMC of macromonomers has been determined from the fluorescence spectroscopy. Previous studies demonstrated the fluorescence of pyrene and pyrene-3-carboxaldehyde as an effective means to determine CMC of selected nonionic, anionic and cationic surfactants.⁷¹⁻⁷² Fluorescence probes such as pyrene and pyrene-3-carboxaldehyde which are sensitive to the polarity of the solubilizing medium will exhibit different fluorescence behavior in micellar and nonmicellar solutions. Such changes of behaviour as a function of surfactant concentration have been used to determine the CMC of surfactants. In case of pyrene-3-carboxaldehyde, emission spectrum was obtained by

exciting samples at 380 nm. The emission spectrum of pyrene-3-carboxaldehyde in water exhibits a single peak at 469 nm. The decrease in the λ_{\max} of pyrene-3-carboxaldehyde in surfactant solution is an indication of the solubilization of the probes in a more hydrophobic environment than water, *i.e.*, hydrophobic micellar cores.⁷²⁻⁷³ In case of pyrene, the excitation spectrum shows one peak at 333 nm characteristic of pyrene in an aqueous environment and one peak at 338.5 nm characteristic of pyrene in a hydrophobic environment (Figure IV-13, A). An increase of the value of $I_{338.5}/I_{333}$ indicate the transfer of pyrene molecules from a water environment to the hydrophobic micellar cores.⁷³

Two macromonomers (**M10** and **M15**) were chosen to perform CMC measurements as **M10** presents an aggregation in water and **M15** contains a high hydrophobic chain -C₁₂H₂₅. All macromonomer solutions were prepared using water in flasks containing a thin layer of pyrene or pyrene-3-carboxaldehyde (concentration: 5×10^{-7} mol/L) and were stirred at room temperature for 24 hours to ensure full dissolution. The change in $I_{338.5}/I_{333}$ as a function of the $\log[M10]_0$ is given in Figure VI-13, B. The first break point indicates a CMC for **M10** at 3 mg/mL.

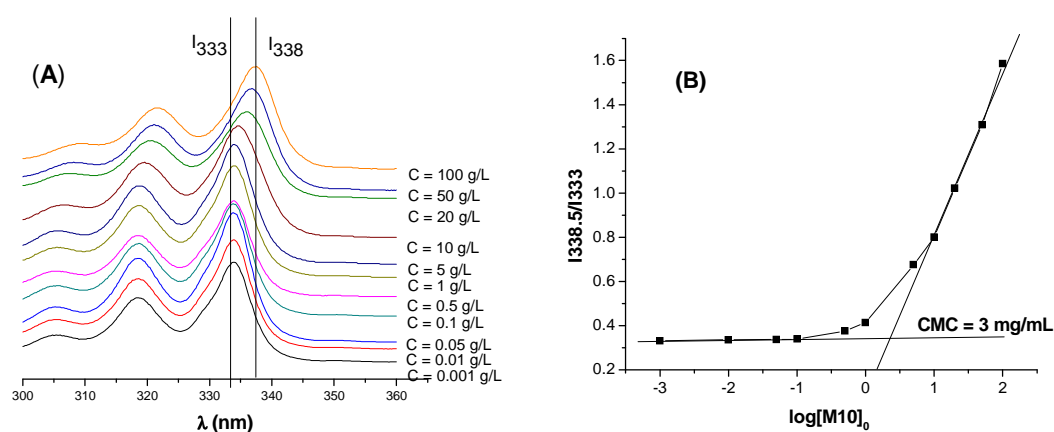


Figure IV-13. (A) Excitation spectra of pyrene (5×10^{-7} mol/L) in aqueous solutions of **M10** at different concentrations, and (B) semilogarithmic plot of the intensity ratio ($I_{338.5}/I_{333}$) from pyrene excitation spectra *versus* the concentration of **M10** in water.

On the other hand, pyrene-3-carboxaldehyde was chosen as fluorescence probe for the CMC determination of **M15** because **M15** presents an absorption band from 250 to 350

nm due to its trithiocarbonate moiety that could influence the absorption and emission of pyrene. Figure IV-14 indicated that the CMC of **M15** was 0.3 mg/mL at which a marked decrease in the λ_{\max} parameter of pyrene-3-carboxaldehyde occurred. The lower CMC of **M15** than that obtained for **M10** is attributed to the higher hydrophobicity induced by the $-C_{12}H_{25}$ group of chain transfer agent RAFT moiety as the hydrophilic part is the same.

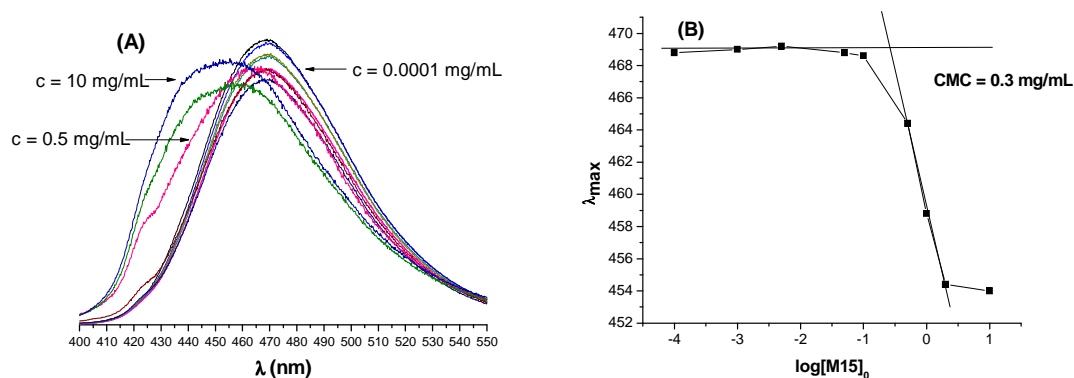


Figure IV-14. (A) Emission spectra of pyrene-3-carboxaldehyde (5×10^{-7} mol/L) in aqueous solutions of **M15** at different concentrations, and (B) semilogarithmic plot of the λ_{\max} of emission band of pyrene-3-carboxaldehyde (5×10^{-7} mol/L) versus the concentration of **M15** in water; $\lambda_{\text{em}} = 380$ nm.

The self-organization of these macromonomers **M10** and **M15** in water is expected to make them good candidates for ROMP in aqueous dispersed media.

II-2. ROMP in dispersed media of oxanorbornenyl- and cyclobutenyl-functionalized macromonomers

II-2.1. ROMP in dispersed aqueous media of oxanorbornenyl macromonomer[#]

Before testing the ROMP in dispersed aqueous media, a kinetic of ROMP of **M2-2000** using **G1** in DCM with a $[M]_0/[I]_0$ ratio of 10 has first been studied by ^1H NMR spectroscopy in order to check the reactivity of oxanorbornenyl PEO macromonomer towards ROMP in the same conditions of macromonomer concentration in oil phase

[#] This work has been done in the LCPO, Bordeaux University, during a 6 weeks stay under the supervision of Dr. V. Héroguez.

than those used for the emulsion technique, *i.e.* 0.23 mol/L. ♦ As shown in Figure IV-15, a quantitative conversion was obtained after 52 minutes of reaction attesting the efficiency of **G1** for the ROMP of **M2-2000**.

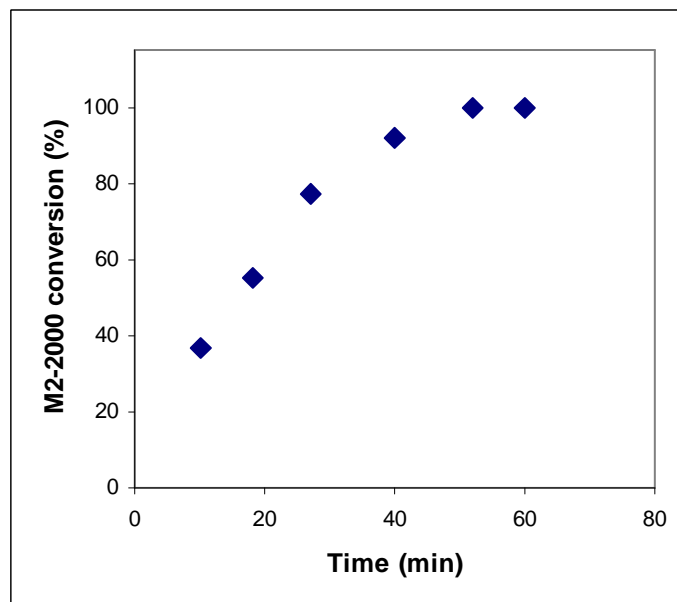


Figure IV-15. Conversion of macromonomer **M2-2000** initiated by **G1** versus time with a $[M]_0/[I]_0$ ratio of 10.

The ROMP of oxanorbornenyl PEO macromonomer **M2-2000** has first been carried out in micro-emulsion. Moreover, the hydrophobic Grubbs' catalyst cannot be added directly into the micro-emulsion medium as water-soluble initiator. Thus, two aqueous micro-emulsions have been prepared. Two identical aqueous phases were first prepared by solubilizing an anionic surfactant such as sodium dodecyl sulfate (SDS) and a co-surfactant (1-pentanol for this work) in degassed deionized water.* The first micro-emulsion was prepared by adding to the first aqueous phase, an oil phase, which was composed of macromonomer solubilized in an organic solvent, whereas the second one was prepared by adding to the second aqueous phase an oil phase composed of Grubbs catalyst solubilized in an organic solvent. Once the two micro-emulsion phases have

♦ This work has been done by Dr. F. Collette within the framework of a 6 months post-doctoral position financed by the ANR under contract ANR_08_BLAN_0104 ("cycloROMP") in the LCPO, Bordeaux University.

* The conditions have been previously optimized by Airaud, C.; Ibarboure, E.; Gaillard, C.; Héroguez, V. in *J. Polym. Sci. Part A: Polym. Chem.* **2009**, *47*, 4014-4027.

been mixed together, exchanges between the droplets of both micro-emulsions enable the initiator to meet the macromonomer and thus trigger off the ROMP.⁷⁴⁻⁷⁸

This test was realized using **G1** as the initiator and a $[M]_0/[I]_0$ ratio of 10 at room temperature. DCM was used as the organic solvent to solubilize both macromonomer **M2-2000** and **G1**. However, the polymerization didn't occur at all after 24 h of reaction. The use of toluene as organic solvent and a reaction temperature of 60 °C did not allow to increase the macromonomer conversion. This behaviour could be explained by the fact that the two micro-emulsion systems did not allow an exchange between the droplets of initiator and of macromonomer.

Mini-emulsion conditions were then selected because they enable to minimize inter-droplet exchanges between macromonomer and catalyst. A droplet emulsion was prepared by mixing under stirring the oil phase containing macromonomer, Grubbs catalyst, hexadecane solubilized in an organic solvent and the water phase containing the surfactant Brij 700. The mixture was subjected to an efficient homogenization by ultrasonication for two minutes to produce the droplet mini-emulsion.[#] The mini-emulsion polymerization data generated with two different $[M]_0/[I]_0$ ratios are summarized in Table IV-6.

Table IV-6. Mini-emulsion of macromonomer **M2-2000** using **G1** as the initiator.

Run	Oil phase	$[M]_0/[I]_0^a$	Time (h)	Conv. NMR ^b (%)	Conv. SEC ^c (%)	D_h^d (nm)
1	DCM	10	24	90	86	109,8
2	DCM	50	24	35	34	169,8

^a Macromonomer to Grubbs' catalyst ratio ^b Determined by comparing the peak areas of vinyl proton of the grafted copolymer and residual macromonomer from ¹H NMR of the crude product. ^c Determined by comparing the peak areas of grafted copolymer and residual macromonomer from SEC measurement of the crude product. ^d Hydrodynamic diameter of particle obtained after 24 h of reaction determined by dynamic light scattering.

[#] The mini-emulsion process has been reported in Airaud, C.; Gnanou, Y.; Héroguez, V. *Macromolecules* **2008**, *41*, 3015-3022

A nearly quantitative conversion was obtained after 24 h (Table IV-6, run 1) for a $[M]_0/[I]_0$ ratio of 10. Particles with an average diameter of 109 nm were generated and were stable over two months. In contrast, the conversion was only 35% after 24 h of reaction for a $[M]_0/[I]_0$ ratio of 50. Such behaviour is related to the low quantity of catalyst in the system or the low efficiency of **G1** for the ROMP of **M2-2000** at high \overline{DP}_n .

II-2.2. ROMP in mini-emulsion of cyclobutenyl macromonomer*

Two macromonomers **M10** and **M15** were chosen to study their ability to polymerize by ROMP in mini-emulsion because of their self-organization properties, which is expected to make them good candidates as they act as monomer and surfactant.

In order to gain more insight into the process, a kinetic study of ROMP in DCM of **M10** and **M15** for different $[M]_0/[I]_0$ ratios in the same macromonomer concentration conditions as those used in the oil phase of mini-emulsion process was performed. The third generation Grubbs catalyst has first been chosen as the ROMP initiator because of its efficiency for the polymerization of cyclobutenyl macromonomers in mild conditions, *i.e.* room temperature. The conversion was determined by comparing the peak areas of vinyl group of cyclobutene of residual macromonomer and of the triazole proton of both polymer and residual macromonomer from ^1H NMR of the crude product.

High conversions were quickly obtained after 10 min of reaction with low $[M]_0/[I]_0$ ratios of 10-20 and 20 of **M10** and **M15**, respectively. The overall polymerization rate decreased with an increasing $[M]_0/[I]_0$ ratio (Figures IV-16 & IV-17). However, the crude polymers obtained could not be totally dissolved in any solvent such as water, DCM, THF and DMF. Such behaviour could be ascribed to the back-biting of 1,4-polybutadiene chains at high macromonomer concentration⁶²⁻⁶⁴ to form multicyclic of polybutadiene backbone that could increase the compactness of copolymers.

* This work has been done in the LCPO, Bordeaux University during a 6 weeks stay under the supervision of Dr. V. Héroguez

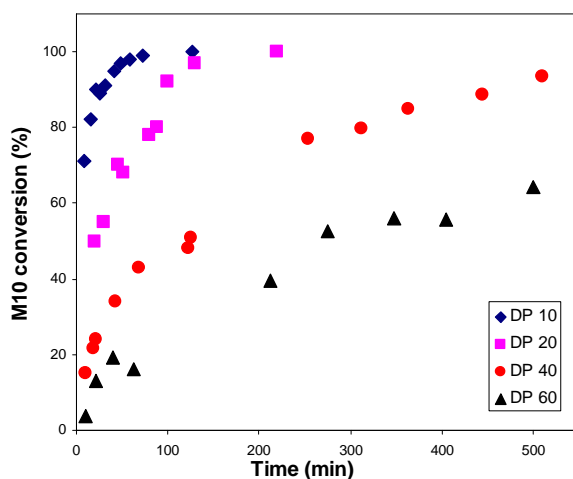


Figure IV-16. Conversion of macromonomer **M10** initiated by **G3** in DCM *versus* time with a range of $[M]_0/[I]_0$ ratios of 10-60 with $[M]_0 = 0.23$ mol/L.

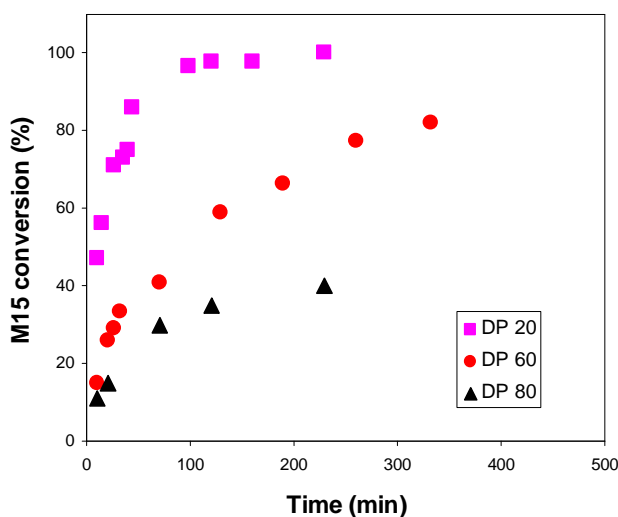


Figure IV-17. Conversion of macromonomer **M15** initiated by **G3** in DCM *versus* time with a range of $[M]_0/[I]_0$ ratios of 10-80 with $[M]_0 = 0.23$ mol/L.

The mini-emulsion system was prepared by applying the same DCM/water ratio of the mini-emulsion of oxanorbornenyl macromonomer, *i.e.* 1.2% because of an evaporation of solvent under heating of the ultrasonication. An increase of DCM/water proportion from 1.2 to 3.3 % and a decrease of the temperature to 1 °C before ultrasonication allow to form a stable mini-emulsion system. The stability of monomer droplets was then monitored as a function of time by DLS. The monomer droplets in the size range of 340 nm were stable over 48h at room temperature.

An aqueous mini-emulsion ROMP of **M10** using a $[M]_0/[I]_0$ ratio of 60 was then triggered (Table IV-7).

Table IV-7. Mini-emulsion of macromonomer **M10** using **G3** as the initiator.

Run	Macromonomer	Oil phase	$[M]_0/[I]_0^a$	Time (h)	Conv. NMR ^b (%)	D_h^c (nm)
1	M10	DCM	60	24	50	340
2	M10	DCM	60	38	56	350

^a Macromonomer to Grubbs' catalyst ratio ^b Determined by comparing the peak areas of vinyl proton of the grafted copolymer and residual macromonomer from ¹H NMR of the crude product. ^c Hydrodynamic diameter of particle obtained after 24 h of reaction determined by dynamic light scattering.

The initial droplets size was 300 nm. After 24 h of reaction, the overall conversion was 50% and increases slowly to 56% after 38 h. A possible explanation of the decrease of the polymerization rate might be related to the decrease macromonomer concentration per particle as the interval III, *i.e.* third period of kinetic curve, in mini-emulsion process.⁷⁹

Conclusion

ROMP of previously synthesized oxanorbornenyl and cyclobutenyl macromonomers has been investigated in solution and in dispersed media.

The ROMP of oxanorbornenyl PEO-based macromonomers was carried out using the Grubbs catalyst **G3**, leading to a variety of well-defined graft copolymers, although the efficiency of the ROMP process was affected by the molecular weight of the macromonomers. A series of polyoxanorbornene-*g*-PEO 500 with various lengths of the overall backbone was prepared by controlling the macromonomer-to-catalyst ratio, giving access to brush copolymers with low polydispersity index ($PDI \leq 1.17$). The long PEO chain macromonomers 2000 and 5000 were able to form polyoxanorbornene-*g*-PEO with relatively short backbone length.

Within the cyclobutenyl PEO-based macromonomers series, the succinimide-based cyclobutenyl PEO macromonomer was only polymerized by Schrock catalyst to form short backbone length because the Π -acceptor carbonyl groups in 3 and 4 positions on the cyclobutene deactivate the double bond towards ROMP initiated by Grubbs catalysts. 3,4-Substituted cyclobutenyl PEO macromonomers with Π -donor group have been successfully polymerized by Grubbs catalysts **G2** and **G3** with a range of $[M]_0/[I]_0$ ratios from 10 to 30. It is noteworthy that ROMP initiated by third generation Grubbs catalyst was efficient but accompanied by chain transfer reactions while ROMP initiated by second generation Grubbs catalyst resulted in well-defined 1,4-polybutadiene-*g*-PEO with low PDI (≤ 1.12).

The behaviour of all PEO macromonomers has been studied in aqueous solution. Two of them show a CMC, *i.e.* cyclobutenyl PEO macromonomer **M10** and CTA-based cyclobutenyl PEO macromonomer **M15**, with a PEO chain 2000 and a large hydrophobic segment. **M10** and oxanorbornenyl macromonomer with PEO chain 2000, **M2-2000**, have been subjected to ROMP in dispersed aqueous media. The preliminary results demonstrated that the mini-emulsion conditions were efficient for the polymerization of both oxanorbornenyl- and cyclobutenyl-functionalized PEO macromonomers. The particle size ranges from 100 to 350 nm after the polymerization with conversion from 35-90%.

References

1. Quéméner, D.; Héroguez, V.; Gnanou, Y. in “*Macromolecular Engineering: Precise Synthesis, Materials Properties, Applications*”, (K. Matyjaszewski, Y. Gnanou, L. Leibler Eds.), Wiley-VCH, Weinheim, **2007**, Vol. 1, Chapter 6.
2. Quéméner, D.; Chemtob, A.; Héroguez, V.; Gnanou, Y. *Polymer* **2005**, *46*, 1067-1075.
3. Liaw, D. J.; Huang, C. C.; Ju, J. Y. *J. Polym. Sci. Part A: Polym. Chem.* **2006**, *44*, 3382-3392.
4. Morandi, G.; Mantovani, G.; Montembault, V.; Haddleton, D. M.; Fontaine L. *New J. Chem.* **2007**, *31*, 1826-1829.
5. Xia, Y.; Kornfield, J. A.; Grubbs R. H. *Macromolecules* **2009**, *42*, 3761-3766.
6. Patton, D. L.; Advincula R. C. *Macromolecules* **2006**, *39*, 8674-8683.
7. Li, Z.; Zhang, K.; Ma, J.; Cheng, C.; Wooley, K. L. *J. Polym. Sci. Part A: Polym. Chem.* **2009**, *47*, 5557-5563.
8. Li, Z.; Ma, J.; Cheng, C.; Zhang, K.; Wooley, K. L. *Macromolecules* **2010**, *43*, 1182-1184.
9. Li, Y.; Themistou, E.; Zou, J.; Das, B. P.; Tsianou, M.; Cheng, C. *ACS Macro Lett.* **2012**, *1*, 52-56.
10. Morandi, G.; Montembault, V.; Pascual, S.; Legoupy, S.; Fontaine, L. *Macromolecules* **2006**, *39*, 2732-2735.
11. Perrott, M. G.; Novak, B. M. *Macromolecules* **1995**, *28*, 3492-3494.
12. Perrott, M. G.; Novak, B. M. *Macromolecules* **1996**, *29*, 1817-1823.
13. Wu, Z.; Grubbs, R. H. *Macromolecules* **1995**, *28*, 3502-3508.
14. G. Black, D. Maher, W. Risse, in *Handbook of Metathesis*; Wiley VCH, Weinheim, **2003**, 3.
15. Benson, S. W.; Cruickshank, F. R.; Golden, D. M.; Haugen, G. R.; O'Neal, H. E.; Rogers, A. S.; Shaw, R.; Walsh, R. *Chem. Rev.* **1969**, *69*, 279-324.
16. Morandi, G.; Montembault, V.; Pascual, S.; Legoupy, S.; Delorme, N.; Fontaine, L. *Macromolecules* **2009**, *42*, 6927-6931.
17. Lapinte, V.; De Frémont, P.; Montembault, V.; Fontaine, L. *Macromol. Chem. Phys.* **2004**, *205*, 1238-1245.
18. Ding, J.; Chuy, C.; Hodcroft, S. *Macromolecules* **2002**, *35*, 1348-1355.

19. Maniruzzaman, M.; Kawaguchi, S.; Ito, K. *Macromolecules* **2000**, *33*, 1583-1592.
20. Capek, I. *Adv. Colloid Interface Sci.* **2000**, *88*, 295-357.
21. Claverie, J. P. ; Soula, R. *Progr. Polym. Sci.* **2003**, *28*, 619-662.
22. Mecking, S.; Held, A.; Bauers, F. M. *Angew. Chem. Int. Ed.* **2002**, *41*, 544-561.
23. Pecher, J.; Mecking, S. *Macromolecules* **2007**, *40*, 7733-7735.
24. Quémener, D.; Héroguez, V.; Gnanou, Y. *J. Polym. Sci. Part A: Polym. Chem.* **2006**, *44*, 2784-2793.
25. Quémener, D.; Bousquet, A.; Héroguez, V.; Gnanou, Y. *Macromolecules* **2006**, *39*, 5589-5591.
26. Airaud, C.; Gnanou, Y.; Héroguez, V. *Macromolecules* **2008**, *41*, 3015-3022
27. Love, J. A.; Morgan, J. P.; Trnka, T. M.; Grubbs, R. H. *Angew. Chem. Int. Ed.* **2002**, *41*, 4035-4037.
28. Slugovc, C.; Demel, S.; Riegler, S.; Hobisch, J.; Stelzer, F. *Macromol. Rapid Commun.* **2004**, *25*, 475-480.
29. Choi, T.-L.; Grubbs, R. H. *Angew. Chem. Int. Ed.* **2003**, *42*, 1743-1746.
30. Li, K.; Zou, J.; Das, B. P.; Tsianou, M.; Cheng, C. *Macromolecules* **2012**, *45*, 4623-4629.
31. Li, Z.; Ma, J.; Lee, N. S.; Wooley, K. L. *J. Am. Chem. Soc.* **2011**, *133*, 1228-1231.
32. Li, Z.; Ma, J.; Cheng, C.; Zhang, K.; Wooley, K. L. *Macromolecules* **2010**, *43*, 1182-1184.
33. Fu, Q. J.; Ren, M.; Qiao, G. G. *Polym. Chem.* **2012**, *3*, 343-351.
34. Jha, S. ; Dutta, S.; Bowden, N. B. *Macromolecules* **2004**, *37*, 4365-4374.
35. Czelusniak, I.; Khosravi, K.; Kenwright, A. M.; Ansell C. W. G. *Macromolecules* **2007**, *40*, 1444-1452.
36. Xia, Y.; Olsen, B. D.; Kornfield, J. A.; Grubbs R. H. *J. Am. Chem. Soc.* **2009**, *131*, 18525-18532.
37. Biagini, S. C. G.; Parry, A. L. *J. Polym. Sci. A: Polym. Chem.* **2007**, *45*, 3178-3190.
38. Alfred, S. F.; Al-Badri, Z. M.; Madkour, A. E.; Lienkamp, K.; Tew, G. N. *J. Polym. Sci. A: Polym. Chem.* **2008**, *46*, 2640-2648.
39. Breitenkamp, K.; Emrick, T. *J. Polym. Sci. Part A: Polym. Chem.* **2005**, *43*, 5715-5721.

40. Gerle, M.; Fisher, K.; Roos, S.; Müller, A. H. E.; Schmidt, M. *Macromolecules* **1999**, *32*, 2629-2637.
41. Runge, M. B.; Dutta, S.; Bowden, N. B. *Macromolecules* **2006**, *39*, 498-508.
42. Breitenkamp, K.; Simeone, J.; Jin, E.; Emrick, T. *Macromolecules* **2002**, *35*, 9249-9252.
43. Héroguez, V.; Breunig, S.; Gnanou, Y.; Fontanille, M. *Macromolecules* **1996**, *29*, 4459-4464.
44. Maughon, B. R.; Grubbs, R. H. *Macromolecules* **1997**, *30*, 3459-3469.
45. Miller, A. F.; Richards, R. W.; Webster, J. R. P. *Macromolecules* **2001**, *34*, 8361-8369.
46. Camm, K. D.; Martinez Castro, N.; Liu, Y.; Czechura, P.; Snelgrove, J. L.; Fogg, D. E. *J. Am. Chem. Soc.* **2007**, *129*, 4168-4169.
47. Matson, J. B.; Grubbs, R. H. *J. Am. Chem. Soc.* **2008**, *130*, 6731-6733.
48. Gauvry, N.; Lescop, C.; Huet, F. *Eur. J. Org. Chem.* **2006**, *71*, 5207-5218.
49. Boucheron, C.; Guillarme, S.; Legoupy, S.; Dubreuil, D.; Huet, F. *Synthesis* **2006**, *4*, 633-636.
50. Gourdel-Martin, M. E.; Huet, F. *Tetrahedron Lett.* **1996**, *37*, 7745-7748.
51. Kirmse, W.; Rondan, N. G.; Houk, K. N. *J. Am. Chem. Soc.* **1984**, *106*, 7989-7991.
52. Rondan, N. G.; Houk, K. N. *J. Am. Chem. Soc.* **1985**, *107*, 2099-2111.
53. Rudolf, K.; Spellmeyer, D. C.; Houk, K. N. *J. Org. Chem.* **1987**, *52*, 3711-3712.
54. Feldman, J.; Murdzek, J. S.; Davis, W. M.; Schrock, R. R. *Organometallics* **1989**, *8*, 2260-2265.
55. Fu, G. C.; Grubbs, R. H. *J. Am. Chem. Soc.* **1992**, *114*, 7324-7325.
56. Furstner, A.; Langemann, K. *Synthesis* **1997**, *29*, 792-803.
57. Song, A.; Parker, K. A.; Sampson, N. S. *J. Am. Chem. Soc.* **2009**, *131*, 3444-3445.
58. Trnka, T. M.; Grubbs, R. H. *Acc. Chem. Res.* **2001**, *34*, 18-29.
59. Lee, J. C.; Parker, K. A.; Sampson, N. S. *J. Am. Chem. Soc.* **2006**, *128*, 4578-4579.
60. Song, A.; Lee, J. C.; Parker, K. A.; Sampson, N. S. *J. Am. Chem. Soc.* **2010**, *132*, 10513-10520.
61. Lee, K. S.; Choi, T.-L. *Org. Lett.* **2011**, *13*, 3908-3911.
62. Schwab, P.; Grubbs, R. B.; Ziller, J. W. *J. Am. Chem. Soc.* **1996**, *118*, 100-110.

63. Thorn-Csanyi, E.; Ruhland, K. *Macromol. Chem. Phys.* **1999**, *200*, 2606-2611.
64. Allaert, B.; Ledoux, N.; Dieltiens, N.; Mierde, H. V.; Stevens, C. V.; Voort, P. V. D.; Verpoort, F. *Catal. Commun.* **2008**, *9*, 1054-1059.
65. Bielawski, C. W.; Grubbs, R. H. *Angew. Chem. Int. Ed.* **2000**, *39*, 2903-2906.
66. Compain, P. *Adv. Synth. Catal.* **2007**, *349*, 1829-1846.
67. Wilson, G. O.; Porter, K. A.; Weissman, H.; White, S. R.; Sottos, N. R.; Moore, J. S. *Adv. Synth. Catal.* **2009**, *351*, 1817-1825.
68. Fürstner, A.; Leitner, A. *Angew. Chem. Int. Ed.* **2003**, *42*, 308-311.
69. Fürstner, A.; Grabowski, J.; Lehmann, C. W. *J. Org. Chem.* **1999**, *64*, 8275-8280.
70. Yang, Q.; Xiao, W. J.; Yu, Z. *Org. Lett.* **2005**, *7*, 871-874.
71. Ananthapadmanabhan, K. P.; Goddard, E. D.; Turro, N. J.; Kuo, P. L. *Langmuir* **1985**, *1*, 352-355.
72. Zhao, C. L.; Winnik, M. A.; Melvin, G. R.; Croucher, D. *Langmuir* **1990**, *6*, 514-516.
73. Ren, X. Z.; Li, G. Z.; Wang, H. L.; Xu, X. H. *Colloids Surfaces A: Physicochem. Eng. Aspects* **1995**, *100*, 165-172.
74. Monteil, V.; Wehrmann, P.; Mecking, S. *J. Am. Chem. Soc.* **2005**, *127*, 14568-14569.
75. Airaud, C.; Héroguez, V.; Gnanou, Y. *Macromolecules* **2008**, *41*, 3015-3022.
76. Airaud, C.; Ibarboure, E.; Gaillard, C.; Héroguez, V. *Macromol. Symp.* **2009**, *281*, 31-38.
77. Airaud, C.; Ibarboure, E.; Gaillard, C.; Héroguez, V. *J. Polym. Sci. Part A: Polym. Chem.* **2009**, *47*, 4014-4027.
78. Nguyen, M. N.; Mougner, S.-J.; Ibarboure, E.; Héroguez, V. *J. Polym. Sci. Part A: Polym. Chem.* **2011**, *49*, 1472-1482.
79. Landfester, K. *Macromol. Rapid. Commun.* **2001**, *22*, 896-936.

Conclusion générale

L'objectif de cette thèse était la synthèse par polymérisation par ouverture de cycle par métathèse (ROMP) de copolymères greffés bien définis possédant un squelette polybutadiène et polyoxanorbornène et une haute densité de greffons poly(oxyde d'éthylène) (POE) selon la stratégie « grafting through » à partir de macromonomères amphiphiles à extrémité cyclobutène et oxanorbornène.

La synthèse des macromonomères a été réalisée par réaction de chimie « click » catalysée au cuivre entre des précurseurs oxanorbornène et cyclobutène fonctionnalisés par un groupement azoture ou alcyne et des POE commerciaux préalablement fonctionnalisés par un groupement complémentaire (alcyne ou azoture).

Afin de mener à bien ce projet, des précurseurs originaux dérivés d'oxanorbornène et de cyclobutène ont d'abord été synthétisés. Toute une gamme de nouveaux monomères polymérisables en ROMP ont été obtenus, possédant un groupement alcyne (**2** et **4**, Schéma 1), deux groupements azoture ou alcyne (**6** et **8**, Schéma 1), un groupe alcyne et une deuxième fonctionnalité autorisant une modification ultérieure (**9**, **10** et **11**, Schéma 1), et enfin un groupe alcyne et/ou une fonction trithiocarbonate (**14** et **15**, Schéma 1) qui permet de contrôler une polymérisation RAFT (*Reversible Addition-Fragmentation chain Transfer*).

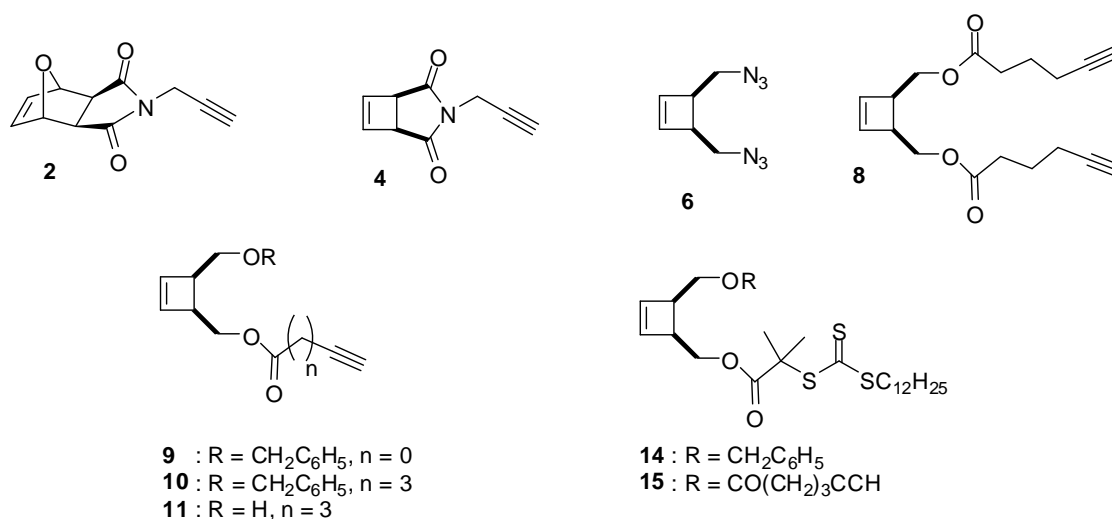


Schéma 1. Précurseurs dérivés de l'oxanorbornène et du cyclobutène synthétisés au cours de ce travail.

La synthèse des macromonomères a été ensuite effectuée par la réaction de chimie « click » à partir des précurseurs fonctionnalisés par un groupement alcyne et

des azotures de POE, ou bien à partir des précurseurs fonctionnalisés par un groupement azoture et de POE à extrémité alcyne.

Une première gamme de macromonomères, dérivés de l'oxanorbornène et renfermant des chaînes POE de masse molaire allant de 500 à 5000 g/mol a été obtenue avec des conversions quantitatives.

Dans la gamme des dérivés du cyclobutène, l'analyse des macromonomères contenant deux chaînes POE (synthétisés à partir des précurseurs avec deux groupements azoture ou alcyne) a mis en évidence la présence de POE en excès ou de macromonomères monofonctionnalisés par du POE dans le produit final, ce qui témoigne de la difficulté d'effectuer une réaction de chimie « click » sur des polymères. En revanche, les macromonomères possédant une chaîne POE ont été synthétisés avec succès, ainsi que l'attestent les analyses spectroscopiques (RMN ^1H , MALDI-TOF) et chromatographique (SEC).

La synthèse de macromonomères cyclobuténiques par polymérisation RAFT a également été réalisée. Ainsi, le dérivé cyclobuténiq ue **14** (Schéma 1) renfermant une fonction trithiocarbonate a été engagé en tant qu'agent de transfert pour le contrôle de la polymérisation de l'acrylate d'éthyle (AE) et du *N*-isopropyl acrylamide (NIPAM) selon le processus RAFT. Les résultats SEC et RMN ^1H confirment que la polymérisation RAFT est bien contrôlée et que la double liaison du cyclobutène demeure intacte durant la polymérisation. Des polymères de masses molaires moyennes prédéfinies et possédant une distribution étroite ($I_p \leq 1,11$) sont accessibles jusqu'à une conversion élevée du monomère (~80% avec le NIPAM et 64% avec l'AE).

La combinaison chimie « click » / polymérisation RAFT a également été utilisée pour accéder à des macromonomères cyclobutényl POE-*b*-PNIPAM. Le macro-agent RAFT α -cyclobutényl POE, synthétisé à partir de l'azoture de POE et du précurseur **9** avec deux groupements orthogonaux alcyne et agent RAFT, a été engagé avec succès dans une polymérisation RAFT du NIPAM ($M_{n,SEC} = 11\ 500$ g/mol, $I_p = 1,11$).

Ces résultats ont permis de démontrer l'orthogonalité de la double liaison cyclobuténiq ue avec le processus RAFT. Compte tenu de la grande variété de monomères utilisables en RAFT et des potentialités de la chimie « click », ces travaux ouvrent la voie à la synthèse d'une large gamme de macromonomères originaux.

La ROMP des macromonomères obtenus a ensuite été étudiée en solution puis en milieu aqueux dispersé.

La polymérisation des macromonomères oxanorbornène à base de POE 500, 2000 et 5000 a permis d'accéder à des copolymères greffés polyoxanorbornène-*g*-POE en utilisant l'amorceur de Grubbs de troisième génération (Grubbs III). Une série de polyoxanorbornène-*g*-POE bien définis de différents rapports $[\text{macromonomère}]_0/[\text{amorceur}]_0$ allant de 10 à 100 ont été obtenus avec un indice de polymolécularité faible ($I_p = 1,06$ à $1,14$) et des masses molaires moyennes en poids de 40 650 à 60 050 g/mol à partir du macromonomère de POE 500 g/mol.

Dans le cas de la ROMP des macromonomères de cyclobutène, différents amorceurs de Grubbs et Schrock ont été testés. L'amorceur de Grubbs s'est révélé inapte à la polymérisation du cyclobutène imide **4** en raison des groupements carbonyle électro-attracteurs en position β de la double liaison du cyclobutène. Par contre, l'utilisation d'un amorceur de Schrock fluoré a permis d'obtenir des 1,4-polybutadiène-*g*-POEs avec des squelettes courts ($M_{n, SEC} : 15\ 000\text{-}22\ 000$ g/mol et $I_p : 1,10\text{-}1,17$).

La ROMP des macromonomères synthétisés par polymérisation RAFT a été également effectuée. Une conversion partielle a été obtenue en utilisant l'amorceur de Grubbs III, qui confirme la comptabilité de la combinaison RAFT / ROMP pour la synthèse de copolymères greffés 1,4-polybutadiène selon la stratégie « *grafting through* ».

Pour les macromonomères non symétriques possédant une chaîne POE, la ROMP avec l'amorceur de Grubbs III est quantitative. Toutefois, elle s'accompagne d'un phénomène de transfert de chaîne qui se traduit en SEC par un chromatogramme dissymétrique. L'amorceur de Grubbs de deuxième génération a permis d'accéder à une série de polybutadiènes-*g*-POE bien définis pour des rapports $[\text{macromonomère}]_0/[\text{amorceur}]_0$ allant de 10 à 30, avec un I_p de 1,07 à 1,11 et une $M_{n, SEC}$ de 19 800 à 38 000 g/mol.

De plus, des essais préliminaires de ROMP en milieu dispersé des macromonomères de l'oxanorbornène et de cyclobutène ont été effectués. Si la ROMP en micro-émulsion n'a pas permis de réaliser la polymérisation, la ROMP en mini-émulsion a conduit à des résultats encourageants puisqu'elle laisse entrevoir la

possibilité de polymériser les macromonomères en milieu dispersé par concentration des sites réactifs à l'intérieur des micelles.

Ces premiers travaux en mini-émulsion devront être poursuivis en effectuant la ROMP de macromonomères présentant une CMC (*Critical Micellar Concentration*) et pouvant jouer le rôle de *surfmers* (*Surfactant-monomers*) en homopolymérisation et en copolymérisation. Il serait également intéressant de poursuivre la caractérisation des propriétés thermosensibles du macromonomère cyclobutényle POE-*b*-PNIPAM en vue d'une ROMP en milieu dispersé.

Enfin, les travaux concernant la synthèse des macromonomères renfermant des chaînes de natures différentes mériteraient également d'être développés. En effet, les groupements hydroxyle ainsi que la fonction trithiocarbonate des macromonomères **M11** et **M15** synthétisés à partir de **11** et **15**, respectivement, pourraient être utilisés pour introduire d'autres types de greffons par polymérisation par ouverture de cycle ou par polymérisation RAFT. Cette méthodologie donnerait accès à des copolymères greffés à squelette 1,4-polybutadiène possédant des greffons de natures différentes régulièrement alternés le long de la chaîne principale, qui sont des précurseurs d'architectures macromoléculaires originales de type « Janus ».

Experimental section

Materials

Toluene (99%+), dioxane (Fisher-Scientific, 99%) and triethylamine (99%), ethyl acrylate (EA, Aldrich, 98.5%) were distilled over CaH_2 . Prior to use, PEO monomethyl ethers (PEO-OH) 500 ($\overline{M_{n,NMR}} = 530$ g/mol), 2 000 ($\overline{M_{n,NMR}} = 2\ 010$ g/mol) and 5 000 ($\overline{M_{n,NMR}} = 4\ 590$ g/mol) were heated at 120°C for 3 h under nitrogen atmosphere to remove excess water. 2,2'-Azobis(isobutyronitrile) (AIBN) was purchased from Acros and recrystallized from methanol before use. N-isopropyl acrylamide (NIPAM, Aldrich, 99%) was twice recrystallized from hexane. *N,N'*-Dimethylformamide (DMF, Aldrich, 99%), dichloromethane (DCM, Aldrich, 99%), hexane (Aldrich), tetrahydrofuran (THF, Aldrich, 99.9%), methanol (Pro labo, 99.8%), MgSO_4 (Fisher chemical), NaCl (Fisher chemical), hydrochloric acid (Aldrich, 37%), silica gel for column chromatography (Kieselgel 60, 230-400 mesh Merck), CuBr (Aldrich, 99.999%), maleic anhydride (Aldrich, 99%), furane (Acros, 99%), sodium azide (NaN_3 , Aldrich, 99.5%), ethylenediaminetetraacetic acid disodium (EDTA, Aldrich, 99%), ethyl vinyl ether (Aldrich, 99%), *N,N'*-dicyclohexylcarbodiimide (DCC, Acros, 99%), 4-(*N,N'*-dimethylamino)pyridine (DMAP, Aldrich, 99%), N-propargylamine (Acros, 99%), methanesulfonyl chloride (MsCl, Fluka, 99%), sodium acetate (Labosi, 98%), hydroxyl potassium (KOH, Acros), (E)-1,2-dichloroethene (Alfa aesar, 98%), Zinc (Aldrich, 99%), Acetic anhydride (Merck, 98.0%), LiAlH_4 (Aldrich, 97.0%), Benzyl bromide (Aldrich, 98%), 5-hexynoic acid (Aldrich, 97%), propynoic acid (Aldrich, 95%), *N,N,N',N'',N'''*-pentamethyldiethylenetriamine (PMDETA, Aldrich, 99%), S-1-dodecyl-S'-(α, α' -dimethyl- α'' -acetic acid) trithiocarbonate (Aldrich, 98%), acyl chloride ($(\text{COCl})_2$, Aldrich, 98%), 4,4'-azobis(4-cyanopentanoyl acid) (ACPA, Aldrich, 98%), pyrene (Aldrich, 99%), pyrene-3-carboxaldehyde (Aldrich, 99%), Grubbs catalyst 1st, 2nd and 3rd generations (Aldrich), Schrock catalyst (Strem chemicals), Brij 700 (Aldrich), 1-pentanol (Aldrich, 99%), hexadecane (Aldrich, 99%) were purchased from commercial sources and used without further purification.

General Characterization

NMR spectra were recorded on a Bruker Avance 400 spectrometer for ^1H NMR (400 MHz) and ^{13}C NMR (100 MHz). Chemical shifts are reported in ppm relative to the deuterated solvent resonances.

Molecular weights and molecular weight distributions were measured using size exclusion chromatography (SEC) on a system equipped with a SpectraSYSTEM AS 1000 autosampler, with a Guard column (Polymer Laboratories, PL gel 5 μm Guard column, 50 x 7.5 mm) followed by two columns (Polymer Laboratories, 2 PL gel 5 μm MIXED-D columns, 2 x 300 x 7.5) and with a SpectraSYSTEM RI-150 detector. The eluent used was tetrahydrofuran (THF) at a flow rate of 1 $\text{mL}\cdot\text{min}^{-1}$ at 35°C. Polystyrene standards (580-4.83 x 10⁵ $\text{g}\cdot\text{mol}^{-1}$) were used to calibrate the SEC.

PNIAM Polymers were characterized on a SEC system operating in DMF eluent at 60°C fitted with a polymer laboratories guard column (PL Gel 5 μm) and two Polymer Laboratories PL Mixed D columns, a Waters 410 differential refractometer (RI) and a Waters 481 UV photodiode array detector. The instrument operated at a flow rate of 1.0 $\text{mL}\cdot\text{min}^{-1}$ and was calibrated with narrow linear polystyrene (PS) standards ranging in molecular weight from 580 $\text{g}\cdot\text{mol}^{-1}$ to 460 000 $\text{g}\cdot\text{mol}^{-1}$. Molecular weights and polydispersity indices (PDI) were calculated using Waters EMPOWER software.

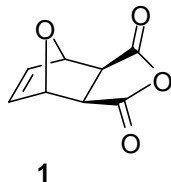
High resolution mass spectra were recorded on Waters-Micromass GCT Premier spectrometers.

MALDI-TOF MS analyses were realized on a Bruker Biflex III using 2-[(2*E*)-3-(4-*tert*-butylphenyl)-2-methylprop-2-enylidene]malononitrile (DCTB) as the matrix.

Thermogravimetric analyses (TGA) were performed on a TA instruments Q500 apparatus measuring the total mass loss on approximately 15 mg samples from 20 °C up to 600 °C at a heating rate of 10 °C $\cdot\text{min}^{-1}$ in a nitrogen flow of 90 $\text{mL}\cdot\text{min}^{-1}$.

Synthesis of precursors, macromonomers and ROMP

exo-7-Oxabicyclo[2.2.1]hept-5-ene-2,3-dicarboxylic anhydride **1**

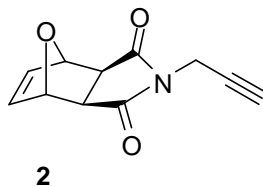


A 50-mL round-bottom flask was charged with maleic anhydride (5 g, 0.05 mol). 30 mL of toluene were added and the reaction flask was swirled until the maleic anhydride completely dissolved. Furan (5.0 mL, 0.075 mol) was added and the resulting solution was stirred for 7 days at room temperature. The crystals were collected by suction filtration and washed with toluene. mp: 116–117 °C. Yield: 65%.

¹H NMR (200 MHz, CDCl₃), δ (ppm): 6.56 (s, 2H, HC=), 5.43 (s, 2H, CHOCH), 3.17 (s, 2H, CHC=O).

¹³C NMR (50 MHz, CDCl₃), δ (ppm): 170.5 (C=O), 137.3 (C=C), 82.1 (CHOCH), 48.3 (CHC=O).

Exo-N-prop-2-ynyl-7-oxabicyclo[2.2.1]hept-5-ene-2,3-dicarboximide **2**



Anhydride **1** (2.00 g, 12.0 mmol) was suspended in MeOH (50 mL) and the mixture cooled to 0 °C. A solution of *N*-propargylamine (1.07 g; 18.0 mmol) in 20 mL of MeOH was added dropwise (10 min), and the resulting solution was stirred for 5 min at 0 °C, then 30 min at ambient temperature, and finally refluxed for 72 h. After cooling the mixture to ambient temperature, the solvent was removed under reduced pressure, and the yellow residue was dissolved in 150 mL of DCM and washed with 3x100 mL of water. The organic layer was dried over MgSO₄ and filtered. Removal of the solvent under reduced pressure furnished **2** as a yellow solid. Yield: 1.97 g (9.72 mmol, 81 %).

¹H NMR (200 MHz, CDCl₃), δ (ppm): 6.54 (s, 2H, =CH), 5.30 (s, 2H, =CH-O), 4.24 (d, *J* = 2.0 Hz, 2H, CH₂-N), 2.90 (s, 2H, CH-CO), 2.20 (t, *J* = 2.0 Hz, 1H, ≡CH).

¹³C NMR (50 MHz, CDCl₃), δ (ppm): 172.8 (C=O), 134.5 (=CH-), 78.9 (CH-O), 74.48 (C≡CH), 69.5 (≡CH), 45.5 (CH-CO), 25.8 (N-CH₂).

HRMS (CI-H⁺). Calc. for C₁₁H₉NO₃ + H⁺: 204.2060; Found: 204.0661.

Azido-terminated PEO monomethyl ethers 500, 2 000, 5 000 g/mol



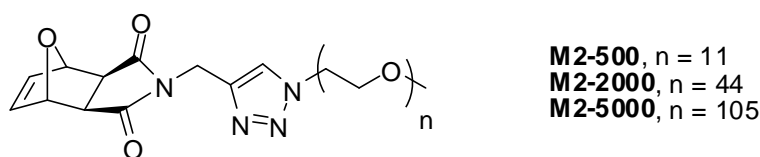
PEO-OH monomethyl ether (5 mmol) and triethylamine (4.2 mL, 30 mmol) were dissolved in 50 mL of DCM. The mixture was cooled to 0 °C. A solution of methanesulfonyl chloride (5.7 g, 50 mmol) in 10 mL DCM was added dropwise (over 30 min). The reaction mixture was then stirred for 24 h at room temperature. The reaction mixture was washed with 50 mL of HCl solution (1M) and 50 mL of distilled water. The organic layer was dried over MgSO₄ and precipitated into diethyl ether. Mesylated-PEO was obtained as a colorless oil (PEO 500) or a white powder (PEO 2 000 and 5 000). Thus, obtained mesylated-PEO was dissolved in 15 mL of DCM (PEO 500) or in 30 mL THF (PEO 2 000, 5 000) and sodium azide (NaN₃) (3.25 g, 50 mmol) was added to this solution. After stirring the reaction mixture overnight at room temperature, DCM was added and the organic layer was washed for another three times with water and dried over MgSO₄. The organic phase was evaporated and precipitated in diethyl ether. The obtained PEO-N₃ was dried for 24 h in a vacuum oven. The yields were ranged between 80 and 90 %.

RMN ¹H (200 MHz, CDCl₃), δ (ppm): 3.60-3.80 (m, 180H, CH₂); 3.38 (s, 3H, CH₃).

RMN ¹³C (50 MHz, CDCl₃), δ (ppm): 71.9 (CH₂-O-CH₃) ; 70.5 (-CH₂-) ; 70.0 (CH₂-CH₂-N₃); 59.0 (CH₃) ; 50.6 (CH₂-N₃).

IR (ν cm⁻¹) : 2882 (ν_{CH₂}), 2097 (ν_{N₃}).

General procedure for the synthesis of macromonomers M2-500, M2-2000 and M2-5000 via “Click” coupling reactions between azido-terminated PEO monomethyl ethers and 2.



In a typical experiment, the azido-terminated PEO monomethyl ether (0.4 mmol) and PMDETA (0.1 g, 0.6 mmol) were charged to a dry Schlenk tube along with degassed DMF (5 mL). The tube was sealed with a rubber septum and subjected to six freeze-pump-thaw cycles. This solution was then cannulated under nitrogen into another Schlenk tube, previously evacuated and filled with nitrogen, containing Cu(I)Br (0.023 g, 0.16 mmol), **2** (0.1 g, 0.4 mmol), and a stir bar. The resulting solution was subsequently stirred at room temperature for 4 h. The reaction mixture was diluted with DCM and then washed with 3x100 mL of an aqueous ethylenediaminetetraacetate solution (0.03 mol/L) to remove the catalyst. The organic layer was dried over MgSO₄ and filtered. The resulting macromonomers were isolated by precipitation into diethyl ether for the ω -*exo*-oxanorbornenyl PEO monomethyl ethers **M2-2000** and **M2-5000** or by removal of the solvent under high vacuum for the ω -*exo*-oxanorbornenyl PEO monomethyl ether **M2-500**.

ω -Exo-oxanorbornenyl PEO monomethyl ether M2-500. Yellow brown oil. Yield: 80 %.

¹H NMR (200 MHz, CDCl₃), δ (ppm): 7.68 (s, 1H, triazole), 6.50 (s, 2H, =CH), 5.29 (s, 2H, CH-O), 4.78 (s, 2H, N-CH₂), 4.49 (t, J = 5.1 Hz, 2H, N_{triazole}-CH₂-CH₂-O), 3.85 (t, J = 5.1 Hz, 2H, N_{triazole}-CH₂-CH₂-O), 3.60-3.70 (m, 40H, CH₂-CH₂-O), 3.38 (s, 3H, O-CH₃), 2.96 (s, 2H, CH-CO).

¹³C NMR (50 MHz, CDCl₃), δ (ppm): 175.5 (CO), 141.9 (C=C-N_{triazole}), 136.5 (=CH), 123.7 (C=C-N_{triazole}), 80.9 (CH-O), 71.9 (CH₂-O-CH₃), 70.4 (-CH₂-O), 69.3 (N_{triazole}-CH₂-CH₂-O), 59.0 (CH₃-O), 50.30 (N_{triazole}-CH₂-CH₂-O), 47.5 (CH-CO), 34.1 (N-CH₂).

ω -Exo-oxanorbornenyl PEO monomethyl ether M2-2000. White powder. Yield: 85 %.

¹H NMR (200 MHz, CDCl₃), δ (ppm): 7.67 (s, 1H, triazole), 6.50 (s, 2H, =CH), 5.29 (s, 2H, CH-O), 4.78 (s, 2H, N-CH₂), 4.49 (t, J = 5.1 Hz, 2H, N_{triazole}-CH₂-CH₂-O), 3.85 (t, J = 5.1 Hz, 2H, N_{triazole}-CH₂-CH₂-O), 3.60-3.70 (m, 172H, CH₂-CH₂-O), 3.38 (s, 3H, O-CH₃), 2.89 (s, 2H, CH-CO).

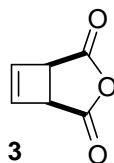
¹³C NMR (50 MHz, CDCl₃), δ (ppm): 175.4 (CO), 141.9 (C=C-N_{triazole}), 136.5 (=CH), 123.6 (C=C-N_{triazole}), 80.9 (CH-O), 71.9 (CH₂-O-CH₃), 70.5 (-CH₂-O), 69.3 (N_{triazole}-CH₂-CH₂-O), 59.0 (CH₃-O), 50.2 (N_{triazole}-CH₂-CH₂-O), 47.5 (CH-CO), 34.1 (N-CH₂).

ω-Exo-oxanorbornenyl PEO monomethyl ether **M2-5000**. White powder. Yield: 78 %.

^1H NMR (200 MHz, CDCl_3), δ (ppm): 7.68 (s, 1H, triazole), 6.52 (s, 2H, =CH), 5.29 (s, 2H, CH-O), 4.79 (s, 2H, N-CH₂), 4.50 (t, $J = 5.1$ Hz, 2H, N_{triazole}-CH₂-CH₂-O), 4.00 (t, $J = 5.1$ Hz, 2H, N_{triazole}-CH₂-CH₂-O), 3.50-3.90 (m, 412H, CH₂-CH₂-O), 3.38 (s, 3H, O-CH₃), 2.90 (s, 2H, CH-CO).

^{13}C NMR (50 MHz, CDCl_3), δ (ppm): 175.4 (CO), 141.9 (C=C-N_{triazole}), 136.5 (=CH), 123.4 (C=C-N_{triazole}), 80.9 (CH-O), 71.9 (CH₂-O-CH₃), 70.4 (-CH₂-O), 69.3 (N_{triazole}-CH₂-CH₂-O), 59.1 (CH₃-O), 50.3 (N_{triazole}-CH₂-CH₂-O), 47.4 (CH-CO), 34.1 (N-CH₂).

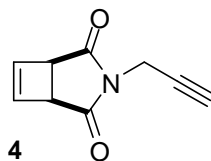
cis-Cyclobut-3ene-1,2-dicarboxylic anhydride **3**



A solution of maleic anhydride (90 g, 0.92 mol) and (*E*)-1,2-dichloroethene (100 g, 1.03 mol) in 1.5 L of EtOAc was purged during 10 min and irradiated 1 week. The solvent was removed, the residue was triturated with Et₂O to afford 3,4-dichlorocyclobutane-1,2-dicarboxylic anhydride. 3,4-Dichlorocyclobutane-1,2-dicarboxylic anhydride (20 g, 0.1 mol) was suspended in 330 mL of toluene and 120 mL of Ac₂O (1.3 mol). The solution was warmed to 40 °C and activated Zn (167 g, 2.5 mol) was then added in one portion. The mixture was mechanically stirred at 85 °C for 72 h, under N₂. The solution was then cooled to rt and filtered through a Celite par. The solid was washed with 3x50 mL of toluene. The organic phase was evaporated. The residue was purified by distillation (80-120 °C/0.3 mbar) through a 2-cm column to afford a white solid that was washed with hexane, yielding **3** as a white powder (6.5 g, 51 %).

^1H NMR (200 MHz, CDCl_3), δ (ppm): 6.50 (s, 2H, =CH-), 4.10 (s, 2H, -CH-).

^{13}C NMR (50 MHz, CDCl_3), δ (ppm): 168.3 (C=O), 139.4 (=CH-), 47.7 (CH-CO).

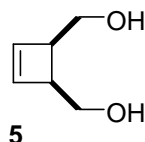
N-prop-2-ynyl-*cis*-cyclobut-3-ene-1,2-dicarboximide **4**

Anhydride **3** (0.100 g, 0.8 mmol) was suspended in dry ethyl ether (1.5 mL). A solution of *N*-propargylamine (0.050 g; 0.9 mmol) in 0.5 mL of dry ethyl ether was added dropwise (20 min), and the resulting thick suspension solution was stirred for 4h at 30 °C. The solvent was then removed by rotary evaporator, anhydrous sodium acetate (26 mg) and acetic anhydride (1 mL) were added, and the resulting suspension is dissolved by stirring and heating for 5h at 60 °C. The reaction mixture was poured into ice water and the solvent was then evaporated by rotary evaporator. The crude product was purified by chromatography on SiO₂ using 1/2 EtOAc/cyclohexane and **4** was obtained as a white powder (95 mg, yield: 70%).

¹H NMR (200 MHz, CDCl₃), δ (ppm): 6.47 (s, 2H, =CH), 4.24 (d, *J* = 2.0 Hz, 2H, CH₂-N), 3.87 (s, 2H, CH-C=O), 2.20 (t, *J* = 2.0 Hz, 1H, ≡CH).

¹³C NMR (50 MHz, CDCl₃), δ (ppm): 173.8 (C=O), 139.2 (=CH-), 77.3 (C≡CH), 71.4 (≡CH), 47.7 (CH-CO), 27.6 (N-CH₂).

HRMS (CI-H⁺). Calc for C₉H₇NO₂ + H⁺: 162.0500; Found: 162.0555.

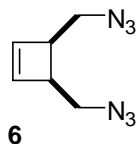
cis-3,4-Bis(hydroxymethyl)cyclobut-2-ene **5**

LiAlH₄ (2.5 g, 66 mmol) was suspended in 70 mL of anhydrous THF, the solution was cooled to 0 °C. **3** (2.0 g, 20 mmol) in 30 mL of anhydrous THF was added dropwise (over 30 min) under N₂. The suspension solution was stirred for 20 h at 75 °C. The solution was then cooled to 0 °C, and 15 mL of KOH solution (2M) was added. 40 mL diethyl ether was added into the mixture, the suspension was filtered and washed with 3x10 mL of DCM and 3x15 mL of diethyl ether. The organic solution was evaporated and the residue was dissolved in 40 mL of DCM, dried over MgSO₄, filtered and evaporated to give a transparent oil (1.69 g, yield of 92 %).

^1H NMR (200 MHz, CDCl_3), δ (ppm): 6.04 (s, 2H, =CH), 4.02 (broad s, 2H, -OH), 3.87 (dd, 2H, $-\text{CH}_2\text{-OH}$, $J = 11.3$ and 3.9 Hz), 3.73 (dd, $-\text{CH}_2\text{-OH}$, $J = 11.3$ and 10.8 Hz), 3.24 (m, 2H, -CH-).

HRMS (CI- H^+). Calc. for $\text{C}_6\text{H}_8\text{O}_2 + \text{H}^+$: 115.0766; Found: 115.0768.

Cis-3,4-Bis(azidomethyl)cyclobut-2-ene **6**

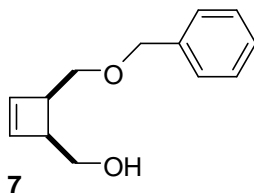


5 (1.5 g, 13 mmol) and triethylamine (4.0 g, 40 mmol) were dissolved in 50 mL of DCM. The solution was cooled to $0\text{ }^\circ\text{C}$, then methanesulfonyl chloride (3.7 g, 32 mmol) in 10 mL DCM was added dropwise (over 30 min). The reaction mixture was then stirred 2 h at room temperature. It was first washed with 15 mL of cold HCl solution (10%), 10 mL of NaHCO_3 solution (10%) and 15 mL of NaCl saturated solution. The organic solution was dried over MgSO_4 and evaporated. The dimesylated-cyclobutene was obtained as a colorless oil (2.6 g) after purification by chromatography on SiO_2 using DCM. Thus obtained dimesylated-cyclobutene was dissolved in 25 mL of DMF and NaN_3 (1.24 g, 19 mmol) was added to this solution. After, the reaction mixture was stirred for 3 h at $75\text{ }^\circ\text{C}$. The mixture was cooled to rt and transferred to cold water (40 mL). The solution was extracted three times with diethyl ether (3x30 mL). The organic phase was dried over MgSO_4 and evaporated. The residue was purified by chromatography on SiO_2 using cyclohexane. The product **6** was obtained as a colorless oil (1.2 g, 66%) and was stored at $-20\text{ }^\circ\text{C}$.

^1H NMR (200 MHz, CDCl_3), δ (ppm): 6.20 (s, 2H, =CH), 3.40-3.60 (m, 4H, $-\text{CH}_2\text{-N}_3$), 3.15-3.35 (m, 2H, -CH-).

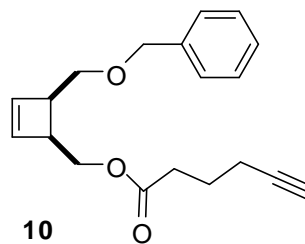
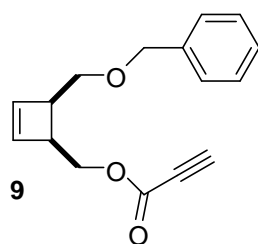
^{13}C NMR (50 MHz, CDCl_3), δ (ppm): 138.50 (=CH-), 51.30 ($-\text{CH}_2\text{-N}_3$), 45.03 (-CH-).

Organic azides are potentially-explosive substances and small molecules containing the azido functionality tend to decompose violently which may result in injury if proper safety precautions are not used. The organic azides with number of carbon/number of nitrogen ratio smaller than 3 should be stored as solutions below room temperature and less than 5 grams of material. Compound 6 having $N_{\text{C}}/N_{\text{N}} = 1$ was thus purified using column chromatography and should be handled with care.

Cis-4-benzyloxymethyl-cis-3-hydroxymethylcyclobut-1-ene 7

5 (1.5 g, 13.3 mmol) was dissolved in 40 mL of anhydrous DMF, the solution was cooled to 0 °C under N₂. NaH (80 % in paraffin, 0.43 g, 14.4 mmol) was added in portion. The mixture was stirred for 15 min at 0 °C. Benzyl bromide (2.49 g, 14.4 mmol) was then added dropwise and the reaction mixture was stirred for 4 h at rt. MeOH (4.5 mL) was slowly added and solvent was then evaporated. The residue was dissolved in 80 mL of DCM, and extracted with 20 mL of water and 20 mL of saturated NaCl solution. Organic phase was dried over MgSO₄, evaporated. The residue was purified by chromatography on SiO₂ using 5/1 cyclohexane/AcOEt. The product was obtained as a colorless oil (1.4 g) with yield of 52 %.

¹H NMR (200 MHz, CDCl₃), δ (ppm) 7.25-7.50 (m, 5H, C₆H₅), 6.05 (d, 1H, =CH-, *J* = 2.9 Hz), 6.00 (d, 1H, =CH-, *J* = 2.9 Hz), 4.50 (s, 2H, -CH₂-C₆H₅), 3.60-3.80 (m, 4H, -CH₂-), 3.50 (broad, OH), 3.20-3.35 (m, 2H, -CH-).

Precursors 9 and 10

To a solution of propynoic acid (0.37 g, 5.3 mmol) or 5-hexynoic acid (0.60 g, 5.3 mmol) and *cis-4-benzyloxymethyl-cis-3-hydroxymethylcyclobut-1-ene* (1.00 g, 4.9 mmol) in diethyl ether (10 mL) was added dropwise a solution of DCC (0.97 g, 0.049 mmol), DMAP (0.038 g, 0.3 mmol) in 30 mL of diethyl ether at -20 °C under N₂. The mixture was stirred for 24h at rt. The mixture was filtered, washed with 2x20 mL of cooled solution of HCl (1M) and 2x20 mL of saturated NaCl solution. Organic phase was then dried over MgSO₄ and evaporated. The products were then purified by chromatography on a silica gel column using DCM as eluent.

Precursor 9. Colorless oil, yield: 45 %.

^1H NMR (200 MHz, CDCl_3), δ (ppm): 7.26-7.37 (m, 5H, C_6H_5), 6.16 (d, 1H, =CH-, $J = 3.0$ Hz), 6.13 (d, 1H, =CH-, $J = 3.0$ Hz), 4.50 (s, 2H, $-\text{CH}_2-\text{C}_6\text{H}_5$), 4.29-4.47 (m, 2H, $-\text{CH}_2-\text{OCO}-$), 3.55-3.60 (m, , 2H, $-\text{CH}_2-\text{O}-$, $J = 2.0$ and 7.0 Hz) 3.26-3.33 (m, 2H, $-\text{CH}-$), 2.90 (s, 1H, $\text{C}\equiv\text{CH}$).

HRMS (FIID). Calc. for $\text{C}_{16}\text{H}_{16}\text{O}_3^+$: 256.1100 Found: 256.1117.

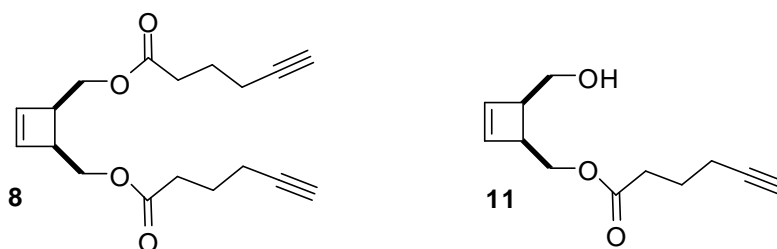
Precursor 10. Colorless oil, yield: 60 %.

^1H NMR (200 MHz, CDCl_3), δ (ppm): 7.25-7.36 (m, 5H, C_6H_5), 6.17 (d, 1H, =CH-, $J = 3.0$ Hz), 6.12 (d, 1H, =CH-, $J = 3.0$ Hz), 4.50 (s, 2H, $-\text{CH}_2-\text{C}_6\text{H}_5$), 4.18-4.33 (m, 2H, $-\text{CH}_2-\text{OCO}-$), 3.60 (d, 2H, $-\text{CH}_2-\text{O}-$, $J = 7.0$ Hz), 3.22-3.29 (m, 2H, $-\text{CH}-$), 2.36-2.44 (t, 2H, $-\text{CH}_2-\text{COO}-$, $J = 7.0$ Hz), 2.19-2.27 (m, 2H, $-\text{CH}_2-\text{C}\equiv\text{CH}$), 1.95-1.98 (t, 1H, $-\text{C}\equiv\text{CH}$, $J = 3.0$ Hz), 1.77-1.84 (m, 2H, $\text{CH}_2-\text{CH}_2-\text{C}\equiv\text{CH}$).

^{13}C NMR (50 MHz, CDCl_3), δ (ppm): 173.3 ($\text{C}=\text{O}$), 139.0 ($\text{CH}_2-\text{C}_{\text{phenyl}}$), 138.1 (=CH-), 137.7 (=CH-), 129.0, 128.1, 127.9 ($\text{CH}(\text{o}, \text{m}, \text{p})$), 77.5 ($\text{C}\equiv\text{CH}$), 73.3 ($\text{CH}_2-\text{Phenyl}$), 70.5 ($\text{CH}-\text{CH}_2-\text{O}-\text{CH}_2-\text{Phenyl}$), 69.0 ($\equiv\text{CH}$), 64.3 ($\text{CH}_2-\text{OCO}-$), 45.5 and 44.2 ($\text{CH}-\text{CH}=\text{}$), 33.3 ($-\text{CH}_2-\text{COO}$), 23.5 ($\text{CH}_2-\text{CH}_2-\text{C}\equiv\text{CH}$), 17.5 ($\text{CH}_2-\text{C}\equiv\text{CH}$).

HRMS (FIID) Calc. for $\text{C}_{19}\text{H}_{22}\text{O}_3^+$: 298.1569 Found: 298.1583.

Precursors 8 and 11



A solution of 5-hexynoic acid (3.92 g, 35 mmol), DCC (7.4 g, 0.36 mmol) and DMAP (0.26 g, 2.1 mmol) in DCM (40 mL) was added dropwise to a solution of **5** (2.6 g, 22.8 mmol) in 60 mL of DCM at rt under N_2 . The mixture was stirred for 24h at rt. The mixture was filtered, washed with 2x40 mL of cooled solution of HCl (1M) and 2x40 mL of saturated NaCl solution. Organic phase was then dried over MgSO_4 and evaporated. Precursor **9** and **10** were then purified by chromatography on a silica gel column using a cyclohexane/AcOEt (5/2) solution as eluent.

Precursor 8. Colorless oil, yield: 40 %

^1H NMR (200 MHz, CDCl_3), δ (ppm): 6.10 (s, 2H, =CH-), 4.20 (d, 4H, -CH₂-OCO-, $J = 7.0$ Hz), 3.22-3.28 (m, 2H, -CH-), 2.41-2.52 (t, 4H, -CH₂-COO-, $J = 7.0$), 2.23-2.34 (m, 4H, -CH₂-C \equiv CH), 1.92-1.97 (t, 2H, -C \equiv CH, $J = 3.0$ Hz), 1.82-1.93 (m, 4H, CH₂-CH₂-C \equiv CH).

^{13}C NMR (50 MHz, CDCl_3), δ (ppm): 173.3 (C=O), 138.1 (=CH-), 77.5 (C \equiv CH), 69.0 (\equiv CH), 63.9 (CH₂-OCO-), 44.2 (CH-CH=), 33.3 (CH₂-COO-), 23.5 (CH₂-CH₂-C \equiv CH), 17.50 (CH₂-C \equiv CH).

Precursor 11. Colorless oil, yield: 35 %

^1H NMR (200 MHz, CDCl_3), δ (ppm): 6.09 (d, 1H, =CH-, $J = 3.0$ Hz), 6.05 (d, 1H, =CH-, $J = 3.0$ Hz), 4.07-4.34 (m, 2H, -CH₂-OCO-), 3.70 (d, 2H, -CH₂-O-, $J = 7.0$ Hz), 3.10-3.22 (m, 2H, -CH-), 2.40 (t, 2H, -CH₂-COO-, $J = 7.0$), 2.17-2.24 (m, 2H, -CH₂-C \equiv CH), 1.91-2.00 (t, 1H, -C \equiv CH, $J = 3$ Hz), 1.70-1.84 (m, 2H, CH₂-CH₂-C \equiv CH).

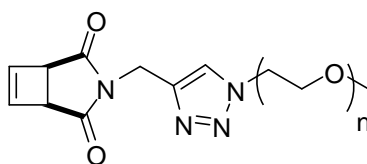
^{13}C NMR (50 MHz, CDCl_3), δ (ppm): 173.3 (C=O), 138.1 (=CH-), 137.7 (=CH-), 77.56 (C \equiv CH), 69.0 (\equiv CH), 64.0 (CH₂-OCO-), 62.9 (CH₂-OH), 48.0 and 44.2 (CH-CH=), 33.3 (CH₂-COO-), 23.5 (CH₂-CH₂-C \equiv CH), 17.5 (CH₂-C \equiv CH).

HRMS (FIID). Calc. for $\text{C}_{12}\text{H}_{16}\text{O}_3^+$: 208.1099 Found: 208.1019.

General procedure for the synthesis of ω -cyclobutenyl PEO macromonomers via “Click” coupling reactions between azido-terminated or alkyne-terminated PEO monomethyl ethers and precursors 4, 6, 8, 9, 10 and 11.

In a typical experiment, the azido-terminated or alkyne-terminated PEO monomethyl ether (0.4 mmol), *N,N,N',N',N''*-pentamethyldiethylenetriamine (PMDETA; 0.1 g, 0.6 mmol) and cyclobutene precursor (0.2 or 0.4 mmol) were charged to a dry Schlenk tube along with degassed DMF (5 mL). The tube was sealed with a rubber septum and subjected to six freeze-pump-thaw cycles. This solution was then cannulated under nitrogen into another Schlenk tube, previously evacuated and filled with nitrogen, containing Cu(I)Br (0.023 g, 0.16 mmol) and a stir bar. The resulting solution was subsequently stirred at room temperature for 4 h. The reaction mixture was diluted with DCM and then washed with 3x100 mL of an aqueous ethylenediaminetetraacetate solution (0.03 mol/L) to remove the catalyst. The organic layer was dried over MgSO_4 and filtered. The resulting macromonomers were isolated by precipitation into diethyl ether.

ω-Cyclobutenyl PEO monomethyl ether **M4-2000**. White powder, yield: 67 %.



M4-2000, n = 44
M4-5000, n = 105

^1H NMR (200 MHz, CDCl_3), δ (ppm): 7.71 (s, 1H, triazole), 6.44 (s, 2H, =CH), 4.76 (s, 2H, N- CH_2 -), 4.50 (t, $J = 5.1$ Hz, 2H, $\text{N}_{\text{triazole}}\text{-CH}_2\text{-CH}_2\text{-O}$), 3.83 (m, 4H, $\text{N}_{\text{triazole}}\text{-CH}_2\text{-CH}_2\text{-O}$, -CH-CH=), 3.60-3.70 (m, 172H, $\text{CH}_2\text{-CH}_2\text{-O}$), 3.38 (s, 3H, O- CH_3).

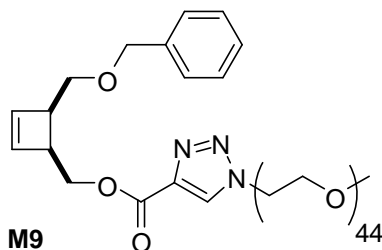
^{13}C NMR (50 MHz, CDCl_3), δ (ppm): 173.8 (CO), 141.86 (C=C- $\text{N}_{\text{triazole}}$), 139.3 (=CH), 124.0 (C=C- $\text{N}_{\text{triazole}}$), 71.9 ($\text{CH}_2\text{-O-CH}_3$), 70.5 (- $\text{CH}_2\text{-O}$), 69.4 ($\text{N}_{\text{triazole}}\text{-CH}_2\text{-CH}_2\text{-O}$), 59.0 ($\text{CH}_3\text{-O}$), 50.29 ($\text{N}_{\text{triazole}}\text{-CH}_2\text{-CH}_2\text{-O}$), 47.7 (CH-CO), 33.8 (N- CH_2).

ω-Cyclobutenyl PEO monomethyl ether **M4-5000**. White powder, yield: 60 %.

^1H NMR (200 MHz, CDCl_3), δ (ppm): 7.71 (s, 1H, triazole), 6.44 (s, 2H, =CH), 4.76 (s, 2H, N- CH_2 -), 4.50 (t, $J = 5.0$ Hz, 2H, $\text{N}_{\text{triazole}}\text{-CH}_2\text{-CH}_2\text{-O}$), 3.83 (m, 4H, $\text{N}_{\text{triazole}}\text{-CH}_2\text{-CH}_2\text{-O}$, -CH-CH=), 3.60-3.70 (m, 172H, $\text{CH}_2\text{-CH}_2\text{-O}$), 3.38 (s, 3H, O- CH_3).

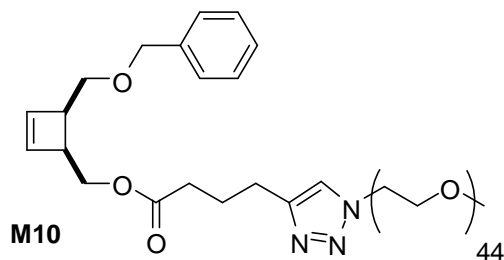
^{13}C NMR (50 MHz, CDCl_3), δ (ppm): 173.8 (CO), 141.8 (C=C- $\text{N}_{\text{triazole}}$), 139.2 (=CH), 124.0 (C=C- $\text{N}_{\text{triazole}}$), 71.9 ($\text{CH}_2\text{-O-CH}_3$), 70.5 (- $\text{CH}_2\text{-O}$), 69.4 ($\text{N}_{\text{triazole}}\text{-CH}_2\text{-CH}_2\text{-O}$), 59.0 ($\text{CH}_3\text{-O}$), 50.2 ($\text{N}_{\text{triazole}}\text{-CH}_2\text{-CH}_2\text{-O}$), 47.7 (CH-CO), 33.8 (N- CH_2).

ω-Cyclobutenyl PEO monomethyl ether **M9**. White powder, yield: 70 %.



^1H NMR (200 MHz, CDCl_3), δ (ppm): 8.22 (s, 1H, triazole), 7.25-7.36 (m, 5H, C_6H_5), 6.19 (s, 2H, =CH), 4.40-4.60 (m, 6H, $\text{N}_{\text{triazole}}\text{-CH}_2$ -, - $\text{CH}_2\text{-C}_6\text{H}_5$ -, - $\text{CH}_2\text{-OCO}$), 3.99 (t, 2H, $\text{N}_{\text{triazole}}\text{-CH}_2\text{-CH}_2\text{-O}$, $J = 5.0$ Hz), 3.60-3.70 (m, 174H, $\text{CH}_2\text{-CH}_2\text{-O}$ -, - $\text{CH}_2\text{-O-CH}_2\text{-C}_6\text{H}_5$), 3.28-3.41 (m, 5H, O- CH_3 -, -CH-CH=).

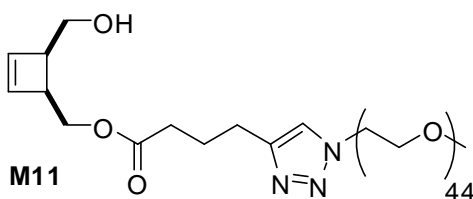
ω-Cyclobutenyl PEO monomethyl ether **M10**. White powder, yield: 75 %.



^1H NMR (200 MHz, CDCl_3), δ (ppm): 7.50 (s, 1H, triazole), 7.25-7.36 (m, 5H, C_6H_5), 6.16 (d, 1H, $=\text{CH}$ -, $J = 3.0$ Hz), 6.12 (d, 1H, $=\text{CH}$ -, $J = 3.0$ Hz), 4.52 (m, 4H, $\text{N}_{\text{triazole}}\text{-CH}_2\text{-CH}_2\text{-O}$, $\text{CH}_2\text{-C}_6\text{H}_5$), 4.17-4.30 (m, 2H, $-\text{CH}_2\text{-OCO}$) 3.99 (t, 2H, $\text{N}_{\text{triazole}}\text{-CH}_2\text{-CH}_2\text{-O}$, $J = 5.0$ Hz), 3.60-3.70 (m, 174H, $\text{CH}_2\text{-CH}_2\text{-O}$, $-\text{CH}_2\text{-O-CH}_2\text{-C}_6\text{H}_5$), 3.37 (s, 3H, O-CH_3), 3.23-3.31 (m, 2H $-\text{CH-CH=}$), 2.66-2.77 (t, 2H, $-\text{CH}_2\text{-C}_{\text{triazole}}$, $J = 7.0$ Hz), 2.30-2.37 (t, 2H, $-\text{CH}_2\text{-COO}$, $J = 7.0$ Hz), 1.93-2.01 (m, 2H, $\text{CH}_2\text{-CH}_2\text{-C}_{\text{triazole}}$).

^{13}C NMR (50 MHz, CDCl_3), δ (ppm): 173.3 (C=O), 146.0 ($\text{C=C-N}_{\text{triazole}}$), 139.0 ($\text{CH}_2\text{-C}_{\text{phenyl}}$), 138.1 ($=\text{CH}$ -), 137.7 ($=\text{CH}$ -), 129.0, 128.1, 127.9 ($\text{CH}(\text{o, p, m})$), 122.0 ($\text{C=C-N}_{\text{triazole}}$), 73.2 ($\text{CH}_2\text{-Phenyl}$), 71.8 ($\text{CH}_2\text{-O-CH}_3$), 70.5 ($-\text{CH}_2\text{-O}$), 70.0 ($\text{CH-CH}_2\text{-O-CH}_2\text{-Phenyl}$), 69.4 ($\text{N}_{\text{triazole}}\text{-CH}_2\text{-CH}_2\text{-O}$), 64.3 ($\text{CH}_2\text{-OCO-}$), 58.9 ($\text{CH}_3\text{-O}$), 50.0 ($\text{N}_{\text{triazole}}\text{-CH}_2\text{-CH}_2\text{-O}$), 45.5 and (CH-CH=), 33.3($\text{CH}_2\text{-COO-}$), 24.8 ($\text{CH}_2\text{-C}_{\text{triazole}}$), 24.7 ($\text{CH}_2\text{-C}_{\text{triazole}}$).

ω-Cyclobutenyl PEO monomethyl ether **M11**. White powder, yield: 73 %.

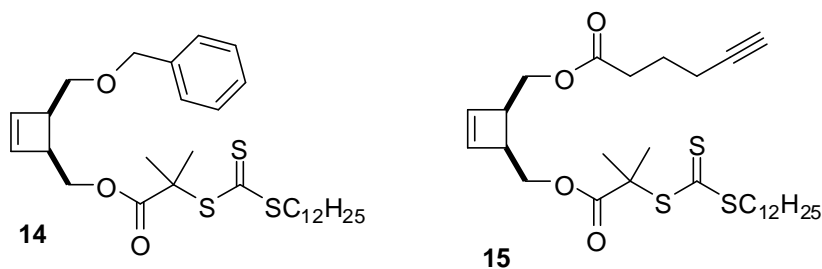


^1H NMR (200 MHz, CDCl_3), δ (ppm): 7.51 (s, 1H, triazole), 6.15 (d, 1H, $=\text{CH}$ -, $J = 2.8$ Hz), 6.10 (d, 1H, $=\text{CH}$ -, $J = 2.8$ Hz), 4.49 (t, 2H, $\text{N}_{\text{triazole}}\text{-CH}_2$ -, $J = 5.0$ Hz), 4.16-4.35 (m, 2H, $-\text{CH}_2\text{-OCO}$) 3.87 (t, 2H, $\text{N}_{\text{triazole}}\text{-CH}_2\text{-CH}_2\text{-O}$, $J = 5.0$ Hz), 3.60-3.70 (m, 172H, $\text{CH}_2\text{-CH}_2\text{-O}$), 3.38 (s, 3H, O-CH_3), 3.17-3.26 (m, 2H $-\text{CH-CH=}$), 2.66-2.77 (t, 2H, $-\text{CH}_2\text{-C}_{\text{triazole}}$, $J = 7.0$ Hz), 2.30-2.37 (t, 2H, $-\text{CH}_2\text{-COO}$, $J = 7$), 1.93-2.01 (m, 2H, $\text{CH}_2\text{-CH}_2\text{-C}_{\text{triazole}}$).

^{13}C NMR (50 MHz, CDCl_3), δ (ppm): 172.9 (C=O), 146.8 ($\text{C=C-N}_{\text{triazole}}$), 138.4 ($=\text{CH}$ -), 137.3 ($=\text{CH}$ -), 122.1 ($\text{C=C-N}_{\text{triazole}}$), 71.9 ($\text{CH}_2\text{-O-CH}_3$), 70.5 ($-\text{CH}_2\text{-O}$), 69.5 ($\text{N}_{\text{triazole}}\text{-}$

CH₂-CH₂-O), 64.3 (CH₂-OCO-), 62.0 (CH₂-OH), 59.0 (CH₃-O), 50.1 (N_{triazole}-CH₂-CH₂-O), 48.0 and 44.5 (CH-CH=), 33.5 (CH-CH₂-OCO), 24.8 (CH₂-C_{triazole}), 24.6 (CH₂-CH₂-C_{triazole}).

Synthesis of cyclobutene-RAFT chain transfer agent **14** and cyclobutenyl-functionalized RAFT-“click” dual agent/group **15**



Oxalyl chloride (COCl)₂ (1 mL, 11.6 mmol) was added via a syringe to S-1-dodecyl-S'-(α , α' -dimethyl- α'' -acetic acid) trithiocarbonate (0.4 g, 1.1 mmol) placed in a Schlenk tube at room temperature with rapid stirring under an argon atmosphere, causing the vigorous evolution of CO₂(g), CO(g), and HCl(g). After 5 h, the evolution of gases has stopped and the reaction mixture is homogeneous. The excess of (COCl)₂ was removed in vacuum to yield the acyl chloride which is used without further purification. *Cis*-4-benzyloxymethyl-3-hydroxymethylcyclobut-1-ene **5** (0.22 g, 1.1 mmol) or **11** (0.23 g, 1.1 mmol) was added via a syringe to the acyl chloride under argon resulting in the vigorous evolution of HCl(g). After 24 h, the Schlenk was opened to air and stirred with 1.0 mL of 2-propanol for 1 h. Excess of 2-propanol was then removed under reduced pressure and the remaining residue was purified by a silica gel chromatography using DCM give **14** or **15**.

Cyclobutene-RAFT chain transfer agent 14. Yield: 80% (0.48 g).

¹H NMR (200 MHz, CDCl₃), δ (ppm): 7.35-7.25 (m, 5H, C₆H₅), 6.17 (d, 1H, =CH-, J = 2.8 Hz), 6.08 (d, 1H, =CH-, J = 2.8 Hz), 4.50 (s, 2H, -CH₂-C₆H₅), 4.35-4.17 (m, 2H, -CH₂-OCO), 3.65-3.55 (m, 2H, -CH₂-O-CH₂-C₆H₅), 3.29-3.21 (m, 4H, -CH-, S-CH₂-), 1.68 (s, 6H, C(CH₃)₂), 1.20-1.47 (m, 20H, (-CH₂)₁₀), 0.88 (t, CH₃-CH₂, J = 6.2 Hz).

¹³C NMR (50 MHz, CDCl₃), δ (ppm): 172.8 (C=O), 138.8 (CH₂-C_{phenyl}), 138.3 and 137.6 (=CH-), 128.4, 127.8, 127.6 (CH(*o*, *m*, *p*)), 73.3 (CH₂-Phenyl), 70.2 (CH-CH₂-O-CH₂-Phenyl), 65.9 (CH₂-OCO-), 56.0 ((CH₃)₂-C-S), 45.5 and 44.1 (CH-CH=), 36.9,

31.9, 29.6, 29.6, 29.4, 29.3, 29.1, 28.9, 27.9, 26.9 (CH₃-CH₂-(CH₂)₁₀-S), 25.4 (-S-C(CH₃)₂-CO), 22.7 (CH₃-CH₂-(CH₂)₉-S), 14.1 (CH₃-(CH₂)₁₀-S).

HRMS (Cl-H⁺). Calc. for C₃₀H₄₇O₃S₃⁺: 551.2687 Found: 551.2687.

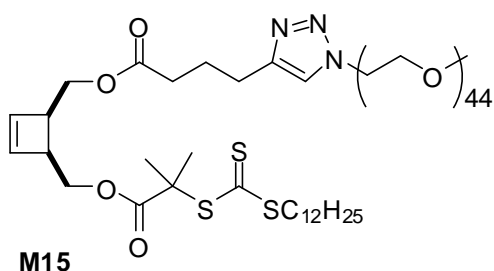
Cyclobutenyl-functionalized “click”-RAFT dual group/agent 15. Yield: 80% (0.48 g).

¹H NMR (200 MHz, CDCl₃), δ (ppm): 6.11 (d, 1H, =CH-, *J* = 3.3 Hz), 6.09 (d, 1H, =CH-, *J* = 3.2 Hz), 4.27-4.21 (m, 4H, -CH₂-OCO-), 3.29-3.21 (m, 4H, -CH-, S-CH₂-), 2.50-2.42 (t, 2H, -CH₂-COO-, *J* = 7.0), 2.31-2.23 (m, 2H, -CH₂-C≡CH), 1.99-1.96 (t, 1H, -C≡CH, *J* = 3 Hz), 1.88-1.81 (m, 2H, CH₂-CH₂-C≡CH), 1.68 (s, 6H, C(CH₃)₂), 1.47-1.20 (m, 20H, (-CH₂)₁₀), 0.88 (t, CH₃-CH₂, *J* = 6.2 Hz).

¹³C NMR (50 MHz, CDCl₃), δ (ppm): 172.8 and 172.8 (C=O), 137.9 (=CH-), 83.2 (C≡CH), 69.2 (≡CH) 65.5 and 64.0 (CH₂-OCO-), 55.9 ((CH₃)₂-C-S), 44.4 and 44.1 (CH-CH=), 32.9 (CH₂-COO) 36.9, 31.9, 29.6, 29.6, 29.4, 29.3, 29.1, 28.9, 27.9, 26.9 (CH₃-CH₂-(CH₂)₁₀-S), 25.47 (-S-C(CH₃)₂-CO), 23.50 (CH₂-CH₂-C≡CH), 22.7 (CH₃-CH₂-(CH₂)₉-S), 17.5 (CH₂-C≡CH), 14.1 (CH₃-(CH₂)₁₀-S).

HRMS (FIID). Calc. for C₂₉H₄₆O₄S₃⁺: 554.2558 Found: 554.2588.

Synthesis of cyclobutene-based PEO macromolecular chain transfer agent M15 via “Click” coupling reaction.



In a typical experiment, the azido-terminated PEO monomethyl ether 2000 (0.8 g, 0.4 mmol), *N,N,N',N',N''*-pentamethyldiethylenetriamine (PMDETA; 0.1 g, 0.6 mmol) and cyclobutene precursor **15** (0.22 g, 0.4 mmol) were charged in a dry Schlenk tube along with degassed DMF (5 mL). The tube was sealed with a rubber septum and subjected to six freeze-pump-thaw cycles. This solution was then cannulated under nitrogen into another Schlenk tube, previously evacuated and filled with nitrogen, containing Cu(I)Br (0.023 g, 0.16 mmol) and a stir bar. The resulting solution was subsequently stirred at room temperature for 4 h. The reaction mixture was diluted with DCM and then washed with 3x100 mL of an aqueous ethylenediaminetetraacetate solution (0.03 mol/L) to

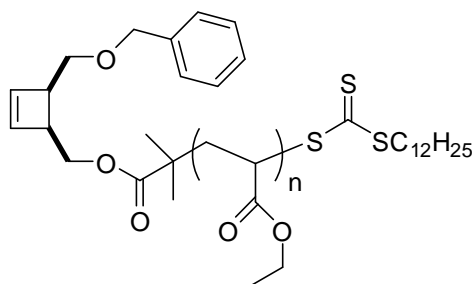
remove the catalyst. The organic layer was dried over MgSO_4 and filtered. The resulting macro-CTA **M15** were isolated by precipitation into diethyl ether. Yellow powder. Yield: 70 %.

^1H NMR (200 MHz, CDCl_3), δ (ppm): 7.50 (s, 1H, triazole), 6.10 (d, 1H, =CH-, $J = 2.8$ Hz), 6.08 (d, 1H, =CH-, $J = 2.8$ Hz), 4.51 (t, 2H, $\text{N}_{\text{triazole}}\text{-CH}_2\text{-}$, $J = 5.0$ Hz), 4.25-4.20 (m, 4H, $\text{-CH}_2\text{-OCO}$), 3.87 (t, 2H, $\text{N}_{\text{triazole}}\text{-CH}_2\text{-CH}_2\text{-O}$, $J = 5.0$ Hz), 3.70-3.60 (m, 172H, $\text{CH}_2\text{-CH}_2\text{-O}$), 3.38 (s, 3H, O-CH_3), 3.22-3.28 (m, 4H -CH-CH= , S-CH_2), 2.76 (t, 2H, $\text{-CH}_2\text{-C}_{\text{triazole}}$, $J = 7.0$ Hz), 2.36 (t, 2H, $\text{-CH}_2\text{-COO}$, $J = 7.0$ Hz), 2.00 (m, 2H, $\text{CH}_2\text{-CH}_2\text{-C}_{\text{triazole}}$), 1.68 (s, 6H, $\text{C-(CH}_3)_2$), 1.20-1.47 (m, 20H, $\text{-(CH}_2\text{)}_{10}$), 0.88 (t, $\text{CH}_3\text{-CH}_2$, $J = 6.2$ Hz).

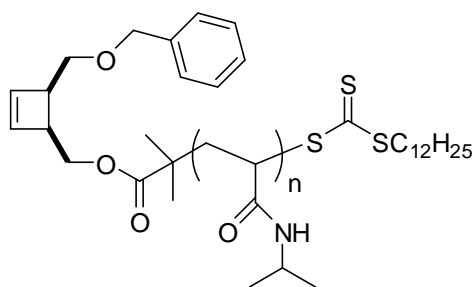
^{13}C NMR (50 MHz, CDCl_3), δ (ppm): 173.0 and 172.7 (C=O), 146.9 ($\text{C=C-N}_{\text{triazole}}$), 137.9 (=CH-), 122.1 ($\text{C=C-N}_{\text{triazole}}$), 71.9 ($\text{CH}_2\text{-O-CH}_3$), 70.5 ($\text{-CH}_2\text{-O}$), 69.5 ($\text{N}_{\text{triazole}}\text{-CH}_2\text{-CH}_2\text{-O}$), 65.5 and 64.0 ($\text{CH}_2\text{-OCO-}$), 55.9 ($\text{(CH}_3)_2\text{-C-S}$), 50.1 ($\text{N}_{\text{triazole}}\text{-CH}_2\text{-CH}_2\text{-O}$), 44.4 and 44.1 (CH-CH=), 32.9 ($\text{CH}_2\text{-COO}$) 36.9, 31.9, 29.6, 29.6, 29.4, 29.3, 29.1, 28.9, 27.9, 26.9 ($\text{CH}_3\text{-CH}_2\text{-(CH}_2\text{)}_{10}\text{-S}$), 25.47 ($\text{-S-C(CH}_3)_2\text{-CO}$), 24.8 ($\text{CH}_2\text{-C}_{\text{triazole}}$), 24.6 ($\text{CH}_2\text{-CH}_2\text{-C}_{\text{triazole}}$), 22.7 ($\text{CH}_3\text{-CH}_2\text{-(CH}_2\text{)}_9\text{-S}$), 14.1 ($\text{CH}_3\text{-(CH}_2\text{)}_{10}\text{-S}$).

General RAFT polymerization procedure.

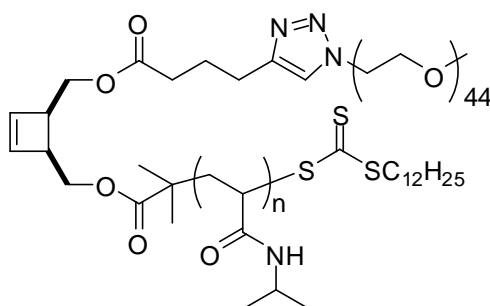
CTA, monomer, initiator, solvent and DMF were added in a Schlenk tube fitted with a rubber septum and a stir bar. RAFT polymerization of NIPAM was realized in dioxane at 70 °C with ACPA as the initiator and a monomer/CTA/initiator/DMF ratio of 100/1/0.2/50 and concentration of CTA **14** or macroCTA **M15** was 0.0091 mol/L. RAFT polymerization of EA was realized in toluene at 65 °C and AIBN as the initiator with a monomer/CTA/initiator/DMF ratio of 100/1/0.1/100 and a monomer/solvent ratio of 1/1 (v/v). In all cases, DMF was used as an internal standard for the determination of monomer conversion. After 5 cycles of freeze-pump-thaw, the polymerization was conducted in a 65 °C or 70 °C oil bath under an argon atmosphere. Every 30 min, aliquots were removed and rapidly quenched by freezing the reaction mixture in a liquid nitrogen bath. Portions of these aliquots were used directly for analysis by ^1H NMR for monomer conversion or purification for SEC analysis. Purified PNIPAM and PEA samples were obtained by precipitation three times in diethyl ether and in water, respectively.

***α*-Cyclobutenyl PEA M14-EA**


^1H NMR (200 MHz, CDCl_3), δ (ppm): 7.32-7.18 (m, 5H, C_6H_5), 6.17 (d, 1H, $=\text{CH}$ -, $J = 2.8$ Hz), 6.08 (d, 1H, $=\text{CH}$ -, $J = 2.8$ Hz), 4.51 (s, 2H, $-\text{CH}_2-\text{C}_6\text{H}_5$), 4.16-4.06 (m, 74H $-\text{CH}_2-\text{OCO}$, $(-\text{O}-\text{CH}_2-\text{CH}_3)_{36}$), 3.65-3.55 (m, 2H, $-\text{CH}_2-\text{O}-\text{CH}_2-\text{C}_6\text{H}_5$), 3.29-3.21 (m, 4H, $-\text{CH}$ -, $\text{S}-\text{CH}_2$ -), 2.35-1.23 (m, 242H, $(\text{C}(\text{CH}_3)_2)$, $(-\text{CH}_2-\text{CH}-)_{36}$, $(\text{O}-\text{CH}_2-\text{CH}_3)_{36}$, $(-\text{CH}_2-)_10$), 0.88 (t, CH_3-CH_2 , $J = 6.2$ Hz).

***α*-Cyclobutenyl PNIPAM M14-NIPAM**


^1H NMR (200 MHz, $\text{DMSO-}d_6$), δ (ppm): 7.80-6.70 (m, C_6H_5 -, $-\text{NH}$ -), 6.17 (d, 1H, $=\text{CH}$ -, $J = 2.8$ Hz), 6.08 (d, 1H, $=\text{CH}$ -, $J = 2.8$ Hz), 4.51 (s, 2H, $-\text{CH}_2-\text{C}_6\text{H}_5$), 4.16-4.06 (m, 74H $-\text{CH}_2-\text{OCO}$, $(-\text{N}-\text{CH}(\text{CH}_3)_2)_{30}$), 3.65-3.55 (m, 2H, $-\text{CH}_2-\text{O}-\text{CH}_2-\text{C}_6\text{H}_5$), 3.29-3.21 (m, 4H, $-\text{CH}$ -, $\text{S}-\text{CH}_2$ -), 2.35-1.23 (m, 242H, $\text{C}-(\text{CH}_3)_2$ -, $(-\text{CH}_2-\text{CH}-)_{30}$, $(\text{N}-\text{CH}(\text{CH}_3)_2)_{30}$, $(-\text{CH}_2-)_10$), 0.88 (t, CH_3-CH_2 , $J = 6.2$ Hz).

Cylobutene-based block copolymers M15-NIPAM


^1H NMR (200 MHz, $\text{DMSO-}d_6$), δ (ppm): 7.80-6.70 (m, proton triazole, $-\text{NH}$ -), 6.10 (m, 2H, $=\text{CH}$ -), 4.51 (t, 2H, $\text{N}_{\text{triazole}}-\text{CH}_2$ -, $J = 5.0$ Hz), 4.20-3.10 (m, $(-\text{N}-\text{CH}(\text{CH}_3)_2)_{30}$, $-\text{CH}_2-$

OCO, (CH₂-CH₂-O)₄₃, O-CH₃, -CH-CH=, S-CH₂, 2.30-0.75 (m, (-CH₃)₂-C, (-CH₂-CH-)₃₀, (-CH₃)₆₀, -CH₂-COO, -CH₂-CH₂-C_{triazole}, (C(CH₃)₂, (-CH₂-)₁₀), CH₃-CH₂).

Preparation of samples for DLS and SLS analysis.

All samples were prepared using Millipore (18.2 MΩ) water in a hood that was kept dust-free by an air circulation system. The polymer sample was weighed into a clean, dust-free sample vial using a four figure balance. Afterwards, Millipore water was added dropwise through a 0.2 μm pore size Anotop syringe filter, with the mass of solvent used recorded for accurate concentration determination. The samples of different concentration of polymer (ranging from 2 mg mL⁻¹ to 12 mg mL⁻¹) were stored at room temperature for a minimum of 24 hours to ensure full dissolution. They were then filtered through 0.2 μm pore size Anotop syringe filters into a disposable glass vessel for static light scattering measurements performed at 20°C. Measurements were made at angles of 30°, 50°, 70°, 90°, 110°, 130° and 150° and the data analysed using a Zimm plot. These measurements provide molecular weight and second virial coefficient and hydrodynamic radius. Separate dynamic light scattering measurements were performed on the samples using a Malvern instruments Zetasizer.

CMC determination by fluorescence spectroscopy.

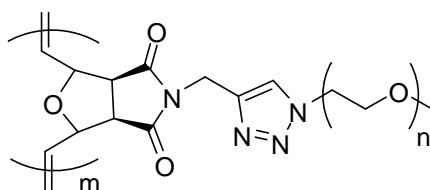
To a series of dry flasks were added aliquots of a acetone solution of pyrene or pyrene-3-carboxaldehyde. A thin layer of pyrene or pyrene-3-carboxaldehyde formed at the bottom of each flask after the solvent was evaporated. Macromonomer solutions of different concentrations in Millipore (18.2 MΩ) water (ranking from 10⁻³ to 10² mg/mL for **M10** and from 10⁻⁴ to 10 mg/mL for **M15**) were then added, and the probe was solubilized in the resulting solutions by stirring for 24h before the fluorescence measurements were made. Emission spectra of pyrene and pyrene-3-carboxaldehyde were obtained by exciting the samples at 332 and 380 nm, respectively.

General procedure for ROMP of macromonomers.

In a typical experiment, a dry Schlenk tube was charged with the macromonomer (100 mg) and a stir bar. The Schlenk was capped with a rubber septum, and cycled three

times between vacuum and nitrogen to remove oxygen. The desired amount of degassed, anhydrous DCM or toluene ($[M]_0 = 0.01 - 0.10$ mol/L) was added *via* syringe under a nitrogen atmosphere to dissolve the macromonomer. A stock solution of Grubbs' catalyst in degassed anhydrous DCM or toluene was prepared in a separate vial. All experiments have been conducted with a catalyst concentration $[G]_0 = 7$ μ mol/L, except that for the polymerization of **M2-500** ($[G]_0 = 24$ μ mol/L). The desired amount of catalyst was injected into the macromonomer solution to initiate the polymerization. The Schlenk tube was stirred under nitrogen at room temperature in case of **G3** or at 70 °C in case of **G2**. The polymerization was terminated by the addition of two drops of ethyl vinyl ether. The solvent was removed under reduced pressure for NMR and SEC measurements. The reaction mixture was then diluted in DCM and precipitated into 10 mL of stirring cold diethyl ether.

Polyoxanorbornene-g-PEO monomethyl ether 500 from M2-500. Brown plastic.



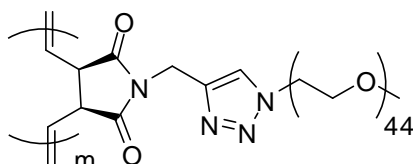
^1H NMR (200 MHz, CDCl_3), δ (ppm): 7.72 (bs, 1H, triazole), 6.05 (bs, 2H, $\text{CH}=\text{CH}$, *trans*), 5.75 (bs, 2H, $\text{CH}=\text{CH}$, *cis*), 5.00 (bs, 2H, $\text{CH}-\text{O}-\text{CH}$, *cis*), 4.75 (bs, 4H, $\text{CH}-\text{O}-\text{CH}$, *trans*; $\text{N}-\text{CH}_2$), 4.49 (bs, 2H, $\text{N}_{\text{triazole}}-\text{CH}_2-\text{CH}_2-\text{O}$), 3.84 (bs, 2H, $\text{N}_{\text{triazole}}-\text{CH}_2-\text{CH}_2-\text{O}$), 3.80-3.50 (m, 40H, $\text{CH}_2-\text{CH}_2-\text{O}$), 3.38 (s, 3H, $\text{CH}-\text{C}=\text{O}$, $\text{O}-\text{CH}_3$). ^{13}C NMR (50 MHz, CDCl_3), δ (ppm): 175.17 (CO), 141.43 ($\text{C}=\text{C}-\text{N}_{\text{triazole}}$), 130.92 ($=\text{CH}$), 123.86 ($\text{C}=\text{C}-\text{N}_{\text{triazole}}$), 80.73 ($\text{CH}-\text{O}$), 71.89 ($\text{CH}_2-\text{O}-\text{CH}_3$), 70.54 ($-\text{CH}_2-\text{O}$), 69.35 ($\text{N}_{\text{triazole}}-\text{CH}_2-\text{CH}_2-\text{O}$), 59.00 (CH_3-O), 53.36 ($\text{N}_{\text{triazole}}-\text{CH}_2-\text{CH}_2-\text{O}$), 50.51 ($\text{CH}-\text{CO}$), 34.07 ($\text{N}-\text{CH}_2$).

Polyoxanorbornene-g-PEO monomethyl ether 2 000 from M2-2000. Brown powder. ^1H NMR (200 MHz, CDCl_3), δ (ppm): 7.76 (bs, 1H, triazole), 6.02 (bs, 2H, $\text{CH}=\text{CH}$, *trans*), 5.70 (bs, 2H, $\text{CH}=\text{CH}$, *cis*), 5.02 (bs, 2H, $\text{CH}-\text{O}-\text{CH}$, *cis*), 4.76 (bs, 4H, $\text{CH}-\text{O}-\text{CH}$, *trans*; $\text{N}-\text{CH}_2$), 4.50 (bs, 2H, $\text{N}_{\text{triazole}}-\text{CH}_2-\text{CH}_2-\text{O}$), 3.82 (bs, 2H, $\text{N}_{\text{triazole}}-\text{CH}_2-\text{CH}_2-\text{O}$), 3.80-3.60 (m, 172H, $\text{CH}_2-\text{CH}_2-\text{O}$), 3.40 (s, 3H, $\text{CH}-\text{C}=\text{O}$, $\text{O}-\text{CH}_3$). ^{13}C NMR (50 MHz, CDCl_3), δ (ppm): 174.99 (CO), 141.41 ($\text{C}=\text{C}-\text{N}_{\text{triazole}}$), 131.72 ($=\text{CH}$), 123.70

(C=C-N_{triazole}), 80.71 (CH-O), 71.89 (CH₂-O-CH₃), 70.52 (-CH₂-O), 69.31 (N_{triazole}-CH₂-CH₂-O), 58.99 (CH₃-O), 53.35 (N_{triazole}-CH₂-CH₂-O), 50.22 (CH-CO), 34.12 (N-CH₂).

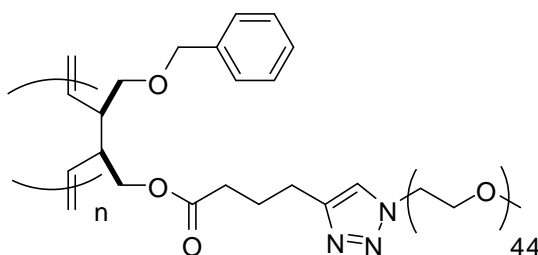
Polyoxanorbornene-g-PEO monomethyl ether 5 000 from M2-5000. Brown powder. ¹H NMR (200 MHz, CDCl₃), δ (ppm): 7.73 (bs, 1H, triazole), 6.05 (bs, 2H, CH=CH, *trans*), 5.78 (bs, 2H, CH=CH, *cis*), 5.04 (bs, 2H, CH-O-CH, *cis*), 4.78 (bs, 4H, CH-O-CH, *trans*; N-CH₂), 4.51 (bs, 2H, N_{triazole}-CH₂-CH₂-O), 3.80 (bs, 2H, N_{triazole}-CH₂-CH₂-O), 3.80-3.60 (m, 412H, CH₂-CH₂-O), 3.38 (s, 3H, CH-C=O, O-CH₃).

1,4-polybutadiene-g-PEO monomethyl ether from M4-2000. White powder.



¹H NMR (200 MHz, CDCl₃), δ (ppm): 7.70 (bs, 1H, triazole), 5.60 (bs, 2H, CH=CH), 4.76 (bs, 2H, N-CH₂-), 4.50 (bs, 2H, N_{triazole}-CH₂-CH₂-O), 3.83 (m, 4H, N_{triazole}-CH₂-CH₂-O, -CH-CH=), 3.60-3.70 (m, 172H, CH₂-CH₂-O), 3.38 (s, 3H, O-CH₃).

1,4-polybutadiene-g-PEO monomethyl ether from M10. White powder.



¹H NMR (200 MHz, CDCl₃), δ (ppm): 7.50 (bs, 1H, triazole), 7.30 (bs, 5H, C₆H₅), 5.40 (bs, 2H, CH=CH), 4.50-4.00 (b, 6H, N_{triazole}-CH₂-CH₂-C₆H₅, -CH₂-OCO) 3.99 (bs, 2H, N_{triazole}-CH₂-CH₂-O), 3.60-3.70 (m, 174H, CH₂-CH₂-O, -CH₂-O-CH₂-C₆H₅), 3.37 (s, 3H, O-CH₃), 3.20 (m, 2H -CH-CH=), 2.70 (bs, 2H, -CH₂-C_{triazole}), 2.30 (bs, 2H, -CH₂-COO, *J* = 7), 1.90 (bs, 2H, CH₂-CH₂-C_{triazole}).

Typical micro-emulsion polymerization

All the micro-emulsions polymerizations were carried out in Schlenk tubes and under nitrogen atmosphere. In a typical recipe, two aqueous phases were prepared by adding 20 mL of degassed deionized water (by nitrogen bubbling for 45 min) and 1-pentanol (0.72 mL, co-surfactant) in a Schlenk tube containing SDS (1.39 g, 4.7mmol) preliminarily degassed by three vacuum/nitrogen filling cycles. The monomer micro-emulsion was prepared by adding to the first aqueous phase, an organic solution, which was composed of macromonomer/solvent ratio of 0.75 g/0.24 mL. The Grubbs' catalyst micro-emulsion was prepared by adding to the second aqueous phase, an organic solution composed of Grubbs catalyst (9.0 mg) and solvent (0.72 mL). When these two micro-emulsions became translucent (after about 30 min of agitation), the micro-emulsion of monomers was transferred into the Schlenk containing the catalyst micro-emulsion. The reaction was stopped by adding ethyl vinyl ether.

Typical mini-emulsion polymerization

All the mini-emulsions polymerizations were carried out in Schlenk tubes and under nitrogen atmosphere. In a typical recipe, aqueous phase was prepared by adding 45 mL of degassed deionized water (by nitrogen bubbling for 45 min) in a Schlenk tube containing Brij 700 (50mg) preliminarily degassed by three vacuum/nitrogen filling cycles. The macromonomer organic phase was prepared by dissolving macromonomer (0.4 g in case of oxanorbornenyl macromonomer or 0.8 g in case of cyclobutenyl macromonomer), co-surfactant (hexadecane, 20 mg) and Grubb's catalyst in DCM (0.8 mL in case of oxanorbornenyl macromonomer or 1.5 mL in case of cyclobutenyl macromonomer). The organic phase was quickly transferred into the aqueous phase. This step was followed by further mixing under magnetic agitation in an ultrasonic homogenizer equipped with a cylindrical probe (Sonic W750) at 60% of the power for 2x2 min. During the sonication step, the vessel containing the mini-emulsion was immersed in an ice-bath to prevent it from heating up. The reaction was stopped by adding ethyl vinyl ether.